Self-assembling PEG-oligoesters
nanoparticle design for drug delivery

Myrra Carstens

This printing of this thesis was financially supported by:
OctoPlus N.V., Leiden, The Netherlands

Utrecht Institute for Pharmaceutical Sciences (UIPS), Utrecht, The Netherlands

Self-assembling PEG-oligoesters *nanoparticle design for drug delivery*
Myrra G. Carstens
Ph.D. Thesis, with a summary in Dutch
Utrecht University, the Netherlands
August 2007
ISBN 978-90-39346358

Cover design and layout: Martine Boonstra
Cover: PEG-*b*-oligolactate and PEG-*b*-oligo(ε-caprolactone) on a schematic representation of a self-assembled particle.

Printed by PrintPartners Ipskamp, Enschede, The Netherlands

Self-assembling PEG-oligoesters
nanoparticle design for drug delivery

Zelf-assemblerende PEG-oligoësters
ontwerp van nanodeeltjes voor de aflevering van geneesmiddelen
(met een samenvatting in het Nederlands)

Proefschrift

ter verkrijging van de graad van doctor aan de Universiteit Utrecht
op gezag van de rector magnificus, prof. dr. W.H. Gispen,
ingevolge het besluit van het college voor promoties
in het openbaar te verdedigen op woensdag 26 september 2007 des middags te 12.45 uur

door

Myrra Gwendolyn Carstens

geboren op 30 januari 1978 te Waalwijk

Promotoren:	Prof. dr. ir. W.E. Hennink Prof. dr. D.J.A. Crommelin
Co-promotoren:	Dr. C.F. van Nostrum Dr. R. Verrijk

The research described in this thesis was financially supported by OctoPlus N.V., Leiden, The Netherlands.
The research was performed at the Department of Pharmaceutics, Utrecht Institute for Pharmaceutical Sciences, Utrecht University, Utrecht, The Netherlands.

"Wisdom begins in wonder"
Socrates (*Greek philosopher, 470–399 BC*)

m
n

m

Table of contents

General Introduction

Polymeric drug delivery systems

Recent advances in proteomics, genomics, combinatorial chemistry and high-throughput screening have resulted in the discovery and selection of numerous highly potent new chemical entities (NCE's). However, a good bioactivity is not the only prerequisite for a lead candidate, and does not guarantee its development into a clinically successful product with the desired therapeutic effect.[1] Drug candidates may have a limited aqueous solubility or low stability, causing formulation problems. Furthermore, the compound may be rapidly cleared from the body, necessitating frequent administration. Finally, it may distribute to other sites than the diseased area, which can result in side effects and/or insufficient localisation at the target-site, thereby reducing the therapeutic index of the drug. To diminish these unfavourable properties, a large variety of drug delivery systems have been designed and investigated. Several of these systems have been approved by the regulatory authorities and are currently on the market. Prime examples are liposomes loaded with the anti-cancer agent doxorubicin (Caelyx®) or with the antimicrobial amphothericin B (Ambisome®).[2-5] Besides lipid-based drug carriers, systems based on polymeric materials have been developed. The major advantage of using (semi-)synthetic polymers for drug delivery purposes is their almost unlimited tailorability.[6, 7] Their size, molecular architecture and chemical composition can be easily adjusted, thereby affecting properties such as physicochemical characteristics and degradability. Furthermore, their synthesis can be performed reproducibly, and is relatively easy to scale up (Box 1).

Box 1

Advantages of the use of polymers for drug delivery systems

- High tailorability
- Reproducible production
- Easy up-scaling

Polymeric drug delivery systems include implants, that are surgically inserted or injected subcutaneously, and microspheres, administered by subcutaneous or intramuscular injection.[8-13] Polymer-based implants and microspheres are used for the controlled release of several agents, such as cytostatics, hormones and proteins.[9-11, 13] In addition, polymer-drug conjugates and nanoparticles have been designed, which can be used for the (targeted) delivery of drugs after intravenous administration. Polymer-drug conjugates are formed by covalent coupling of (protein) drugs to a

synthetic polymer, in order to improve their solubility, stability, pharmacokinetics and/or biodistribution.[2, 5, 14, 15] As an example, poly(ethylene glycol) (PEG) has been coupled to therapeutic proteins (so-called PEGylation), which has led for instance to the commercially available products Neulasta® (PEG-granulocyte colony stimulating factor),[16] PEG-Asys® (PEG-interferon α 2a), and PEG-Intron® (PEG-interferon α 2b).[5, 14, 15, 17-21] Several polymer-conjugated anti-cancer drugs have been developed in the last 25 years, for instance poly(N-(2-hydroxypropyl)methacrylamide) (PHPMA)-doxorubicin (PK1, PK2),[22-24] poly(glutamate)-paclitaxel (Xyotax®)[25] and PEG-camptothecin (Prothecan®).[26, 27] These polymer-drug conjugates demonstrated promising results as compared to the commercially available formulations of the free drugs, and have entered clinical trials.[5, 15, 18-20, 23-25, 27]

Polymeric nanoparticles are defined as sub-micron colloidal dispersions, and may consist of a nano-sized polymeric matrix, in which the drug is dispersed or dissolved (nanosphere), or a reservoir system surrounded by a polymeric wall (nanocapsule).[3, 28-30] A variety of polymers have been used for the preparation of nanospheres or nanocapsules, including polyesters[31-38] and poly(alkylcyanoacrylates).[39-41] Nanocapsules have been used for the encapsulation of *e.g.* insulin,[39, 40] the anti-viral azidothymidine[41] or xanthones,[33] and nanospheres for the formulation of photosensitisers,[35] or the taxoids paclitaxel[38] and docetaxel.[32]

Self-assembling polymers

A specific class of polymeric nanoparticles are the self-assembled systems. These are based on amphiphilic block copolymers that, upon their self-assembly in water, can yield various morphologies. Well known examples are spherical micelles, composed of a hydrophobic core and a hydrophilic shell, and vesicles (also called polymersomes), comprising a bilayer structure with an aqueous interior, similar to liposomes. Furthermore, worm-like or disk-shaped micelles, rods, lamellar structures, tubules and many other structures can be formed (Figure 1).[28, 42-44] The type of morphology formed upon self-assembly depends on several factors related to characteristics of the polymer itself, as well as the preparation method and the properties of the aqueous phase. An important polymer-related morphogenic factor is the polymer composition, and in particular the weight ratio between the hydrophobic and the hydrophilic block.[6, 28, 42-46] For example, it was demonstrated that the morphology of a series of PEG-*b*-polybutadiene (PBD) block copolymers in water changed from vesicles to worm-like micelles and finally spherical micelles, when increasing the PEG-weight fraction from 0.25 to 0.65.[43] A similar trend was observed upon increasing the poly(acrylic acid) (PAA) block of PAA-*b*-polystyrene (PS) block copolymers.[47]

Self-assembled block copolymer nanoparticles can be prepared by the film-hydration (also called 'film-casting') method, which is a common procedure for the preparation of liposomes.[4] The block copolymer is dissolved in a volatile solvent, which is evaporated to form a polymer film, followed by hydration in an aqueous phase. This method has been applied for the formation of polymeric micelles composed of *e.g.* PEG-*b*-phosphatidylethanolamine (PE),[48] PEG-*b*-polylactate (PLA),[49] PEG-

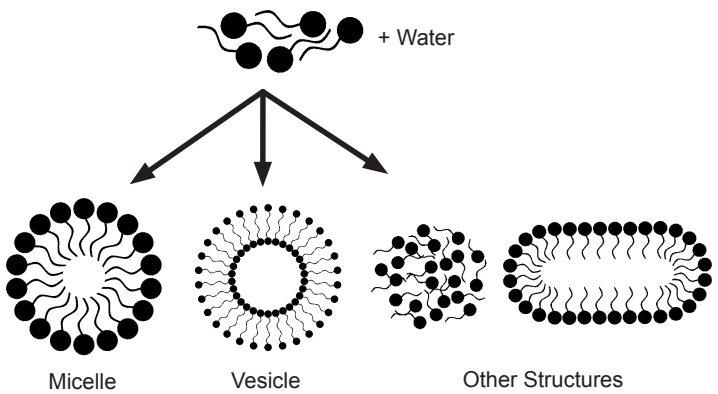

Figure 1 Self-assembly of amphiphilic block copolymers in water.

b-poly(aspartic acid) (P(Asp)),[50] and polymersomes composed of PEG-*b*-PBD or PEG-*b*-poly(ethyl ethylene).[51] Self-assembly also occurs when a solution of block copolymer in an organic solvent is added to an aqueous phase, followed by removal of the organic solvent by evaporation ('solvent-evaporation method' or 'o/w emulsion method') or dialysis ('dialysis method'). The solvent evaporation method was for example applied to form PEG-*b*-butylacrylate,[52] PEG-*b*-PLA[53] and PEG-*b*-P(Asp)[50] micelles, whereas PAA-*b*-PS micelles and vesicles were prepared by the dialysis method.[47] With respect to the morphology, important factors are the selected solvent, and the polymer concentration. When hydrophilic blocks with acidic, basic or charged groups are used, the pH and salt concentration of the aqueous phase are morphogenic factors as well.[28, 42, 43, 45, 46]

Obviously, these self-assembled systems are interesting carriers for the delivery of drugs. Polymer vesicles (or polymersomes) are an attractive alternative for liposomes, but they represent a relatively new area of research. The first *in vivo* results were recently reported by the group of Discher, who observed good anti-tumour efficacy in mice using PEG-polyester polymersomes, loaded with doxorubicin in the aqueous vesicle interior, and paclitaxel in the hydrophobic bilayer.[54, 55] Polymeric micelles are of particular interest for the delivery of hydrophobic drugs. These drugs are usually difficult to formulate, due to their poor aqueous solubility. Several examples of the successful use of polymeric micelles for drug delivery have been reported,[44, 56-59] as will be discussed in detail in chapter two of this thesis.

Aim and outline of this thesis

An attractive class of amphiphilic block copolymers for the formation of self-assembled drug delivery systems are PEG-polyesters, illustrated by the large number of systems that have been developed based on this type of block copolymers.[60-72] The two PEG-polyesters that are most often used are PEG-*b*-PLA and PEG-*b*-poly(ε-caprolactone) (PCL), the latter being more hydrophobic. The ubiquitous use of these polymers is related to the good biocompatibility and low toxicity of both blocks. Moreover, the hydrophilic PEG-block confers the drug delivery system long circulating properties, and the hydrophobic polyester-block is biodegradable, which may enable controlled release of the loaded drug and prevent the accumulation of the carrier after administration.[31, 73-79] A phase I clinical trial with paclitaxel-loaded PEG-*b*-PLA micelles demonstrated a better toxicity profile than the conventional formulation,[80] illustrating the potential of these type of systems for pharmaceutical applications.

The above mentioned drug delivery systems are based on high molecular weight polymers. In this **thesis**, the use of low molecular weight PEG-oligoesters to design novel nano-sized drug delivery systems is evaluated. It was demonstrated previously that low molecular weight oligolactates can be easily fractionated by preparative reversed phase HPLC, to obtain monodisperse materials.[81] This technique was applied to prepare well defined block oligomers, in particular PEG-oligo(L-lactate)s and PEG-oligo(ε-caprolactone)s. This offers the possibility to study the effects of block oligomer composition on self-assembling properties in detail, and to gain insight into the degradation mechanisms.

Chapter two presents an overview of the literature on polymeric micelles, focussing on their long circulating properties, stability and stimuli sensitivity. Strategies to improve the longevity of polymeric micelles after intravenous administration are discussed, including the adjustments of surface properties and size. Furthermore, several methods are described to stabilise polymeric micelles by physical or chemical crosslinking, and to improve drug retention by optimising the compatibility between the drug and the micellar core. The last part of this chapter focuses on the possibilities and mechanisms to release the payload from the polymeric micelles in a controlled manner by local and/or external stimuli.

In **Chapter three** low molecular weight mPEG-*b*-oligo(L-lactate)s with monodisperse hydrophobic blocks were prepared. The effect of the composition of the block oligomers on their critical aggregation concentration and temperature sensitivity was studied, and the particle formation was studied by several techniques, including dynamic and static light scattering (DLS, SLS) and NMR spectroscopy.

Since this study demonstrated the miscibility of both blocks of the mPEG-*b*-oligo(L-lactate)s, which limits proper micelle formation, in **Chapter four** a more hydrophobic oligoester was used. PEG-*b*-oligo(ε-caprolactone)s were synthesised and fractionated, and the end group of the hydrophobic block was modified with a benzoyl or a naphthoyl group. The influence of terminal derivatisation of PEG-*b*-oligo(ε-caprolactone)s with a benzoyl or naphthoyl group on the self-assembling properties was evaluated, and it was demonstrated that sub-20 nm micelles could be formed, which may have attractive properties for drug delivery applications in terms of biodistribution and tumour penetration.[82-86]

To obtain insight into the degradation-induced destabilisation of these carrier systems, the *in vitro* degradation of monodisperse oligomers was studied in **Chapter five**. First, the hydrolysis rate and hydrolysis mechanism of monodisperse oligo(ε-caprolactone) was investigated, and the effect of pH and dielectric constant thereon. Next, the degradation behaviour of its amphiphilic block oligomer with PEG was studied, both as a molecularly dissolved block oligomer and in a micellar dispersion, including the influence of ester bond hydrolysis on the stability of the micelles. Besides chemical hydrolysis, the enzymatic degradation and destabilisation of these block oligomer micelles by lipase was investigated.

Chapter six presents the loading of PEG-*b*-oligo(ε-caprolactone)-based micelles with the taxanes paclitaxel and docetaxel, focusing on the effect of the composition of the micellar core on the encapsulation and retention of the drug. Their *in vitro* drug release and cytotoxicity are reported in this chapter as well.

In **Chapter seven** the results are summarised and discussed. A preliminary *in vivo* study with paclitaxel-loaded micelles in mice is presented, and directions for future research and applications are given.

References

1. Pritchard JF; Jurima-Romet M; Reimer ML; Mortimer E; Rolfe B; Cayen MN, Making better drugs: Decision gates in non-clinical drug development. *Nat Rev Drug Discov* 2, 542-553 (2003).
2. Allen TM; Cullis PR, Drug delivery systems: entering the mainstream. *Science* 303, 1818-1822 (2004).
3. Barratt GM, Therapeutic applications of colloidal drug carriers. *Pharm Sci Technol To* 3, 163-171 (2000).
4. Storm G; Crommelin DJA, Liposomes: quo vadis? *Pharm Sci Technol To* 1, 19-31 (1998).
5. Khandare J; Minko T, Polymer-drug conjugates: Progress in polymeric prodrugs. *Prog Polym Sci* 31, 359-397 (2006).
6. Qiu LY; Bae YH, Polymer architecture and drug delivery. *Pharm Res* 23, 1-30 (2006).
7. Hawker CJ; Wooley KL, The convergence of synthetic organic and polymer chemistries. *Science* 309, 1200-1205 (2005).
8. Packhaeuser CB; Schnieders J; Oster CG; Kissel T, In situ forming parenteral drug delivery systems: an overview. *Eur J Pharm Biopharm* 58, 445-455 (2004).
9. Fung LK; Saltzman WM, Polymeric implants for cancer chemotherapy. *Adv Drug Deliver Rev* 26, 209-230 (1997).
10. Dash AK; Cudworth II GC, Therapeutic applications of implantable drug delivery systems. *J Pharmacol Toxicol* 40, 1-12 (1998).
11. Freiberg S; Zhu XX, Polymer microspheres for controlled drug release. *Int J Pharm* 282, 1-18 (2004).
12. Sinha VR; Trehan A, Biodegradable microspheres for protein delivery. *J Control Release* 90, 261-280 (2003).
13. Malik DK; Baboota S; Ahuja A; Hasan S; Ali J, Recent advances in protein and peptide drug delivery systems. *Curr Drug Deliv* 4, 141-151 (2007).
14. Molineux G, Pegylation: engineering improved biopharmaceuticals for oncology. *Pharmacotherapy* 23, 3S-8S (2003).
15. Duncan R, Polymer conjugates as anticancer nanomedicines. *Nat Rev Cancer* 6, 688-701 (2006).
16. Molineux G, The design and development of pegfilgrastim (PEG-rmetHuG-CSF, Neulasta). *Curr Pharm Design* 10, 1235-1244 (2004).
17. Wang YS; Youngster S; Grace M; Bausch J; Bordens R; Wyss DF, Structural and biological characterization of pegylated recombinant interferon alpha-2b and its therapeutic implications. *Adv Drug Deliver Rev* 54, 547-570 (2002).
18. Vicent MJ; Duncan R, Polymer conjugates: nanosized medicines for treating cancer. *Trends Biotechnol* 24, 39-47 (2006).
19. Duncan R, The dawning era of polymer therapeutics. *Nat Rev Drug Discov* 2, 347-360 (2003).
20. Haag R; Kratz F, Polymer therapeutics: concepts and applications. *Angew Chem Int Edit* 45, 1198-1215 (2006).
21. Luxon BA; Grace M; Brassard D; Bordens R, Pegylated interferons for the treatment of chronic hepatitis C infection. *Clin Ther* 24, 1363-1383 (2002).
22. Seymour LW; Ulbrich K; Strohalm J; Kopecek J; Duncan R, The pharmacokinetics of polymer-bound adriamycin. *Biochem Pharmacol* 39, 1125-1131 (1990).
23. Vasey PA; Kaye SB; Morrison R; Twelves C; Wilson P; Duncan R; Thomson AH; Murray LS; Hilditch TE; Murray T; Burtles S; Fraier D; Frigerio E; Cassidy J, Phase I clinical and pharmacokinetic study of PK1 [N-(2-hydroxypropyl)methacrylamide copolymer doxorubicin]: first member of a new class of chemotherapeutic agents-drug-polymer conjugates. Cancer Research Campaign Phase I/II Committee. *Clin Cancer Res* 5, 83-94 (1999).
24. Seymour LW; Ferry DR; Anderson D; Hesslewood S; Julyan PJ; Poyner R; Doran J; Young AM; Burtles S; Kerr DJ, Hepatic drug targeting: phase I evaluation of polymer-bound doxorubicin. *J Clin Oncol* 20, 1668-1676 (2002).
25. Singer JW, Paclitaxel poliglumex (XYOTAX, CT-2103): a macromolecular taxane. *J Control Release* 109, 120-126 (2005).

26. Greenwald RB; Choe YH; McGuire J; Conover CD, Effective drug delivery by PEGylated drug conjugates. *Adv Drug Deliver Rev* 55, 217-250 (2003).
27. Posey JA, 3rd; Saif MW; Carlisle R; Goetz A; Rizzo J; Stevenson S; Rudoltz MS; Kwiatek J; Simmons P; Rowinsky EK; Takimoto CH; Tolcher AW, Phase 1 study of weekly polyethylene glycol-camptothecin in patients with advanced solid tumors and lymphomas. *Clin Cancer Res* 11, 7866-7871 (2005).
28. Letchford K; Burt H, A review of the formation and classification of amphiphilic block sopolymer nanoparticulate structures: micelles, manospheres, nanocapsules and polymersomes. *Eur J Pharm Biopharm* 65, 259-269 (2007).
29. Meier W, Polymer nanocapsules. *Chem Soc Rev* 29, 295-303 (2000).
30. Brigger I; Dubernet C; Couvreur P, Nanoparticles in cancer therapy and diagnosis. *Adv Drug Deliver Rev* 54, 631-651 (2002).
31. Sinha VR; Bansal K; Kaushik R; Kumria R; Trehan A, Poly-ε-caprolactone microspheres and nanospheres: an overview. *Int J Pharm* 278, 1-23 (2004).
32. Musumeci T; Ventura CA; Giannone I; Ruozi B; Montenegro L; Pignatello R; Puglisi G, PLA/PLGA nanoparticles for sustained release of docetaxel. *Int J Pharm* 325, 172-179 (2006).
33. Teixeira M; Alonso MJ; Pinto MM; Barbosa CM, Development and characterization of PLGA nanospheres and nanocapsules containing xanthone and 3-methoxyxanthone. *Eur J Pharm Biopharm* 59, 491-500 (2005).
34. Soppimath KS; Aminabhavi TM; Kulkarni AR; Rudzinski WE, Biodegradable polymeric nanoparticles as drug delivery devices. *J Control Release* 70, 1-20 (2001).
35. Leroux J-C; Allemann E; De Jaeghere F; Doelker E; Gurny R, Biodegradable nanoparticles — From sustained release formulations to improved site specific drug delivery. *J Control Release* 39, 339-350 (1996).
36. Abdelwahed W; Degobert G; Fessi H, A pilot study of freeze drying of poly(epsilon-caprolactone) nanocapsules stabilized by poly(vinyl alcohol): Formulation and process optimization. *Int J Pharm* 309, 178-188 (2006).
37. Zweers MLT; Grijpma DW; Engbers GHM; Feijen J, The preparation of monodisperse biodegradable polyester nanoparticles with a controlled size. *J Biomed Mater Res B* 66B, 559-566 (2003).
38. Jin C; Wu H; Liu J; Bai L; Guo G, The effect of paclitaxel-loaded nanoparticles with radiation on hypoxic MCF-7 cells. *J Clin Pharm Ther* 32, 41-47 (2007).
39. Watnasirichaikul S; Davies NM; Rades T; Tucker IG, Preparation of biodegradable insulin nanocapsules from biocompatible microemulsions. *Pharm Res* 17, 684-689 (2000).
40. Aboubakar M; Puisieux F; Couvreur P; Deyme M; Vauthier C, Study of the mechanism of insulin encapsulation in poly(isobutylcyanoacrylate) nanocapsules obtained by interfacial polymerization. *J Biomed Mater Res* 47, 568-576 (1999).
41. Hillaireau H; Le Doan T; Besnard M; Chacun H; Janin J; Couvreur P, Encapsulation of antiviral nucleotide analogues azidothymidine-triphosphate and cidofovir in poly(iso-butylcyanoacrylate) nanocapsules. *Int J Pharm* 324, 37-42 (2006).
42. Allen C; Maysinger D; Eisenberg A, Nano-engineering block copolymer aggregates for drug delivery. *Colloid Surface B* 16, 3-27 (1999).
43. Jain S; Bates FS, On the origins of morphological complexity in block copolymer surfactants. *Science* 300, 460-464 (2003).
44. Gaucher G; Dufresne MH; Sant VP; Kang N; Maysinger D; Leroux JC, Block copolymer micelles: preparation, characterization and application in drug delivery. *J Control Release* 109, 169-188 (2005).
45. Opsteen JA; Cornelissen JJLM; van Hest JCM, Block copolymer vesicles. *Pure Appl Chem* 76, 1309-1319 (2004).
46. Soo PL; Eisenberg A, Preparation of block copolymer vesicles in solution. *J Polym Sci Pol Phys* 42, 923-938 (2004).
47. Zhang L; Eisenberg A, Multiple morphologies and characteristics of "crew-cut" micelle-like aggregates of polystyrene-b-poly(acrylic acid) diblock copolymers in aqueous solutions. *J Am Chem Soc* 118, 3168-3181 (1996).
48. Lukyanov AN; Torchilin VP, Micelles from lipid derivatives of water-soluble polymers as delivery systems for poorly soluble drugs. *Adv Drug Deliver Rev* 56, 1273-1289 (2004).
49. Zhang X; Jackson JK; Burt HM, Development of amphiphilic diblock copolymers as micellar carriers of taxol. *Int J Pharm* 132, 195-206 (1996).

50. Yokoyama M; Opanasopit P; Okano T; Kawano K; Maitani Y, Polymer design and incorporation methods for polymeric micelle carrier system containing water-insoluble anti-cancer agent camptothecin. *J Drug Target* 12, 373-384 (2004).
51. Lee JC; Bermudez H; Discher BM; Sheehan MA; Won YY; Bates FS; Discher DE, Preparation, stability, and in vitro performance of vesicles made with diblock copolymers. *Biotechnol Bioeng* 73, 135-145 (2001).
52. Sant VP; Smith D; Leroux JC, Novel pH-sensitive supramolecular assemblies for oral delivery of poorly water soluble drugs: preparation and characterization. *J Control Release* 97, 301-312 (2004).
53. Avgoustakis K; Beletsi A; Panagi Z; Klepetsanis P; Livaniou E; Evangelatos G; Ithakissios DS, Effect of copolymer composition on the physicochemical characteristics, in vitro stability, and biodistribution of PLGA-mPEG nanoparticles. *Int J Pharm* 259, 115-127 (2003).
54. Ahmed F; Pakunlu RI; Srinivas G; Brannan A; Bates F; Klein ML; Minko T; Discher DE, Shrinkage of a rapidly growing tumor by drug-loaded polymersomes: pH-triggered release through copolymer degradation. *Mol Pharm*, (2006).
55. Ahmed F; Pakunlu RI; Brannan A; Bates F; Minko T; Discher DE, Biodegradable polymersomes loaded with both paclitaxel and doxorubicin permeate and shrink tumors, inducing apoptosis in proportion to accumulated drug. *J Control Release* 116, 150-158 (2006).
56. Kwon GS, Polymeric micelles for delivery of poorly water-soluble compounds. *Crit Rev Ther Drug* 20, 357-403 (2003).
57. Torchilin VP, Micellar nanocarriers: pharmaceutical perspectives. *Pharm Res* 24, 1-16 (2007).
58. Kataoka K; Harada A; Nagasaki Y, Block copolymer micelles for drug delivery: design, characterization and biological significance. *Adv Drug Deliver Rev* 47, 113-131 (2001).
59. Nishiyama N; Kataoka K, Current state, achievements, and future prospects of polymeric micelles as nanocarriers for drug and gene delivery. *Pharmacol Therapeut* 112, 630-648 (2006).
60. Ould-Ouali L; Arien A; Rosenblatt J; Nathan A; Twaddle P; Matalenas T; Borgia M; Arnold S; Leroy D; Dinguizli M; Rouxhet L; Brewster M; Preat V, Biodegradable self-assembling PEG-copolymer as vehicle for poorly water-soluble drugs. *Pharm Res* 21, 1581-1590 (2004).
61. Lee H; Zeng F; Dunne M; Allen C, Methoxy poly(ethylene glycol)-block-poly(δ-valerolactone) copolymer micelles for formulation of hydrophobic drugs. *Biomacromolecules* 6, 3119-3128 (2005).
62. Ahmed F; Discher DE, Self-porating polymersomes of PEG-PLA and PEG-PCL: hydrolysis-triggered controlled release vesicles. *J Control Release* 96, 37-53 (2004).
63. Aliabadi HM; Brocks DR; Lavasanifar A, Polymeric micelles for the solubilization and delivery of cyclosporine A: pharmacokinetics and biodistribution. *Biomaterials* 26, 7251-7259 (2005).
64. Forrest ML; Won CY; Malick AW; Kwon GS, In vitro release of the mTOR inhibitor rapamycin from poly(ethylene glycol)-*b*-poly(ε-caprolactone) micelles. *J Control Release* 110, 370-377 (2005).
65. Yasugi K; Nagasaki Y; Kato M; Kataoka K, Preparation and characterization of polymer micelles from poly(ethylene glycol)-poly(D,L-lactide) block copolymers as potential drug carrier. *J Control Release* 62, 89-100 (1999).
66. Dong Y; Feng S-S, Methoxy poly(ethylene glycol)-poly(lactide) (MPEG-PLA) nanoparticles for controlled delivery of anticancer drugs. *Biomaterials* 25, 2843-2849 (2004).
67. Burt HM; Zhang X; Toleikis P; Embree L; Hunter WL, Development of copolymers of poly(D,L-lactide) and methoxypolyethylene glycol as micellar carriers of paclitaxel. *Colloid Surface B* 16, 161-171 (1999).
68. Govender T; Riley T; Ehtezazi T; Garnett MC; Stolnik S; Illum L; Davis SS, Defining the drug incorporation properties of PLA-PEG nanoparticles. *Int J Pharm* 199, 95-110 (2000).
69. Shuai X; Ai H; Nasongkla N; Kim S; Gao J, Micellar carriers based on block copolymers of poly(ε-caprolactone) and poly(ethylene glycol) for doxorubicin delivery. *J Control Release* 98, 415-426 (2004).
70. Kim SY; Lee YM, Taxol-loaded block copolymer nanospheres composed of methoxy poly(ethylene glycol) and poly(epsilon-caprolactone) as novel anticancer drug carriers. *Biomaterials* 22, 1697-1704 (2001).
71. Aliabadi HM; Mahmud A; Sharifabadi AD; Lavasanifar A, Micelles of methoxy poly(ethylene oxide)-b-poly(epsilon-caprolactone) as vehicles for the solubilization and controlled delivery of cyclosporine A. *J Control Release* 104, 301-311 (2005).

72. Lim Soo P; Lovric J; Davidson P; Maysinger D; Eisenberg A, Polycaprolactone-block-poly(ethylene oxide) micelles: A nanodelivery system for 17beta-estradiol. *Mol Pharm* 2, 519-527 (2005).
73. Woodle MC; Lasic DD, Sterically stabilized liposomes. *Biochim Biophys Acta* 1113, 171-199 (1992).
74. Storm G; Belliot SO; Daemen T; Lasic DD, Surface modification of nanoparticles to oppose uptake by the mononuclear phagocyte system. *Adv Drug Deliver Rev* 17, 31-48 (1995).
75. Torchilin VP; Trubetskoy VS, Which polymers can make nanoparticulate drug carriers long-circulating? *Adv Drug Deliver Rev* 16, 141-155 (1995).
76. Edlund U; Albertsson AC, Polyesters based on diacid monomers. *Adv Drug Deliver Rev* 55, 585-609 (2003).
77. Panyam J; Labhasetwar V, Biodegradable nanoparticles for drug and gene delivery to cells and tissue. *Adv Drug Deliver Rev* 55, 329-347 (2003).
78. Vert M, Aliphatic polyesters: great degradable polymers that cannot co everything. *Biomacromolecules* 6, 538-546 (2005).
79. Albertsson AC; K.Varma I, Recent developments in ring opening polymerization of lactones for biomedical applications. *Biomacromolecules* 4, 1446-1486 (2003).
80. Kim TY; Kim DW; Chung JY; Shin SG; Kim SC; Heo DS; Kim NK; Bang YJ, Phase I and pharmacokinetic study of Genexol-PM, a cremophor-free, polymeric micelle-formulated paclitaxel, in patients with advanced malignancies. *Clin Cancer Res* 10, 3708-3716 (2004).
81. de Jong SJ; van Dijk-Wolthuis WNE; Kettenes-van den Bosch JJ; Schuyl PWJ; Hennink WE, Monodisperse enantiomeric lactic acid oligomers: Preparation, characterization, and stereocomplex formation. *Macromolecules* 31, 6397-6402 (1998).
82. Vonarbourg A; Passirani C; Saulnier P; Benoit JP, Parameters influencing the stealthiness of colloidal drug delivery systems. *Biomaterials* 27, 4356-4373 (2006).
83. Sun X; Rossin R; Turner JL; Becker ML; Joralemon MJ; Welch MJ; Wooley KL, An assessment of the effects of shell cross-linked nanoparticle size, core composition, and surface PEGylation on in vivo biodistribution. *Biomacromolecules* 6, 2541-2554 (2005).
84. Weissig V; Whiteman KR; Torchilin VP, Accumulation of protein-loaded long-circulating micelles and liposomes in subcutaneous Lewis lung carcinoma in mice. *Pharm Res* 15, 1552-1556 (1998).
85. Hobbs SK; Monsky WL; Yuan F; Roberts WG; Griffith L; Torchilin VP; Jain RK, Regulation of transport pathways in tumor vessels: role of tumor type and microenvironment. *P Natl Acad Sci USA* 95, 4607-4612 (1998).
86. Yuan F; Dellian M; Fukumura D; Leunig M; Berk DA; Torchilin VP; Jain RK, Vascular permeability in a human tumor xenograft: molecular size dependence and cutoff size. *Cancer Res* 55, 3752-3756 (1995).

Pharmaceutical micelles

combining longevity, stability and stimuli sensitivity

2

Myrra G. Carstens,[a,b,#] Cristianne J.F. Rijcken,[a,#]

Cornelus F. van Nostrum,[a] Wim E. Hennink[a]

[a] Department of Pharmaceutics, Utrecht Institute for Pharmaceutical Sciences (UIPS), Faculty of Pharmaceutical Sciences, Utrecht University, Utrecht, The Netherlands

[b] OctoPlus N.V., Leiden, the Netherlands

[#] *Both authors contributed equally to this manuscript*

Submitted for publication

Abstract

During the last decades, polymeric micelles have been extensively studied as potential drug delivery systems, in particular for hydrophobic drugs. To achieve selective and tissue specific delivery of the encapsulated drugs after intravenous injection, these micellar carriers need to have long circulating properties without premature loss of encapsulated agents. After accumulation at the target site via the enhanced permeability and retention effect, controlled release of the drugs is required, preferably as a consequence of time or site specific degradation, or as a result of an external trigger.

In this chapter, the various aspects encountered during the design of long circulating, stable polymeric micelles are presented, including strategies to improve the longevity in the blood, such as surface coating and size adjustments. Further, a variety of methods to stabilise the polymeric micelles by physical or chemical crosslinking are described, as well as the approach to improve drug retention by optimising the compatibility between the drug and the micellar core.

Furthermore, the possibilities and mechanisms to obtain a triggered drug release from the polymeric micelles at the site of action are discussed. Various stimuli like temperature, pH, light and (enzymatic) degradation may increase the polarity of the hydrophobic block, thereby inducing micellar disintegration and drug release. Finally, the possibilities to co-encapsulate imaging agents in the micellar core to follow the fate of micelles *in vivo* is mentioned.

In conclusion, the enormous versatility of polymeric micelles and the many possibilities presented in this chapter indicate that polymeric micelles are very promising systems for site specific delivery of drugs. It is anticipated that several attractive polymeric micelles will be further developed as delivery systems for hydrophobic drugs and will soon be clinically applied in the effective treatment of several diseases.

1. Introduction

Targeted drug delivery is of particular importance for the treatment of life-threatening diseases such as cancer, since the adverse effects of cytostatic drugs can be very detrimental.[1-3] Nowadays, polymer micelles are extensively studied as drug delivery systems to fulfil the requirements for selective and tissue specific drug delivery.[4-18] The most attractive feature is their hydrophobic core with a relatively large capacity to accommodate hydrophobic agents, which are normally difficult to formulate. Polymeric micelles have been used to encapsulate a great variety of highly potent but hydrophobic drugs,[19-29] such as doxorubicin (DOX),[18, 30-35] paclitaxel (PTX),[36-44] amphotericin B [45] and photosensitisers used for the treatment of cancer.[46-48] Some of these micellar formulations have already entered clinical trials and showed promising results with regard to their therapeutic index in cancer patients.[13, 36, 49, 50] A drug delivery system, such as polymeric micelles, needs to fulfil several (pharmaceutical) requirements such as a significant increase in therapeutic effect with respect to the free drug, good biocompatibility and the possibility to scale-up its production. In addition, the ideal micellar system i) has long circulating properties and adequate stability in the blood stream, ii) has a high drug loading capacity, iii) is able to selectively accumulate at the target site and iv) offers the possibility to control the release of drugs at the target site, for example by external stimuli.[4-11, 13, 16, 51] Other desirable properties of polymeric micelles are the ability to be (degraded and) excreted from the body after the drug is released and the possibility to track and trace the micellar structure by co-encapsulating an imaging agent.[52]

The primary focus of this chapter is the description and discussion of longevity and stability of drug-loaded polymeric micelles after intravenous injection, and the possibility to release their payload in a controlled manner upon local and/or external stimuli.

2. Longevity

Drug delivery systems such as polymeric micelles should deliver their payloads selectively at the target sites, and therefore longevity in the blood circulation is a prerequisite. Provided that the encapsulated drug will remain associated with the nanocarrier, a long circulating nanocarrier will longer maintain the blood level of its loaded drug, thereby enhancing the therapeutic effect of the drug as a result of the prolonged interactions in the target organ.[4, 8, 13] In addition, a long circulation time allows the accumulation of polymeric micelles themselves in pathological tissue via the so-called enhanced permeability and retention (EPR) effect. This EPR effect was proposed by Maeda *et al.* in the eighties, and is attributed to the higher permeability of the vasculature in diseased areas due to discontinuous endothelium and impaired lymphatic drainage.[4, 7, 53-55] These two features enable extravasation of colloidal particles through the 'leaky' endothelial layer into the tumour and inflamed areas, and subsequent retention there.

However, the human immune system rapidly recognises and eliminates foreign objects via adsorption of opsonic proteins onto their surface. Therefore, a key issue for prolonged circulation of colloidal drug carriers is to reduce the rate and extent of this opsonisation, and the recognition by cells of the reticulo-endothelial system (RES). It has been shown that so-called steric stabilisation, *i.e.* coating of the particle surface with hydrophilic polymers (*e.g.* poly(ethylene glycol), poloxamer) effectively reduces the interaction with opsonic proteins, and thereby the uptake by the RES cells of the liver, spleen and bone marrow.[56-61] Next to surface characteristics, the biodistribution of polymeric micelles depends on many other factors including predominantly particle size[7, 9, 51, 62] and particle rigidity[62, 63] as will be described in this section.

2.1 Steric stabilisation

2.1.1 Poly(ethylene glycol)

Poly(ethylene glycol) (PEG) (also called poly(ethylene oxide) (PEO)) is the most frequently used hydrophilic segment of amphiphilic micelle-forming copolymers, for example in PEG-*b*-poly(propyleneglycol) (PPO),[5] PEG-*b*-polyesters,[64-68] PEG-*b*-phospholipids (PL),[69, 70] and various PEG-*b*-poly(meth)acrylamide derivatives.[71-74] The ubiquitous use of PEG results from its low toxicity and immunogenicity, and FDA-approval in various pharmaceutical formulations. Moreover, it has unique physicochemical properties, such as excellent water solubility, high flexibility and a large exclusion volume, resulting in good 'stealth' properties.[12, 56, 75-78]

Since the discovery of these 'stealth' properties and the positive effect of a PEG-coating on the circulation kinetics of colloidal drug delivery systems in the early nineties,[79] the responsible mechanisms and factors that influence this effect have been extensively studied but are not fully elucidated yet, as reviewed recently by Vonarbourgh *et al.*[62] In general, the reduction of opsonisation by PEG is ascribed to shielding of surface charge and an increased hydrophilicity of the surface, thereby preventing the two main driving forces for protein adsorption, *i.e.* electrostatic and hydrophobic interactions. In addition, reduction of the Van der Waals interactions, enhanced repulsive forces and the formation of an impermeable polymeric layer on the particle surface, but also the binding of dysopsonins (*i.e.* naturally occurring substances known to inhibit phagocytosis) are considered to attribute to the protective effect.[13, 59, 62, 75, 80] Prolonged circulation times as a result of effective blocking of opsonisation can only be achieved when the protective polymer layer is sufficiently thick. On the other hand, the PEG-chains should retain their flexibility for an optimal protection against recognition by the immune system. Both factors are related to the molecular weight, conformation and the surface density of the PEG-chains (Figure 1A).[7, 59, 62, 80, 81]

The positive effect of a higher PEG molecular weight to reduce protein adsorption, and to prolong circulation times of colloidal particles was amongst others demonstrated for ^{14}C-benzylamine labelled PEG-*b*-P(aspartic acid) (P(Asp)) micelles with covalently bound doxorubicin. An increase in the molecular weight of PEG from 5000 to 12000 Da resulted in a five fold increase of the blood level of the micelles at 4 h post injection (13 vs 68% of the injected dose), and decreased hepatosplenic uptake.[82, 83] The favourable influence of a longer PEG-chain on blood circulation times was also reported for a series of Pluronic® (PEG-PPO-PEG) block copolymers.[84] Although usually PEG with a molecular weight between 1000 and 15000 Da is used to design polymeric micelles for drug delivery, also smaller PEGs may be able to form a protective layer. For instance, coating of lipid nanocapsules using PEG with a molecular weight of 660 Da resulted in steric stabilisation and reduced protein opsonisation, which was ascribed to a high surface chain density.[85] Remarkably, regarding the PEG-chain conformation on the surface, it was shown that the attachment of both ends of the PEG-chain onto the surface resulted in better protection than single chain end attachment, despite a lower chain mobility.[86, 87] It was suggested that single chain end attachment allows easier penetration of the PEG-layer by proteins (Figure 1B), and that it results in a less dense PEG-layer, when compared to double chain end attachment.[86, 87]

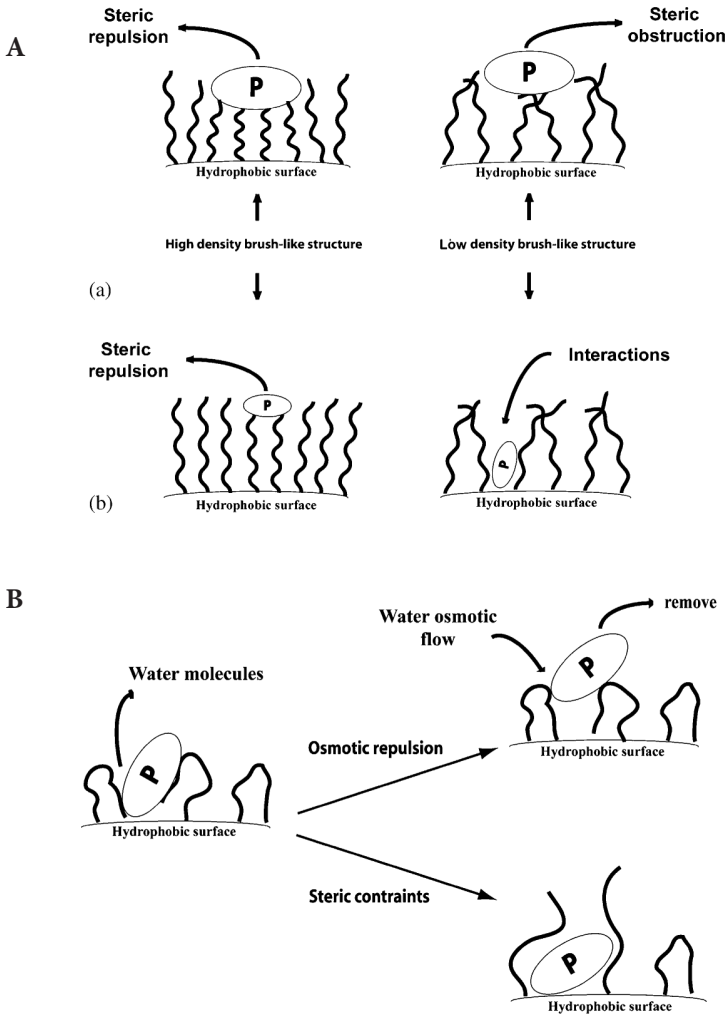

Figure 1 Effect of chain density (A, large (a) and small (b) proteins) and conformation (B) on the repulsion of opsonic proteins (P). This figure was published by Vonarbourg *et al.*[62] Copyright Elsevier (2006).

Although nowadays PEG is considered to be the gold standard for the steric stabilisation of nanoparticles, it is not as inert as generally assumed. Several studies with PEGylated liposomes indicate the binding of blood proteins,[88] and disappearance of the stealth properties at low lipid doses and/or upon repeated administration.[89-92] The repeated administration of drug-loaded polymeric micelles has been reported in several studies. However, these studies focused on the anti-tumour effect of the micellar formulation of a cytostatic drug, rather than the biodistribution of the carrier itself, or the loaded drug.[24, 26, 37, 38, 47, 93]

It is anticipated that the loss of the long circulation behaviour upon repeated administration or at low doses is not limited to PEGylated liposomes, and that micelles with a hydrophilic PEG-shell may be subject to this phenomenon as well. This warrants the search for alternative protective coatings, as will be described in the next section.

2.1.2 Alternative coatings

Based on the above mentioned mechanistical aspects, alternative hydrophilic polymers (Table 1) have to be biocompatible, hydrophilic, water soluble and highly flexible. Polymeric coatings that successfully prolonged the circulation times of liposomal carriers are based on poly(oxazoline),[94] poly(glycerol),[95] poly(N-vinyl pyrrolidone) (PVP),[96, 97] poly(acryl amide) (P(AAm)),[97] poly(vinylalcohol) (PVA),[98] poly(N-(2-hydroxypropyl) methacryl amide) (PHPMA)[99] and poly(amino acids).[100, 101] Several of these polymers have also been used as hydrophilic part of amphiphilic block copolymers in the development of polymeric micelles, which will be described in this section.

2.1.2.1 Poly(N-vinylpyrrolidone)

An attractive PEG-alternative is poly(N-vinyl pyrrolidone) (PVP), which is highly hydrophilic, flexible and biocompatible, similar to PEG. In recent years micelle formation has been reported of several amphiphilic PVP-containing block copolymers, for example copolymers with poly(lactic acid) (PLA),[47, 102, 103] poly(ε-caprolactone) (PCL)[104-106] and poly(N-isopropyl acryl amide) (PNIPAAm).[107] The effective encapsulation of hydrophobic drugs such as indomethacin,[103] chloro aluminum phthalocyanine,[107] and PTX[47] was demonstrated. It has been shown that PVP effectively prolongs the circulation time of liposomes,[96, 97] but these data are not available for micellar systems yet. *In vivo* studies with PVP coated micelles focused on the biodistribution and tumour accumulation of micelles loaded with chloro aluminum phthalocyanine[107] or PTX.[47] For both drugs no improvement in blood circulation times, tumour accumulation nor in therapeutic effect was observed when compared to a similar dose formulated in Cremophor EL®. This may be related to a fast release of the drug from the micelles or disintegration of the micelles themselves. However, the maximum tolerated dose of PTX-loaded PVP-*b*-PLA micelles in mice was more than five times higher than that of Taxol® (PTX formulated in Cremophor EL®). By using a higher dose, a better anti-tumour activity could be achieved.[47]

Table 1 Various hydrophilic polymers used for the steric stabilisation of micelles

Polymer	Abbreviation	Chemical structure	Reference
Poly(ethylene glycol)	PEG	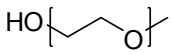	5, 24, 64-74, 82
Poly(N-vinyl pyrrolidone)	PVP	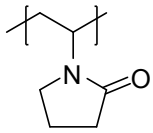	47, 102-107
Poly(vinyl alcohol)	PVA	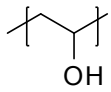	108
Poly(2-ethyl-2-oxazoline)	PEtOz	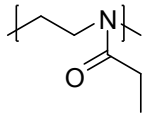	104, 109-112
Poly(N-(2-hydroxypropyl) methacrylamide)	PHPMA	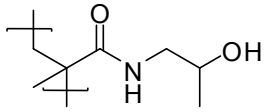	105
Poly(acrylamide)	P(AAm)	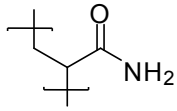	6, 75
Dextran	Dex	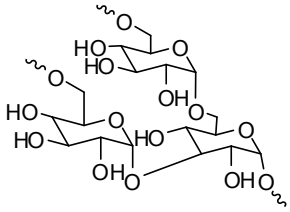	113, 114

2.1.2.2 Polysaccharides

Another class of polymers used as PEG-alternative is the group of polysaccharides, which play a role in the surface characteristics of several cells, *e.g.* red blood cells. These cells effectively evade the immune system, which may be related to the presence of oligosaccharide groups on their surface.[8, 115] It was demonstrated that dextran-*g*-PCL-nanoparticles, and dextran-coated PLA-nanoparticles showed a lower protein adsorption than bare polyester nanoparticles.[113, 114] Whereas these studies did not investigate the circulation kinetics of these dextran-coated nanoparticles, prolonged circulation times were reported for poly(methyl methacylate) (PMMA) nanoparticles coated with dextran or heparin, compared to bare PMMA nanoparticles.[116] Recently micelles of hydroxyethyl starch (HES) grafted with acyl chains were reported, which may also evade the RES.[117] However, the pharmacokinetics of these HESylated nanoparticles *in vivo* have not been investigated yet. It was demonstrated that the conformation of polysaccharides is of high importance when minimising the interactions with plasma proteins.[118] In contrast to PEG (section 2.1.1), a brush-like configuration conferred a more effective protection than the presence of dextran loops at the surface. Although poly- and oligosaccharides present at the nanoparticles' surface may protect against RES-uptake, saccharide-receptors are present in the membranes of several cells.[115] This enables their use in active targeting approaches (section 2.4), and is illustrated by the recognition of galactose presenting nanoparticles by hepatocytes.[119]

2.1.2.3 Other hydrophilic blocks

Several other biocompatible hydrophilic polymers have been used as shell-forming component in polymeric micelles, for example poly(N,N-dimethylamino-2-ethyl methacrylate) (PDMAEMA),[120] poly(ethylene imine) (PEI),[121] poly(acrylic acid) (PAA),[6, 122] and poly(asparagine).[123] However, the longevity of these micelles *in vivo* is questionable, because of the charges present on the micellar shell surface. In addition, P(NIPAAm-*co*-N,N-dimethylacrylamide (DMAAm)) was suggested as the shell-forming block.[124] Since this copolymer displays thermosensitive behaviour, it can be used for the temperature triggered release of encapsulated drugs, as will be discussed further on in this chapter. Micelles composed of poly(2-ethyl-2-oxazoline)-*b*-polyester,[104, 109-112] PHPMA-*b*-PCL,[105] P(AAm)-*b*-palmitate[6, 75] and PVA-*b*-oleylamine[108] may exhibit prolonged circulation times *in vivo*, since these hydrophilic blocks effectively protected liposomes against rapid RES-uptake (*vide supra*), but evidence has not yet been obtained.

2.2 Micellar size

The size of micelles is another predominant parameter determining its fate after i.v. injection. Nanoparticles larger than 200 nm are removed by mechanical filtration by the interendothelial cell-slits in the spleen, and particles with a molecular weight smaller than 50 kDa (a hydrodynamic diameter of 5-10 nm) are subject to renal excretion.[8, 11, 84, 125] The size of polymeric micelles (10-100 nm) prevents elimination via these routes, but it was shown that the extent of RES uptake and tumour penetration were related to their size as well.[7, 9, 11, 51, 84] For example shell crosslinked poly(*tert*-butylacrylate)-*b*-polystyrene (PBA-*b*-PS) micelles with a size of 20 nm had significantly higher blood residence times than their two times bigger counterparts (50% vs 5% of the injected dose at 1 h after injection).[63] The same trend was found with PEG-*b*-poly(cyanoacrylate) micelles of 80 and 170 nm.[126] However, it should be mentioned that in the latter study the longer circulation times of the 80 nm micelles may be related to a higher surface density of PEG as a result of the smaller size. As pointed out in section 2.1.1 a higher PEG-density results in more effective shielding. Furthermore, it was suggested that the particle size itself is of importance, since small particles have a higher curvature, thereby hampering the adsorption of proteins.[62]

In contrast, Weissig *et al*. demonstrated that i.v. injected PEG5000-*b*-distearoyl phosphatidyl ethanolamine (PEG-*b*-DSPE) micelles of 15 nm circulated shorter than 100 nm liposomes in mice with a subcutaneously established Lewis lung carcinoma. Remarkably, the tumour accumulation of the small micelles was much higher than that of the liposomes.[70] This is ascribed to the low cut-off size of the tumour vessel wall, which is different in each tumour type, and determines the ability of nanoparticles to penetrate the tumour tissue.[127, 128] Especially in solid tumours, such as Lewis lung carcinoma, the small size of micelles is indeed an additional advantage over *e.g.* liposomal and other bigger nanoparticulate systems. A different tumour penetration was also reported for DOX-loaded PEG-*b*-poly(aspartate hydrazone adriamycin) micelles of 65 nm and liposomes of 150 nm.[9, 129] The micelles were found inside tumoural spheroids, whereas the 150 nm liposomes were found only in the periphery.[9] Thus, small sized nanoparticles benefit more from the EPR effect as a result of their higher ability to penetrate into tumour tissue.

2.3 Other strategies to improve circulation times

Next to surface characteristics and particle size, the rigidity of the particle influences the circulation kinetics. It has been reported that liposomes with a rigid lipid bilayer exhibit long circulation times despite the absence of a protective PEG-layer.[130, 131] Sun *et al.* compared the biodistribution of poly(*tert*-butylacrylate) (PBA)-*b*-polystyrene (PS) micelles with a high T_g and glassy PS core, to that of PBA-*b*-poly(methyl acrylate) (PMA) micelles with a low T_g and fluid-like PMA core, and demonstrated that a more rigid, glassy micellar core results in a longer blood retention.[63]

In addition to changing particle-related parameters such as surface characteristics, size and rigidity, another strategy to improve the circulation times of nanoparticles may be predosing with empty micelles to saturate the elimination mechanisms. In fact, this was the first strategy to improve the circulation time of liposomes,[132] but so far it has not been investigated for micellar systems.

2.4 Longevity of actively targeted polymeric micelles

Although long circulation times promote the passive targeting of polymeric micelles and thus the delivery of the entrapped drug at its site of action, their delivery may be further improved by active targeting. Specific ligands such as internalising antibodies,[44, 133] sugar moieties,[134] transferrin, RGD and folate[135, 136] have been coupled to the micellar shell to promote cellular recognition and internalisation of the drug carrier.[136-139] The delivery of drugs by actively targeted long circulating micelles is a promising approach to improve its site specific action, but the properties of such carriers are paradoxal. On the one hand, the presence of a targeting ligand, especially antibodies or other proteins, on the micellar surface may enhance its recognition by the immune system and thereby removal from the circulation. On the other hand, the presence of a protective polymer such as PEG may interfere with the binding of the ligand to its target. A strategy to tackle the above mentioned paradox is the use of a 'sheddable' coating, *i.e.* a coating that is removed after arrival at the target site. Recently, a pH-sensitive deshielding of a TAT-peptide coupled to the surface of PEG-*b*-PLA micelles was reported. The cationic TAT ligand was shielded at pH 7.4 by the anionic pH-sensitive poly(methacryloyl sulfadimethoxine) (PSD) block of a PEG-*b*-PSD copolymer. Upon lowering the pH to 6.6, the complex was disrupted and TAT was exposed, resulting in enhanced cellular uptake and localisation at the surface of the nucleus.[140]

3. Micellar stability

Even with a prolonged circulation, selective drug accumulation can only take place if premature leakage of drug molecules from the micelles is prevented or the release of the drug is slow during the first few hours after administration. Essentially the core-forming segment determines the micellar stability, its drug loading capacity and drug release profile, which explains why so many core-forming mainly hydrophobic polymers have been investigated (Table 2).[4, 6, 11, 24, 40, 46, 64, 84, 141, 142]

Table 2 Hydrophobic polymers used as core-forming block in polymeric micelles

Polymer	Abbreviation	Chemical structure	Reference
Poly(lactic acid)	PLA	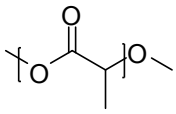	47, 143
Poly(ε-caprolactone)	PCL	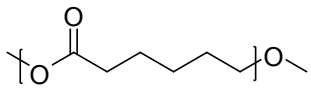	66, 68, 102
Poly(N-isopropyl acrylamide)	PNIPAAm	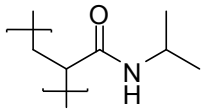	74, 144
Poly(β-benzyl L-aspartate) / poly(γ-benzyl L-glutamate)	PBLA / PBLG	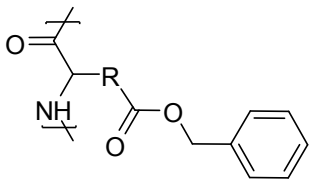 $R = CH_2$ or C_2H_4	134, 145-147
Poly(propylene oxide)	PPO	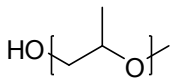	5, 32, 148
Poly(methacrylamide oligolactates)	PHEMA-Lac_n, PHPMA-Lac_n	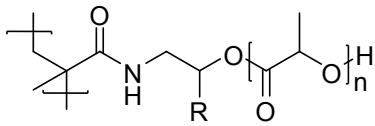 $R = H$ or CH_3; $n = 1\text{-}4$	71, 73

The stability of a polymeric micelle can be considered either thermodynamically or kinetically. Polymeric micelles are thermodynamically stable when the polymer concentration in aqueous solution is above the critical micelle concentration (CMC), also called the critical aggregation concentration (CAC). Below the CMC, amphiphilic block copolymers in water are present as single chains in the bulk and at the air-water interface. At concentrations above the CMC, the Gibbs free energy (ΔG) of the system is minimised by the self-assembly of the amphiphiles, as a result of the hydrophobic interactions between the hydrophobic blocks.[11, 149] Since polymeric micelles are subjected to dilution in the circulation upon intravenous injection, it is important to know their CMC, and to administer a sufficiently high dose.[6, 14]

The kinetic stability of a micellar system is related to the exchange rate of single polymer chains between the micelles and the bulk, and even upon dilution below the CMC, the micellar system may still be kinetically stable.[6, 11, 149, 150] The rate of disassembly is related to the strength of the interactions in the micellar core, which depends on many factors, such as the physical state of the core-forming polymer (crystalline or amorphous), the presence of solvent (*e.g.* methanol or dioxane residues due to the preparation procedure) in the micellar core, the ratio between the hydrophilic and the hydrophobic block of the copolymer, and the encapsulation of hydrophobic compounds.[6, 7, 11, 24] Preferably, polymeric micelles have a (semi-)crystalline or glassy core at body temperature, and are composed of block copolymers with a low CMC.[6, 7, 11, 151]

In addition to micellar stability, several other factors influence the release of the loaded drug, such as the length of the core-forming polymer segment and the amount of loaded drug.[152] Importantly, the compatibility between the core-forming polymer and the drug affects the drug loading and release.[6, 7] By a proper selection of the block copolymer, the compatibility with the drug was optimised for various micellar systems, which is expected to result in an increased drug retention *in vivo*.[4, 37, 43, 47, 83, 153-158]

However, the presence of blood components often leads to premature drug release, either by provoking micelle destabilisation, or by extraction of encapsulated drug from intact micelles.[159-163] Therefore much effort is currently undertaken to improve the thermodynamic and kinetic stability of drug-loaded micelles. Several strategies have been investigated, including modification of the micelle-forming polymers to reduce their CMC (section 3.1), physical and covalent crosslinking (sections 3.2 and 3.3), and improving the drug-polymer compatibility (section 3.4).

3.1 Reducing the CMC

The thermodynamic stability of polymeric micelles can be improved by reducing the CMC of the amphiphilic block copolymers. This is easily achieved by adjusting the sizes of the blocks.[6, 7] Both a larger hydrophobic block and a smaller hydrophilic block result in a higher overall hydrophobicity, thereby reducing the CMC.[11, 47, 68, 84, 164] In addition to size, the nature of the hydrophobic block is an important parameter determining the CMC. Chemical modification of the hydrophobic block, for example by the introduction of aromatic groups, has been demonstrated to effectively reduce the CMC.[68, 146, 147, 165, 166] For instance, changing the amount of benzyl groups in the modified poly(β-benzyl L-aspartate) ($PBLA_{mod}$) block of PEG-*b*-$PBLA_{mod}$ copolymer from 44% to 75% resulted in a ten fold reduction of the CMC.[165] A 60- to 200-fold reduction was obtained by the end group modification of mPEG750-*b*-oligo(ε-caprolactone)s with a benzoyl or a naphthoyl moiety.[68] Similarly, an increase in the level of fatty acids[167] or hydrophobic oligolactates[71] attached to the polymer backbone resulted in a reduced CMC.

3.2 Physical interactions

The introduction of aromatic groups does not only improve the thermodynamic stability by decreasing the CMC, but may also improve the kinetic stability of the micelles by strengthening the interactions inside the micellar core through π-π-stacking. Mahmud *et al*. studied the viscosity of the core of PEG-*b*-PCL micelles and PEG-*b*-poly(α-benzyl-ε-caprolactone) micelles with fluorescence spectroscopy and found, besides a decreased CMC (*vide supra*), an increased rigidity of the micellar core as a result of the presence of aromatic groups.[166] The introduction of crystallinity or stereocomplex formation was shown to enhance the stability of micelles as compared to the amorphous counterparts.[168, 169] An increase in physical interactions was also obtained by hydrogen bonding.[170] A summary of physical interactions that can play a role in the kinetic stability of micelles is illustrated in Figure 2.

In addition to interactions between the core-forming polymers, the incorporation of a hydrophobic drug may also enhance the micellar stability. For example, Yokoyama *et al*. demonstrated that the stability of PEG-*b*-P(Asp) micelles was not only increased by the amount of chemically bound doxorubicin (DOX), but also by the amount of physically entrapped DOX.[24]

Micelle formation may also be driven by the electrostatic interaction forces of oppositely charged block copolymers, to form so-called polyion complex (PIC) or complex coacervate micelles (Figure 3).[171-173]

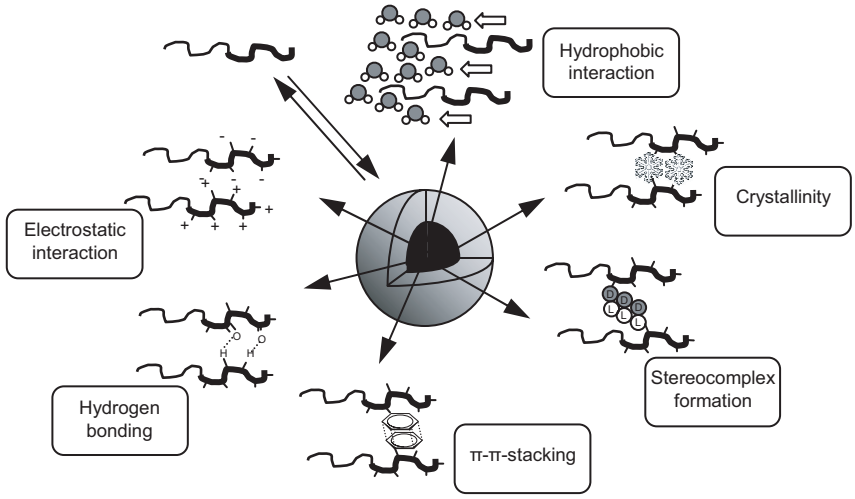

Figure 2 Interactions in the micellar core that enhance the kinetic stability of polymeric micelles .

Examples of polyion-couples are PEG-*b*-poly(L-lysine) (P(Lys)) and PEG-*b*-P(Asp),[171, 174] PEG-*b*-poly(methacrylic acid) (PMA) and poly(N-ethyl-4-vinylpyridinium) (PEVP),[175] or PEG-*b*-poly(2-vinylpyridinium) (P2VP) and poly(styrene sulfonate) (PSS).[176] PIC micelles that comprise thermosensitive shells were described,[173, 177] as well as PIC micelles composed of PEG-*b*-PMA and Ca^{2+} with a crosslinked PMA core.[178] Polymers having negatively charged units, such as PMA and P(Asp) (co)polymers, were used to form micelles with cationic drugs or peptides, and polycations such as PEG-*b*-P(Lys) were used to form micelles with siRNA/DNA.[179] The advantage of PIC micelles is their ease of preparation, *i.e.* simple mixing of aqueous solutions of drug and polymer. However, their application is limited due to the low stability in physiological saline and the drug's prerequisite to be hydrophilic, although this could be overcome by copolymerising phenylalanine in the polymer backbone, thereby enhancing the hydrophobic/aromatic interactions.[157] On the other hand, the saline-induced micelle destabilisation can be utilised to control the release of the loaded drug. This concept was demonstrated for cisplatin-complexed PEG-*b*-poly(glutamic acid), as will be discussed in section 4.7.[26]

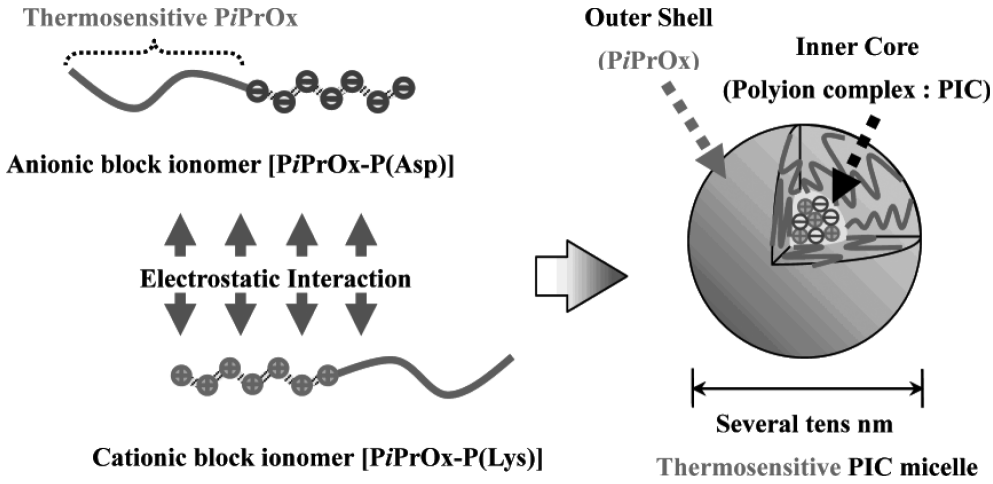

Figure 3 Formation of PIC micelles with a thermosensitive shell composed of poly(2-isopropyl-2-oxazoline) (P*i*PrOx) shell and a core composed of the anionic ionomer poly(aspartic acid) P(Asp) and cationic poly(L-lysine) (P(Lys)). Reprinted with permission from Park *et al.*[177] Copyright (2007), American Chemical Society.

3.3 Covalent crosslinking

In addition to the above mentioned physical means to enhance stability of micelles, chemical crosslinking of either the shell, the interfacial layer, or the core of the micelles has been used to prepare stable particles with a micellar morphology (Figure 4).[172, 179-181] The increased stability of covalently crosslinked micelles versus their non-crosslinked counterparts was proven (among other techniques) by the insensitivity of micelles towards a destabilising agent (*e.g.* sodium dodecyl sulphate (SDS)).[182-184] While the micellar morphology was fixed by the crosslinking procedure, drug release could be controlled by the crosslink density,[185] and stimuli responsiveness was retained (*e.g.* to pH, temperature, salt concentration).[183, 186-188] However, in contrast to physical crosslinking, the covalent crosslinking approach may adversely affect the overall degradability of the micelle and the structural integrity of the encapsulated drug (when the crosslinking procedure is performed in the presence of the drug).

3.3.1 Shell crosslinking

The hydrophilic shell of polymeric micelles has been covalently crosslinked by chemical or photo-induced reactions.[63, 179, 181, 189-194] For example, in polypeptide-*b*-polydiene micelles, covalent bonds were formed between either the amine or carboxylic acid groups in the hydrophilic polypeptide block using glutaraldehyde or a diamine, respectively, as crosslinking agents. Crosslinking by amide bond formation was induced by the addition of an activating agent (*e.g.* a water soluble carbodiimide).[194] The shell consisting of poly(N,N-dimethylaminoethyl methacrylate) (PDMAEMA) was crosslinked by alkylation with a bifunctional alkyl iodide[195] and the shell of poly(4-vinylpyridine) (P4VP)-*b*-polystyrene was crosslinked by addition of a water soluble radical initiator, followed by UV-irradiation at 50 °C.[196] Besides shape fixation, shell crosslinking provides a tool to control the permeability of the micellar shell for drug molecules.[185] The surface stabilisation can also be applied in stimuli sensitive micelles to further control the drug release[187, 191, 195] (see section 4). A major disadvantage of crosslinking the shell segments is that all reactions have to be performed at high polymer dilution, in order to selectively crosslink the micellar shell while avoiding the formation of intermicellar crosslinking.[181] Furthermore, the shell fixation may hamper the chain flexibility of the shell-forming polymers, thereby impairing the steric stabilisation.

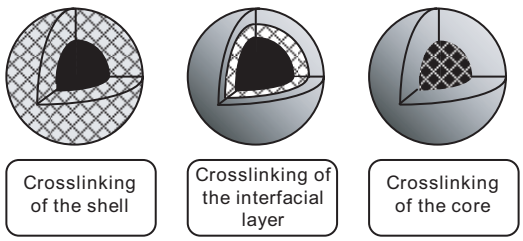

Figure 4 Covalent crosslinking of the micellar shell, the interfacial layer or the micellar core.

3.3.2 Interfacial crosslinking

Alternatively, the interfacial layer between the micellar core and shell can be crosslinked by the introduction of a crosslinkable spacer between the hydrophobic and the hydrophilic block.[192, 197, 198] This approach will leave both the micellar core and shell, and consequently the loaded drug and steric stabilisation, respectively, unaffected, while it may provide a way to control drug release. Examples of spacers used are poly(glycerol monomethacrylate) (PGMA) and poly(2-hydroxyethyl methacrylate), which can be crosslinked by the addition of divinyl sulfone,[188, 197] or by modifying PGMA with cinnamoyl chloride followed by UV-irradiation of the aqueous micellar solution.[192]

3.3.3 Core crosslinking

Core crosslinked (CCL) micelles can be prepared using functional groups present at the chain end or along the core-forming block. Hydroxyl moieties present in the hydrophobic block are often functionalised with (meth)acrylate groups.[39, 184, 199] After micelle formation, the hydrophobic blocks are crosslinked by thermal[184, 199] or photo-induced polymerisation.[182, 200] Other strategies to obtain CCL micelles from (meth)acrylate functional block copolymers are Michael addition with multifunctional thiol compounds,[201] or formation of an interpenetrating network using a hydrophobic polyfunctional acrylate.[202] Another example are PIC micelles composed of anionic PEG-*b*-P(Asp) and the cationic protein trypsin, which were crosslinked by Schiff-base formation of gluteraldehyde with the protein. An interpenetrating network of crosslinked trypsin was formed in the core which was stable even at high ionic strength (0.6 M NaCl), indicating that, next to protein-protein crosslinks, also covalent bonds between the primary amino groups at the ω-end of the P(Asp) segments and aldehyde groups in glutaraldehyde were formed. Besides, the protein retained its enzymatic activity.[203] PIC micelles composed of PEG-*b*-P(methacrylic acid) (PMA)/Ca^{2+} were crosslinked by reaction of the carboxylic acid groups in PMA with 1,2-diethylene diamine in presence of a carbodiimide.[178, 186]

3.3.4 Cleavable crosslinks

A drawback of crosslinked micelles may be that covalent linkages in the shell, the core or the interfacial layer can negatively affect the biodegradability of the polymeric assemblies. The use of reversible or degradable crosslinks may (partly) circumvent this. Reversibly crosslinked micelles were formed by the introduction of thiol groups

on the lysine units in PIC micelles, followed by their oxidation to disulfide bonds.[204] In addition, disulfide bonds were used to stabilise the interfacial layer of PEG-*b*-(poly(N,N-dimethylacrylamide)-*stat*-(N-acryloxysuccinimide))-*b*-PNIPAAm micelles The resulting particles were susceptible to reduction by agents such as gluthatione or dithiothreitol. Therefore, the reducing environment in the cytoplasm of cells is also a potential trigger for disintegration and drug release from these particles.[191]

Recently, hydrolysable CCL micelles were developed via introduction of methacrylate moieties at degradable oligolactate grafts of a core-forming polymer backbone. These crosslinked micelles showed superior physical stability as compared to their non-crosslinked counterparts and the degradation time could be controlled by their crosslink density.[183]

3.3.5 Effects of crosslinking on drug loading and release

The above described crosslinking strategies of the shell, interfacial layer or micellar core not only fixed the micellar morphology, but also retarded the release of the loaded drug.[185, 191, 205, 206] In addition, crosslinking can influence the drug loading capacity. An eight fold higher amount of triclosan was encapsulated in PEG-lipid micelles after polymerisation of the chain ends, which was attributed to a higher stability of CCL micelles as compared to unmodified ones.[207] Obviously, one should always be aware that the structural integrity of the loaded drug molecules should be preserved upon the chemical crosslinking of the core. To avoid unwanted modification of entrapped drug molecules, the micelles can be crosslinked first and subsequently loaded with drugs. For example, mPEG-*b*-PLA micelles were crosslinked by thermally initiated polymerisation of methacrylate groups in the core. Next, via a microemulsion method and subsequent evaporation of the organic solvent, PTX was loaded into these CCL micelles. A loading capacity of 3 to 6 weight percent (% (w/w)) was achieved, equal to non-crosslinked micelles.[182] Crosslinked PEG-*b*-PMA micelles were loaded with cisplatin by incubation with an aqueous drug solution for 48 h. After removal of the unbound cisplatin by ultracentrifugation, a drug loading of 22% (w/w) was obtained.[186]

3.4 Micellar core – drug compatibility

Even at high micellar stability, the retention of the loaded drug cannot be guaranteed. Upon contact with blood, extraction and redistribution of the drug between the micellar core and blood components might take place.[160, 161] The retention and release of a drug is related to the amount of drug loaded, the size of the core,[152] the compatibility between the micellar core and the drug, and the effect of external stimuli (*vide infra*). The compatibility between the polymer and the drug can be quantified and predicted by the Flory-Huggings interaction parameter:

$$\chi_{sp} = (\delta_s - \delta_p)^2 \frac{V_s}{RT}$$

where χ_{sp} is the interaction parameter between the drug (solubilisate, s) and the core-forming polymer (p), δ_s is the Scatchard -Hildebrand solubility parameter of the drug and δ_p that of the polymer, and V_s is the molar volume of the drug.[4, 6] To obtain an optimal compatibility between the drug and the core-forming polymer, χ_{sp} should be as low as possible. This means that there is not a universal micellar system that can be used for all drugs, but an optimal combination has to be found for each drug to improve its retention.[4, 6, 7, 24, 37, 43, 47, 82, 83, 146, 147, 153-158, 208] This approach was proven for example by Liu *et al*. who compared the interaction parameters of a series of core-forming polymers with a drug (ellipticine). It was demonstrated that in this way a good polymer selection could be made, resulting in high drug loading capacities and slow release.[155] Similarly, the core-forming polymer can be modified to get a better compatibility with the drug. For example, the loading efficiency in PEG-*b*-poly(β-benzyl L-aspartate) (PBLA) micelles and the *in vivo* therapeutic effect of the aromatic drug camptothecin was improved by increasing the number of aromatic groups on the polymer backbone, which was ascribed to aromatic interactions between the benzyl groups and the drug.[146, 147] A similar approach was used to design a micellar system for DOX[209] and PTX.[37] Chemical modification of the drug can be an alternative way to increase the compatibility with the micellar core. Forrest *et al*. synthesised prodrugs of the anti-cancer drug geldanamycin and indeed demonstrated that a higher encapsulation efficiency could be obtained when the chemical structure of the prodrug was 'matched' with the core-forming segment.[158]

The drug is stably retained in the micellar core when the drug is chemically attached to the micelle-forming polymer. This approach was applied by Yokoyama *et al.,* who covalently bound DOX to the P(Asp) block of PEG-*b*-P(Asp) copolymers. The resulting PEG-*b*-P(Asp)-DOX conjugate formed micelles.[24, 83, 208] In addition to the bound DOX, large amounts of free DOX could be loaded through π–π stacking in these micelles, and the encapsulation efficiency depended on the amount of conju-

gated drug.[24] *In vivo* studies demonstrated that these DOX-loaded micelles had a considerably higher anti-tumour activity compared to free DOX in C26 bearing mice after i.v. injection.[34] A phase I clinical trial was conducted with this formulation (NK911, Figure 5) in 23 patients with metastatic or recurrent solid tumours refractory to conventional chemotherapy. It was found that the toxicity profile of NK911 was similar to free DOX. However, NK911 exhibited longer half-lives, a lower clearance, and a larger area under the curve (AUC), suggesting prolonged circulation times compared to free DOX. A phase II clinical trial is currently ongoing.[50]

In summary, the ideal micellar system should circulate long and reach the target site intact, with the drug still loaded in the micellar core. However, this does not implicate that completely inert, non-degrading and non-releasing micelles are desired, since this may cause long-term accumulation in the body, especially after repeated administration. Moreover, the drug should eventually be released to interact with the therapeutic target. Therefore, ideally the encapsulated agents should be selectively released at the target site, and the micelles should dissociate into single block copolymer chains or even chain fragments, with a molecular weight less than 50 kDa to enable clearance via the renal pathway.[17, 210] At the target site the drug can be released by degradation of the carrier system, but preferably via a more controlled mechanism, *i.e.* being the result of specific stimuli as will be discussed in the next sections of this chapter.

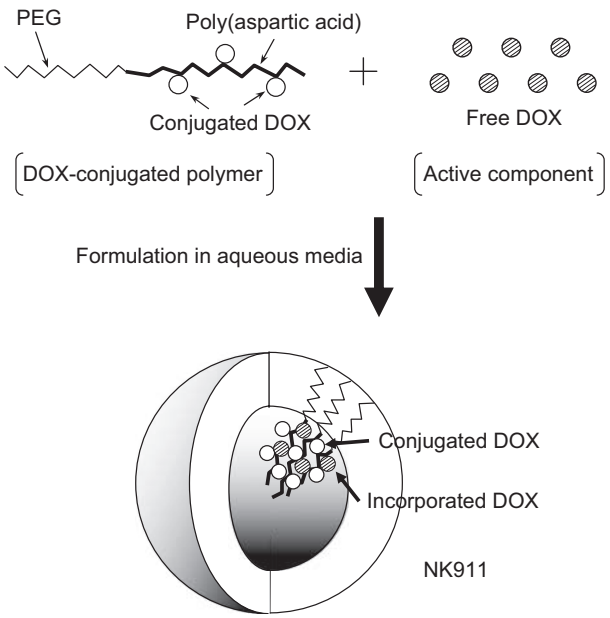

Figure 5 PEG-*b*-poly(aspartic acid) micelles with covalently bound and physically entrapped doxorubicin, also known as NK911. Reprinted with permission from Macmillan Publishers Ltd: British Journal of Cancer,[50] copyright (2004).

4. Stimuli sensitivity

As pointed out in the previous sections, in an ideal micellar system, the drug is stably retained in the micelle during circulation, and after accumulation in the targeted tissue, only here the drug is released as a result of environmental triggers. A release mechanism utilising the locally different conditions in pathological tissue compared to healthy tissue is attractive to achieve a high concentration of the drug in the target tissue. Besides, the loaded drug can be released by an external trigger including temperature, light, or ultrasound. Micelles which are destabilised as a result of either physiological or external triggers are referred to as 'stimuli sensitive micelles'. After micelle formation, stimuli sensitive micelles disassemble only after certain triggers, for example as a result of changed polymers properties (*e.g.* polarity). Moreover, the originally stably encapsulated drug is expected to be released concomitantly with the disintegration of the micelles. A variety of triggers have been investigated to destabilise drug-loaded polymeric micelles, including temperature (section 4.1), pH (section 4.2), hydrolysis (section 4.3), enzymatic reactions (section 4.4), redox processes (section 4.5), light (section 4.6), other (*e.g.* ultrasound in section 4.7), as well as combinations hereof (section 4.8) (Figure 6). These approaches have been described for micelle-forming amphiphilic block copolymers,[172] and for peptide amphiphiles.[211] A sophisticated stimuli sensitive release system is obtained by co-loading of an imaging agent, which enables tracking of the micelles *in vivo* as will be discussed in section 4.9.

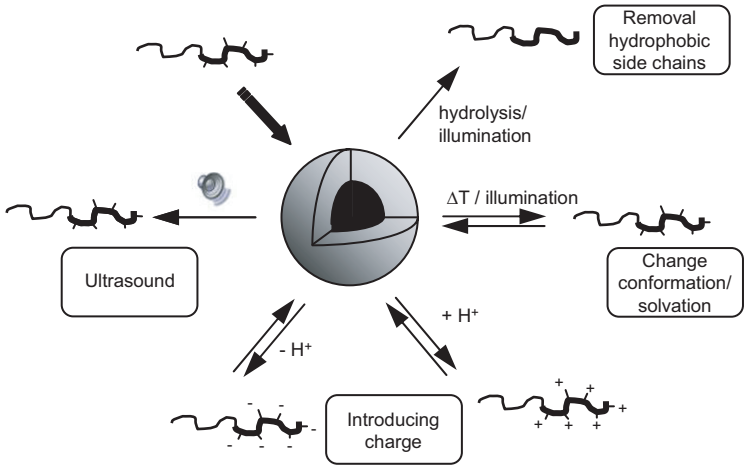

Figure 6 Examples of stimuli sensitive polymeric micelle destabilisation. Adapted from a figure published by Rijcken *et al.*[212] Copyright Elsevier Ltd. (2007).

4.1 Thermosensitive polymeric micelles

An aqueous solution of a thermosensitive polymer is characterised by a so-called cloud point (CP). Below the CP, the polymer is hydrated and intra- and inter-polymer interactions are prevented, thus rendering the polymer water soluble. Once the polymer solution is heated above the CP, the hydrogen bonds between the water molecules and the polymer chain are disrupted and water is expelled from the polymer chains. Interactions between the hydrophobic moieties of the polymer chain can now take place, which is associated with the collapse of the polymer, and finally results in phase separation (aggregation/precipitation of the polymer). Various thermosensitive block polymers are presently under investigation for the development of polymeric micelles for pharmaceutical applications.[84, 213-215] Poly(N-isopropyl acrylamide) (PNIPAAm) is the most extensively studied thermosensitive polymer with a CP of 32 °C.[216-218] The CP of a thermosensitive polymer can be tailored by copolymerisation with hydrophobic or hydrophilic comonomers, resulting in a decreased or increased CP, respectively.[71, 144, 219-222] Via this strategy, polymers with a CP around body temperature were designed to create polymeric micelles, which are suitable for temperature-induced micelle dissociation. Thermosensitive copolymers can be used either as a hydrophilic, shell-forming segment (for example P(NIPAAm-*co*-DMAAm) and poly(2-isopropyl-2-oxazoline))[124, 177] or as a hydrophobic, core-forming segment of block copolymers (for example PNIPAAm and PHPMA-Lac_n)[73, 74] (Figure 7).

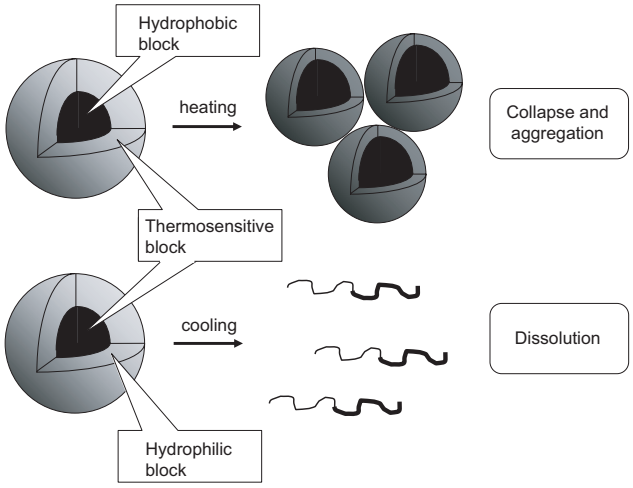

Figure 7 Drug-loaded block copolymer micelles comprising a thermosensitive block either as the hydrophilic shell below the CP (top) or as the hydrophobic core above the CP (bottom). Heating or cooling will accomplish distortion of the micellar structures with concomitant release of the loaded drug. This figure was published by Rijcken *et al.*[212] Copyright Elsevier Ltd. (2007).

The advantage of thermosensitive core-forming segments is that micelles are simply prepared by heating an aqueous polymer solution (above the CMC) till above the CP of the thermosensitive part; *i.e.* no organic solvents are required. The heating rate is a critical factor for the ultimate size of the formed nanoparticles; fast heating resulted in smaller micelles than when slow heating was applied.[72, 223, 224] A major drawback for the first generation of thermosensitive polymeric micelles based on non-degradable polymers (*e.g.* PNIPAAm) is that thermal treatment (hyperthermia or hypothermia) is required for their destabilisation and concurrent drug release, which is not always feasible in clinical practice. Therefore, thermosensitivity is frequently combined with an other stimuli responsive mechanism, such as pH or light sensitivity, and degradability (section 4.8).

4.2. pH-sensitive polymeric micelles

The mildly acidic pH encountered in tumours and inflammatory tissues (pH ~ 6.8) as well as in the endosomal and lysosomal compartments of cells (pH ~ 5-6) provides a potential trigger for the destabilisation of a pH sensitive carrier.[225, 226] The major mechanism to induce pH sensitivity is changing the charges in (polyion complex) micelles; pH dependent cleavage and destabilisation will be discussed in section 4.3. Typically, block copolymeric micelles that contain basic groups such as L-histidine (His),[138, 227] pyridine[228] and tertiary amine groups[229, 230] are pH-sensitive. The block copolymers assemble into micelles at a pH one unit above the pKa of the amines, where the pH-sensitive block is essentially uncharged and hydrophobic, thereby forming the core of the micelles. Decreasing the pH below the pKa results in protonation of the polymer, which in turn leads via an increased hydrophilicity and electrostatic repulsions to destabilisation of the micelles. The transition pH can be controlled by mixing different block copolymers. For instance, a mixture of PEG-*b*-P(His) and PEG-*b*-PLA formed stable micelles at pH 7.4 and dissociated at pH 6.0 to 7.2, depending on the ratio of the two block copolymers in the micelles.[138, 227] Another example of pH-sensitive micelles are the sulphonamide-containing nanoparticles which collapsed upon protonation of the sulphonamide units (pKa = 6.1), thereby releasing the loaded DOX at pH<7.[231, 232]

Block copolymers that are in their protonated (= water soluble) form at pH < pKa can be easily loaded with active compounds. Upon increasing the pH of an aqueous solution of poly(2-(methacryloyloxy)ethyl phosphorylcholine)-*b*-poly(2-(diisopropylamino)ethyl methacrylate) (PMPC-*b*-PDPA) block copolymers from pH 3 to 7, the PDPA block (pKa 6-7) became deprotonated (*i.e.* hydrophobic) and self-assembly took place. In presence of a model compound (dipyridamole, only soluble below pH 5.8), this neutralisation resulted in the formation of dipyridamole-loaded

micelles.[233] Furthermore, tamoxifen and PTX could be stably encapsulated in these PMPC-*b*-PDPA micelles at pH 7.4. Lowering of the pH below the pKa of the PDPA block resulted in a fast release of the drugs. This pH-triggered release might be advantageous when loaded micelles permeate into relatively acidic tumour tissue, or when they are taken up via the endocytotic pathway.[234]

4.3 Chemical hydrolysis to induce micellar disintegration

Micellar disintegration and concomitant drug release can be established by chemical hydrolysis, which includes degradation of the polymer backbone (section 4.3.1), cleavage of side groups (section 4.3.2), and hydrolysis of covalent bonds between drug and polymer in micelle-forming polymer-drug conjugates (section 4.3.3).

4.3.1 Chemical hydrolysis of the polymer backbone

Backbone hydrolysis of the hydrophobic block of an amphiphilic block copolymer is a frequently applied method to destabilise micelles used for drug delivery[235] (Table 3). For example, the chemical degradation of the polyester block in PEG-*b*-poly(DL-lactic-*co*-glycolic acid) (PLGA),[236] PCL-*b*-PEG-*b*-PCL[237] and mPEG-*b*-oligo(ε-caprolactone)s[238] was associated with changes in particle size, indicating micelle destabilisation. Furthermore, transition of PEG-*b*-PCL worm micelles into spherical micelles was observed upon hydrolysis of the ester bonds in the PCL block.[239] The ester hydrolysis is pH dependent and the ester bonds in oligolactates[240] and oligo(ε-caprolactone)s[238] displayed an optimal stability at pH ~ 4-5. However, even at physiological pH and temperature, chemical hydrolysis of ε-caprolactone-based polymers and oligomers is slow and will hardly play a role *in vivo*. It is anticipated that in the body these polymers will be mainly cleaved by enzymatic degradation (*vide infra*).[238] Moreover, when the drug should be released in the mildly acidic tumour tissue and endosomal compartments of cells and, consequently, degradation of micelles is desired at relatively low pH, other type of polymers such as poly(ortho esters) (POE) have a better degradation profile[241] (Table 3). Indeed, PEG-*b*-POE micelles displayed a higher stability at pH 7.5 than at pH 5.5.[242] The effect of hydrolytic degradation on micelle stability has been extensively studied, and although it is generally believed that micelle destabilisation leads to the release of the loaded drugs, experimental data on the relation between degradation and drug release are scarce. One of the few examples was described by Geng *et al.,* who correlated the degradation-induced transition of PEG-*b*-PCL worm-to-sphere micelles with the release of the loaded PTX. PTX release from these micelles was caused by a reduction of the drug-carrying capacity, since spherical micelles have a smaller volume-to-surface ratio than worm micelles.[243]

Table 3 Biodegradable moieties embedded in polymeric micelles

Degradable group	Structure	Degradation products	Reference
Ester	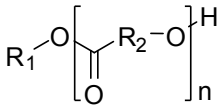	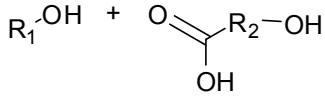	71, 238
Orthoester	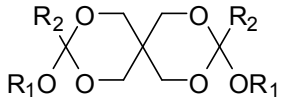	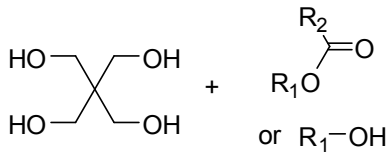	241
Acetal	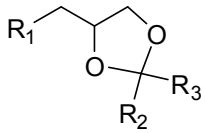	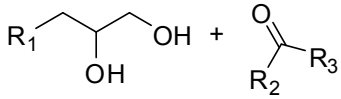	244
Hydrazone	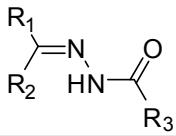	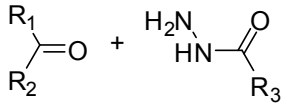	31, 129, 245

4.3.2 Cleavable side chains

When hydrophobic side chains in the core-forming block, which are contributing to the stability of the micelles, are removed by hydrolysis, the hydrophilicity of the micellar core will increase and micelles undergo destabilisation. A good example is PEG-*b*-P(Asp) that is stabilised by cyclic benzylidene acetals in the hydrophobic core via π-π-stacking. The micelles were stable at physiological pH, whereas hydrolysis of the acetal bonds at pH 5 generated the more polar diols (Table 3). The overall hydrophilicity of the polymer increased, resulting in micellar dissolution and release of an encapsulated hydrophobic dye.[244] A similar mechanism was applied for linear-dendritic block copolymers. *In vitro*, these polymeric micelles displayed an accelerated release of entrapped DOX at acidic pH as a result of micelle disruption.[30, 246] Thermosensitive (block co) polymers containing biodegradable side chains will be discussed in section 4.8.2.

4.3.3 Cleavage of polymer-drug conjugates

In the case of polymer-drug conjugates, drug release from polymeric micelles can be established by the acid-catalysed cleavage of a labile linkage by which the drugs are attached to the polymer. For example, the acid labile hydrazone linkage between DOX and PEG-*b*-P(Asp) resulted in an accelerated release of DOX at acidic pH *in vitro* (Table 3). In comparison to free DOX, these pH sensitive DOX-hydrazone-micelles had a 15-fold greater AUC_{blood}, a higher anti-tumour activity and a reduced toxicity *in vivo*. Moreover, micelles in which DOX was bound via a non-degradable amide bond did not exert any anti-tumour activity.[31, 129, 245] In a recent study, a triblock copolymer ((PLA-*co*-glycolic acid-*alt*-glutamic acid)-*b*-PEG-*b*-(PLA-*co*-glycolic acid-*alt*-glutamic acid)) was used to couple PTX via an acid labile ester linkage and the resulting micelles displayed a three fold higher release of PTX at pH 4.2 than at 7.4.[247]

4.4 Enzymatically triggered destabilisation of polymeric micelles

The abundant presence of certain enzymes in pathological tissues has been applied as an environmental trigger to destabilise (drug-loaded) polymeric micelles. Similar to hydrolytic degradation, enzymes may cleave either the backbone of the hydrophobic block, their side chains, or the bonds between the polymer and drug. It was demonstrated that polyesters are not only degraded hydrolytically, but they are also susceptible to enzymatic degradation, for example by lipases. This lipase-catalysed degradation was shown for PEG-*b*-poly(3-hydroxybutyrate) (PHB)-*b*-PEG micelles,[248] PEG-*b*-PCL nanoparticles,[249] accompanied by the release of encapsulated pyrene, and for PEG-*b*-oligo(ε-caprolactone) micelles.[238] Furthermore, the peptide bonds in poly(amino acid)s, used as hydrophobic blocks, can be cleaved by proteases, as demonstrated for example for poly(γ-glutamic acid)-*g*-L-phenylalanine (PGA-*g*-L-PEA) micelles.[250]

4.5 Oxidation and reduction sensitive polymeric micelles

The reduction of disulphide bonds in polymeric assemblies by intracellular glutathione can be used for micellar decrosslinking (see section 3.3) or for full destabilisation.[191, 204, 251, 252] Furthermore, the reversible redox reactions of organo-metal compounds, *e.g.* viologen and ferrocene, are an attractive trigger to alter the charge density and thus to change the solubility of viologen or ferrocene containing polymers.[253] Oxidation of redox-active micelles, containing a hydrophobic ferrocenylalkyl moiety in the block copolymer, was demonstrated to shift the

hydrophobic/hydrophilic balance, and the micelles disintegrated into water soluble unimers. The release of a model hydrophobic drug (perylene) from these micelles was precisely controlled by a selective electrochemical oxidation of the ferrocenylalkyl moiety and zero-order kinetics could be obtained.[254] Selective drug release at pathogenic sites may be accomplished via externally applied electric current or by taking advantage of the accumulation of activated macrophages in inflamed tissues and certain tumours. These macrophages release oxygen-reactive species, which may also trigger the transformation of redox sensitive micelles. However, so far, these redox sensitive polymeric micelles have not been investigated *in vivo*.

4.6 Light-induced micellar deformation

Light-responsive polymeric micelles ideally release their entrapped guest molecules only upon either ultraviolet (UV), visible (VIS) or (near-) infrared ((N)IR) light exposure. The use of NIR is of particular interest for biomedical applications because of its deep tissue penetration and minimal detrimental effects on healthy cells.

4.6.1 Irreversible reactions upon illumination (photolysis)

Light-induced micellar disruption can be applied using UV- or IR-illumination to cleave photolabile hydrophobic side chains. An amphiphilic block copolymer composed of PEG and a polymethacrylate bearing photolabile pyrene methyl esters in the side chain (PPy) as the hydrophobic core-forming domain was synthesised.[205, 255] Upon illumination, these ester side groups were split off, thereby transforming the hydrophobic micellar block into a hydrophilic poly(methacrylic acid) (PMA) block, which caused dissociation of the micelles. A controlled release of encapsulated Nile red could be accomplished, since the dissociation kinetics were controlled by the intensity of the light.[255] Moreover, upon core crosslinking of these micelles, the photolysis-induced micellar destabilisation was prevented by the crosslinks. Nevertheless, the overall hydrophilicity of the polymer increased upon illumination, and the micelle swelled, thereby still releasing the loaded hydrophobic guests, although at a lower rate.[205]

In addition, irreversible rearrangements upon illumination were used to eradicate the hydrophobic micellar interaction forces. For example, hydrophobic 2-diazo-1,2-naphthoquinone derivatives were attached to alkyl-PEG-chains, which self-assembled into micelles. The so-called Wolff rearrangement (Figure 8) that takes place upon illumination of these chromophores drastically changed their polarity, destabilised the micelles, and released the encapsulated Nile red.[256]

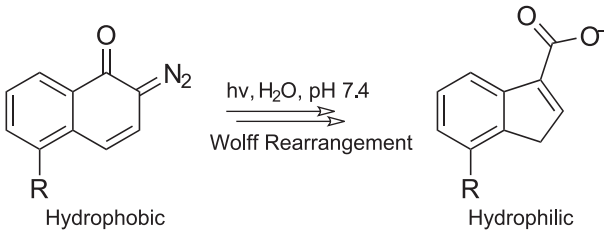

Figure 8 Solubility change of 2-diazo-1,2-naphthoquinone derivatives after Wolff rearrangement to 3-indenecarboxylate in buffer.

4.6.2 Light-induced reversible changes

Besides irreversible micellar disintegration, environmental light can induce reversible and non-destructive destabilisation. Several photoactive groups that undergo reversible structural changes upon illumination have been attached to amphiphilic block copolymers, thereby mainly shifting the hydrophobic/hydrophilic balance. Chemical entities that display photochemically induced transitions include azobenzenes (change in dipole moment),[257] cinnamoyl (isomerisation into a more hydrophilic residue or photodimerisation),[193] spyrobenzopyran (formation of zwitterionic species)[258] and triphenylmethane leucohydroxide (generation of charges),[259] as recently reviewed in detail.[212]

For instance, exposure of azobenzenes-containing methacrylate-*b*-(*tert*-butyl acrylate-*co*-acrylic acid) polymers to UV-light results in a *trans*-to-*cis* isomerisation and a more hydrophilic polymer is generated, causing dissolution of the assemblies.[257] Another example is the reversible *trans*-to-*cis* photoisomerisation upon UV-irradiation of cinnamoyl-containing PEG-*b*-poly(methacrylate) polymers, which creates compounds with an increased hydrophilicity or leads to reversible photodimerisation (Figure 9).[192, 193] Some of these photosensitive moieties were also embedded in thermosensitive block copolymers as will be discussed in section 4.8.3.

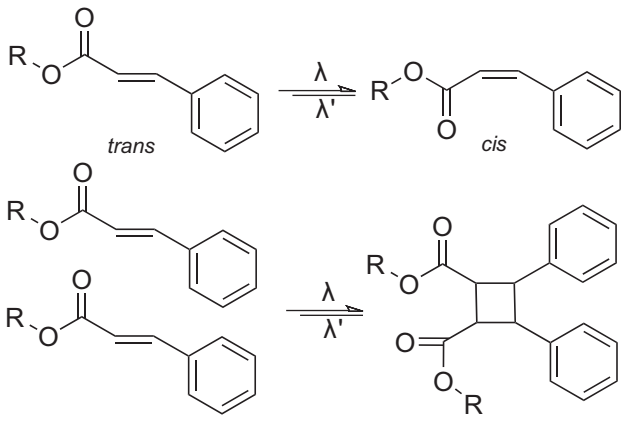

Figure 9 Reversible *trans*-to-*cis* isomerisation (top) and photodimerisation (bottom) of the cinnamoyl photoreactive group upon irradiation with UV-light.

4.7 Other physical triggers to destabilise polymeric micelles

Besides the above mentioned temperature, pH, hydrolysis, and light triggers, ultrasound and ion exchange have also been explored to induce drug-release. The use of ultrasound as an external trigger to release drugs from Pluronic® micellar systems *in vitro* and *in vivo* was extensively studied by Rapoport *et al.*[260-262] The cellular cytotoxicity of DOX-loaded micelles in combination with ultrasound was 66%, without ultrasound 53%, while free DOX without applying ultrasound resulted only in 15% in cell death.[261] *In vivo*, an increased uptake of both free drug (in PBS) and DOX-loaded Pluronic® micelles was observed for sonicated tumour cells *in vivo.*[260, 262] The mechanisms of the ultrasound effect might be: i) enhanced permeability of blood vessels resulting in extravasation of the carriers; ii) dissociation of micelles into unimers with concomitant drug release, iii) accelerated diffusion in the interstitium and tumour, and iv) enhanced membrane permeability leading to increased cellular uptake of the drug.[260-262]

Ion sensitive polymer-metal micelles were formed by complexation of cisplatin to the carboxylate groups of PEG-*b*-poly(glutamic acid) block copolymer. In 0.15 M NaCl, ion exchange reactions occurred, thereby slowly releasing cisplatin from the micelles, accompanied by the dissociation of the micellar structure (Figure 10). Intravenous injection of these micelles led to a significantly increased plasma level and tumour accumulation of cisplatin as compared to free drug.[26] Cellular uptake and release of cisplatin was recently also demonstrated with cisplatin-loaded crosslinked PIC micelles.[186]

Magnetic micelles (220 ~ 430 nm) were obtained in water by coating iron-oxide nanoparticles with peptide-based polymers (polybutadiene-*b*-poly(glutamic acid)). It is anticipated that the micellar shape is manipulable in a magnetic field but experimental data are not available yet. These superparamagnetic self-assembled hybrids might be of interest for future drug delivery systems but also as contrast agents in MRI[263, 264] as will be described in section 4.9.

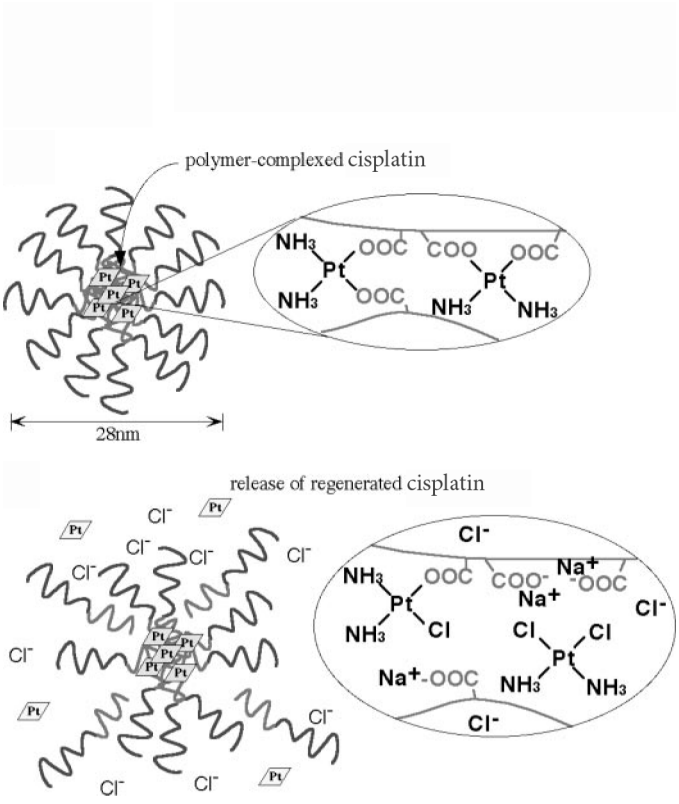

Figure 10 Cisplatin-complexation with carboxylate containing polymers (PEG-*b*-poly(glutamic acid)) results in stabilised micelles (above), while ligand exchange reactions in saline lead to gradual release of cisplatin (below). Reproduced with permission from Nishiyama *et al.*[26] Copyright 2003, American Association for Cancer Research.

4.8 Polymeric micelles sensitive to a combination of triggers

4.8.1 pH and temperature sensitivity

Random copolymers based on NIPAAm, N,N-dimethylacrylamide and 10-undecenoic acid displayed a CP that was not only dependent on the copolymer composition but also on the pH. The polymer was designed in such a way that the polymer was below its CP and thus highly hydrated at pH 7.4 and 20 °C, with the hydrophobic undecenoic acids side chains clustering together to form core-shell morphologies of approximately 200 nm. The hydrophobic drug DOX could be loaded in the undecenoic acid core by a dialysis method. Lowering the pH to 6.6 caused protonation of the undecenoic carboxylate group and decreased the CP below 20 °C. Thereby the micelles disintegrated, which was accompanied by the release of the encapsulated DOX.[137, 265] A similar effect was seen at pH 7.4, when increasing the temperature to above the CP of 40 °C.[265] Furthermore, a broad range of other block copolymeric assemblies that use this pH dependency to control the temperature sensitivity have been reported in literature.[266-270]

4.8.2 Biodegradable temperature sensitive polymers

Dual sensitive micellar systems that are based on biodegradable thermosensitive (block co) polymers have been described.[71, 73, 144, 271-273] The polymers self-assemble into micelles in aqueous solution above their critical micelle temperature (CMT), which is the temperature above which phase separation of the thermosensitive block takes place. A pH-dependent cleavage of hydrophobic side chains resulted in a "hydrophobic- to-hydrophilic" conversion of the micellar core. Consequently, the CMT gradually increases, which ultimately results in micelle destabilisation and polymer dissolution. Our department designed biodegradable thermosensitive polymers that have methacrylamide backbones with oligolactates attached via hydrolytically sensitive ester bonds (*e.g.* 2-hydroxypropyl methacrylamide lactate (HPMAm-Lac$_n$, n is the number of lactic acid units in the oligolactate chain).[71, 221, 273] The CMT of these methacrylamide-oligolactate copolymers is precisely tailored by the monomer feed ratio. The CMT of copolymers of HPMAm-Lac$_1$ with HPMAm-Lac$_2$ covers a temperature range of 10 to 63 °C (corresponding to 0 to 100% HPMAm-Lac$_1$ respectively). The slightly more hydrophilic homopolymer poly(N-(2-hydroxyethyl)methacryl amide-dilactate) (P(HEMAm-Lac$_2$)) has a CP of 22 °C, which could be lowered by copolymerisation with HEMAm-Lac$_4$. Generally, the CMT of the block copolymers can be tuned to be below the temperature at which micelles are desired (*e.g.* ambient or body temperature). PEG-*b*-P(HPMAm-Lac$_2$) (CMT 8 °C)

displayed a transient stability at physiological conditions: after one week a sufficient amount of lactate side chains were hydrolysed to increase the CMT to above body temperature, which resulted in polymer dissolution and thus the micelles disintegrated (Figure 11).[274] A much shorter destabilisation time of 8 h was obtained with PEG-*b*-P(HEMAm-Lac$_n$) micelles since the hydrolysis of HEMAm-Lac$_n$ was much faster than that of HPMAm-Lac$_n$.[71]

Recently, other biodegradable thermosensitive polymers with different hydrolysable groups were reported. A cyclic ester is the degradable moiety in poly(NIPAAm-*co*-dimethyl-γ-butyrolactone acrylate),[275] whereas hydrazone bonds in poly(NIPAAm-hydrazone-alkyl$_n$)[276] or ortho-esters in poly(N-(2-(m)ethoxy-1,3-dioxan-5-yl) methacrylamide)[277] have been used as acid-labile groups. It is anticipated that by applying these type of polymers in block copolymer architectures, a second generation of controlled biodegradable thermosensitive micelles can be created.

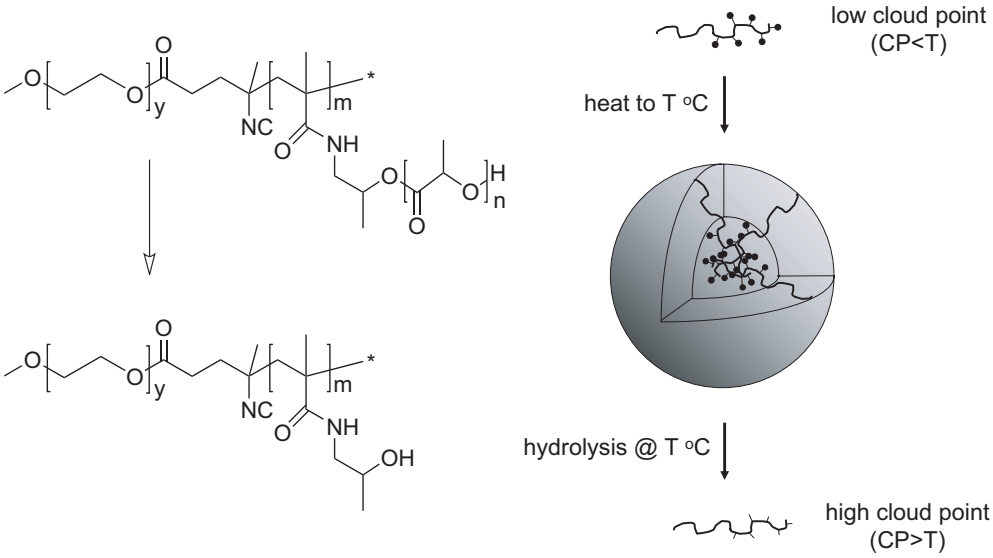

Figure 11 Hydrolysis of PEG-*b*-poly(HPMAm-Lac$_2$) (left) causes an increase of the critical micelle temperature (CMT) of the block copolymer by removal of the hydrophobic lactic acid groups (black dots; right). Thus, micelles formed above the cloud point of PEG-*b*-poly(HPMAm-Lac$_2$) destabilise when the CMT passes the incubation temperature. This figure was published by Rijcken *et al.*[212] Copyright Elsevier Ltd. (2007).

4.8.3 Various combinations of triggers

Photoresponsive thermosensitive copolymers do not only respond to temperature, but also display a photo-induced change in CP. UV-illumination of a thermosensitive copolymer that contains light sensitive compounds (such as those mentioned in section 4.6.2) can result in increased hydrogen bonding capacity, and consequently an increased CP.[278-280] In the case of poly(2-(dimethylamino)ethylmethacrylate)-*b*-poly(6-(4-phenylazo)phenoxy)-hexylmethacrylate) micelles, the application of only light was not sufficient to induce dissociation, since the light-induced *trans*-to-*cis* isomerisation did not overcome the hydrophobic interactions.[281] Additionally, pH sensitivity could be obtained by the introduction of carboxylic acid units.[282] The photodimerisation of cinnamoyl units was used to design crosslinked polymeric micelles that responded to pH, temperature and ionic strength.[283]

So-called schizophrenic micelles were developed by Armes *et al*. and are based on the pH-induced micellar inversion of zwitterionic diblock copolymers assemblies. For example, a diblock copolymer composed of 2-(diethylamino)ethyl methacrylate (PDEA) and 2-(N-morpholino)ethyl methacrylate (PMEMA) is fully dissolved at pH 6 and 20 °C, since the PDEA is protonated and the neutral PMEMA is hydrophilic. At pH 8.5 the PDEA block is deprotonated and micelles are formed with PDEA as the core-forming part. Lowering the pH and addition of sufficient electrolyte causes the PMEMA block to be selectively salted out to yield PMEMA-core micelles.[284] An overview of these type of micelles bearing pH and ionic strength dependency was recently published.[285]

The combination of enzyme and temperature sensitivity was introduced in a PNIPAAm-based polymer with peptide side chains. Upon phosphorylation of the peptide by protein kinase A, the CP of the copolymers increased (from 36.7 to 40 °C) caused by the hydrophilisation of the peptide chains.[286] At physiological conditions, as a result from the action of this enzyme, the polymers gradually dissolved in time. However, this concept has not been used to design responsive micelles so far.

4.9 Imaging-guided drug delivery

Encapsulation of drugs in stimuli sensitive polymeric micelles aims at achieving an optimal pharmacotherapeutic effect, *e.g.* drug release as a result of (external) stimuli after accumulation of the loaded nanocarrier at its site of action. The possibility to detect the presence of the drug-loaded micelles at their aimed site of action by *in vivo* imaging, and to subsequently trigger the release of the loaded drug would be an important new feature.[287]

For imaging purposes, polymeric micelles were loaded with either magnetic resonance imaging (MRI) contrast agents (mainly Fe, Mn, or Gd), γ-emitting radiolabels (such as ^{111}indium or ^{99m}technetium),[288] heavy elements (*e.g.* I, Br and Ba) for CT imaging, or with quantum dots (QDs).[51, 52, 289] Importantly, encapsulation of these agents in micelles is favourable since in that form they are less susceptible to renal clearance while their accumulation in tumour tissue (via the EPR-effect) will enhance the signal strength and specificity, respectively.[290, 291]

Co-loading diacyllipid micelles with Fe_3O_4 and a photosensitiser (a drug that is activated via illumination) enabled to monitor *in vitro* cellular uptake in real time.[292] Furthermore, applying an external magnetic field to cells incubated with these magnetic nanoparticles resulted in a so-called magnetophoretic control of the cellular uptake.[292, 293] Future *in vivo* administration of iron and drug-loaded micelles in combination with a local magnetic field might thus increase the concentration of the drug at the target site. Another sophisticated carrier for imaging-guided drug delivery was developed by Reddy *et al.* PEGylated polyacrylamide nanoparticles were loaded with both iron-oxide and photofrin (photosensitiser) and also a targeting ligand directing to tumour vasculature was coupled onto the micellar shell. *In vivo*, a higher photodynamic therapeutic effect (*i.e.* killing of tumours) was observed when compared to non-targeted nanoparticles or free photofrin. The multifunctional targeted nanoparticles were internalised while the iron-oxide allowed to monitor the tissue localisation of the micelles real-time by MRI, and the optimal time for illumination could be chosen.[294, 295]

Semiconductor quantum dots (QD) also have a potential for image-guided drug delivery using polymeric micelles. Several markers can be probed simultaneously since QDs absorb over a very broad spectral range, while their extreme high photostability enables real-time monitoring over long periods of time.[289, 296] Furthermore, since QDs generate highly reactive free radicals upon illumination, these QD-containing micelles can be used for diagnostic as well as for (photodynamic) therapeutic purposes (Figure 12).[297] The most extensively studied QD in biology is CdSe, which has been encapsulated in phospholipids[298] and in antibody decorated multiblock copolymeric micelles. The latter type of micelles gave a clear imaging signal *in vivo* and enabled very precise tracking of the active tumour uptake.[299]

5. Combining longevity, stability and stimuli sensitivity

In conclusion, polymeric micelles are very attractive drug delivery carriers for hydrophobic drugs in particular because of their unique morphology, high versatility, and high drug loading capacity. The ideal micellar system should be able to stably encapsulate drugs, also when circulating *in vivo*. Several strategies have been investigated to improve the circulation times ('longevity') of the micellar carriers, their stability, and the retention of the loaded drugs in the micellar core. Once the polymeric micelle has reached the aimed target site, the desired release of the entrapped drug poses conflicting requirements on the micellar building blocks. Internal or external triggers create possibilities to develop transiently stable polymeric micelles from which the time and site of release of entrapped drug can be precisely tailored.

The most popular approach to combine longevity and triggered release properties is the use of building blocks that contain a hydrophilic PEG-block in combination with a degradable or stimuli sensitive hydrophobic block, accounting for both desired properties, respectively. However, only a few systems combine additional stabilising strategies with stimuli triggered drug release. For example, biodegradable PEG-*b*-PCL micelles were stabilised either by reducing the CMC[68, 166] or by core crosslinking.[39] Furthermore, thermosensitive PEG-*b*-P(HEMA-Lac$_n$) micelles were core crosslinked, and demonstrated transient stability upon pH-dependent degradation.[183] A third example are PEG-*b*-P(Asp) micelles with covalently coupled doxorubicin, which increased the compatibility of the micellar core with additional physically encapsulated doxorubicin.[24]

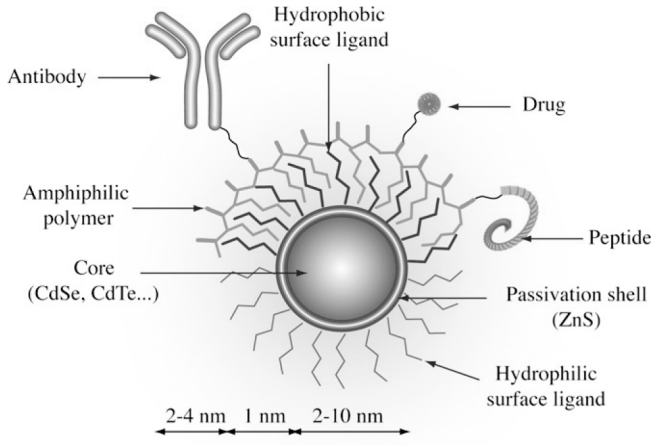

Figure 12 Multifunctional QD-containing micelles. This figure was published by Maysinger *et al.*[297] Copyright Elsevier Ltd. (2007).

Despite all promising aspects, so far, only few micellar formulations have entered clinical trials; well known concepts are Genexol-PM® (paclitaxel-loaded mPEG-*b*-PLA micelles) and PEG-*b*-P(Asp) micelles with either encapsulated paclitaxel (NK105) or covalently bound and physically entrapped doxorubicin (NK911).[36, 50, 300] Phase I studies with these formulations indicated prolonged circulation times when compared to the conventional formulations[50, 300] or a better toxicity profile, allowing higher dosing.[36]

Concluding, it is anticipated that a proper combination of long circulating properties with sophisticated stabilising strategies will generate highly stable micelles that are able to reach the target site in their intact form. Introduction of stimuli sensitive building blocks will control the release behaviour while further improvement is obtained by attaching targeting ligands. Incorporation of imaging agents allows detection of the drug-loaded micelles at the target site and application of the external trigger at the appropriate site and time. The building blocks of polymeric micelles are synthetic polymers, which offer almost unlimited possibilities to tailor and optimise the micellar structures towards the desired morphology, drug compatibility and drug release profile. It is therefore expected that within the coming years their favourable properties will be exploited to successfully encapsulate various hydrophobic compounds, and that these drug-loaded micelles will display superior performance in the treatment of several diseases.

References

1. Moses MA; Brem H; Langer R, Advancing the field of drug delivery: taking aim at cancer. *Cancer Cell* 4, 337-341 (2003).
2. Crommelin DJA; Scherphof G; Storm G, Active targeting with particulate carrier systems in the blood compartment. *Adv Drug Deliver Rev* 17, 49-60 (1995).
3. Gros L; Ringsdorf H; Schupp H, Polymeric antitumor agents on a molecular and on a cellular level? *Angew Chem Int Edit* 20, 305-325 (1981).
4. Torchilin VP, Structure and design of polymeric surfactant-based drug delivery systems. *J Control Release* 73, 137-172 (2001).
5. Kabanov AV; Batrakova EV; Melik-Nubarov NS; Fedoseev NA; Dorodnich TY; Alakhov VY; Chekhonin VP; Nazarova IR; Kabanov VA, A new class of drug carriers: micelles of poly(oxyethylene)-poly(oxypropylene) block copolymers as microcontainers for drug targeting from blood in brain. *J Control Release* 22, 141-157 (1992).
6. Allen C; Maysinger D; Eisenberg A, Nano-engineering block copolymer aggregates for drug delivery. *Colloid Surface B* 16, 3-27 (1999).
7. Gaucher G; Dufresne MH; Sant VP; Kang N; Maysinger D; Leroux JC, Block copolymer micelles: preparation, characterization and application in drug delivery. *J Control Release* 109, 169-188 (2005).
8. Moghimi SM; Hunter AC; Murray JC, Long-circulating and target-specific nanoparticles: theory to practice. *Pharmacol Rev* 53, 283-318 (2001).
9. Nishiyama N; Kataoka K, Current state, achievements, and future prospects of polymeric micelles as nanocarriers for drug and gene delivery. *Pharmacol Therapeut* 112, 630-648 (2006).
10. Jones M-C; Leroux J-C, Polymeric micelles - a new generation of colloidal drug carriers. *Eur J Pharm Biopharm* 48, 101-111 (1999).
11. Kwon GS, Polymeric micelles for delivery of poorly water-soluble compounds. *Crit Rev Ther Drug Carrier Syst* 20, 357-403 (2003).
12. Adams ML; Lavasanifar A; Kwon GS, Amphiphilic block copolymers for drug delivery. *J Pharm Sci* 92, 1343-1355 (2003).
13. Torchilin VP, Multifunctional nanocarriers. *Adv Drug Deliver Rev* 58, 1532-1555 (2006).
14. Liu J; Zeng F; Allen C, In vivo fate of unimers and micelles of a poly(ethylene glycol)-block-poly(caprolactone) copolymer in mice following intravenous administration. *Eur J Pharm Biopharm* 65, 309-319 (2007).
15. Kataoka K; Harada A; Nagasaki Y, Block copolymer micelles for drug delivery: design, characterization and biological significance. *Adv Drug Deliver Rev* 47, 113-131 (2001).
16. Kreuter J, Nanoparticles- a historical perspective. *Int J Pharm* 331, 1-10 (2006).
17. Lavasanifar A; Samuel J; Kwon GS, Poly(ethylene oxide)-block-poly(-amino acid) micelles for drug delivery. *Adv Drug Deliver Rev* 54, 169-190 (2002).
18. Yokoyama M; Kwon GS; Okano T; Sakurai Y; Seto T; Kataoka K, Preparation of micelle-forming polymer-drug conjugates. *Bioconjugate Chem* 3, 295-301 (1992).
19. Lee SC; Huh KM; Lee J; Cho YW; Galinsky RE; Park K, Hydrotropic polymeric micelles for enhanced paclitaxel solubility: In vitro and in vivo characterization. *Biomacromolecules* 8, 202 - 208 (2007).
20. Zamboni WC, Liposomal, nanoparticle and conjugated formulations of anticancer agents. *Clin Cancer Res* 11, 8230-8234 (2005).
21. Cheng J; Teply BA; Sherifi I; Sung J; Luther G; Gu FX; Levy-Nissenbaum E; Radovic-Moreno AF; Langer R; Farokhzad OC, Formulation of functionalized PLGA-PEG nanoparticles for in vivo targeted drug delivery. *Biomaterials* 28, 869-876 (2007).
22. Avgoustakis K; Beletsi A; Panagi Z; Klepetsanis P; Karydas AG; Ithakissios DS, PLGA-mPEG nanoparticles of cisplatin: in vitro nanoparticle degradation, in vitro drug release and in vivo drug residence in blood properties. *J Control Release* 79, 123-135 (2002).
23. Yi Y; Kim JH; Kang HW; Oh HS; Kim SW; Seo MH, A polymeric nanoparticle consisting of mPEG-PLA-Toco and PLMA-COONa as a drug carrier: improvements in cellular uptake and biodistribution. *Pharm Res* 22, 200-208 (2005).

24. Yokoyama M; Fukushima S; Uehara R; Okamoto K; Kataoka K; Sakurai Y; Okano T, Characterization of physical entrapment and chemical conjugation of adriamycin in polymeric micelles and their design for in vivo delivery to a solid tumor. *J Control Release* 50, 79-92 (1998).
25. Lin WJ; Chen YC; Lin CC; Chen CF; Chen JW, Characterization of pegylated copolymeric micelles and in vivo pharmacokinetics and biodistribution studies. *J Biomed Mater Res B* 77, 188-194 (2005).
26. Nishiyama N; Okazaki S; Cabral H; Miyamoto M; Kato Y; Sugiyama Y; Nishio K; Matsumura Y; Kataoka K, Novel cisplatin-incorporated polymeric micelles can eradicate solid tumors in mice. *Cancer Res* 63, 8977–8983 (2003).
27. Lin WJ; Juang LW; Lin CC, Stability and release performance of a series of pegylated copolymeric micelles. *Pharm Res* V20, 668-673 (2003).
28. Nishiyama N; Kato Y; Sugiyama Y; Kataoka K, Cisplatin-loaded polymer-metal complex micelle with time-modulated decaying property as a novel drug delivery system. *Pharm Res* V18, 1035-1041 (2001).
29. Djordjevic J; Barch M; Uhrich KE, Polymeric micelles based on amphiphilic scorpion-like macromolecules: novel carriers for water-insoluble drugs. *Pharm Res* 22, 24-32 (2005).
30. Gillies ER; Frechet JM, pH-Responsive copolymer assemblies for controlled release of doxorubicin. *Bioconjugate Chem* 16, 361-368 (2005).
31. Hruby M; Konak C; Ulbrich K, Polymeric micellar pH-sensitive drug delivery system for doxorubicin. *J Control Release* 103, 137-148 (2005).
32. Kabanov AV; Batrakova EV; Alakhov VY, Pluronic block copolymers for overcoming drug resistance in cancer. *Adv Drug Deliver Rev* 54, 759-779 (2002).
33. Lee ES; Na K; Bae YH, Super pH sensitive multifunctional polymeric micelle. *Nano Lett* 5, 325-329 (2005).
34. Nakanishi T; Fukushima S; Okamoto K; Suzuki M; Matsumura Y; Yokoyama M; Okano T; Sakurai Y; Kataoka K, Development of the polymer micelle carrier system for doxorubicin. *J Control Release* 74, 295-302 (2001).
35. Rapoport N, Combined cancer therapy by micellar-encapsulated drug and ultrasound. *Int J Pharm* 277, 155-162 (2004).
36. Kim TY; Kim DW; Chung JY; Shin SG; Kim SC; Heo DS; Kim NK; Bang YJ, Phase I and pharmacokinetic study of Genexol-PM, a cremophor-free, polymeric micelle-formulated paclitaxel, in patients with advanced malignancies. *Clin Cancer Res* 10, 3708-3716 (2004).
37. Hamaguchi T; Matsumura Y; Suzuki M; Shimizu K; Goda R; Nakamura I; Nakatomi I; Yokoyama M; Kataoka K; Kakizoe T, NK105, a paclitaxel-incorporating micellar nanoparticle formulation, can extend in vivo antitumour activity and reduce the neurotoxicity of paclitaxel. *Brit J Cancer* 92, 1240-1246 (2005).
38. Kim SC; Kim DW; Shim YH; Bang JS; Oh HS; Wan Kim S; Seo MH, In vivo evaluation of polymeric micellar paclitaxel formulation: toxicity and efficacy. *J Control Release* 72, 191-202 (2001).
39. Shuai X; Merdan T; Schaper AK; Xi F; Kissel T, Core-cross-linked polymeric micelles as paclitaxel carriers. *Bioconjugate Chem* 15, 441-448 (2004).
40. Liggins RT; Burt HM, Polyether-polyester diblock copolymers for the preparation of paclitaxel loaded polymeric micelle formulations. *Adv Drug Deliver Rev* 54, 191-202 (2002).
41. Cavallaro G; Licciardi M; Giammona G; Caliceti P; Semenzato A; Salmaso S, Poly(hydroxyethylaspartamide) derivatives as colloidal drug carrier systems. *J Control Release* 89, 285-295 (2003).
42. Krishnadas A; Rubinstein I; Önyüksel H, Sterically stabilized phospholipid mixed micelles: in vitro evaluation as a novel carrier for water-insoluble drugs. *Pharm Res* V20, 297-302 (2003).
43. Huh KM; Lee SC; Cho YW; Lee J; Jeong JH; Park K, Hydrotropic polymer micelle system for delivery of paclitaxel. *J Control Release* 101, 59-68 (2005).
44. Torchilin VP; Lukyanov AN; Gao Z; Papahadjopoulos-Sternberg B, Immunomicelles: targeted pharmaceutical carriers for poorly soluble drugs. *P Natl Acad Sci USA* 100, 6039-6044 (2003).
45. Lavasanifar A; Samuel J; Sattari S; Kwon GS, Block copolymer micelles for the encapsulation and delivery of amphotericin B. *Pharm Res* V19, 418-422 (2002).
46. van Nostrum CF, Polymeric micelles to deliver photosensitizers for photodynamic therapy. *Adv Drug Deliver Rev* 56, 9-16 (2004).
47. Le Garrec D; Gori S; Luo L; Lessard D; Smith DC; Yessine MA; Ranger M; Leroux JC, Poly(N-vinylpyrrolidone)-block-poly(D,L-lactide) as a new polymeric solubilizer for hydrophobic anticancer drugs: in vitro and in vivo evaluation. *J Control Release* 99, 83-101 (2004).

48. Zhang G-D; Harada A; Nishiyama N; Jiang D-L; Koyama H; Aida T; Kataoka K, Polyion complex micelles entrapping cationic dendrimer porphyrin: effective photosensitizer for photodynamic therapy of cancer. *J Control Release* 93, 141-150 (2003).
49. Barratt GM, Therapeutic applications of colloidal drug carriers. *Pharm Sci Technol To* 3, 163-171 (2000).
50. Matsumura Y; Hamaguchi T; Ura T; Muro K; Yamada Y; Shimada Y; Shirao K; Okusaka T; Ueno H; Ikeda M; Watanabe N, Phase I clinical trial and pharmacokinetic evaluation of NK911, a micelle-encapsulated doxorubicin. *Brit J Cancer* 91, 1775-1781 (2004).
51. Torchilin VP, Micellar nanocarriers: pharmaceutical perspectives. *Pharm Res* 24, 1-16 (2007).
52. Torchilin VP, PEG-based micelles as carriers of contrast agents for different imaging modalities. *Adv Drug Deliver Rev* 54, 235-252 (2002).
53. Matsumura Y; Maeda H, A new concept for macromolecular therapeutics in cancer chemotherapy: mechanism of tumoritropic accumulation of proteins and the antitumor agent smancs. *Cancer Res* 46, 6387-6392 (1986).
54. Maeda H; Wu J; Sawa T; Matsumura Y; Hori K, Tumor vascular permeability and the EPR effect in macromolecular therapeutics: a review. *J Control Release* 65, 271-284 (2000).
55. Maeda H; Fang J; Inutsuka T; Kitamoto Y, Vascular permeability enhancement in solid tumor: various factors, mechanisms involved and its implications. *Int Immunopharmacol* 3, 319-328 (2003).
56. Woodle MC; Lasic DD, Sterically stabilized liposomes. *Biochim Biophys Acta* 1113, 171-199 (1992).
57. Illum L; Jacobsen LO; Muller RH; Mak E; Davis SS, Surface characteristics and the interaction of colloidal particles with mouse peritoneal macrophages. *Biomaterials* 8, 113-117 (1987).
58. Moghimi SM; Porter CJH; Illum L; Davis SS, The effect of poloxamer-407 on liposome stability and targeting to bone marrow: comparison with polystyrene microspheres. *Int J Pharm* 68, 121-126 (1991).
59. Owens DE, 3rd; Peppas NA, Opsonization, biodistribution, and pharmacokinetics of polymeric nanoparticles. *Int J Pharm* 307, 93-102 (2006).
60. Leroux J; De Jaeghere F; Anner B; Doelker E; Gurny R, An investigation on the role of plasma and serum opsonins on the internalization of biodegradable poly(D,L-lactic acid) nanoparticles by human monocytes. *Life Sci* 57, 695-703 (1995).
61. Stolnik S; Illum L; Davis SS, Long circulating microparticulate drug carriers. *Adv Drug Deliver Rev* 16, 195-214 (1995).
62. Vonarbourg A; Passirani C; Saulnier P; Benoit JP, Parameters influencing the stealthiness of colloidal drug delivery systems. *Biomaterials* 27, 4356-4373 (2006).
63. Sun X; Rossin R; Turner JL; Becker ML; Joralemon MJ; Welch MJ; Wooley KL, An assessment of the effects of shell cross linked nanoparticle size, core composition and surface pegylation on in vivo distribution. *Biomacromolecules* 6, 2541-2554 (2005).
64. Hagan SA; Coombes AGA; Garnett MC; Dunn SE; Davies MC; Illum L; Davis SS; Harding SE; Purkiss S; Gellert PR, Polylactide-poly(ethylene glycol) copolymers as drug delivery systems. 1. Characterization of water dispersible micelle-forming systems. *Langmuir* 12, 2153 - 2161 (1996).
65. Luo L; Tam J; Maysinger D; Eisenberg A, Cellular internalization of poly(ethylene oxide)-b-poly(epsilon-caprolactone) diblock copolymer micelles. *Bioconjugate Chem* 13, 1259-1265 (2002).
66. Shi B; Fang C; You MX; Zhang Y; Fu S; Pei Y, Stealth MePEG-PCL micelles: effects of polymer composition on micelle physicochemical characteristics, *in vitro* drug release, *in vivo* pharmacokinetics in rats and biodistribution in S180 tumor bearing mice. *Colloid Polym Sci* 283, 954-967 (2005).
67. Yamamoto Y; Nagasaki Y; Kato Y; Sugiyama Y; Kataoka K, Long-circulating poly(ethylene glycol)-poly(D,L-lactide) block copolymer micelles with modulated surface charge. *J Control Release* 77, 27-38 (2001).
68. Carstens MG; Bevernage JJL; van Nostrum CF; van Steenbergen MJ; Flesch FM; Verrijk R; de Leede LGJ; Crommelin DJA; Hennink WE, Small oligomeric micelles based on end group modified mPEG-oligocaprolactone with monodisperse hydrophobic blocks. *Macromolecules* 40, 116-122 (2007).
69. Lukyanov AN; Torchilin VP, Micelles from lipid derivatives of water-soluble polymers as delivery systems for poorly soluble drugs. *Adv Drug Deliver Rev* 56, 1273-1289 (2004).
70. Weissig V; Whiteman KR; Torchilin VP, Accumulation of protein-loaded long-circulating micelles and liposomes in subcutaneous lewis lung carcinoma in mice. *Pharm Res* V15, 1552-1556 (1998).
71. Rijcken CJF; Veldhuis TFJ; Ramzi A; Meeldijk JD; Van Nostrum CF; Hennink WE, Novel fast degradable thermosensitive polymeric micelles based on PEG-block-poly(N-(2-hydroxyethyl)methacrylamide-oligolactates). *Biomacromolecules* 6, 2343-2351 (2005).

72. Neradovic D; Soga O; Van Nostrum CF; Hennink WE, The effect of the processing and formulation parameters on the size of nanoparticles based on block copolymers of poly(ethylene glycol) and poly(N-isopropylacrylamide) with and without hydrolytically sensitive groups. *Biomaterials* 25, 2409-2418 (2004).
73. Soga O; Van Nostrum CF; Ramzi A; Visser T; Soulimani F; Frederik PM; Bomans PHH; Hennink WE, Physicochemical characterization of degradable thermosensitive polymeric micelles. *Langmuir* 20, 9388-9395 (2004).
74. Topp MDC; Dijkstra PJ; Talsma H; Feijen J, Thermosensitive micelle-forming block copolymers of poly(ethylene glycol) and poly(N-isopropylacrylamide). *Macromolecules* 30, 8518-8520 (1997).
75. Torchilin VP; Trubetskoy VS, Which polymers can make nanoparticulate drug carriers long-circulating? *Adv Drug Deliver Rev* 16, 141-155 (1995).
76. Allen TM; Hansen C, Pharmacokinetics of stealth versus conventional liposomes: effect of dose. *Biochim Biophys Acta* 1068, 133-141 (1991).
77. Lee KY; Ha WS; Park WH, Blood compatibility and biodegradability of partially N-acylated chitosan derivatives. *Biomaterials* 16, 1211-1216 (1995).
78. Molineux G, PEGylation: engineering improved pharmaceuticals for enhanced therapy. *Cancer Treat Rev* 28, 13-16 (2002).
79. Klibanov AL; Maruyama K; Torchilin VP; Huang L, Amphipathic polyethyleneglycols effectively prolong the circulation time of liposomes. *FEBS Lett* 268, 235-237 (1990).
80. Soppimath KS; Aminabhavi TM; Kulkarni AR; Rudzinski WE, Biodegradable polymeric nanoparticles as drug delivery devices. *J Control Release* 70, 1-20 (2001).
81. Michel R; Pasche S; Textor M; Castner DG, Influence of PEG architecture on protein adsorption and conformation. *Langmuir* 21, 12327-12332 (2005).
82. Kwon GS; Yokoyama M; Okano T; Sakurai Y; Kataoka K, Biodistribution of micelle-forming polymer-drug conjugates. *Pharm Res* 10, 970-974 (1993).
83. Kwon G; Suwa S; Yokoyama M; Okano T; Sakurai Y; Kataoka K, Enhanced tumor accumulation and prolonged circulation times of micelle-forming poly (ethylene oxide-aspartate) block copolymer-adriamycin conjugates. *J Control Release* 29, 17-23 (1994).
84. Kabanov AV; Batrakova EV; Alakhov VY, Pluronic block copolymers as novel polymer therapeutics for drug and gene delivery. *J Control Release* 82, 189-212 (2002).
85. Vonarbourg A; Passirani C; Saulnier P; Simard P; Leroux JC; Benoit JP, Evaluation of PEGylated lipid nanocapsules versus complement system activation and macrophage uptake. *J Biomed Mater Res A* 78A, 620-628 (2006).
86. Peracchia MT; Vauthier C; Passirani C; Couvreur P; Labarre D, Complement consumption by poly(ethylene glycol) in different conformations chemically coupled to poly(isobutyl 2-cyanoacrylate) nanoparticles. *Life Sci* 61, 749-761 (1997).
87. Hu Y; Xie J; Tong YW; Wang CH, Effect of PEG conformation and particle size on the cellular uptake efficiency of nanoparticles with the HepG2 cells. *J Control Release* 118, 7-17 (2007).
88. Moghimi SM; Szebeni J, Stealth liposomes and long circulating nanoparticles: critical issues in pharmacokinetics, opsonization and protein-binding properties. *Prog Lipid Res* 42, 463-478 (2003).
89. Dams ET; Laverman P; Oyen WJ; Storm G; Scherphof GL; van Der Meer JW; Corstens FH; Boerman OC, Accelerated blood clearance and altered biodistribution of repeated injections of sterically stabilized liposomes. *J Pharmacol Exp Ther* 292, 1071-1079 (2000).
90. Laverman P; Brouwers AH; Dams ET; Oyen WJ; Storm G; van Rooijen N; Corstens FH; Boerman OC, Preclinical and clinical evidence for disappearance of long-circulating characteristics of polyethylene glycol liposomes at low lipid dose. *J Pharmacol Exp Ther* 293, 996-1001 (2000).
91. Ishida T; Harashima H; Kiwada H, Liposome clearance. *Bioscience Rep* 22, 197-224 (2002).
92. Carstens MG; Romberg B; Laverman P; Boerman OC; Oussoren C; Storm G, Observations on the disappearance of the stealth property of PEGylated liposomes. Effects of lipid dose and dosing frequency. In: *Liposome Technology*, 3rd ed.; Gregoriadis G, Ed. CRC press: London, Vol. III (2006).
93. Yokoyama M; Okano T; Sakurai Y; Fukushima S; Okamoto K; Kataoka K, Selective delivery of adriamycin to a solid tumor using a polymeric micelle carrier system. *J Drug Target* 7, 171-186 (1999).
94. Woodle MC; Engbers CM; Zalipsky S, New amphipatic polymer-lipid conjugates forming long-circulating reticuloendothelial system-evading liposomes. *Bioconjugate Chem* 5, 493-496 (1994).

95. Maruyama K; Okuizumi S; Ishida O; Yamauchi H; Kikuchi H; Iwatsuru M, Phosphatidyl polyglycerols prolong liposome circulation in vivo. *Int J Pharm* 111, 103-107 (1994).

96. Torchilin VP; Levchenko TS; Whiteman KR; Yaroslavov AA; Tsatsakis AM; Rizos AK; Michailova EV; Shtilman MI, Amphiphilic poly-N-vinylpyrrolidones: synthesis, properties and liposome surface modification. *Biomaterials* 22, 3035-3044 (2001).

97. Torchilin VP; Shtilman MI; Trubetskoy VS; Whiteman K; Milstein AM, Amphiphilic vinyl polymers effectively prolong liposome circulation time in vivo. *BBA -Biomembranes* 1195, 181-184 (1994).

98. Takeuchi H; Kojima H; Yamamoto H; Kawashima Y, Evaluation of circulation profiles of liposomes coated with hydrophilic polymers having different molecular weights in rats. *J Control Release* 75, 83-91 (2001).

99. Whiteman K; Subr V; Ulbrich K; Torchilin V, Poly(HPMA)-coated liposomes demonstrated prolonged circulation in mice. *J Liposome Res* 11, 153-164 (2001).

100. Metselaar JM; Bruin P; de Boer LW; de Vringer T; Snel C; Oussoren C; Wauben MH; Crommelin DJ; Storm G; Hennink WE, A novel family of L-amino acid-based biodegradable polymer-lipid conjugates for the development of long-circulating liposomes with effective drug-targeting capacity. *Bioconjugate Chem* 14, 1156-1164 (2003).

101. Romberg B; Oussoren C; Snel CJ; Carstens MG; Hennink WE; Storm G, Pharmacokinetics of poly(hydroxyethyl-L-asparagine)-coated liposomes is superior over that of PEG-coated liposomes at low lipid dose and upon repeated administration. *BBA -Biomembranes* 1768, 737-743 (2007).

102. Luo L; Ranger M; Lessard DG; Garrec DL; Gori S; Leroux J-C; Rimmer S; Smith D, Novel amphiphilic diblock copolymer of low molecular weight poly(N-vinylpyrrolidone)-block-poly(D,L-lactide): Synthesis, characterization, and micellization. *Macromolecules* 37, 4008-4013 (2004).

103. Benahmed A; Ranger M; Leroux JC, Novel polymeric micelles based on the amphiphilic diblock copolymer poly(N-vinyl-2-pyrrolidone)-block-poly(D,L-lactide). *Pharm Res* 18, 323-328 (2001).

104. Lee SC; Lee HJ, pH-Controlled, polymer-mediated assembly of polymer micelle nanoparticles. *Langmuir* 23, 488-495 (2007).

105. Lele BS; Leroux J-C, Synthesis and micellar characterization of novel amphiphilic A-B-A triblock copolymers of *N*-(2-hydroxypropyl)methacrylamide or *N*-vinyl-2-pyrrolidone with poly(ε-caprolactone). *Macromolecules* 35, 6714-6723 (2002).

106. Chung TW; Cho KY; Lee HC; Nah JW; Yeo JH; Akaike T; Cho CS, Novel micelle-forming block copolymer composed of poly(ε-caprolactone) and poly(vinyl pyrrolidone). *Polymer* 45, 1591-1597 (2004).

107. Le Garrec D; Taillefer J; Van Lier JE; Lenaerts V; Leroux J-C, Optimizing pH-responsive polymeric micelles for drug delivery in a cancer photodynamic therapy model. *J Drug Target* 10, 429-437 (2002).

108. Zuccari G; Carosio R; Fini A; Montaldo PG; Orienti I, Modified polyvinylalcohol for encapsulation of all-trans-retinoic acid in polymeric micelles. *J Control Release* 103, 369-380 (2005).

109. Kim C; Lee SC; Shin JH; Yoon J-S; Kwon IC; Jeong SY, Amphiphilic diblock copolymers based on poly(2-ethyl-2-oxazoline) and poly(1,3-trimethylene carbonate): Synthesis and micellar characteristics. *Macromolecules* 33, 7448-7452 (2000).

110. Lee SC; Chang Y; Yoon J-S; Kim C; Kwon IC; Kim Y-H; Jeong SY, Synthesis and micellar characterization of amphiphilic diblock copolymers based on poly(2-ethyl-2-oxazoline) and aliphatic polyesters. *Macromolecules* 32, 1847-1852 (1999).

111. Hsiue GH; Wang CH; Lo CL; Li JP; Yang JL, Environmental-sensitive micelles based on poly(2-ethyl-2-oxazoline)-b-poly(L-lactide) diblock copolymer for application in drug delivery. *Int J Pharm* 317, 69-75 (2006).

112. Volet G; Chanthavong V; Wintgens V; Amiel C, Synthesis of monoalkyl end-capped poly(2-methyl-2-oxazoline) and its micelle formation in aqueous solution. *Macromolecules* 38, 5190-5197 (2005).

113. Lemarchand C; Gref R; Lesieur S; Hommel H; Vacher B; Besheer A; Maeder K; Couvreur P, Physico-chemical characterization of polysaccharide-coated nanoparticles. *J Control Release* 108, 97-111 (2005).

114. Rouzes C; Gref R; Leonard M; De Sousa Delgado A; Dellacherie E, Surface modification of poly(lactic acid) nanospheres using hydrophobically modified dextrans as stabilizers in an o/w emulsion/evaporation technique. *J Biomed Mater Res* 50, 557-565 (2000).

115. Lemarchand C; Gref R; Couvreur P, Polysaccharide-decorated nanoparticles. *Eur J Pharm Biopharm* 58, 327-341 (2004).

116. Passirani C; Barratt G; Devissaguet JP; Labarre D, Long-circulating nanoparticles bearing heparin or dextran covalently bound to poly(methyl methacrylate). *Pharm Res* 15, 1046-1050 (1998).

117. Besheer A; Hause G; Kressler J; Mader K, Hydrophobically modified hydroxyethyl starch: synthesis, characterization, and aqueous self-assembly into nano-sized polymeric micelles and vesicles. *Biomacromolecules* 8, 359-367 (2007).

118. Lemarchand C; Gref R; Passirani C; Garcion E; Petri B; Muller R; Costantini D; Couvreur P, Influence of polysaccharide coating on the interactions of nanoparticles with biological systems. *Biomaterials* 27, 108-118 (2006).

119. Maruyama A; Ishihara T; Adachi N; Akaike T, Preparation of nanoparticles bearing high density carbohydrate chains using carbohydrate-carrying polymers as emulsifier. *Biomaterials* 15, 1035-1042 (1994).

120. Bougard F; Jeusette M; Mespouille L; Dubois P; Lazzaroni R, Synthesis and supramolecular organization of amphiphilic diblock copolymers combining poly(N,N-dimethylamino-2-ethyl methacrylate) and poly(e-caprolactone). *Langmuir* 23, 2339-2345 (2007).

121. Nam YS; Kang HS; Park JY; Park TG; Han S-H; Chang I-S, New micelle-like polymer aggregates made from PEI-PLGA diblock copolymers: micellar characteristics and cellular uptake. *Biomaterials* 24, 2053-2059 (2003).

122. Inoue T; Chen G; Nakamae K; Hoffman AS, An AB block copolymer of oligo(methyl methacrylate) and poly(acrylic acid) for micellar delivery of hydrophobic drugs. *J Control Release* 51, 221-229 (1998).

123. Jeong JH; Kang HS; Yang SR; Park K; Kim J-D, Biodegradable poly(asparagine) grafted with poly(caprolactone) and the effect of substitution on self-aggregation. *Colloid Surface A* 264, 187-194 (2005).

124. Kohori F; Sakai K; Aoyagi T; Yokoyama M; Yamato M; Sakurai Y; Okano T, Control of adriamycin cytotoxic activity using thermally responsive polymeric micelles composed of poly(N-isopropylacrylamide-co-N,N-dimethylacrylamide)-b-poly(-lactide). *Colloid Surface B* 16, 195-205 (1999).

125. Moghimi SM; Porter CJ; Muir IS; Illum L; Davis SS, Non-phagocytic uptake of intravenously injected microspheres in rat spleen: influence of particle size and hydrophilic coating. *Biochem Bioph Res Co* 177, 861-866 (1991).

126. Fang C; Shi B; Pei YY; Hong MH; Wu J; Chen HZ, In vivo tumor targeting of tumor necrosis factor-alpha-loaded stealth nanoparticles: effect of MePEG molecular weight and particle size. *Eur J Pharm Sci* 27, 27-36 (2006).

127. Hobbs SK; Monsky WL; Yuan F; Roberts WG; Griffith L; Torchilin VP; Jain RK, Regulation of transport pathways in tumor vessels: role of tumor type and microenvironment. *P Natl Acad Sci USA* 95, 4607-4612 (1998).

128. Yuan F; Dellian M; Fukumura D; Leunig M; Berk DA; Torchilin VP; Jain RK, Vascular permeability in a human tumor xenograft: molecular size dependence and cutoff size. *Cancer Res* 55, 3752-3756 (1995).

129. Bae Y; Nishiyama N; Fukushima S; Koyama H; Yasuhori M; Kataoka K, Preparation and biological characterization of polymeric micelle drug carriers with intracellular pH-triggered drug release property: tumor permeability, controlled subcellular drug distribution, and enhanced in vivo antitumor efficacy. *Bioconjugate Chem* 16, 122-130 (2005).

130. Oku N; Namba Y, Long-circulating liposomes. *Crit Rev Ther Drug* 11, 231-270 (1994).

131. Senior J; Gregoriadis G, Stability of small unilamellar liposomes in serum and clearance from the circulation: the effect of the phospholipid and cholesterol components. *Life Sci* 30, 2123-2136 (1982).

132. Abra RM; Bosworth ME; Hunt CA, Liposome disposition in vivo: effects of pre-dosing with lipsomes. *Res Commun Chem Path* 29, 349-360 (1980).

133. Gao Z; Lukyanov AN; Chakilam AR; Torchilin VP, PEG-PE/phosphatidylcholine mixed immunomicelles specifically deliver encapsulated taxol to tumor cells of different origin and promote their efficient killing. *J Drug Target* 11, 87-92 (2003).

134. Jeong YI; Seo SJ; Park IK; Lee HC; Kang IC; Akaike T; Cho CS, Cellular recognition of paclitaxel-loaded polymeric nanoparticles composed of poly(gamma-benzyl L-glutamate) and poly(ethylene glycol) diblock copolymer endcapped with galactose moiety. *Int J Pharm* 296, 151-161 (2005).

135. Park EK; Kim SY; Lee SB; Lee YM, Folate-conjugated methoxy poly(ethylene glycol)/poly(epsilon-caprolactone) amphiphilic block copolymeric micelles for tumor-targeted drug delivery. *J Control Release* 109, 158-168 (2005).

136. Xiong XB; Mahmud A; Uludag H; Lavasanifar A, Conjugation of arginine-glycine-aspartic acid peptides to poly(ethylene oxide)-b-poly(epsilon-caprolactone) micelles for enhanced intracellular drug delivery to metastatic tumor cells. *Biomacromolecules* 8, 874-884 (2007).

137. Liu S-Q; Wiradharma N; Gao S-J; Tong YW; Yang Y-Y, Bio-functional micelles self-assembled from a folate-conjugated block copolymer for targeted intracellular delivery of anticancer drugs. *Biomaterials* 28, 1423-1433 (2007).

138. Lee ES; Na K; Bae YH, Polymeric micelle for tumor pH and folate-mediated targeting. *J Control Release* 91, 103-113 (2003).

139. Torchilin VP, Targeted polymeric micelles for delivery of poorly soluble drugs. *Cell Mol Life Sci* 61, 2549-2559 (2004).

140. Sethuraman VA; Bae YH, TAT peptide-based micelle system for potential active targeting of anti-cancer agents to acidic solid tumors. *J Control Release* 118, 216-224 (2007).

141. Allen C; Han J; Yu Y; Maysinger D; Eisenberg A, Polycaprolactone-b-poly(ethylene oxide) copolymer micelles as a delivery vehicle for dihydrotestosterone. *J Control Release* 63, 275-286 (2000).

142. Zhang Z; Grijpma DW; Feijen J, Thermo-sensitive transition of monomethoxy poly(ethylene glycol)-block-poly(trimethylene carbonate) films to micellar-like nanoparticles. *J Control Release* 112, 57-63 (2006).

143. Dong Y; Feng S, Methoxy poly(ethylene glycol)-poly(lactide) (MPEG-PLA) nanoparticles for controlled delivery of anticancer drugs. *Biomaterials* 25, 2843-2849 (2004).

144. Neradovic D; Van Nostrum CF; Hennink WE, Thermoresponsive polymeric micelles with controlled instability based on hydrolytically sensitive N-isopropylacrylamide copolymers. *Macromolecules* 34, 7589-7591 (2001).

145. Kwon GS; Naito M; Yokoyama M; Okano T; Sakurai Y; Kataoka K, Micelles based on AB block copolymers of poly(ethylene oxide) and poly(β-benzyl L-aspartate). *Langmuir* 9, 945-949 (1993).

146. Yokoyama M; Opanasopit P; Okano T; Kawano K; Maitani Y, Polymer design and incorporation methods for polymeric micelle carrier system containing water-insoluble anti-cancer agent camptothecin. *J Drug Target* 12, 373-384 (2004).

147. Watanabe M; Kawano K; Yokoyama M; Opanasopit P; Okano T; Maitani Y, Preparation of camptothecin-loaded polymeric micelles and evaluation of their incorporation and circulation stability. *Int J Pharm* 308, 183-189 (2006).

148. Rapoport N; Marin A; Luo L; Prestwich GD; Muniruzzaman MD, Intracellular uptake and trafficking of pluronic micelles in drug-sensitive and MDR cells: effect on the intracellular drug localization. *J Pharm Sci* 91, 157-170 (2002).

149. Attwood D; Florence AT, In: *Surfactant Systems: Their chemistry, pharmacy and biology*, Chapman and Hall Ltd.: London, p 108-111 (1983).

150. Kwon GS; Okano T, Polymeric micelles as new drug carriers. *Adv Drug Deliver Rev* 21, 107-116 (1996).

151. Teng Y; Morrison ME; Munk P; Webber SE; Prochazka K, Release kinetics studies of aromatic molecules into water from block polymer micelles. *Macromolecules* 31, 3578-3587 (1998).

152. Kim SY; Shin IG; Lee YM; Cho CS; Sung YK, Methoxy poly(ethylene glycol) and epsilon-caprolactone amphiphilic block copolymeric micelle containing indomethacin. II. Micelle formation and drug release behaviours. *J Control Release* 51, 13-22 (1998).

153. Wilhelm M; Zhao CL; Wang Y; Xu R; Winnik MA; Mura JL; Riess G; Croucher MD, Poly(styrene-ethylene oxide) block copolymer micelle formation in water: a fluorescence probe study. *Macromolecules* 24, 1033-1040 (1991).

154. Lavasanifar A; Samuel J; Kwon GS, The effect of fatty acid substitution on the in vitro release of amphotericin B from micelles composed of poly(ethylene oxide)-block-poly(N-hexyl stearate-aspartamide). *J Control Release* 79, 165-172 (2002).

155. Liu J; Xiao Y; Allen C, Polymer-drug compatibility: a guide to the development of delivery systems for the anticancer agent, ellipticine. *J Pharm Sci* 93, 132-143 (2004).

156. Lee J; Lee SC; Acharya G; Chang CJ; Park K, Hydrotropic solubilization of paclitaxel: analysis of chemical structures for hydrotropic property. *Pharm Res* 20, 1022-1030 (2003).

157. Prompruk K; Govender T; Zhang S; Xiong CD; Stolnik S, Synthesis of a novel PEG-block-poly(aspartic acid-stat-phenylalanine) copolymer shows potential for formation of a micellar drug carrier. *Int J Pharm* 297, 242-253 (2005).

158. Forrest ML; Zhao A; Won CY; Malick AW; Kwon GS, Lipophilic prodrugs of Hsp90 inhibitor geldanamycin for nanoencapsulation in poly(ethylene glycol)-b-poly(epsilon-caprolactone) micelles. *J Control Release* 116, 139-149 (2006).

159. Lo CL; Huang CK; Lin KM; Hsiue GH, Mixed micelles formed from graft and diblock copolymers for application in intracellular drug delivery. *Biomaterials* 28, 1225-1235 (2007).

160. Konan-Kouakou YN; Boch R; Gurny R; Allemann E, In vitro and in vivo activities of verteporfin-loaded nanoparticles. *J Control Release* 103, 83-91 (2005).

161. Liu J; Zeng F; Allen C, Influence of serum protein on polycarbonate-based copolymer micelles as a delivery system for a hydrophobic anti-cancer agent. *J Control Release* 103, 481-497 (2005).

162. Opanasopit P; Yokoyama M; Watanabe M; Kawano K; Maitani Y; Okano T, Influence of serum and albumins from different species on stability of camptothecin-loaded micelles. *J Control Release* 104, 313-321 (2005).

163. Savic R; Azzam T; Eisenberg A; Maysinger D, Assessment of the integrity of poly(caprolactone)-b-poly(ethylen eoxide)micelles under biological conditions: a fluorogenic based approach. *Langmuir* 22, 3570-3578 (2006).

164. Letchford K; Zastre J; Liggins R; Burt H, Synthesis and micellar characterization of short block length methoxy poly(ethylene glycol)-block-poly(caprolactone) diblock copolymers. *Colloid Surface B* 35, 81-91 (2004).

165. Opanasopit P; Yokoyama M; Watanabe M; Kawano K; Maitani Y; Okano T, Block copolymer design for camptothecin incorporation into polymeric micelles for passive tumor targeting. *Pharm Res* 21, 2001-2008 (2004).

166. Mahmud A; Xiong XB; Lavasanifar A, Novel self-associating poly(ethylene oxide)-block-poly(ε-caprolactone) block copolymers with functional side groups on the polyester block for drug delivery. *Macromolecules* 39, 9419-9428 (2006).

167. Lavasanifar A; Samuel J; Kwon GS, The effect of alkyl core structure on micellar properties of poly(ethylene oxide)-block-poly(L-aspartamide) derivatives. *Colloid Surface B* 22, 115-126 (2001).

168. Zhang J; Wang L-Q; Wang H; Tu K, Micellization phenomena of amphiphilic block copolymers based on methoxy poly(ethylene glycol) and either crystalline or amorphous poly(caprolactone-*b*-lactide). *Biomacromolecules* 7, 2492-2500 (2006).

169. Kang N; Perron M-E; Prud'homme RE; Zhang Y; Gaucher G; Leroux J-C, Stereocomplex block copolymer micelles: Core-shell nanostructures with enhanced stability. *Nano Lett* 5, 315-319 (2005).

170. Yoshida E; Kunugi S, Micelle formation of poly(vinyl phenol)-block-polystyrene by alfa,omega-diamines. *J Polym Sci Pol Chem* 40, 3063-3067 (2002).

171. Harada A; Kataoka K, Chain length recognition: core-shell supramolecular assembly from oppositely charged block copolymers. *Science* 283, 65-67 (1999).

172. Rodriguez-Hernandez J; Checot F; Gnanou Y; Lecommandoux S, Toward 'smart' nano-objects by self-assembly of block copolymers in solution. *Prog Polym Sci* 30, 691-724 (2005).

173. Cohen Stuart MA; Hofs B; Voets IK; de Keizer A, Assembly of polyelectrolyte-containing block copolymers in aqueous media. *Curr Opin Colloid In* 10, 30-36 (2005).

174. Harada A; Kataoka K, Formation of polyion complex micelles in an aqueous milieu from a pair of oppositely-charged block copolymers with poly(ethylene glycol) segments. *Macromolecules* 28, 5294-5299 (1995).

175. Kabanov AV; Bronich TK; Kabanov VA; Yu K; Eisenberg A, Soluble stoichiometric complexes from poly(N-ethyl-4-vinylpyridinium) cations and poly(ethylene oxide)-block-polymethacrylate anions. *Macromolecules* 29, 6797-6802 (1996).

176. Gohy JF; Varshney SK; Antoun S; Jerome R, Water-soluble complexes formed by sodium poly(4-styrenesulfonate) and a poly(2-vinylpyridinium)-block-poly(ethyleneoxide) copolymer. *Macromolecules* 33, 9298-9305 (2000).

177. Park JS; Akiyama Y; Yamasaki Y; Kataoka K, Preparation and characterization of polyion complex micelles with a novel thermosensitive poly(2-isopropyl-2-oxazoline) shell via the complexation of oppositely charged block ionomers. *Langmuir* 23, 138-146 (2007).

178. Bronich TK; Keifer PA; Shlyakhtenko LS; Kabanov AV, Polymer micelle with cross-linked ionic core. *J Am Chem Soc* 127, 8236-8237 (2005).

179. Harada A; Kataoka K, Supramolecular assemblies of block copolymers in aqueous media as nanocontainers relevant to biological applications. *Prog Polym Sci* 31, 949-982 (2006).

180. Rosler A; Vandermeulen GW; Klok HA, Advanced drug delivery devices via self-assembly of amphiphilic block copolymers. *Adv Drug Deliver Rev* 53, 95-108 (2001).

181. O'Reilly RK; Hawker CJ; Wooley KL, Cross-linked block copolymer micelles: functional nanostructures of great potential and versatility. *Chem Soc Rev* 35, 1068-1083 (2006).

182. Kim J; Emoto K; Iijima M; Nagasaki Y; Aoyagi T; Okano T; Sakurai Y; Kataoka K, Core-stabilized polymeric micelle as potential drug carrier: increased solubilization of taxol. *Polym Advan Technol* 10, 647-654 (1999).

183. Rijcken CJF; Snel CJ; Schiffelers RM; van Nostrum CF; Hennink WE, Hydrolysable core crosslinked thermosensitive polymeric micelles: synthesis, characterisation and *in vivo* studies. *Submitted for publication.*

184. Iijima M; Nagasaki Y; Okada T; Kato M; Kataoka K, Core-polymerized reactive micelles from heterotechelic amphiphilic block copolymers. *Macromolecules* 32, 1140-1146 (1999).

185. Hu F-Q; Ren G-F; Yuan H; Du Y-Z; Zeng S, Shell cross-linked stearic acid grafted chitosan oligosaccharide self-aggregated micelles for controlled release of paclitaxel. *Colloid Surface B* 50, 97-103 (2006).

186. Bontha S; Kabanov AV; Bronich TK, Polymer micelles with cross-linked ionic cores for delivery of anticancer drugs. *J Control Release* 114, 163-174 (2006).

187. Bae KH; Choi SH; Park SY; Lee Y; Park TG, Thermosensitive pluronic micelles stabilized by shell cross-linking with gold particles. *Langmuir* 22, 6380-6384 (2006).

188. Liu S; Weaver HVM; Tang B; Billingham NC; Armes SP, Synthesis of shell cross-linked micelles with pH-responsive cores using ABC triblock copolymers. *Macromolecules* 35, 6121-6131 (2002).

189. Li X; Ji J; Shen J, Synthesis of hydroxyl-capped comb-like poly(ethylene glycol) to develop shell cross-linkable micelles. *Polymer* 47, 1987-1994 (2006).

190. Joralemon MJ; O'Reilly RK; Hawker CJ; Wooley KL, Shell Click-Crosslinked (SCC) Nanoparticles: A New Methodology for Synthesis and Orthogonal Functionalization. *J Am Chem Soc* 127, 16892-16899 (2005).

191. Li Y; Lokitz BS; Armes SP; McCormick CL, Synthesis of reversible shell cross-linked micelles for controlled release of bioactive agents. *Macromolecules* 39, 2726-2728 (2006).

192. Jiang X; Luo S; Armes SP; Shi W; Liu S, UV irradiation-induced shell cross-linked micelles with pH-responsive cores using ABC triblock copolymers. *Macromolecules* 39, 5987-5994 (2006).

193. Jiang J; Qi B; Lepage M; Zhao Y, Polymer micelles stabilization on demand through reversible photo-cross-linking. *Macromolecules* 40, 790-792 (2007).

194. Rodriguez-Hernandez J; Babin J; Zappone B; Lecommandeux S, Preparation of shell cross-linked nano-objects from hybrid-peptide block copolymers. *Biomacromolecules* 6, 2213-2220 (2005).

195. Pilon LN; Armes SP; Findlay P; Rannard SP, Synthesis and characterization of shell cross-linked micelles with hydroxy-functional coronas: a pragmatic alternative to dendrimers? *Langmuir* 21, 3808-3813 (2005).

196. Thurmond II KB; Huang H; Clark Jr. CG; Kowalewski T; Wooley KL, Shell cross-linked polymer micelles: stabilized assemblies with great versatility and potential. *Colloid Surface B* 16, 45-54 (1999).

197. Liu S; Weaver JVM; Save M; Armes SP, Synthesis of pH-responsive shell crosslinked micelles and their use as nanoreactors for the preparation of gold nanoparticles. *Langmuir* 18, 8350-8357 (2002).

198. Zhang L; Katapodi K; Davis TP; Barner-Kowollik C; Stenzel MH, Using the reversible addition-fragmentation chain transfer process to synthesize core-crosslinked micelles. *J Polym Sci Pol Chem* 44, 2177-2194 (2006).

199. Li Z; Ding J; Day M; Tao Y, Molecularly imprinted polymeric nanospheres by diblock copolymer self-assembly. *Macromolecules* 39, 2629-2636 (2006).

200. Rheingans O; Hugenberg N; Harris JR; Fischer K; Maskos M, Nanoparticles built of cross-linked heterotechelic amphiphilic poly(dimethylsiloxane)-b-poly(ethylene oxide) diblock copolymers. *Macromolecules* 33, 4780-4790 (2000).

201. Lee BH; West B; McLemore R; Pauken C; Vernon BL, In-situ injectable physically and chemically gelling NIPAAm-based copolymer system for embolization. *Biomacromolecules* 7, 2059-2064 (2006).

202. Petrov P; Bozukov M; Tsvetanov CB, Innovative approach for stabilizing poly(ethylene oxide)-b-poly(propylene oxide)-b-poly(ethylene oxide) micelles by forming nano-sized networks in the micelle. *J Mater Chem* 15, 1481-1486 (2005).

203. Jaturanpinyo M; Harada A; Yuan X; Kataoka K, Preparation of bionanoreactor based on core-shell structured polyion complex micelles entrapping trypsin in the core cross-linked with glutaraldehyde. *Bioconjugate Chem* 15, 344-348 (2004).

204. Kakizawa Y; Harada A; Kataoka K, Environment-sensitive stabilization of core-shell structured polyion complex micelle by reversible cross-linking of the core through disulfide bond. *J Am Chem Soc* 121, 11247-11248 (1999).

205. Jiang J; Tong X; Morris D; Zhao Y, Toward photocontrolled release using light-dissociable block copolymer micelles. *Macromolecules* 39, 4633-4640 (2006).

206. Liu D-Z; Hsieh J-H; Fan X-C; Yang J-D; Chung T-W, Synthesis, characterization and drug delivery behaviors of new PCP polymeric micelles. *Carbohyd Polym* 68, 544–554 (2007).

207. Tian L; Yam L; Wang J; Tat H; Uhrich K, Core crosslinkable polymeric micelles from PEG-lipid amphiphiles as drug carriers. *J Mater Chem* 14, 2317-2324 (2004).

208. Yokoyama M; Okano T; Sakurai Y; Kataoka K, Improved synthesis of adriamycin-conjugated poly (ethylene oxide)-poly (aspartic acid) block copolymer and formation of unimodal micellar structure with controlled amount of physically entrapped adriamycin. *J Control Release* 32, 269-277 (1994).

209. Kataoka K; Matsumoto T; Yokoyama M; Okano T; Sakurai Y; Fukushima S; Okamoto K; Kwon GS, Doxorubicin-loaded poly(ethylene glycol)-poly([beta]-benzyl-aspartate) copolymer micelles: their pharmaceutical characteristics and biological significance. *J Control Release* 64, 143-153 (2000).

210. Seymour LW; Duncan R; Strohalm J; Kopecek J, Effect of molecular weight (Mw) of N-(2-hydroxypropyl)me thacrylamide copolymers on body distribution and rate of excretion after subcutaneous, intraperitoneal, and intravenous administration to rats. *J Biomed Mater Res* 21, 1341-1358 (1987).

211. Mart RJ; Osborne RD; Stevens MM; Ulijn RV, Peptide-based stimuli-responsive biomaterials. *Soft Matter* 2, 822-835 (2006).

212. Rijcken CJF; Soga O; Hennink WE; Van Nostrum CF, Triggered destabilisation of polymeric micelles and vesicles by changing polymers polarity: an attractive tool for drug delivery. *J Control Release* 120, 121-148 (2007).

213. Jeong B; Bae YH; Lee DS; Kim SW, Biodegradable block copolymers as injectable drug-delivery systems. *Nature* 388, 860-862 (1997).

214. Hoffman AS; Stayton PS; Volga B; Chen G; Chen J; Cheung C; Chilkoti A; Ding Z; Dong L; Fong R; Lackey CA; Long CJ; Miura M; Morris JE; Murthy N; Nabeshima Y; Park TG; Press OW; Shimoboji T; Shoemaker S; Yang HJ; Monji N; Nowinski RC; Cole CA; Priest JH; Harris JM; Nakamae K; Nishino T; Miyata T, Really smart bioconjugates of smart polymers and receptor proteins. *J Biomed Mater Res* 52, 577-586 (2000).

215. Chilkoti A; Dreher MR; Meyer DE; Raucher D, Targeted drug delivery by thermally responsive polymers. *Adv Drug Deliver Rev* 54, 613-630 (2002).

216. Heskins M; Guillet JE, Solution properties of poly (N-isopropylacrylamide). *J Macromol Sci* A2, 1441-1455 (1968).

217. Pelton R, Temperature-sensitive aqueous microgels. *Adv Colloid Interfac* 85, 1-33 (2000).

218. Schild HG, Poly (N-isopropylacrylamide) experiment, theory and application. *Prog Polym Sci* 17, 163-249 (1992).

219. Feil H; You H, Bae; Feijen J; Sung W, Kim, Effect of comonomer hydrophilicity and ionization on the lower critical solution temperature of N-isopropylacrylamide copolymers. *Macromolecules* 26, 2496-2500 (1993).

220. Shibayama M; Mizutani S; Nomura S, Thermal properties of copolymer gels containing N-isopropylacrylamide. *Macromolecules* 29, 2019-2024 (1996).

221. Soga O; van Nostrum CF; Hennink WE, Poly(N-2-hydroxylpropyl) methacrylamide mono/di lactate): A new class of biodegradable polymers with tuneable thermosensitivity. *Biomacromolecules* 5, 818-821 (2004).

222. Park JS; Kataoka K, Precise control of lower critical solution temperature of thermosensitive poly(2-isopropyl-2-oxazoline) via gradient copolymerization with 2-ethyl-2-oxazoline as a hydrophilic comonomer. *Macromolecules* 39, 6622-6630 (2006).

223. Zhu PW; Napper DH, Effect of heating rate on nanoparticle formation of poly(N-isopropylacrylamide)-poly(ethylene glycol) block copolymer microgels. *Langmuir* 16, 8543-8545 (2000).

224. Qiu XP; Wu C, Study of the core-shell nanoparticle formed through the "coil-to-globule" transition of poly(N-isopropylacrylamide) grafted with poly(ethylene oxide). *Macromolecules* 30, 7921-7926 (1997).

225. Engin K; Leeper DB; Cater JR; Thistlethwaite AJ; Tupchong L; McFarlane JD, Extracellular pH distribution in human tumours. *Int J Hyperther* 11, 211-216 (1995).

226. Haag R, Supramolecular drug delivery systems based on polymeric core-shell architectures. *Angew Chem Int Edit* 43, 278-282 (2004).

227. Lee ES; Shin HJ; Na K; Bae YH, Poly(L-histidine)-PEG block copolymer micelles and pH-induced destabilization. *J Control Release* 90, 363-374 (2003).

228. Martin TJ; Prochazka K; Munk P; Webber SE, pH-dependent micellization of poly(2-vinylpyridine)-block-poly(ethylene oxide). *Macromolecules* 29, 6071-6073 (1996).

229. Tang Y; Liu SY; Armes SP; Billingham NC, Solubilization and controlled release of a hydrophobic drug using novel micelle-forming ABC triblock copolymers. *Biomacromolecules* 4, 1636-1645 (2003).

230. Lee AS; Gast AP; Butun V; Armes SP, Characterizing the structure of pH dependent polyelectrolyte block copolymer micelles. *Macromolecules* 32, 4302-4310 (1999).

231. Na K; Bae KH, Self-assembled hydrogel nanoparticles responsive to tumor extracellular pH from pullulan derivative/sulfonamide conjugate: characterization, aggregation, and adriamycin release in vitro. *Pharm Res* 19, 681-688 (2002).

232. Na K; Lee KH; Bae YH, pH-sensitivity and pH-dependent interior structural change of self-assembled hydrogel nanoparticles of pullulan acetate/oligo-sulfonamide conjugate. *J Control Release* 97, 513-525 (2004).

233. Giacomelli C; Le Men L; Borsali R; Lai-Kee-Him J; Brisson A; Armes SP; Lewis AL, Phosphorylcholine-based pH-responsive diblock copolymer micelles as drug delivery vehicles: light scattering, electron microscopy, and fluorescence experiments. *Biomacromolecules* 7, 817-828 (2006).

234. Licciardi M; Giammona G; Du J; Armes SP; Tang Y; Lewis AL, New folate-functionalized biocompatible block copolymer micelles as potential anti-cancer drug delivery systems. *Polymer* 47, 2946-2955 (2006).

235. Kumar N; Ravikumar MN; Domb AJ, Biodegradable block copolymers. *Adv Drug Deliver Rev* 53, 23-44 (2001).

236. Zweers MLT; Engbers GHM; Grijpma DW; Feijen J, In vitro degradation of nanoparticles prepared from polymers based on DL-lactide, glycolide and poly(ethylene oxide). *J Control Release* 100, 347-356 (2004).

237. Hu Y; Zhang L; Cao Y; Ge H; Jiang X; Yang C, Degradation behavior of poly(ε-caprolactone-*b*-poly(ethylene glycol)-*b*-poly(ε-caprolactone) micelles in aqueous solution. *Biomacromolecules* 5, 1756-1762 (2004).

238. Carstens MG; van Nostrum CF; Verrijk R; de Leede LGJ; Crommelin DJA; Hennink WE, A mechanistic study of the chemical and enzymatic degradation of PEG-oligo(ε-caprolactone) micelles. *J Pharm Sci* In Press (2007).

239. Geng Y; Discher DE, Hydrolytic degradation of poly(ethylene oxide)-*block*-polycaprolactone worm micelles. *J Am Chem Soc* 127, 12780-12781 (2005).

240. de Jong SJ; Arias ER; Rijkers DTS; van Nostrum CF; Kettenes-van den Bosch JJ; Hennink WE, New insights into the hydrolytic degradation of poly(lactic acid): participation of the alcohol terminus. *Polymer* 42, 2795-2802 (2001).

241. Heller J; Barr J, Poly(ortho esters) - from concept to reality. *Biomacromolecules* 5, 1625-1632 (2004).

242. Heller J; Barr J; Ng SY; Abdellauoi KS; Gurny R, Poly(ortho esters): synthesis, characterization, properties and uses. *Adv Drug Deliver Rev* 54, 1015-1039 (2002).

243. Geng Y; Discher DE, Visualization of degradable worm micelle breakdown in relation to drug release. *Polymer* 47, 2519-2525 (2006).

244. Gillies ER; Frechet JM, A new approach towards acid sensitive copolymer micelles for drug delivery. *Chem Commun* 14, 1640-1641 (2003).

245. Bae Y; Fukushima S; Harada A; Kataoka K, Design of environment-sensitive supramolecular assemblies for intracellular drug delivery: polymeric micelles that are responsible to intracellular pH change. *Angew Chem Int Edit* 42, 4640-4643 (2003).

246. Gillies ER; Jonsson TB; Frechet JMJ, Stimuli-responsive supramolecular assemblies of linear-dendritic copolymers. *J Am Chem Soc* 126, 11936-11943 (2004).

247. Xie Z; Guan H; Chen X; Lu C; Chen L; Hu X; Shi Q; Jing X, A novel polymer-paclitaxel conjugate based on amphiphilic triblock copolymer. *J Control Release* 117, 210-216 (2007).

248. Chen C; Yu CH; Cheng YC; Yu PHF; Cheung MK, Biodegradable nanoparticles of amphiphilic triblock copolymers based on poly(3-hydroxybutyrate) and poly(ethylene glycol) as drug carriers. *Biomaterials* 27, 4804-4814 (2006).

249. Gan Z; Jim TF; Li M; Yuer Z; Wang S; Wu C, Enzymatic biodegradation of poly(ethylene oxide-e-caprolactone) diblock copolymer and its potential biomedical applications. *Macromolecules* 32, 590-594 (1999).

250. Akagi T; Higashi M; Kaneko T; Kida T; Akashi M, Hydrolytic and enzymatic degradation of nanoparticles based on amphiphilic poly(gamma-glutamic acid)-graft-L-phenylalanine copolymers. *Biomacromolecules* 7, 297-303 (2006).

251. Kakizawa Y; Harada A; Kataoka K, Glutathione-sensitive stabilization of block copolymer micelles composed of antisense DNA and thiolated poly(ethylene glycol)-block-poly(L-lysine): a potential carrier for systemic delivery of antisense DNA. *Biomacromolecules* 2, 491-497 (2001).

252. Ghosh S; Basu S; Thayumanavan S, Simultaneous and reversible functionalization of copolymers for biological applications. *Macromolecules* 39, 5595-5597 (2006).

253. Anton P; Heinze J; Laschewsky A, Redox-active monomeric and polymeric surfactants. *Langmuir* 9, 77-85 (1993).

254. Takeoka Y; Aoki T; Sanui K; Ogata N; Yokoyama M; Okano T; Sakurai Y; Watanabe M, Electrochemical control of drug release from redox-active micelles. *J Control Release* 33, 79-87 (1995).

255. Jiang J; Tong X; Zhao Y, A new design for light-breakable polymer micelles. *J Am Chem Soc* 127, 8290-8291 (2005).

256. Goodwin AP; Mynar JL; Ma Y; Fleming GR; Frechet JMJ, Synthetic micelle sensitive to IR light via a two-photon process. *J Am Chem Soc* 127, 9952-9953 (2005).

257. Tong X; Wang G; Soldera A; Zhao Y, How can azobenzene block copolymer vesicles be dissociated and reformed by light. *J Phys Chem B* 109, 20281-20287 (2005).

258. Konak C; Rathi RC; Kopeckova P; Kopecek J, Photoassociation of water-soluble copolymers containing photochromic spirobenzopyran moieties. *Polym Advan Technol* 9, 641-648 (1998).

259. Kono K; Nishihara Y; Takagishi T, Photoresponsive permeability of polyelectrolyte complex capsule membrane containing triphenylmethane leucohydroxide residues. *J Appl Poly Sci* 56, 707-713 (1995).

260. Rapoport NY; Christensen DA; Fain HD; Barrows L; Gao Z, Ultrasound-triggered drug targeting of tumors in vitro and in vivo. *Ultrasonics* 42, 943-950 (2004).

261. Rapoport N; Pitt WG; Sun H; Nelson JL, Drug delivery in polymeric micelles: from in vitro to in vivo. *J Control Release* 91, 85-95 (2003).

262. Gao Z-G; Fain HD; Rapoport N, Controlled and targeted tumor chemotherapy by micellar-encapsulated drug and ultrasound. *J Control Release* 102, 203-222 (2005).

263. Lecommandoux S; Sandre O; Checot F; Perzynski R, Smart hybrid magnetic self-assembled micelles and hollow capsules. *Prog Solid State Ch* 34, 171-179 (2006).

264. Lecommandoux S; Sandre O; Checot F; Rodriguez-Hernandez J; Perzynski R, Self-assemblies of magnetic nanoparticles and di-block copolymers: Magnetic micelles and vesicles. *J Magn Magn Mater* 300, 71-74 (2006).

265. Soppimath KS; Tan DC-W; Yang Y-Y, pH-triggered thermally responsive polymer core-shell nanoparticles for drug delivery. *Adv Mater* 17, 318-323 (2005).

266. Liu X-M; Wang LSL-S; Wang L; Huang J; He C, The effect of salt and pH on the phase-transition behaviors of temperature-sensitive copolymers based on N-isopropylacrylamide. *Biomaterials* 25, 5659-5666 (2004).

267. Mertoglu M; Garnier S; Laschewsky A; Skrabania K; Storsberg J, Stimuli responsive amphiphilic block copolymers for aqueous media synthesised via reversible addition fragmentation chain transfer polymerisation (RAFT). *Polymer* 46, 7726-7740 (2005).

268. Yin X; Hoffman AS; Stayton PS, Poly(N-isopropylacrylamide-co-propylacrylic acid) copolymers that respond sharply to temperature and pH. *Biomacromolecules* 7, 1381-1385 (2006).

269. Piskin E, Molecularly designed water soluble, intelligent, nanosize polymeric carriers. *Int J Pharm* 277, 105-118 (2004).

270. Salgado-Rodriguez R; Licea-Claverie A; Arndt KF, Random copolymers of N-isopropylacrylamide and methacrylic acid monomers with hydrophobic spacers: pH-tunable temperature sensitive materials. *Eur Polym J* 40, 1931-1946 (2004).

271. Shah SS; Wertheim J; Wang CT; Pitt CG, Polymer-drug conjugates: manipulating drug delivery kinetics using model LCST systems. *J Control Release* 45, 95-101 (1997).

272. Neradovic D; Hinrichs WLJ; Kettenes-van den Bosch JJ; van Nostrum CF; Hennink WE, Poly(N-isopropylacrylamide) with hydrolyzable lactic acid ester side groups: a new type of thermosensitive polymer. *Macromol Rapid Comm* 20, 577-581 (1999).

273. Lee BH; Vernon B, Copolymers of N-isopropylacrylamide HEMA-lactate and acrylic acid with time-dependent lower critical solution temperature as a bioresorbable carrier. *Polym Int* 54, 418-422 (2005).

274. Soga O; van Nostrum CF; Fens M; Rijcken CJF; Schiffelers RM; Storm G; Hennink WE, Thermosensitive and biodegradable polymeric micelles for paclitaxel delivery. *J Control Release* 103, 341-353 (2005).

275. Cui Z; Lee BH; Vernon BL, New hydrolysis-dependent thermosensitive polymer for an injectable degradable system. *Biomacromolecules* 8, 1280-1286 (2007).

276. Hruby M; Kueka J; Lebeda O; Mackova H; Babie M; Kooak E; Studenovsky M; Sikora A; Kozempel J; Ulbrich K, New bioerodable thermoresponsive polymers for possible radiotherapeutic applications. *J Control Release* 119, 25-33 (2007).

277. Huang X; Rong FD; Li JZ, Novel acid-labile, thermoresponsive poly(methacrylamide)s with pendent ortho ester moieties. *Macromol Rapid Comm* 28, 597-603 (2007).

278. Sugiyama K; Sono K, Characterization of photo- and thermoresponsible amphiphilic copolymers having azobenzene moieties as side groups. *J Appl Poly Sci* 81, 3056-3063 (2000).

279. Laschewsky A; Rekai ED, Photochemical modification of the lower critical solution temperature of cinnamoylated poly(N-2-hydropropylmethacrylamide) in water. *Macromol Rapid Comm* 21, 937-940 (2000).

280. Ivanov AE; Eremeev NL; Wahlund P-O; Galaev IY; Mattiasson B, Photosensitive copolymer of N-isopropylacrylamide and methacryloyl derivative of spyrobenzopyran. *Polymer* 43, 3819-3823 (2002).

281. Ravi P; Sin SL; Gan LH; Gan YY; Tam KC; Xia XL; Hu X, New water soluble azobenzene-containing diblock copolymers: synthesis and aggregation behavior. *Polymer* 46, 137-146 (2005).

282. Desponds A; Freitag R, Synthesis and characterization of photoresponsive N-isopropylacrylamide cotelomers. *Langmuir* 19, 6261-6270 (2003).

283. Szczubialka K; Moczek L; Blaskiewicz S; Nowakowska M, Photocrosslinkable smart terpolymers responding to pH, temperature and ionic strength. *J Polym Sci Pol Chem* 43, 3879-3886 (2004).

284. Butun V; Billingham NC; Armes SP, Unusual aggregation behavior of a novel tertiary amine methacrylate-based diblock copolymer: formation of micelles and reverse micelles in aqueous solution. *J Am Chem Soc* 120, 11818-11819 (1998).

285. Butun V; Liu S; Weaver JVM; Bories-Azeau X; Cai Y; Armes SP, A brief review of 'schizophrenic' block copolymers. *React Funct Polym* 66, 157-165 (2006).

286. Katayama Y; Sonoda T; Maeda M, A polymer micelle responding to the protein kinase A signal. *Macromolecules* 34, 8569-8573 (2001).

287. Wickline SA; Lanza GM, Nanotechnology for molecular imaging and targeted therapy. *Circulation* 107, 1092-1095 (2003).

288. Trubetskoy VS; Frank-Kamenetsky MD; Whiteman KR; Wolf GL; Torchilin VP, Stable polymeric micelles: lymphangiographic contrast media for gamma scintigraphy and magnetic resonance imaging. *Acad Radiol* 3, 232-238 (1996).

289. Otsuka H; Nagasaki Y; Kataoka K, PEGylated nanoparticles for biological and pharmaceutical applications. *Adv Drug Deliver Rev* 55, 403-419 (2003).

290. Nakamura E; Makino K; Okano T; Yamamoto T; Yokoyama M, A polymeric micelle MRI contrast agent with changeable relaxivity. *J Control Release* 114, 325-333 (2006).

291. Ai H; Flask C; Weinberg B; Shuai X; Pagel MD; Farrell D; Duerk J; Gao J, Magnetite-loaded polymeric micelles as ultrasensitive magnetic-resonance probes. *Adv Mater* 17, 1949-1952 (2005).

292. Cinteza LO; Ohulchanskyy TY; Sahoo Y; Bergey EJ; Pandey RK; Prasad PN, Diacyllipid micelle-based nanocarrier for magnetically guided delivery of drugs in photodynamic therapy. *Mol Pharm* 3, 415-423 (2006).

293. Yoon TJ; Kim JS; Kim BG; Yu KN; Cho MH; Lee JK, Multifunctional nanoparticles possessing a 'magnetic motor effect' for drug or gene delivery. *Angew Chem Int Edit* 117, 1092-1095 (2005).

294. Reddy GR; Bhojani MS; McConville P; Moody J; Moffat BA; Hall DE; Kim G; Koo YEL; Woolliscroft MJ; Sugai JV; Johnson TD; Philbert MA; Kopelman R; Rehemtulla A; Ross BD, Vascular targeted nanoparticles for imaging and treatment of brain tumors. *Clin Cancer Res* 12, 6677-6686 (2006).

295. Kopelman R; Lee Koo Y-E; Philbert M; Moffat BA; Ramachandra Reddy G; McConville P; Hall DE; Chenevert TL; Bhojani MS; Buck SM; Rehemtulla A; Ross BD, Multifunctional nanoparticle platforms for in vivo MRI enhancement and photodynamic therapy of a rat brain cancer. *J Magn Magn Mater* 293, 404-410 (2005).

296. Sahoo S; Ma; Labhasetwar, Nanotech approaches to drug delivery and imaging. *Drug Discov Today* 8, 1112-1120 (2003).

297. Maysinger D; Lovric J; Eisenberg A; Savic R, Fate of micelles and quantum dots in cells. *Eur J Pharm Biopharm* 65, 270-281 (2007).

298. Dubertret B; Skourides P; Norris DJ; Noireaux V; Brivanlou AH; Libchaber A, In vivo imaging of quantum dots encapsulated in phospholipid micelles. *Science* 298, 1759-1762 (2002).

299. Gao X; Cui Y; Levenson RM; W K Chung LWK; Nie S, In vivo cancer targeting and imaging with semiconductor quantum dots. *Nature* 22, 969-976 (2004).

300. Kato K; Hamaguchi T; Yasui H; Okusaka T; Ueno H; Ikeda M; Shirao K; Shimada Y; Nakahama H; Muro K; Matsumura Y, Phase I study of NK105, a paclitaxel-incorporating micellar nanoparticle, in patients with advanced cancer. *J Clin Oncol* 24, 2018 (2006).

Poly(ethylene glycol)-oligo(L-lactate)s with monodisperse hydrophobic blocks

preparation, characterisation and behaviour in water

3

Myrra G. Carstens,[a,b] Cornelus F. van Nostrum,[a] Aissa Ramzi,[a] Johannes D. Meeldijk,[c] Ruud Verrijk,[b] Leo G.J. de Leede,[b] Daan J.A. Crommelin,[a] Wim E. Hennink[a]

[a] Department of Pharmaceutics, Utrecht Institute for Pharmaceutical Sciences (UIPS), Faculty of Pharmaceutical Sciences, Utrecht University, The Netherlands

[b] OctoPlus N.V., Leiden, the Netherlands

[c] Electron Microscopy Utrecht (EMU), Utrecht University, The Netherlands

Langmuir **2005**, *21 (24): p. 11446-11454*

Abstract

Methoxy poly(ethylene glycol)-*b*-oligo(L-lactate) (mPEG-*b*-OLA) diblock oligomers with monodisperse oligo(L-lactate) (OLA) blocks were obtained by fractionation of polydisperse block oligomers using preparative HPLC. The fractionated oligomers were composed of an mPEG-block with a molecular weight of 350, 550, or 750 Da and an OLA-block with a degree of polymerisation of 4, 6, 8, or 10. The diblock oligomers with a low PEG-content were fully amorphous, with glass transition temperatures ranging from -60 to -20 °C, indicating that the blocks were miscible. Upon heating aqueous dispersions of the block oligomers, cloud points, which depend on the PEG/OLA ratio of the block oligomer, were observed at temperatures above 40 °C. The monodispersity of the hydrophobic block enabled the amphiphilic molecules to form nanoparticles in water with a hydrodynamic radius of 130-300 nm, at concentrations above the critical aggregation concentration (0.4-1 mg/mL). In contrast, polydisperse mPEG-*b*-OLAs gave formation of large aggregates. Static light scattering measurements showed that the nanoparticles had a low density (0.6-25 mg/mL) indicating that the particles were highly hydrated. In agreement herewith, the ^{1}H NMR spectra of nanoparticles in D_2O closely resembled spectra in a good solvent for both blocks ($CDCl_3$). It is therefore suggested that the nanoparticles contain a hydrated core of mPEG-*b*-OLA block oligomers, stabilised by a thin outer PEG-layer. The particles were stable for two weeks, except for the mPEG350-series and mPEG750-*b*-OLA_4, indicating that both the PEG block size and the PEG weight fraction of the oligomers determine the nanoparticles' stability. The evident self-emulsifying properties of mPEG-*b*-oligo(L-lactate)s with monodisperse hydrophobic blocks as demonstrated in this study, together with their expected biocompatibility and biodegradability, make these systems well suitable for pharmaceutical applications.

Introduction

Poly(lactic acid) (PLA) is a hydrophobic, biodegradable, and biocompatible polyester, which is used for biomedical and pharmaceutical applications.[1-4] Drug delivery systems based on PLA and copolymers of lactic acid and glycolic acid (PLGA) in the form of injectable microspheres are currently used in the clinical practice.[5] To modify the properties of PL(G)A, for example to improve the compatibility with protein drugs, blending or copolymerisation with hydrophilic polymers such as poly(ethylene glycol) (PEG),[6-13] poly(N-vinyl pyrrolidone) (PVP),[14] and dextran[13, 15] has been investigated. Copolymers of PEG and PL(G)A possess thermosensitive properties.[8, 9] PEG is a commonly used hydrophilic polymer, because it is non-toxic and non-immunogenic and has been shown to have little interactions with blood components.[16-18] This results in decreased uptake of PEGylated particles and proteins by the reticuloendothelial system, conferring enhanced circulation times.[16-18]

As a result of the nature of the two building blocks, PEG-*b*-PLA diblock copolymers are amphiphilic molecules. In an aqueous environment they self-assemble, resulting in the formation of nanoparticles,[6, 11, 19-25] micelles,[26-33] and vesicles.[34-36] *In vitro* studies demonstrated the expected protective effect of the PEG-block with regard to cellular uptake and opsonisation by plasma proteins when PEG-*b*-PLA nanoparticles were compared to PLA-nanoparticles.[20-22] *In vivo* studies confirmed these findings by showing enhanced circulation times after intravenous administration.[6, 19] The potential of these type of particles for drug delivery was recently demonstrated by effective treatment of sarcoma tumours in mice with camptothecin-loaded PEG-*b*-PLA nanoparticles.[25]

So far, mainly the formation and characteristics of nanoparticles composed of PEG-*b*-PLA with relatively high molecular weight PLA-blocks (>10 kDa) have been studied. These compounds are rather polydisperse as a result of the synthetic route. In this study low molecular weight diblock mPEG-*b*-oligo(L-lactate) oligomers were prepared, and their behaviour in an aqueous environment was evaluated. After synthesis, these block oligomers were fractionated by HPLC to obtain polymers with monodisperse hydrophobic blocks to gain detailed insight into the properties of these systems in relation to the polymer composition. The critical aggregation concentration, the particle formation, and the temperature sensitivity of the fractionated mPEG-*b*-oligo(L-lactate)s were studied for different oligomer compositions. The type of particles formed was investigated in detail by dynamic and static light scattering and NMR spectroscopy.

Experimental section

Materials

L-lactide ((3-*S*-*cis*)-3,6-dimethyl-1,4-dioxane-2,5-dione; >99.5%) was supplied by Purac Biochem BV (Gorinchem, The Netherlands). Stannous octoate (tin(II) bis(2-ethylhexanoate), $SnOct_2$; >95%), chloroform-*d* ($CDCl_3$; 99.8%D) and deuterium oxide (D_2O; 99.9 %D) were purchased from Sigma Aldrich Chemie BV (Zwijndrecht, The Netherlands). Toluene and poly(ethylene glycol) mono methyl ether (methoxy PEG) with average molecular weights of 350, 550, and 750 Da (mPEG350, mPEG550, and mPEG750) were obtained from Acros Organics (Geel, Belgium), and dichloromethane (DCM; peptide synthesis grade) and acetonitrile (ACN; HPLC gradient grade) from Biosolve LTD (Valkenswaard, The Netherlands). Pyrene was obtained from Fluka Chemie AG (Buchs, Switzerland), acetone, sodium chloride, ammonium acetate, and acetic acid were obtained from Merck (Darmstadt, Germany), and magnesium sulphate exsiccatus was purchased from Bufa BV (Uitgeest, The Netherlands). All chemicals were used as received; buffers were filtered through a 0.2 μm filter (Schleicher & Schuell MicroScience GmbH, Dassel, Germany) prior to use.

Preparation of poly(ethylene glycol)-*b*-oligo(L-lactate)s with monodisperse hydrophobic blocks

The preparation and fractionation of the different mPEG-*b*-oligo(L-lactate)s was performed according to the method of De Jong *et al.* for the preparation of monodisperse 2-(2-methoxyethoxy)ethanol (MEE)-oligo(L-lactate).[37] In detail, polydisperse block oligomers were synthesised by ring opening polymerisation of L-lactide initiated by methoxy PEG (mPEG350, mPEG550, or mPEG750) and catalysed by stannous octoate (Scheme 1). L-Lactide (10 g) and mPEG at a molar ratio of 3/1 or 5/1 were heated to 130 °C, followed by the addition of the catalyst (5 mole% with respect to mPEG) dissolved in 1 mL of toluene. The mixture was stirred for 4 h at 130 °C and cooled to room temperature. A 10 g portion of the polydisperse mPEG-*b*-OLA was dissolved in 100 mL of 40/60 (w/w) ACN/H_2O, and fractionated by preparative HPLC (column Waters Xterra Prep MS C18, 10 μm, 19×250 mm, including a guard column) with a system consisting of a Waters 600EF quaternary gradient pump and a Waters 2700 sample manager. The injection volume was 5 mL and the detection wavelength 210 nm (Waters 2487 absorbance detector with a semipreparative flow cell). A gradient was run from 70% A (5/95 (w/w) ACN/H_2O) to 70% B (95/5 (w/w) ACN/H_2O) in 60 min with a flow rate of 10 mL/min. Four fractions were collected and after evaporation of the solvents the identity was established by electrospray ionisation mass spectrometry (ESI-MS) and ^1H NMR, and the purity by analytical

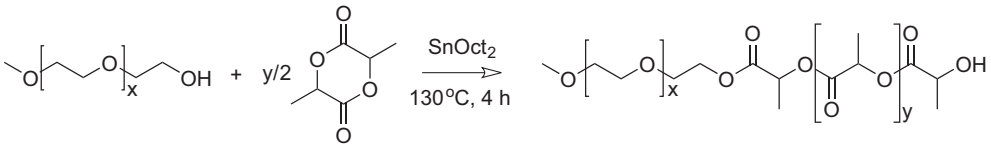

Scheme 1 Synthesis of mPEG-*b*-oligo(L-lactate).

HPLC as described below. To determine the total number average molecular weight (M_n) of the oligomers and hydrophilic and lipophilic molecular weight fractions (F_H and F_L), the molecular weight of the mPEG-block as provided by the supplier was used; the molecular weight of the OLA-block was calculated from the degree of polymerisation (DP) determined by mass spectrometry by DP = (m/z - 44x - q)/72, in which m/z is the mass/charge ratio as detected by ESI-MS, x the amount of ethylene glycol units and q the mass of the end groups and attached ion (q = 50, methoxy group, proton, and ammonium; 72 corresponds to one lactic acid unit).

Electrospray ionisation mass spectrometry

Spectra were recorded on a Shimadzu LCMS QP8000. The cone voltage was +4.5 kV with a detector voltage of 1.5 kV. The CDL voltage was set at –55 V, and the CDL temperature was 230 °C. A deflector voltage of 50 V was used. The flow of the nebulising gas (N_2) was 4.5 L/min. Instrumental control was performed with a CLASS 8000 LCMS software package. Samples (0.1 mg/mL) were dissolved in 95/5 (w/w) ACN/10 mM ammonium acetate buffer (pH 5), followed by centrifugation at 10000*g* for 1 min prior to injection into the system.

NMR spectroscopy

^{1}H NMR spectra were recorded using a Gemini spectrometer (Varian Associates Inc. NMR Instruments, Palo Alto, CA) operating at 300 MHz with $CDCl_3$ as the solvent. As the reference line the chloroform peak at 7.24 ppm was used. Chemical shifts of mPEG-*b*-OLA (δ, ppm): 5.22-5.11 (m, C*H*), 4.36-4.23 (m, overlapping 3H, CH_2-CH_2-O-CO; C*H*(CH_3)-OH), 3.67-3.50 (m, O-CH_2-CH_2-O), 3.35 (s, 3H, O-CH_3), 1.70-1.40 (m, CH-CH_3). To determine the DP of the OLA-block the ratio of the integrals of the methine protons of the lactate (5.22-5.11 ppm) and the protons of the methoxy group (3.35 ppm) was calculated, increased with one for the methine proton of the lactyl end group. A similar procedure was followed to calculate the DP of the mPEG-block from the ratio of the integrals of the ethyleneglycol units (3.67-3.50 ppm) and the protons of the methoxy group (3.35 ppm).

Analytical HPLC

Polydisperse mPEG-*b*-OLAs and their fractionated products were analysed by HPLC using a method similar to the method described by De Jong *et al.*[37] The system used consists of a model 2695 Alliance (consisting of a pump, autosampler and injector), and a model 2487 absorbance meter (Waters Chromatography BV). A 100 µL portion of a solution of 10 mg/mL in a mixture of 50/50 (w/w) ACN/10 mM ammonium acetate buffer, pH 5, was injected onto the column (Waters XTerra MS C18, 5 µm, 4.6×250 mm, including a guard column). A gradient was run from 70% A (5/95 (w/w) ACN/H_2O) to 70% B (95/5 (w/w) ACN/H_2O) in 30 min at a flow rate of 1 mL/min. Peaks were detected by UV (λ = 210 nm). The HPLC chromatograms were analysed using Empower software (Empower Pro, Waters Chromatography BV).

Differential scanning calorimetry

The glass transition (T_g) and the melting temperature (T_m) of mPEG-*b*-OLAs were determined by differential scanning calorimetry (DSC). The measurements were carried out with a Q1000 differential scanning calorimeter (TA Instruments). Indium was used for temperature and heat flow calibration. Samples of approximately 5 mg in hermetically closed aluminium pans were cooled to -70 °C, and then heated to 150 °C at 10 °C/min. Next, the samples were cooled to -70 °C at the same rate or at 2 °C/min, followed by a second heating cycle at 10 °C/min. Calculations were performed with the results of the second heating cycle, in which all samples have an equal thermal history.

Determination of the critical aggregation concentration

The critical aggregation concentration (CAC) of the fractionated oligomers was determined using pyrene as a fluorescent probe.[38, 39] Samples were prepared in 10 mM ammonium acetate buffer, pH 5, at concentrations ranging from 0.005 to 10 mg/mL. A pH of 5 was used to minimise the hydrolysis of the oligo(L-lactate) blocks.[40] Subsequently, 7 µL of a pyrene solution in acetone (0.18 mM) were added to 2 mL of polymer solution/dispersion, followed by incubation for 20 h at room temperature. Excitation spectra of pyrene were recorded from 300 to 360 nm at an emission wavelength of 390 nm using a Horiba Fluorolog fluorimeter at a 90° angle, at 25 and 37 °C. Excitation and emission band slits were 4 and 2 nm, respectively. To determine the CAC, the intensity ratio I_{338}/I_{333} of pyrene was plotted against the polymer concentration. Of some selected oligomers the CAC was also determined in acetate buffered saline (10 mM ammonium acetate buffer, pH 5, 140 mM NaCl).

Formation of particles

Particles from the polydisperse and fractionated oligomers, with variable mPEG-size (M_w = 350, 550, and 750) and variable OLA-length (DP of 4, 6, 8, and 10), were formed by the film-hydration method. This method has been widely used for the preparation of liposomes,[18] and recently of polymersomes as well.[35] Briefly, 20 mg of each block oligomer was dissolved in 2 mL of dichloromethane and coated on the inside wall of a round-bottomed 25 mL flask by evaporation of the solvent. After the film was dried for 30 min under a nitrogen stream, it was hydrated with 2 mL of 10 mM ammonium acetate buffer pH 5, with the aid of some glass pearls (25 mm diameter) to facilitate the release of the oligomer film from the wall, yielding a 10 mg/mL dispersion. Dispersions were also prepared in acetate buffered saline (10 mM ammonium acetate buffer, pH 5, 140 mM NaCl).

Efficiency of particle formation analysed by HPLC

The efficiency of the film-hydration method (% of the film material going into dispersion) was determined by analytical HPLC as described above. Particle dispersions in buffer were diluted 1/1 (v/v) with ACN and compared with reference samples prepared by dissolution of 5 mg of the block oligomer in 0.5 mL of ACN, followed by 1/1 (v/v) dilution with acetate buffer. By comparison of the peak areas, the amount of material in the dispersion relative to the reference sample was calculated. A linear relationship between the peak area and the concentration was shown over a concentration range of 0.5 to 10 mg/mL in the final solution (50/50 (w/w) ACN/buffer).

Determination of the temperature sensitivity

The temperature sensitivity of the different oligomers was determined by static light scattering using a Horiba Fluorolog fluorimeter (λ = 650 nm, 90° angle). Polymer dispersions of mPEG-*b*-OLA in 10 mM ammonium acetate buffer, pH 5, were prepared at a concentration of 10 mg/mL. The dispersions were heated from 0 to 75 °C at 1 °C/min and scattering intensities were measured at 0.3 °C intervals.

Particle analysis by light scattering

The size of the particles and their size distribution were measured by dynamic light scattering (DLS) using a Malvern CGS-3 multi-angle goniometer (Malvern Ltd., Malvern), consisting of a HeNe laser source (λ = 632.8 nm, 22 mW output power), temperature controller (Julabo water bath), and a digital correlator ALV-5000/EPP.

Time correlation functions were analysed using the ALV-60X0 software V.3.X provided by Malvern, to obtain the hydrodynamic radius of the particles (R_h) and the particle size distribution (polydispersity index, PDI). The determination of the hydrodynamic radius (R_h) by dynamic light scattering is based on the Stokes-Einstein equation (eq. 1),

$$R_h = \frac{k_B T q^2}{6\pi\eta\Gamma} \qquad \text{(Eq. 1)}$$

in which k_B is the Boltzmann constant, q is the scattering vector, ($q=(4\pi n \sin(q/2))/\lambda$, where n is the refractive index of the solution, q is the scattering angle, and λ is the wavelength of the incident laser light), η is the solvent viscosity, and Γ is the decay rate. The scattering of the mPEG-*b*-OLA dispersions was measured in an optical quality 4 mL borosilicate cell at a 90° angle. The samples were analysed at 25 °C, both directly after preparation and after incubation at room temperature for several days.

Some of the samples were analysed by multiangle static light scattering (SLS) with use of the equipment described above for DLS. The scattering intensity was measured at angles between 30° and 150° in steps of 2° for four different concentrations (0.75, 1.5, 3, and 5 mg/mL) at 25 °C. The samples were prepared one day before measurement, and the R_h and PDI were determined by DLS before the SLS measurements were started. The data were analysed by the graphical method first reported by Zimm,[41] which involves the extrapolation of the scattering data to both zero angle and zero concentration, simultaneously. The relationship between the concentration and the intensity of the scattered light is given by the following equation:

$$\frac{Kc}{R(q)} = \frac{1}{M_W}\left(1 + \frac{1}{3}R_g^2 q^2\right) + 2A_2 c \qquad \text{(Eq. 2)}$$

where c is the concentration, M_w is the weight average molecular weight of the nanoparticles ($M_{w,NP}$), R_g is the radius of gyration, A_2 is the second virial coefficient, and $R(q)$ is the excess Rayleigh ratio of the solute. The optical constant K is defined as:

$$K = \frac{4\pi^2}{N_A \lambda^4} n_T^2 \left(\frac{dn}{dc}\right)^2 \qquad \text{(Eq. 3)}$$

where n_T is the refractive index of toluene (1.494), (dn/dc) the specific refractive index increment of the mPEG-*b*-OLA dispersion and N_A Avogadro's number. The specific refractive index increments of PEG-*b*-PLA dispersions have been determined by Riley *et al.*, who described a linear relationship with the mass fraction of PEG ($\varphi_{m,PEG} = F_H$) in the copolymer (eq. 4).[30]

$$(dn/dc) = 0.030\,\varphi_{m,\,PEG} + 0.106 \qquad \text{(Eq. 4)}$$

The absolute excess time-averaged scattered intensity, *i.e.* Rayleigh ratio $R(q)$ is expressed by equation 5, where $R_{tol,90}$ is the Rayleigh ratio of toluene at an angle of 90° (*i.e.* 13.7×10^{-6} cm^{-1}), n is the refractive index of the solvent, I, I_o and I_{tol} are the scattering intensities of the solution, solvent, and toluene, respectively, and θ is the measurement angle.

$$R(q) = R_{tol,90}\left(\frac{n}{n_{tol}}\right)^2 \frac{I - I_0}{I_{tol}}\sin(\theta) \qquad \text{(Eq. 5)}$$

From the results the density of the nanoparticles (ρ_{NP}) in the dispersion was calculated by $\rho_{NP} = M_{wNP}/N_A V$, where N_A is Avogadro's number and V is the average volume of the nanoparticles. V was calculated based on the hydrodynamic radius (R_h) of the nanoparticles as determined by DLS. The aggregation number of the micelles (N_{agg}) was calculated by dividing M_{wNP} by the molecular weight of block oligomers as given in Table 1.

Cryogenic transmission electron microscopy

Cryogenic transmission electron microscopy (Cryo-TEM) analysis was performed on oligomer dispersions with a concentration of 10 or 1 mg/mL in 10 mM ammonium acetate buffer, pH 5. Samples were prepared in a temperature- and humidity-controlled chamber using a "Vitrobot". A thin aqueous film of oligomer dispersion was formed by blotting a 200 mesh copper grid covered with Quantifoil holey carbon foil (Micro Tools GmbH, Germany) at 25 or 37 °C and at 100% relative humidity (glow-discharged grid; one blot during 0.5 s). The thin film was rapidly vitrified by plunging the grid into liquid ethane. The grids with the vitrified thin films were transferred into the microscope chamber using a GATAN 626 cryoholder system. A Tecnai12 transmission electron microscope (Philips) operating at 120 kV was used with the specimen at -180 °C and using low-dose imaging conditions to avoid melting of the vitrified film. Images were recorded on a SIS-CCD camera and processed with AnalySIS software.

^{1}H NMR analysis of polymer dispersions in D_2O

Dispersions of block oligomers in D_2O were prepared by the film-hydration method as described above. ^{1}H NMR spectra were recorded using the equipment described previously and compared with the spectra of the polymers dissolved in $CDCl_3$.

Results and discussion

Synthesis and characterisation of mPEG-*b*-oligo(L-lactate)

The OLA-blocks of the synthesised polydisperse mPEG-*b*-OLAs had an average degree of polymerisation (DP) of 6 or 10, which was in correspondence with the initial molar ratios of L-lactide and mPEG of 3/1 and 5/1 (one L-lactide results in two lactic acid units in the polymer chain, Scheme 1). The HPLC chromatograms of the different mPEG-*b*-OLAs, using elution with a water/ACN gradient, showed separate fractions, which corresponded to different chain lengths of the OLA-block as shown previously for MEE-oligo(L-lactate).[37] Figure 1a shows that during the polymerisation reaction, besides mPEG-*b*-$OLA_{y=2,4,6,etc}$, also mPEG-*b*-$OLA_{y=3,5,7,etc.}$ are formed, which can be ascribed to transesterification reactions.[37] For each mPEG block size, four fractions with oligolactate block sizes of DP = 4, 6, 8, and 10 were collected using preparative HPLC. The yield per fraction was 5 to 10% relative to the overall amount of polydisperse block oligomer. The separation of mPEG2000-*b*-oligolactate using HPLC has previously been described by Lee *et al.*, who used critical condition HPLC.[42] At the critical condition of liquid chromatography the retention of a polymer becomes independent of the chain length. By using the critical conditions for the PEG-block (C18 column, isocratic elution using a mixture of 60/40 (v/v) ACN/water at 60 °C), the retention time of the block oligomer depends solely on the size of the oligolactate block.[42] Our results show, however, that with short block lengths of PEG separation can also be obtained at non-critical conditions.

In Figure 2 examples of ESI-MS spectra are shown, recorded from two isolated fractions of mPEG550-*b*-OLA. A regular series of peaks is observed, with a repeating unit of 44 Da, which corresponds to one ethylene glycol unit. For instance, the highest peak in Figure 2a has an *m*/*z* of 822, which corresponds to the ammonium adduct of mPEG-*b*-OLA, with block lengths of 11 and 4 units for the mPEG-block and the OLA-block, respectively. In the spectrum of the next fraction (Figure 2b) the series of peaks have shifted to *m*/*z* values that are 144 higher, indicating that these molecules have two additional units of lactic acid (72 Da). From the ESI-MS spectra it can be derived that each fraction contains a block oligomer with a polydisperse mPEG-block and a monodisperse OLA-block. Only in the highest fraction for each mPEG-series OLA-blocks with DP 9 and 11 detected, next to the main peaks of mPEG-*b*-OLA_{10}. This can be explained by the higher extent of peak overlap in the chromatogram at longer retention times.

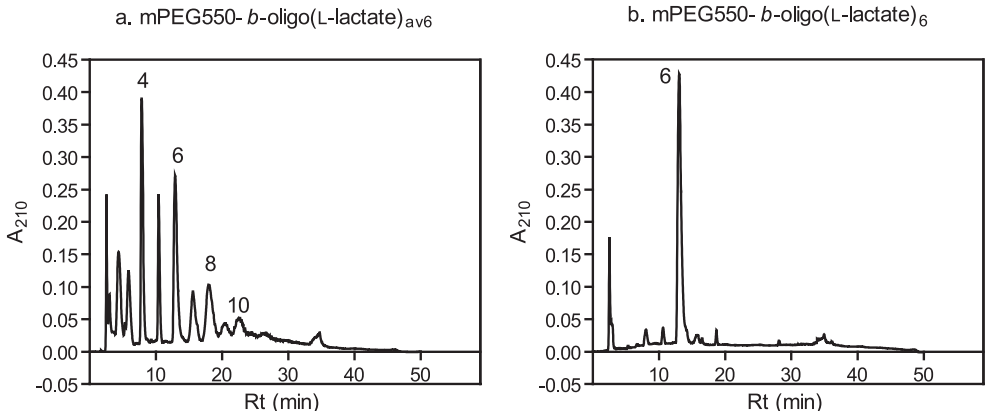

Figure 1 HPLC chromatogram of mPEG550-*b*-oligo(L-lactate) with an average degree of polymerisation of 6 (a) and the fractionated mPEG550-*b*-OLA_6 (b).

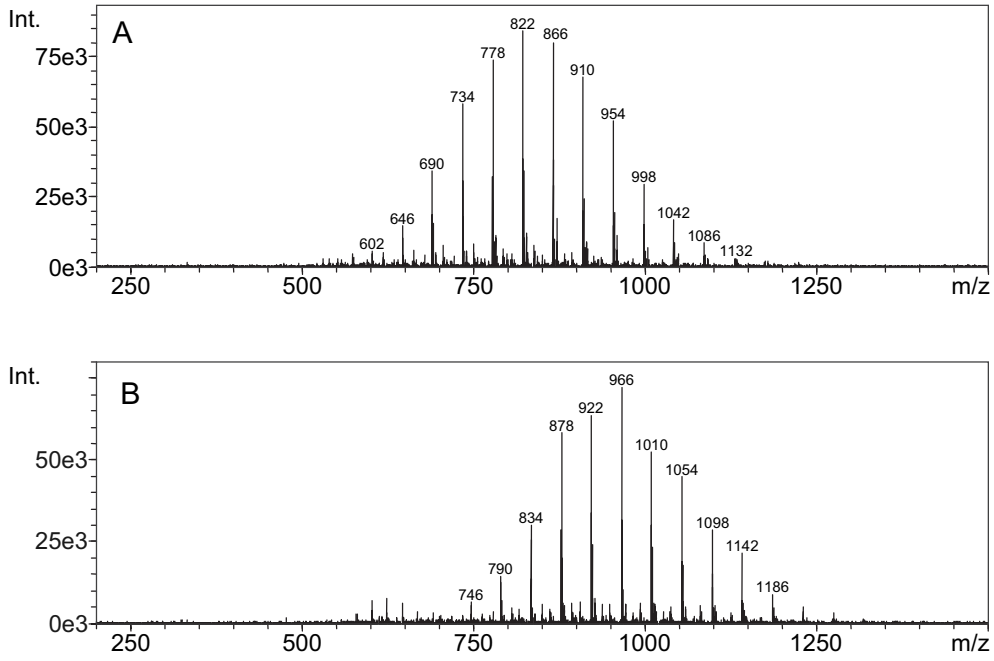

Figure 2 ESI-MS spectrum of mPEG550-*b*-oligo(L-lactate) with four (a) and six (b) lactic acid units.

The results were confirmed by analytical HPLC. An example is given in Figure 1b. From the relative peak areas corresponding to the different OLA chain lengths, the purity of the samples was determined. Generally, the purity of the samples was 80-90%, and the oligomers with the smallest hydrophobic blocks showed the highest purity. The main contaminants detected were mPEG-*b*-OLAs with one or sometimes traces of two lactate units deviation from the main product. Table 1 summarises the characteristics of the different fractions, including the degree of polymerisation of the OLA-blocks as determined using the ^{1}H NMR-spectra. The calculated chain lengths obtained from the NMR spectra correspond well to those derived from the ESI-MS spectra.

DSC measurements on the fractionated block oligomers were performed using a heat-cool-heat cycle. Figure 3a shows representative thermograms of mPEG550, mPEG550-*b*-OLA$_4$, and mPEG550-*b*-OLA$_8$. A single glass transition for the two block oligomers was observed at low temperatures (-55 and -45 °C). The T_g of the oligomers increases with the size of the OLA-block (Figure 3b). The amorphous state of the hydrophobic blocks at these chain lengths and the relationship between the T_g and the block size are in line with the observations by de Jong *et al.* for MEE-oligo(L-lactate)s.[37] However, the observed glass transition temperatures of the PEG-*b*-OLA block oligomers were lower than those observed for MEE-OLA,[37] and decreased with the size of the mPEG-block (Figure 3b). Plotting the reciprocal T_g versus the weight fraction of the oligo(L-lactate) part of the oligomer (F_L) results in a linear relationship (Figure 3c). This indicates that the T_g of the block oligomers follows Fox' law (eq. 6), in which F_A and F_B are the weight fractions of polymers A and B, respectively.

$$1/T_g = F_A/T_{gA} + F_B/T_{gB} \qquad \text{(Eq. 6)}$$

Extrapolation to weight fractions of OLA of 0 (100% PEG) or 1 (100% OLA) gives a calculated T_g of -77 °C for PEG and 6 °C for OLA, respectively. These values correspond well to literature data.[37, 43] The results indicate that the two blocks of the oligomers are miscible. It has been demonstrated before that high molecular weight PEG and PLLA are partially miscible.[44-46] Also, miscibility between the blocks in PEG-PL(G)A block copolymers has been reported.[6, 29, 47] It has been suggested that rapid cooling (10 °C/min) prevented phase separation in PEG-PLGA block copolymers.[6, 47] However, we found that slow cooling (2 °C/min) of PEG-*b*-OLA block oligomers did not result in a shift of the T_g to higher values (data not shown). This suggests that the PEG- and OLA-blocks in the oligomers are thermodynamically miscible.

Table 1 Characteristics of the fractionated mPEG-*b*-oligo(L-lactate)s

No. of lactic acid units	mPEG350-*b*-OLA				mPEG550-*b*-OLA				mPEG750-*b*-OLA			
	M_n [a]	F_H [b]	F_L [b]	DP[c]	M_n [a]	F_H [b]	F_L [b]	DP[c]	M_n [a]	F_H [b]	F_L [b]	DP[c]
4	639	0.55	0.45	4.0	839	0.76	0.34	3.9	1039	0.72	0.28	3.6
6	783	0.45	0.55	6.0	983	0.66	0.44	5.9	1183	0.63	0.37	4.9
8	927	0.38	0.62	7.7	1127	0.49	0.51	7.8	1327	0.57	0.43	7.3
10	1071	0.33	0.67	9.8	1271	0.43	0.57	10.2	1471	0.51	0.49	8.9

[a] *Molecular weight of the total block oligomer, determined from the molecular weight of the mPEG-block as provided by the supplier, and the molecular weight of the OLA-block as calculated from the MS results.*
[b] *Weight fraction of the hydrophilic (F_H) and the lipophilic (F_L) blocks, PEG and OLA, respectively.*
[c] *L-lactate degree of polymerisation as determined by ^1H NMR in $CDCl_3$.*

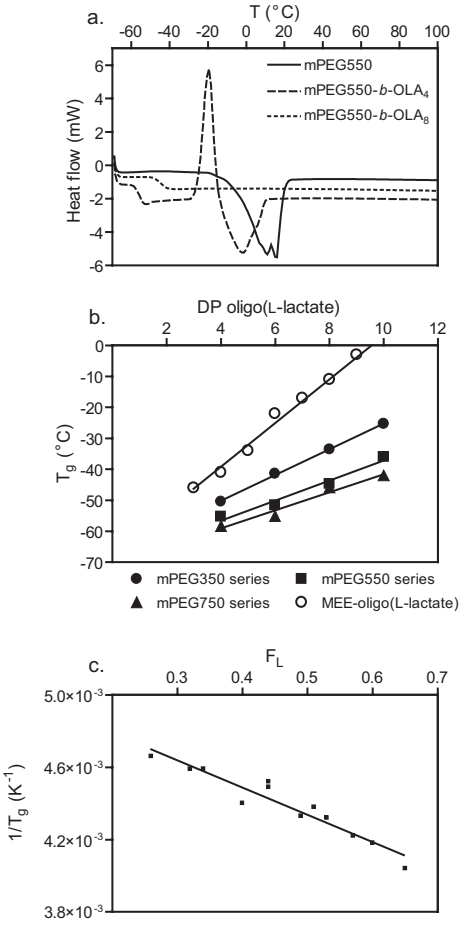

Figure 3 Thermograms of mPEG 550, mPEG550-*b*-OLA_4, and mPEG550-*b*-OLA_8 (a). T_g as a function of the degree of polymerization (DP) of OLA for the mPEG350- (circles), mPEG550- (squares), and mPEG750- (triangles) series, including the data published for MEE-oligo(L-lactate) (open circles)[37] (b). $1/T_g$ (T_g in degrees Kelvin) as a function of the weight fraction of OLA (F_L) in the mPEG-*b*-OLA oligomers (c).

Besides a glass transition temperature, the oligomers with a large PEG-fraction (F_H>0.57) showed a melting endotherm at -10 to 15 °C, preceded by a recrystallisation peak (Figure 3a), which is ascribed to the PEG-block of the oligomer. The observed melting temperature is lower than that of the mPEG homopolymer (0 - 20 °C, Figure 3a). The decrease and ultimately the disappearance of a melting peak of the mPEG-block, when the size of the attached hydrophobic block increases, confirms the miscibility of the two blocks.

The behaviour of mPEG-*b*-oligo(L-lactate)s in water

The critical aggregation concentration (CAC) of the different block oligomers was determined using pyrene as a fluorescent probe. Transfer of pyrene from a hydrophilic to a more hydrophobic environment results in a red shift in the excitation spectrum.[38, 39] This red shift in the pyrene excitation spectra, as well as an increase in the intensity of the fluorescence signal, was indeed observed with increasing mPEG-*b*-OLA concentrations. For one series of block oligomers (mPEG750-series), the intensity ratio of I_{338}/I_{333} is plotted against the block oligomer concentration (Figure 4). The increase in the intensity ratio I_{338}/I_{333} starts at lower concentrations when the OLA-block is longer. This was observed for the other PEG-series as well. Logically, larger OLA-chains are more hydrophobic, and consequently have a lower aqueous solubility.[48] Similar results were described for the CAC determination of other surfactants with increasing size of the hydrophobic block, such as phospholipids, mPEG-oligo(ε-caprolactone)[49] and high molecular weight PEG-*b*-PLA.[23] Furthermore, the slope of the intensity versus concentration curve above the CAC is lower for oligomers with low DPs of 4 or 6, than for those with high DPs of 8 or 10 (Figure 4). This is likely related to the difference in hydrophobicity as well.[38, 49] The observed shift in the curves (Figure 4) is not reflected by the CAC values as presented in Table 2. This can be ascribed to a relatively high variation of 0.3 mg/mL in the values, and it indicates that the CACs of the different oligomers do not differ significantly. The CAC values of 0.4-1 mg/mL obtained in this study are 10-1000-fold higher than those of PEG-*b*-PLA with higher molecular weights.[23, 28, 32] This can be explained by the higher hydrophobicity of high molecular weight PLA compared to low molecular weight oligolactate. In addition, the mobility of the hydrophobic chains likely plays a role. For high molecular weight PEG-*b*-PDLLA a sudden increase (factor of 2-5) in the CAC has been observed when the temperature is increased above the glass transition temperature of the poly(DL-lactate) chain.[32] In contrast to poly(DL-lactate), the T_g of the oligomers described here is far below room temperature (Figure 3), resulting in highly mobile oligomers at the experimental conditions, which may contribute to the high CAC. Furthermore, the effect of temperature and ionic

strength on the CAC was investigated. Neither an increase in temperature (37 °C) nor an increase in salt concentration (150 mM NaCl) resulted in significantly different CAC values.

Dispersions of the mPEG-*b*-OLAs were formed by the film-hydration method and the hydrodynamic radius (R_h) and size distribution (polydispersity index, PDI) of the particles were measured by DLS. HPLC analysis showed that after film-hydration of the fractionated block oligomers, more than 80% of the material was present in the dispersions. Directly after film-hydration at room temperature with 10 mM ammonium acetate buffer, pH 5, at a concentration of 10 mg/mL, mPEG350-*b*-OLA_{10} and mPEG550-*b*-OLA_{10} formed highly turbid dispersions, while all other fractionated block oligomers formed opaque to clear dispersions. In the latter dispersions particles with an R_h of 130-300 nm were detected using DLS (Table 3). To measure

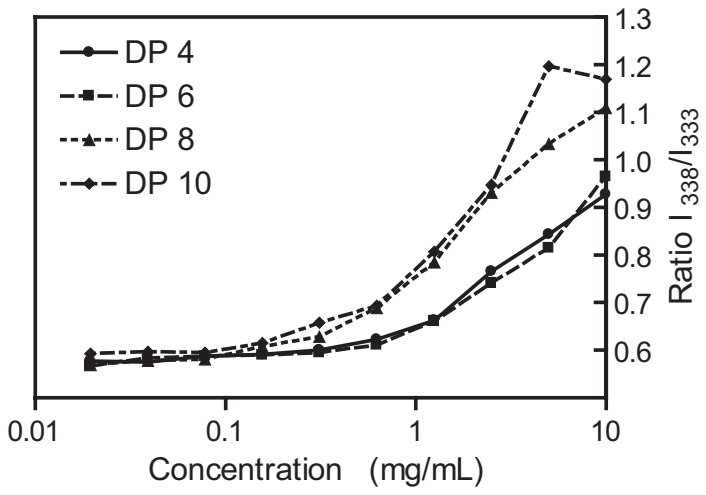

Figure 4 Fluorescence intensity ratio I_{338}/I_{333} of pyrene as a function of the concentration of mPEG750-*b*-oligo(L-lactate) with different OLA chain lengths.

Table 2 Critical aggregation concentrations of mPEG-b-oligo(L-lactate) (mg/mL) in 10 mM ammonium acetate buffer, pH 5, at room temperature[a]

No. of lactic acid units	mPEG350-*b*-OLA	mPEG550-*b*-OLA	mPEG750-*b*-OLA
4	1.0	1.0	0.6
6	0.8	1.0	0.6
8	0.9	0.7	0.5
10	0.5	1.0	0.4

[a] *Variations in the values are 0.2-0.3 mg/mL (n=3).*

the two highly turbid dispersions by DLS, the samples were diluted 10-fold with buffer, which resulted in opaque to clear dispersions. Nanoparticles with a 130 nm radius were measured in the diluted mPEG550-*b*-OLA_{10} dispersion; the dispersion of the mPEG350-*b*-OLA_{10} contained structures with a size larger than 1 μm. Table 3 shows that there are no significant differences in size between the dispersions of the nanoparticle forming block oligomers. Remarkably, hydration of a film of polydisperse, non-fractionated mPEG-*b*-OLA with an average DP of 6 or 10, did not result in the formation of stable nanoparticles, but rather in large aggregates (> 1 μm). This indicates that the monodispersity of the hydrophobic block favours the formation of small particles. Given the size of the nanoparticles (130-300 nm) and the molecular dimensions of the oligomers (the end-to-end distance is a few nanometers), it can be excluded that mPEG-*b*-OLA self-assembled into micelles. To obtain more insight into the structure of the nanoparticles, static light scattering experiments were performed, as discussed in the next section.

Interestingly, the two samples that formed highly turbid dispersions at room temperature showed changes in turbidity upon heating. For example, the static light scattering intensity of mPEG550-*b*-OLA_{10} decreased at 25 °C, but increased again upon further heating above 45 °C (Figure 5). As will be explained below, these phase transition temperatures can probably be attributed to a Krafft point and a cloud point, respectively. The more hydrophobic mPEG350-*b*-OLA_{10} and the more hydrophilic mPEG750-*b*-OLA_{10} showed an increase in scattering intensity at 35 and at 66 °C, respectively, representing the cloud points of these polymers (Figure 5). Two of the other block oligomers, mPEG350-*b*-OLA_8 and mPEG550-*b*-OLA_8 exhibited a cloud point as well, at 41 and 60 °C, respectively (data not shown). A positive linear relation is observed between the cloud point and the size of the PEG-fraction (F_H) of the polymer. Upon further heating the dispersions above the cloud point, a drop in scattering intensity, likely due to aggregation and subsequent sedimentation of the nanoparticles, was observed at 37, 53, and 71 °C for mPEG350-*b*-OLA_{10}, mPEG550-*b*-OLA_{10}, and mPEG750-*b*-OLA_{10}, respectively (Figure 5).

Table 3 Particle formation of mPEG-*b*-oligo(L-lactate) by the film-hydration method at a concentration of 10 mg/mL in 10 mM ammonium acetate buffer, pH 5[a]

No. of	mPEG350-*b*-OLA		mPEG550-*b*-OLA		mPEG750-*b*-OLA	
lactic acid units	R_h (nm)	PDI	R_h (nm)	PDI	R_h (nm)	PDI
4	162 ±35	0.36±0.06	127±13	0.41±0.05	295±95	0.37±0.04
6	164±37	0.33±0.14	172±25	0.42±0.08	226±121	0.43±0.06
8	287±51	0.19±0.12	246±170	0.27±0.14	190±62	0.39±0.11
10	>1 μm	ND[b]	133±23[c]	0.30±0.08[c]	187±12	0.23±0.19

[a] *Data are given as average hydrodynamic radius (R_h) and polydispersity index (PDI) ± standard deviation (n=3-8 individual preparations).*
[b] *ND = Not determined.*
[c] *1 mg/mL.*

Because of the observed temperature dependent light scattering intensities, we studied the particle sizes of two oligomers at elevated temperatures. With mPEG350-*b*-OLA_{10}, nanosized particles were still not observed at 50 °C. However, upon heating of the highly turbid 10 mg/mL dispersion of mPEG550-*b*-OLA_{10} from room temperature to 37 °C, a clear dispersion was obtained which contained particles with an R_h of 89 ± 52 nm (mean ± SD) and a PDI of 0.49 ± 0.05 (n = 3). Therefore, the Krafft point (= the temperature at which the solubility equals the CAC) can be ascribed to a temperature-induced transition from large aggregates to nanoparticles (*vide infra*). The more hydrophilic mPEG750-*b*-OLA_{10} (and also the other block oligomers) already formed nanoparticles at room temperature, and the absence of a Krafft point may be explained by a 'virtual Krafft point' below 0 °C. On the other hand, it can be expected that the Krafft point of the more hydrophobic mPEG350-*b*-OLA_{10} occurs at a temperature above the cloud point of this polymer, which prevents the formation of nanoparticles. The observed cloud points are likely caused by the dehydration of the PEG-block, as found by Jeong *et al.* for the phase behaviour (sol-gel transition) of aqueous systems of PEG-PL(G)A based block copolymers.[8, 9, 50-52] The dehydration of PEG has also been suggested to be responsible for the observed cloud point in mPEG-oligo(ε-caprolactone) dispersions at temperatures above 50 °C.[49]

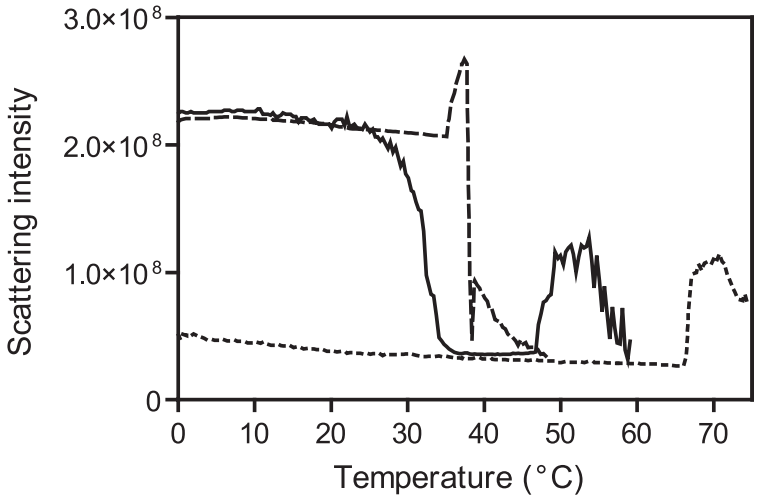

Figure 5 Temperature sensitive behaviour by static light scattering from mPEG350-*b*-OLA_{10} (dashed line), mPEG550-*b*-OLA_{10} (solid line), and and mPEG750-*b*-OLA_{10} (dotted line) in 10 mM ammonium acetate buffer, pH 5, at a concentration of 10 mg/mL.

Characterisation of mPEG-*b*-oligo(L-lactate) nanoparticles

The stability of the nanoparticles in time was studied upon incubation in buffer pH 5 at room temperature. A pH of 5 was used to retard hydrolytic degradation of the oligomers.[40] Most mPEG-*b*-OLA oligomers gave rather stable dispersions, with the exception of the mPEG350-series and mPEG750-*b*-OLA_4, as shown in Figure 6. The scattering intensity and polydispersity measured in the other samples remained constant, and the size only slightly increased during two weeks of incubation at room temperature. These results indicate that both the size of the PEG-block and the total hydrophilicity (as reflected by the PEG-fraction, F_H) of the block oligomer are important factors that determine the stability of the nanoparticles. Apparently, an mPEG block size of 350 Da does not provide protection to prevent aggregation (Figure 6). This suggests the presence of an outer PEG-layer in the nanoparticles. The effect of the total hydrophilicity of the polymers becomes clear from the low stability of mPEG750-*b*-OLA_4 particles as compared to mPEG550-*b*-OLA_4 particles (Figure 6a). The former oligomer contains the highest PEG-fraction (F_H) of the oligomers investigated in this study.

Uptake of water by the nanoparticles or dissolution of this relatively hydrophilic oligomer may cause the rapid increase in particle size. Although the presence of salt ions did not significantly influence the size of the particles directly after preparation, the particle size measured in the dispersion in acetate buffered saline increased more rapidly than in 10 mM buffer. For example, mPEG550-*b*-OLA_4 formed particles with an R_h of 120 nm after hydration with acetate buffered saline. Their size increased rapidly, to > 500 nm within 3 h, indicating a low stability. Dehydration of the PEG-chain by the ions present may result in a less effective barrier, causing aggregation.

The weight average molecular weight of the nanoparticles (M_{wNP}) and their radius of gyration (R_g) were determined by multiangle static light scattering measurements (SLS) at 25 °C (Table 4). The M_{wNP} ranged between 0.8×10^8 and 4×10^8 g/mol, and the R_g between 200 and 250 nm. The ratio R_g/R_h provides information about the morphology of the particles. Three of the investigated particles showed an R_g/R_h ratio of 1.2. This value is higher than the one expected for uniform spheres (0.775) or vesicular structures (1.0),[53-55] and lower than values obtained with random coil chains in good solvents or wormlike/rodlike chains (1.5 and 2, respectively).[53, 54] The value of 1.2 lies between 1 and 1.3, which have been described for a branching chain.[53] An R_g/R_h ratio of 1.17 was found for random aggregates,[56] and 1.1 for self-assembled polycaprolactone-*b*-PEG-*b*-polycaprolactone (PCL-PEG-PCL) copolymers in water.[53] It was suggested that the latter polymers formed particles in which some of the PCL-chains stretched out of the hydrophobic core, thereby increasing R_g without

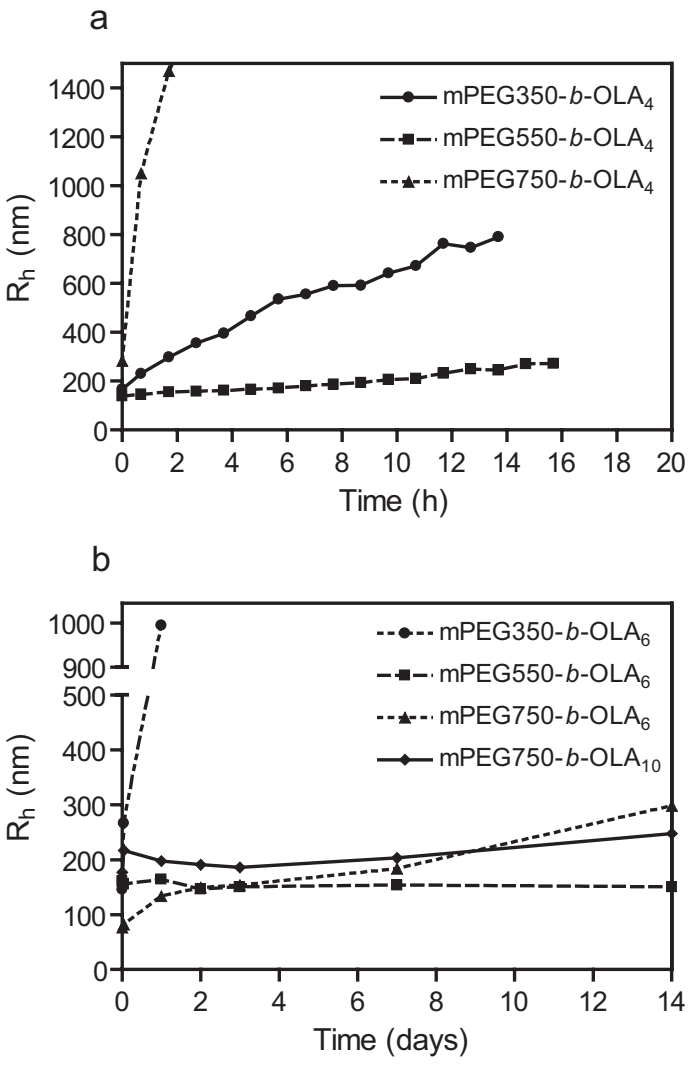

Figure 6 Hydrodynamic radius of mPEG-*b*-oligo(L-lactate) particles as function of time in hours (a) or days (b) at room temperature at pH 5.

an effect on the R_h.[53] This may also apply to the oligomers investigated in this study, which likely form nanoaggregates. The particles of the relatively hydrophilic oligomer mPEG750-*b*-OLA$_6$ had an R_g/R_h ratio of 0.58. This value is lower than for uniform spheres and indicates the presence of a thick hydration layer.[55] All nanoparticles investigated have an N_{agg} around 1×10^5. This is a high value compared to those of other self-assembled systems such as the previously mentioned PCL-*b*-PEG-*b*-PCL particles (maximum N_{agg} of 3600)[53] and assemblies composed of high molecular weight PEG-*b*-PLA (N_{agg} of 1100 for the largest copolymer).[30] The low molecular weight of the oligomers used here, and the type of particles formed, may explain the differences. The densities of the particles are very low, *i.e.* between 0.6 and 25 mg/mL, and increase with the OLA-fraction (F_L) of the oligomer (Table 4).

An estimation of the density of PEG-*b*-PLA micelles described by Riley *et al.* indicates that these high molecular weight polymers form particles with slightly higher densities.[30] For example, the density of PEG5000-*b*-PLA4000 is 52 mg/mL, and increases up to 200 mg/mL for PEG5000-*b*-PLA45000 particles.[30] The lower density of the mPEG-*b*-OLA particles suggests that they are highly hydrated. Likely, PEG is present inside the nanoaggregates, caused by the miscibility of the both blocks of the oligomers as shown by DSC (Figure 3).

Attempts were made to investigate the morphology of the nanoparticles by cryo-TEM. Interestingly, the highly turbid 10 mg/mL dispersion of mPEG550-*b*-OLA$_{10}$ that was formed at room temperature (*vide supra*) shows the presence of large (micrometer-sized) lamellar structures (Figure 7). These structures could not be detected after the sample was heated above the Krafft point (>37 °C) or after 10-fold dilution of the sample with buffer, though nanoparticles were measured in these samples by DLS. In the dispersions formed with the other block oligomers structures were not observed by cryo-TEM either, whereas nanoparticles were detected by DLS. These observations can be explained by the lack of contrast due to the presence of water in the nanoparticles and their low density as demonstrated by SLS. Apparently, mPEG550-*b*-OLA$_{10}$ forms highly organised structures below its Krafft point. Dilution

Table 4 Characteristics of mPEG-*b*-oligo(L-lactate) nanoparticles in 10 mM ammonium acetate buffer, pH 5, at 25 °C, one day after preparation as determined by dynamic (R_h) and static light scattering

Oligomer (F_H)	R_h (nm)	R_g (nm)	R_g/R_h	M_{wNP} (g/mol)	ρ_{NP} (g/mL)	N_{agg}
MPEG550-*b*-OLA6 (0.56)	177	203	1.15	9.6×10^7	6.9×10^{-3}	9.8×10^4
MPEG750-*b*-OLA6 (0.63)	390	227	0.58	8.5×10^7	5.6×10^{-4}	7.2×10^4
MPEG750-*b*-OLA8 (0.57)	200	245	1.23	1.6×10^8	7.8×10^{-3}	1.2×10^5
MPEG750-*b*-OLA10 (0.51)	191	224	1.17	4.3×10^8	2.5×10^{-2}	3.0×10^5

to a concentration close to the CAC or heating to a temperature above the Krafft point results in the loss of the lamellar structure and the formation of nanoparticles that, because of their high hydration, cannot be observed by cryo-TEM.

^{1}H NMR measurements in D_2O give information about the mobility of polymer chains in aqueous dispersions, and have been used to confirm core-shell structures of self-assembled amphiphilic molecules. As a result of the formation of a 'solid-like' core by hydrophobic blocks upon self-assembly in D_2O, only the peaks of the hydrophilic block are visible in the NMR-spectrum.[26, 32, 33, 39] ^{1}H NMR spectra obtained from 10 mg/mL dispersions of the block oligomers in D_2O closely resembled the spectra of solutions of the block oligomers in $CDCl_3$, except for mPEG350-*b*-OLA_{10} and mPEG550-*b*-OLA_{10} (data not shown). With the latter oligomers, which formed highly turbid dispersions, the peaks of the OLA-part (relative to the mPEG-part) were 10-20% lower in the NMR spectrum in D_2O than in the spectrum of the oligomers in $CDCl_3$. DLS measurements of the aqueous dispersions in D_2O revealed that, except for mPEG350-*b*-OLA_{10} and mPEG550-*b*-OLA_{10}, the oligomers formed nanoparticles with the same size as in ammonium acetate buffer. The NMR results indicate that the mPEG-*b*-OLA nanoparticles do not contain a 'solid-like' core. This may result from the water-absorbing capacity of the particle core, which is in agreement with the SLS data. Also the high mobility of the oligomers at temperatures far above their glass transition temperature may contribute to these results.

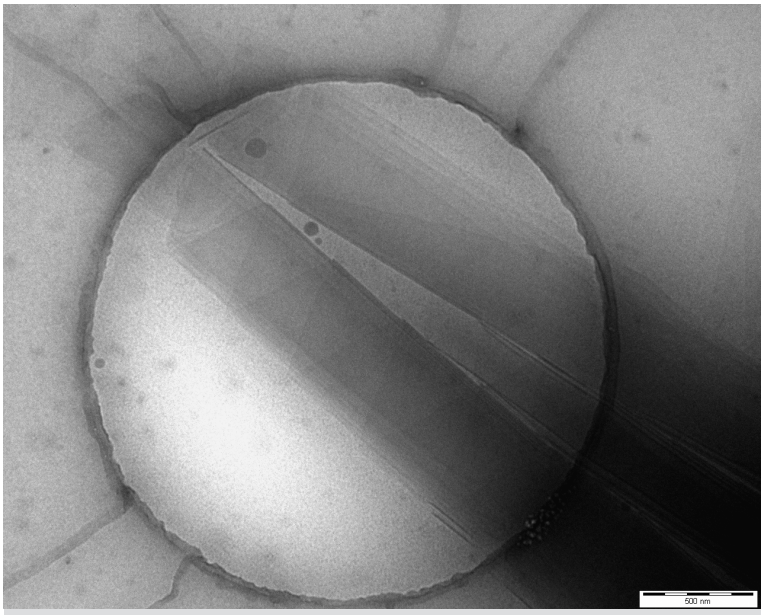

Figure 7 Cryo-TEM image of 10 mg/mL mPEG550-*b*-OLA_{10} dispersion in acetate buffer, pH 5, at room temperature. Folded lamellar structures are visible spanning a hole in the microscope grid. The bar corresponds to 500 nm.

Conclusions

MPEG-*b*-oligo(L-lactate) block oligomers (mPEG 350, mPEG 550, and mPEG 750; OLA DP 4-10) with monodisperse hydrophobic OLA-blocks have self-emulsifying properties to yield nanosized particles (radius ranging from 130-300 nm). The presence of OLA-signals in the ^{1}H NMR spectrum in D_2O and the SLS data suggests that the particles have a liquid nature. This results from the presence of water as reflected by the low density measured by SLS. In addition, the polymers in the absence of water are above their T_g as shown by DSC. Likely, PEG is present inside the nanoaggregates, caused by the miscibility of the both blocks of the oligomer, and thereby contributing to the high water absorbing capacity of the particles. The stability of the particles composed of oligomers with mPEG550 and mPEG750 suggests that these mPEG-blocks form the outer layer of the particles. A schematic representation of the mPEG-*b*-OLA nanoaggregates is given in Figure 8. Their self-emulsifying properties, together with the expected biodegradability and biocompatibility, make these mPEG-*b*-oligo(L-lactate)s very suitable molecules for pharmaceutical applications, such as the solubilisation of therapeutic proteins and drugs. This is currently being investigated.

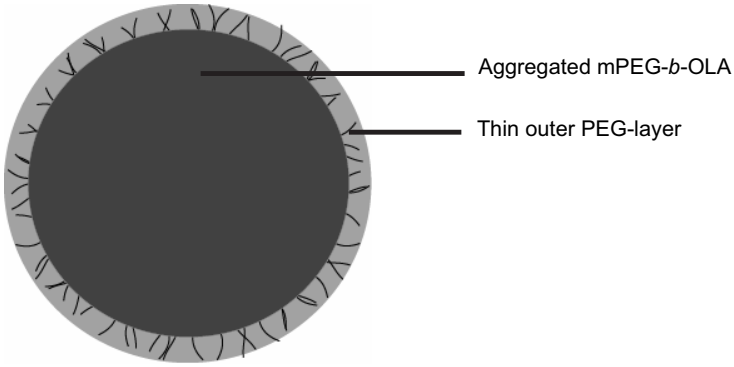

Figure 8 Schematic representation of an mPEG-*b*-oligo(L-lactate) nanoparticle formed by the film-hydration method.

References

1. Edlund U; Albertsson AC, Polyesters based on diacid monomers. *Adv Drug Deliver Rev* 55, 585-609 (2003).
2. Panyam J; Labhasetwar V, Biodegradable nanoparticles for drug and gene delivery to cells and tissue. *Adv Drug Deliver Rev* 55, 329-347 (2003).
3. Vert M, Aliphatic polyesters: great degradable polymers that cannot do everything. *Biomacromolecules* 6, 538-546 (2005).
4. Jiang W; Gupta RK; Deshpande MC; Schwendeman SP, Biodegradable poly(lactic-co-glycolic acid) microparticles for injectable delivery of vaccine antigens. *Adv Drug Deliver Rev* 57, 391-410 (2005).
5. Cleland JL; Johnson OL; Putney S; Jones AJS, Recombinant human growth hormone poly(lactic-co-glycolic acid) microsphere formulation development. *Adv Drug Deliver Rev* 28, 71-84 (1997).
6. Gref R; Domb A; Quellec P; Blunk T; Muller RH; Verbavatz JM; Langer R, The controlled intravenous delivery of drugs using PEG-coated sterically stabilized nanospheres. *Adv Drug Deliver Rev* 16, 215-233 (1995).
7. Leroux J-C; Allemann E; De Jaeghere F; Doelker E; Gurny R, Biodegradable nanoparticles - From sustained release formulations to improved site specific drug delivery. *J Control Release* 39, 339-350 (1996).
8. Jeong B; Bae YH; Kim SW, Drug release from biodegradable injectable thermosensitive hydrogel of PEG-PLGA-PEG triblock copolymers. *J Control Release* 63, 155-163 (2000).
9. Jeong B; Bae YH; Lee DS; Kim SW, Biodegradable block copolymers as injectable drug-delivery systems. *Nature* 388, 860-862 (1997).
10. Ruan G; Feng S-S, Preparation and characterization of poly(lactic acid)-poly(ethylene glycol)-poly(lactic acid) (PLA-PEG-PLA) microspheres for controlled release of paclitaxel. *Biomaterials* 24, 2037-5044 (2003).
11. Govender T; Riley T; Ehtezazi T; Garnett MC; Stolnik S; Illum L; Davis SS, Defining the drug incorporation properties of PLA-PEG nanoparticles. *Int J Pharm* 199, 95-110 (2000).
12. Lucke A; Tessmar J; Schnell E; Schmeer G; Gopferich A, Biodegradable poly(lactic acid)-poly(ethylene glycol)-monomethyl ether diblock copolymers: structures and surface properties relevant to their use as biomaterials. *Biomaterials* 21, 2361-2370 (2000).
13. Breitenbach A; Li YX; Kissel T, Branched biodegradable polyesters for parenteral drug delivery systems. *J Control Release* 64, 167-178 (2000).
14. Luo L; Ranger M; Lessard DG; Garrec DL; Gori S; Leroux J-C; Rimmer S; Smith D, Novel amphiphilic diblock copolymer of low molecular weight poly(N-vinylpyrrolidone)-block-poly(D,L-lactide): Synthesis, characterization, and micellization. *Macromolecules* 37, 4008-4013 (2004).
15. Hennink WE; de Jong SJ; Bos GW; Veldhuis TFJ; van Nostrum CF, Biodegradable dextran hydrogels crosslinked by stereocomplex formation for the controlled release of pharmaceutical proteins. *Int J Pharm* 277, 99-104 (2004).
16. Torchilin VP; Trubetskoy VS, Which polymers can make nanoparticulate drug carriers long-circulating? *Adv Drug Deliver Rev* 16, 141-155 (1995).
17. Allen TM; Hansen C, Pharmacokinetics of stealth versus conventional liposomes: effect of dose. *Biochim Biophys Acta* 1068, 133-141 (1991).
18. Woodle MC; Lasic DD, Sterically stabilized liposomes. *Biochim Biophys Acta* 1113, 171-199 (1992).
19. Verrecchia T; Spenlehauer G; Bazile DV; Murry-Brelier A; Archimbaud Y; Veillard M, Non-stealth (poly(lactic acid/albumin)) and stealth (poly(lactic acid-polyethylene glycol)) nanoparticles as injectable drug carriers. *J Control Release* 36, 49-61 (1995).
20. Gref R; Luck M; Quellec P; Marchand M; Dellacherie E; Harnisch S; Blunk T; Muller RH, 'Stealth' corona-core nanoparticles surface modified by polyethylene glycol (PEG): influences of the corona (PEG chain length and surface density) and of the core composition on phagocytic uptake and plasma protein adsorption. *Colloid Surface B* 18, 301-313 (2000).
21. Zambaux MF; Bonneaux F; Gref R; Dellacherie E; Vigneron C, MPEO-PLA nanoparticles: effect of MPEO content on some of their surface properties. *J Biomed Mater Res* 44, 109-115 (1999).
22. Nguyen CA; Allemann E; Schwach G; Doelker E; Gurny R, Cell interaction studies of PLA-MePEG nanoparticles. *Int J Pharm* 254, 69-72 (2003).

23. Chognot D; Six JL; Leonard M; Bonneaux F; Vigneron C; Dellacherie E, Physicochemical evaluation of PLA nanoparticles stabilized by water-soluble MPEO-PLA block copolymers. *J Colloid Interf Sci* 268, 441-447 (2003).
24. Zweers MLT; Engbers GHM; Grijpma DW; Feijen J, In vitro degradation of nanoparticles prepared from polymers based on DL-lactide, glycolide and poly(ethylene oxide). *J Control Release* 100, 347-356 (2004).
25. Miura H; Onishi H; Sasatsu M; Machida Y, Antitumor characteristics of methoxypolyethylene glycol-poly(-lactic acid) nanoparticles containing camptothecin. *J Control Release* 97, 101-113 (2004).
26. Hrkach JS; Peracchia MT; Bomb A; Lotan N; Langer R, Nanotechnology for biomaterials engineering: structural characterization of amphiphilic polymeric nanoparticles by 1H NMR spectroscopy. *Biomaterials* 18, 27-30 (1997).
27. Hagan SA; Coombes AGA; Garnett MC; Dunn SE; Davies MC; Illum L; Davis SS; Harding SE; Purkiss S; Gellert PR, Polylactide-poly(ethylene glycol) copolymers as drug delivery systems. 1. Characterization of water dispersible micelle-forming systems. *Langmuir* 12, 2153 - 2161 (1996).
28. Yasugi K; Nagasaki Y; Kato M; Kataoka K, Preparation and characterization of polymer micelles from poly(ethylene glycol)-poly(D,L-lactide) block copolymers as potential drug carrier. *J Control Release* 62, 89-100 (1999).
29. Kim SY; Kim JH; Kim D; An JH; Lee DS; Kim SC, Drug-releasing kinetics of MPEG/PLLA block copolymer micelles with different PLLA block lengths. *J Appl Poly Sci* 82, 2599-2605 (2001).
30. Riley T; Stolnik S; Heald CR; Xiong CD; Garnett MC; Illum L; Davis SS; Purkiss SC; Barlow RJ; Gellert PR, Physicochemical evaluation of nanoparticles assembled from poly(lactic acid)-poly(ethylene glycol) (PLA-PEG) block copolymers as drug delivery vehicles. *Langmuir* 17, 3168 - 3174 (2001).
31. Riley T; Heald CR; Stolnik S; Garnett MC; Illum L; Davis SS; King SM; Heenan RK; Purkiss SC; Barlow RJ; Gellert PR; Washington C, Core-shell structure of PLA-PEG nanoparticles used for drug delivery. *Langmuir* 19, 8428-8435 (2003).
32. Yamamoto Y; Yasugi K; Harada A; Nagasaki Y; Kataoka K, Temperature-related change in the properties relevant to drug delivery of poly(ethylene glycol)-poly(D,L-lactide) block copolymer micelles in aqueous milieu. *J Control Release* 82, 359-371 (2002).
33. Heald CR; Stolnik S; Kujawinski KS; De Matteis C; Garnett MC; Illum L; Davis SS; Purkiss SC; Barlow RJ; Gellert PR, Poly(lactic acid)-poly(ethylene oxide) (PLA-PEG) nanoparticles: NMR studies of the central solidlike PLA core and the liquid PEG corona. *Langmuir* 18, 3669-3675 (2002).
34. Meng F; Hiemstra C; Engbers GHM; Feijen J, Biodegradable polymersomes. *Macromolecules* 36, 3004-3006 (2003).
35. Ahmed F; Discher DE, Self-porating polymersomes of PEG-PLA and PEG-PCL: hydrolysis-triggered controlled release vesicles. *J Control Release* 96, 37-53 (2004).
36. Meng F; Engbers GHM; Feijen J, Biodegradable polymersomes as a basis for artificial cells: encapsulation, release and targeting. *J Control Release* 101, 187-198 (2005).
37. de Jong SJ; van Dijk-Wolthuis WNE; Kettenes-van den Bosch JJ; Schuyl PWJ; Hennink WE, Monodisperse enantiomeric lactic acid oligomers: Preparation, characterization, and stereocomplex formation. *Macromolecules* 31, 6397-6402 (1998).
38. Wilhelm M; Zhao CL; Wang Y; Xu R; Winnik MA; Mura JL; Riess G; Croucher MD, Poly(styrene-ethylene oxide) block copolymer micelle formation in water: a fluorescence probe study. *Macromolecules* 24, 1033-1040 (1991).
39. Soga O; van Nostrum CF; Ramzi A; Visser T; Soulimani F; Frederik PM; Bomans PHH; Hennink WE, Physicochemical characterization of degradable thermosensitive polymeric micelles. *Langmuir* 20, 9388-9395 (2004).
40. de Jong SJ; Arias ER; Rijkers DTS; van Nostrum CF; Kettenes-van den Bosch JJ; Hennink WE, New insights into the hydrolytic degradation of poly(lactic acid): participation of the alcohol terminus. *Polymer* 42, 2795-2802 (2001).
41. Zimm BJ, Apparatus and methods for measurement and interpretation of the angular variation of light scattering; Preliminary results on polystyrene solutions. *J Chem Phys* 16, 1099-1116 (1948).
42. Lee H; Lee W; Chang T; Choi S; Lee D; Ji H; Nonidez WK; Mays JW, Characterization of poly(ethylene oxide)-block-poly(L-lactide) by HPLC and MALDI-TOF mass spectrometry. *Macromolecules* 32, 4143-4146 (1999).

43. Polymer Handbook. 3rd ed.; John Wiley and Sons, Inc: New York, USA (1989).
44. Lai W-C; Liau W-B; Lin T-T, The effect of end groups of PEG on the crystallization behaviors of binary crystalline polymer blends PEG/PLLA. *Polymer* 45, 3073-3080 (2004).
45. Nijenhuis AJ; Colstee E; Grijpma DW; Pennings AJ, High molecular weight poly(L-lactide) and poly(ethylene oxide) blends: thermal characterization and physical properties. *Polymer* 37, 5849-5857 (1996).
46. Younes H; Cohn D, Phase separation in poly(ethylene glycol)/poly(lactic acid) blends. *Eur Polym J* 24, 765-773 (1988).
47. Göpferich A; Gref R; Minamitake Y; Shieh L; Alonso M-J; Tabata Y; Langer R Drug delivery from bioerodible polymers: systemic and intravenous administration, In: *Protein Formulations and Delivery*, (J. Cleland and R. Langer, Eds.) American Chemical Society, Washington, p 242 - 277 (1994).
48. Braud C; Devarieux R; Garreau H; Vert M, Capillary electrophoresis to analyze water-soluble oligo(hydroxyacids) issued from degraded or biodegraded aliphatic polyesters. *J Environ Polym Degr* 4, 135-148 (1996).
49. Letchford K; Zastre J; Liggins R; Burt H, Synthesis and micellar characterization of short block length methoxy poly(ethylene glycol)-block-poly(caprolactone) diblock copolymers. *Colloid Surface B* 35, 81-91 (2004).
50. Jeong B; Bae YH; Kim SW, Biodegradable thermosensitive micelles of PEG-PLGA-PEG triblock copolymers. *Colloid Surface B* 16, 185-193 (1999).
51. Jeong B; Kibbey MR; Birnbaum JC; Won Y-Y; Gutowska A, Thermogelling biodegradable polymers with hydrophilic backbones: PEG-g-PLGA. *Macromolecules* 33, 8317-8322 (2000).
52. Jeong B; Windisch CFJ; Park MJ; Sohn YS; Gutowska A; Char K, Phase transition of the PLGA-g-PEG copolymer aqueous solutions. *J Phys Chem B* 107, 10032-10039 (2003).
53. Nie T; Zhao Y; Xie Z; Wu C, Micellar formation of poly(caprolactone-*block*-ethylene oxide-*block*-caprolactone) and its enzymatic biodegradation in aqueous dispersion. *Macromolecules* 36, 8825-8829 (2003).
54. Checot F; Lecommandoux S; Klok H-A; Gnanou Y, From supromolecular polymersomes to stimuli-responsive nano-capsules based on poly(diene-b-peptide) diblock copolymers. *Eur Phys J E* 10, 25-35 (2003).
55. Dai S; Ravi P; Tam KC; Mao BW; Gan LH, Novel pH-responsive amphiphilic diblock copolymers with reversible micellization properties. *Langmuir* 19, 5175-5177 (2003).
56. Bloomfield VA, Static and dynamic light scattering from aggregating particles. *Biopolymers* 54, 168-172 (2000).

Small oligomeric micelles based on end group modified mPEG-oligo(ε-caprolactone) with monodisperse hydrophobic blocks

4

Myrra G. Carstens,[a,b] Jan J.L. Bevernage,[a]

Cornelus F. van Nostrum,[a] Mies J. van Steenbergen,[a]

Frits M. Flesch,[a] Ruud Verrijk,[b] Leo G.J. de Leede,[b]

Daan J.A. Crommelin,[a] Wim E. Hennink[a]

[a] Department of Pharmaceutics, Utrecht Institute for Pharmaceutical Sciences (UIPS), Faculty of Pharmaceutical Sciences, Utrecht University, Utrecht, The Netherlands

[b] OctoPlus N.V., Leiden, the Netherlands

Macromolecules **2007**, *40 (1): p. 116-122*

Abstract

To design stable biodegradable micelles with a size smaller than 20 nm, the self-assembly of methoxy poly(ethylene glycol)-*b*-oligo(ε-caprolactone)s (mPEG-*b*-OCLs), and the effect of OCL-block length and terminal derivatisation with an aromatic group were studied. The studied oligomers consisted of an mPEG-block with a molecular weight of 750 Da and a monodisperse OCL-block of 1-7 units with a hydroxyl end group that was either unmodified, benzoylated or naphthoylated. They were prepared by preparative HPLC of the polydisperse block oligomers. Differential scanning calorimetry demonstrated that the two blocks were phase separated and crystallised separately. These block oligomers formed small and almost monodisperse oligomeric micelles with a hydrodynamic diameter of 8-15 nm, which could be tailored by the size of the hydrophobic block. The critical aggregation concentration (CAC) of the unmodified mPEG-*b*-OCLs was 0.03 - 4 mg/mL, and it decreased with increasing length of the OCL-chain. End group modification resulted in an extensive reduction of the CAC to values as low as 0.003 mg/mL. This is expected to result in a better stability of these oligomeric micelles towards dilution upon intravenous administration, which makes these modified mPEG-*b*-OCLs very promising candidates for drug delivery purposes.

Introduction

Polymeric micelles are nanoparticles with a core-shell structure that are formed by the self-assembly of amphiphilic block copolymers in water. They have interesting properties for a number of applications, in particular for drug delivery.[1-4] Generally, polymeric micelles have a size of 10-100 nm and their hydrophobic core can accommodate hydrophobic drugs, such as several anti-cancer agents.[1-4] Their small size and hydrophilic surface reduce uptake by the reticuloendothelial system (RES), resulting in long circulation times after intravenous injection. Consequently, polymeric micelles can extravasate and accumulate at tumours and other pathological sites, through the so-called enhanced permeability and retention (EPR) effect.[5] Poly(ethylene glycol)-*b*-polyesters are attractive and frequently studied polymers for the design of polymeric micelles. In particular polyesters such as poly(lactic acid) (PLA) and poly(ε-caprolactone) (PCL), have been used as the hydrophobic block of the amphiphilic polymers, because of their biodegradability and biocompatibility.[6-8] Poly(ethylene glycol) (PEG) is the most frequently used hydrophilic block, because of its low toxicity and 'stealth' properties.[9-11] The self-assembly of PEG-*b*-polyesters, as well as loading of several types of hydrophobic drugs, have been extensively studied in recent years.[12-20] These studies mainly focused on high molecular weight block copolymers, which form micelles with a diameter greater than 30 nm. Micelles with a smaller size however benefit more from the EPR-effect,[21] because of their longer circulation times and better tissue penetration, as demonstrated for shell crosslinked poly(*tert*-butyl acrylate)-*b*-poly(methyl acrylate) (PBA-*b*-PMA) and PBA-*b*-polystyrene (PBA-*b*-PS) nanoparticles.[22] Moreover, PEG5000-distearoyl phosphatidyl ethanolamine (PEG-DSPE) micelles of 15 nm showed superior tumour accumulation when compared to 100 nm liposomes, after intravenous administration to mice with a subcutaneously established Lewis lung carcinoma.[23] Considering the end-to-end distance of the block copolymers in relation to the required micellar size, the formation of small micelles necessitates the use of low molecular weight block oligomers, such as the biodegradable mPEG-*b*-oligo(ε-caprolactone)s (mPEG-*b*-OCL), as studied in this chapter. It is anticipated that the micellar size will depend on the size of the hydrophobic block, and, consequently, that the use of monodisperse hydrophobic blocks will result in better size control of the micelles.

Besides size, the stability of a polymeric micelle is a key factor for its efficacy as drug delivery system. In order to achieve long circulation times and to obtain accumulation at the target site, the micelle should remain intact *in vivo*. However, destabilisation of polymeric micelles may already occur upon injection into the bloodstream, since dilution may result in polymer concentrations below the critical aggregation concentration (CAC). This likely explains the limited number of reports on stable sub-20 nm

nanoparticles, because the high CAC is inherent to the low molecular weight of the block oligomers forming these small micelles. Several strategies have been proposed to improve the micellar stability, including covalent[24-26] and physical[4, 25] crosslinking of the micellar core or shell, as well as modification of the polymers to reduce their CAC.[4, 27-30] The covalent crosslinking approach has been successfully applied by Shuai *et al.* to stabilise PEG-*b*-PCL micelles[26] and by Sun *et al.* to prepare the before mentioned small PBA-*b*-PMA and PBA-*b*-PS nanoparticles.[22] This strategy, however, carries the risk that the crosslinking procedure causes changes in the degradability of the block copolymer, as well as in the structural integrity of the loaded drug. Improved micellar stability has also been achieved by physical interactions between the amphiphilic block copolymers or with the encapsulated drug, for example by ionic interactions,[31] hydrogen bonding,[32] or stereocomplex formation.[33] The third strategy, reducing the polymer CAC by chemical modification of the hydrophobic block,[4, 27-30] is followed in the present study.

Here, we use mPEG-*b*-OCL with monodisperse hydrophobic blocks. This approach allows a detailed study of the effect of the block oligomer composition for the design of stable sub-20 nm micelles. We demonstrate that terminal derivatisation of mPEG-*b*-OCL with a benzoyl or naphthoyl group greatly improves its self-assembling properties, with regard to their future application *in vivo*.

Experimental section

Materials

Poly(ethylene glycol) mono(methyl ether) with a molecular weight of 750 Da and an M_w/M_n of 1.05 (methoxyPEG, mPEG750), ε-caprolactone (99%) and toluene were obtained from Acros Organics (Geel, Belgium). Stannous octoate (tin(II) bis(2-ethylhexanoate), $SnOct_2$, >95%), 2-(2-methoxyethoxy)ethanol (MEE, 99%), benzoyl chloride (99%), 2-naphthoyl chloride (98%), chloroform-*d* ($CDCl_3$, 99.8%D) and 8-anilino-1-naphthalene sulfonic acid magnesium salt (1,8-ANS) were purchased from Sigma Aldrich Chemie BV (Zwijndrecht, The Netherlands) and dichloromethane (DCM, peptide synthesis grade), acetonitrile (ACN, HPLC gradient grade), chloroform ($CHCl_3$, HPLC grade) and N,N-dimethylformamide (DMF, peptide synthesis grade) from Biosolve Ltd (Valkenswaard, The Netherlands). Acetone, triethylamine (TEA, >99%) and ammonium acetate were obtained from Merck (Darmstadt, Germany), pyrene from Fluka Chemie AG (Buchs, Switzerland), magnesium sulfate exsiccatus from Bufa BV (Uitgeest, The Netherlands) and phosphate buffered saline (PBS, pH 7.4) from Braun Melsungen AG (Melsungen, Germany). All chemicals were used as received; buffers were filtered through a 20 nm filter (Anotop®, Whatmann, Breda, The Netherlands) prior to use.

Synthesis, end group modification and fractionation of poly(ethylene glycol)-*b*-oligo(ε-caprolactone)

Poly(ethylene glycol)-*b*-oligo(ε-caprolactones) (mPEG-*b*-OCLs) were synthesised by ring opening polymerisation of ε-caprolactone, initiated by mPEG750, and catalysed by $SnOct_2$ (Scheme 1a).[7, 16, 34] In detail, ε-caprolactone (20 g) and mPEG750 in a molar ratio of 4/1 were heated to 130 °C. $SnOct_2$ (0.05 equiv.) dissolved in 1 mL of toluene was added and the mixture was stirred overnight at 130 °C and cooled down to room temperature. To yield benzoylated and naphthoylated mPEG-*b*-OCL, the hydroxyl end group of mPEG750-*b*-OCL was reacted with benzoyl chloride or 2-naphthoyl chloride, respectively, as follows (Scheme 1b): A 20 g sample of mPEG750-*b*-OCL was dissolved in 20 mL of dry DCM with a five fold excess of TEA. This solution was added dropwise to a solution of 5 equiv. of either benzoyl chloride or 2-naphthoyl chloride in 20 mL of dry DCM, and stirred overnight under nitrogen atmosphere. Finally, the solvent was removed under reduced pressure.

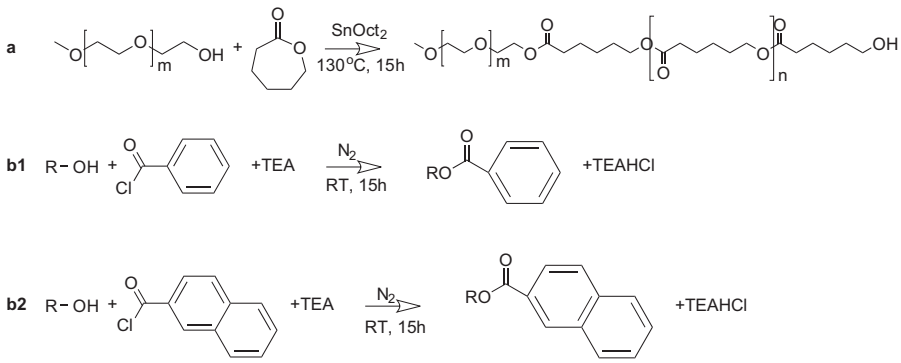

Scheme 1 Synthesis of MEE- and mPEG-*b*-oligo(ε-caprolactone) (a) and modification of the hydroxyl group by benzoylation (b1) or naphthoylation (b2).

The polydisperse oligomers were fractionated by preparative reversed phase HPLC (RP-HPLC), as reported in chapter 3 for mPEG-*b*-oligo(L-lactates)[35] with slight adaptations. The system consisted of a Waters 600EF Quaternary gradient pump and a Waters 2700 sample manager. A 5 mL aliquot of a 10% (w/w) solution of polydisperse block oligomer in 40/60 (w/w) ACN/1 M ammonium acetate buffer (pH 5) was injected onto the column (Waters Xterra Prep MS C18 10 µm, 19×250 mm, including a guard column). A gradient was run from 70% A (5/95 (w/w) ACN/H_2O) to 100% B (95/5 (w/w) ACN/H_2O) in 30 min and from 60% A to 100% B in 25 min for the unmodified and the modified oligomers, respectively. The flow rate was 17 mL/min, and the detection wavelengths were 195 and 210 nm, respectively. Fractions were collected, and after evaporation of the solvents the products were characterised.

To investigate the thermal behaviour (*vide infra*) of the hydrophobic blocks separately, 2-(2-methoxyethoxy)ethanol (MEE)-OCL was synthesised and fractionated as well, using the same procedure as for the synthesis and fractionation of mPEG750-*b*-OCL.

Characterisation of the block oligomers

The purity of the fractions was assessed by analytical RP-HPLC, using a model 2695 Alliance (consisting of a pump, autosampler and injector), and a model 2487 absorbance meter (Waters Chromatography BV). A 50 µL aliquot of a solution of 10 mg/mL in a mixture of 50/50 (w/w) ACN/10 mM ammonium acetate buffer pH 5 was injected onto the column (Waters XTerra MS C18, 5 µm, 4.6×250 mm, including a guard column). A gradient was run from 100% A (5/95 (w/w) ACN/H_2O) to 100% B (95/5 (w/w) ACN/H_2O) in 30 min at a flow rate of 1 mL/min. Peaks were detected by UV (λ=210 nm). The chromatograms were analysed using Empower software (Empower Pro, Waters Chromatography BV).

Electrospray ionisation mass spectrometry of oligomer samples of 0.1 mg/mL in 50/50 (v/v) ACN/10 mM ammonium acetate buffer pH 5 was performed using a Shimadzu LCMS QP8000. The cone voltage was +4.5 kV with a detector voltage of 1.5 kV. The CDL voltage was set at -10 V, the CDL temperature was 250 °C, and the deflector voltage was 80 V. The flow of the nebulising gas (N_2) was 4.5 L/min. Instrumental control was performed with a CLASS 8000 LCMS Software Package.

^{1}H NMR spectra were recorded using a Gemini spectrometer (Varian Associates Inc. NMR Instruments, Palo Alto, CA) operating at 300 MHz with $CDCl_3$ as a solvent. As reference line the chloroform peak at 7.24 ppm was used. Chemical shifts of MEE- and mPEG-*b*-OCL (δ, ppm): 4.19 (t, 2H, O-CH_2-C*H*$_2$-O-CO), 4.03 (t, 2H, CH_2-CH_2-C*H*$_2$-O-CO), 3.67-3.50 (m, O-C*H*$_2$-C*H*$_2$-O; C*H*$_2$-OH), 3.35 (s, 3H, O-C*H*$_3$), 2.33-2.27 (m, CO-C*H*$_2$-CH_2-CH_2), 1.64-1.53 (m, CO-CH_2-C*H*$_2$-CH_2-C*H*$_2$-CH_2-O), 1.37 (q, CO-CH_2-CH_2-C*H*$_2$-CH_2-CH_2-O). Chemical shifts of the benzoyl end group (δ, ppm): 8.0 (d, 2H, aromatic CH), 7.53 (t, 1H, aromatic CH), 7.41 (t, 2H, aromatic CH), 4.29 (t, 2H, C*H*$_2$-O-CO-(C_6H_5)). Chemical shifts of the naphthoyl end group (δ, ppm): 8.57 (s, 1H, aromatic CH), 8.02 (d, 1H, aromatic CH), 7.94 (d, 1H, aromatic CH), 7.86 (d, 2H, aromatic CH), 7.54 (m, 2H, aromatic CH), 4.29 (t, 2H, C*H*$_2$-O-CO-($C_{10}H_7$)).

Both fractionated and polydisperse oligomers were characterised by gel permeation chromatography (GPC), using a PLgel OligoPore column (300×7.5 mm, including a Guard column, 50×7.5 mm) (Polymer Laboratories) and low molecular weight PEG standards. The system used consists of a model 2695 Alliance, and a model 2142 RI-detector (Waters Chromatography BV). The eluens was $CHCl_3$ at an elution rate of 1 mL/min and a temperature of 40 °C. This method was also used to determine the recovery of block oligomers after the particle formation process (*vide infra*). In detail, one mL of filtered and non-filtered particle dispersion of 10 mg/mL in 150 mM ammonium acetate solution (pH 6.8) was freeze-dried and the residue was dissolved in 3 mL $CHCl_3$. The concentration was determined by GPC and compared with the amount of material used for the film formation. A linear relationship between the peak area and the concentration was shown in a concentration range of 1-5 mg of oligomer/mL of $CHCl_3$.

The melting temperature (T_m) of the fractionated MEE- and mPEG-*b*-oligo(ε-caprolactones) was determined by differential scanning calorimetry (DSC), using a Q1000 differential scanning calorimeter (TA Instruments). Calibration of temperature and heat flow was performed with indium. Samples of approximately 5 mg in hermetically closed aluminium pans were subjected to a heat-cool-heat program from -80 to 100 °C at a heating rate of 10 °C/min and a cooling rate of 2 °C/min.

Determination of the critical aggregation concentration

For the determination of the critical aggregation concentration (CAC) of the various block oligomers two methods were used, each with a different fluorescent probe, pyrene and 8-anilino-1-naphthalenesulfonic acid magnesium salt (1,8-ANS), respectively. The fluorescence of pyrene as a function of different concentrations of block oligomer in phosphate buffered saline (PBS) was measured as described in the previous chapter.[35, 36] Briefly, samples were prepared in PBS at concentrations ranging from 0.0005 to 10 mg/mL, to which a pyrene solution in acetone was added (end concentration 6.0×10^{-7} M). Excitation spectra of pyrene were recorded from 300 to 360 nm at an emission wavelength (λ_{em}) of 390 nm using a Horiba Fluorolog fluorimeter at a 90° angle. The intensity ratio I_{338}/I_{333} of pyrene was plotted against the oligomer concentration to determine the CAC. 1,8-ANS was used according to a modified literature procedure.[37-40] In detail, block oligomer samples were prepared in PBS at concentrations ranging from 0.001 to 10 mg/mL. In a black 96 well plate (Greiner), 1 µL of a 5 mM 1,8-ANS-solution in 1/10 (v/v) DMF/H_2O was added to 100 µL of an oligomer dispersion in PBS. Fluorescence was measured using a FluoSTAR OPTIMA fluorimeter; the excitation wavelength (λ_{ex}) was 355 nm, and λ_{em} was 520 nm. Since 1,8-ANS only has fluorescent properties in hydrophobic environment, the CAC was determined by plotting the fluorescence intensity vs the concentration. As a control, the fluorescence of the samples was measured before the addition of the 1,8-ANS solution.

Particle formation and characterisation

Block oligomer dispersions were formed by hydration of an oligomer film, coated on the inside wall of a round bottomed flask by solvent evaporation of an oligomer solution in dichloromethane. The resulting dispersion had a concentration of 10 mg/mL in phosphate buffered saline (PBS), and was filtered through a 0.2 µm Anotop® filter.

The size of the particles and their size distribution were measured by dynamic light scattering (DLS) using a Malvern CGS-3 multiangle goniometer (Malvern Ltd., Malvern), consisting of a HeNe laser source (λ = 632.8 nm, 22 mW output power), temperature controller (Julabo water bath) and a digital correlator ALV-5000/EPP. Time correlation functions were analysed using the ALV-60X0 Software V.3.X provided by Malvern, to obtain the hydrodynamic diameter of the particles (Z_{ave}) and the particle size distribution (polydispersity index, PDI). The samples were analysed at 25 and 37 °C, both directly after preparation and after incubation at room temperature or 37 °C for several days.

Cryogenic transmission electron microscopy (Cryo-TEM) analysis was performed using a Tecnai12 transmission electron microscope (Philips) operating at 120 kV, with the specimen at -180 °C and under low-dose imaging conditions. Samples were prepared in a temperature and humidity-controlled chamber, using a 'Vitrobot'. A thin aqueous film of oligomer dispersion was formed by blotting a 200 mesh copper grid covered with Quantifoil holey carbon foil (Micro Tools GmbH, Germany) at 25 °C and at 100% relative humidity (glow discharged grid; 1 blot during 0.5 sec). The thin film was rapidly vitrified by plunging the grid into liquid ethane, and transferred into the microscope chamber using a GATAN 626 cryo-holder system. Images were recorded on a TemCam-0124 camera and processed with AnalySIS software.

Determination of the temperature sensitivity

The temperature sensitivity of the different oligomers was determined by static light scattering using a Horiba Fluorolog fluorimeter (λ=650 nm, 90° angle).[35, 36] Oligomer dispersions in PBS at a concentration of 10 mg/mL were heated from 0 to 75 °C at 1 °C/min, and scattering intensities were measured at 0.3 °C intervals.

Results and discussion

Preparation and characterisation of unmodified and modified mPEG-*b*-oligo(ε-caprolactone)s

Fractionation of the synthesised polydisperse mPEG-*b*-OCL with three different end groups (the unmodified hydroxyl group, and its benzoyl and naphthoyl derivative) yielded a series of block oligomers with monodisperse hydrophobic blocks. In the mass spectra of each fraction a regular series of peaks was observed, with a repeating unit of 44 Da, corresponding to one ethylene glycol unit (Figure 1). This indicates the presence of an oligomer with a polydisperse PEG-block and a discrete OCL chain length. GPC demonstrated a decrease in the M_w/M_n upon fractionation (Table 1). The M_w/M_n was still slightly higher than one, due to the polydispersity of the PEG-block. The molecular weight values calculated from ^{1}H NMR and the values obtained with GPC correlate well with the values calculated from the degree of polymerisation (DP) of the OCL-block determined by ESI-MS (Table 1). With analytical reversed phase (RP) HPLC it was found that the purity of the fractions was higher than 90%, except for the fractions with the highest DP: benzoylated mPEG-*b*-OCL$_7$ was contaminated with some DP 6, and naphthoylated mPEG-*b*-OCL$_6$ contained DP 7.

Differential scanning calorimetry (DSC) showed a clear melting endotherm in the thermograms of the fractionated MEE-OCL when the DP is 3 or higher (Figure 2a). The melting temperature (T_m) increased with the OCL chain length, from -25 to 31 °C for DP 3 to 7. This trend has also been observed for polydisperse OCL: melting temperatures of 31, 46 and 50 °C were reported for OCLs with average DPs of 5, 10 and 18, respectively.[41] The higher T_m of polydisperse OCLs compared to monodisperse OCLs can be ascribed to the presence of longer chains in the polydisperse oligomers. In the thermograms of mPEG750-*b*-OCL$_{2 \text{ and } 3}$ melting endotherms were observed at 25 and 23 °C , respectively (Figure 2b). These are likely caused by the crystallisation of the mPEG-block, since the thermograms of MEE-OCL did not show any endotherms at these temperatures. The observed T_m's and ΔH's (147 J/g and 135 J/g, respectively, corrected for the weight fraction of OCL) are slightly lower than those of mPEG750 (30 °C, 161 J/g), likely due to imperfections in the crystallisation of mPEG-*b*-OCL block oligomers.[42, 43] This may also explain the peak at -5 °C in the thermogram of mPEG750-*b*-OCL$_4$ which can be considered a sub-endotherm of the melting peak of the mPEG-block. MPEG750-*b*-OCL$_4$ showed a second endotherm at -25 °C, representing the melting of the OCL-block. This T_m and the ΔH (32 J/g, corrected for the weight fraction of PEG) are lower than those of MEE-OCL$_4$ (-1 °C and 85 J/g, respectively), most likely due to imperfect crystallisation as well.

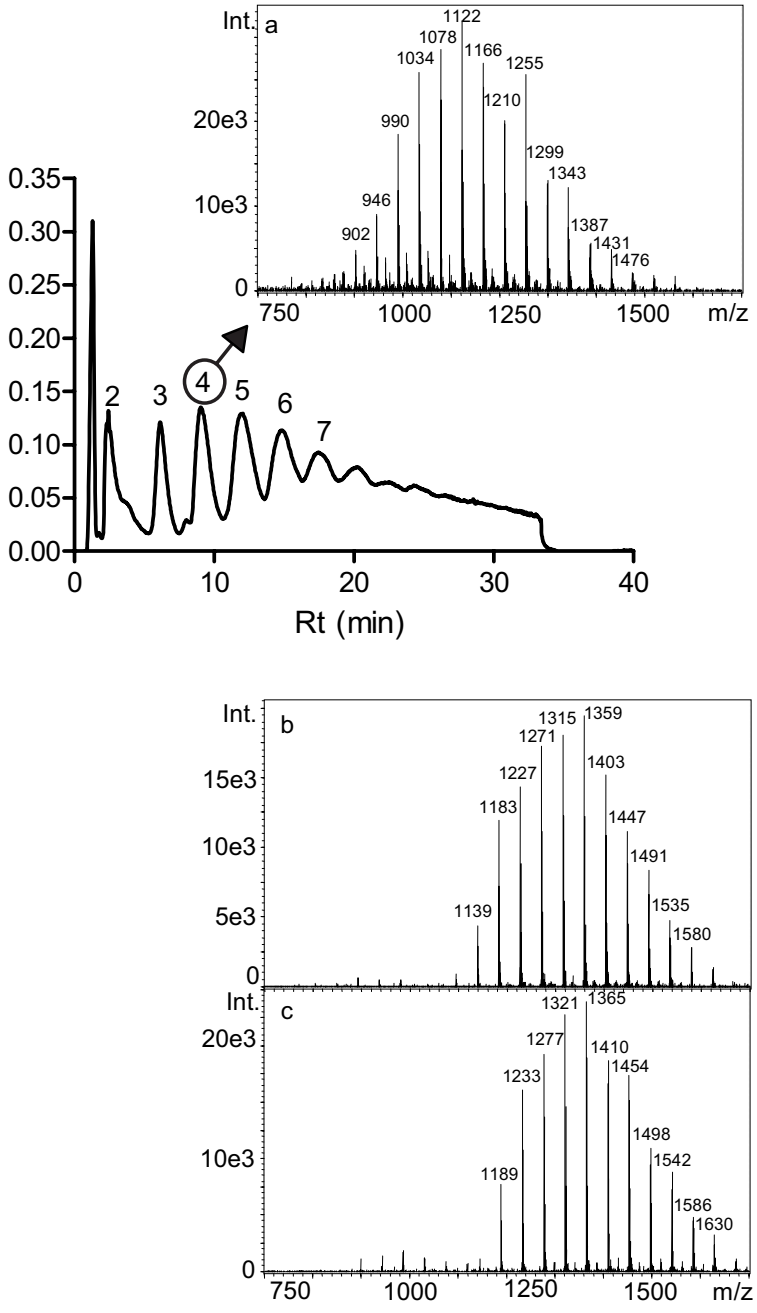

Figure 1 Preparative HPLC chromatogram of mPEG750-*b*-OCL_{av4} and the ESI-MS spectra of mPEG750-*b*-OCL_4 (a), benzoylated mPEG750-*b*-OCL_4 (b) and naphtoylated mPEG750-*b*-OCL_4 (c). The numbers in the chromatogram represent the number of caprolactone units. Mass spectra show the ammonium adduct of the product, with a polydisperse PEG-block and a monodisperse OCL-block, as reflected by the PEG-distribution.

Table 1 Molecular weights (in kDa) of the fractionated and polydisperse block oligomers

x	mPEG750-*b*-OCL$_x$				Benzoylated mPEG750-*b*-OCL$_x$				Naphthoylated mPEG750-*b*-OCL$_x$			
	M_n (Th)[a]	M_n (NMR)[b]	M_n (GPC)	M_w/M_n	M_n (Th)[a]	M_n (NMR)[b]	M_n (GPC)	M_w/M_n	M_n (Th)[a]	M_n (NMR)[b]	M_n (GPC)	M_w/M_n
Poly[c]	1.20	1.23	1.28	1.15	1.31	1.35	1.05	1.33	1.36	1.31	1.23	1.20
1	NA[d]				0.97	0.98	0.95	1.06	1.02	0.97	1.06	1.04
2	0.98	1.13	0.98	1.06	1.08	1.16	1.18	1.03	1.13	1.13	1.14	1.05
3	1.09	1.27	1.13	1.05	1.20	1.18	1.26	1.04	1.25	1.27	1.27	1.05
4	1.20	1.42	1.28	1.05	1.31	1.28	1.38	1.04	1.36	1.39	1.39	1.05
5	1.32	1.50	1.38	1.07	1.42	1.41	1.51	1.04	1.47	1.47	1.53	1.06
6	1.43	1.57	1.50	1.06	1.54	1.42	1.64	1.04	1.59	1.74	1.78	1.05
7	1.55	1.77	1.63	1.06	1.65	1.55	1.77	1.04	NA[d]			

[a] *Theoretical value of the molecular weight, calculated from the molecular weight of the mPEG-block as provided by the supplier (750 Da), of the OCL-block using the M/I ratio or the DP determined by ESI-MS (DP×114), and of the end group (H=1, benzoyl=105, naphthoyl=155).*

[b] *Calculated from ^{1}H NMR in deuterated chloroform, from the signal ratio of the methylene protons of the OCL-block and the mPEG-block to the protons of the methoxy group.*

[c] *Polydisperse block oligomer, mPEG750-b-OCL, synthesised with a molar ratio of mPEG750/ε-caprolactone of 1/4.*

[d] *NA = Not available.*

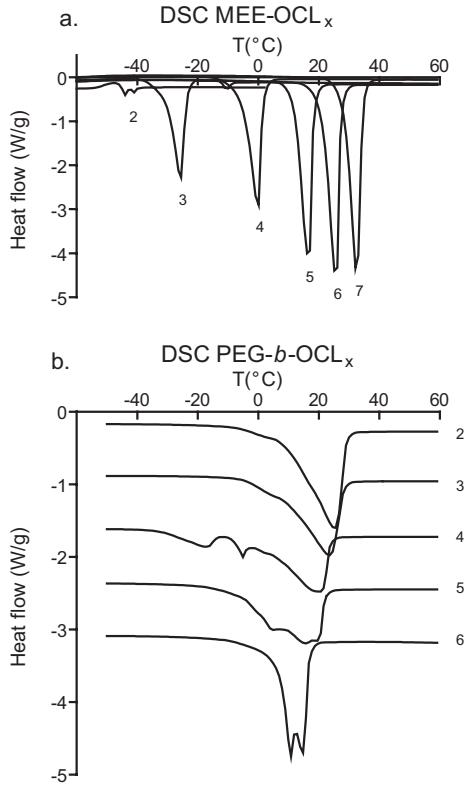

Figure 2 Thermograms of fractionated MEE-*b*-OCL (a) and mPEG750-*b*-OCL (b). Data of the second heating cycle are presented. Numbers represent the degree of polymerisation (DP) of the OCL-blocks.

At higher DPs, the melting endotherm of the OCL-block shifts to higher temperatures and overlaps with the melting peak of mPEG750. The DSC data demonstrate that the two blocks of mPEG-*b*-OCL are phase separated and crystallise separately. Phase separation was also observed in polydisperse PEG-OCL triblock oligomers,[43] and in high molecular weight PEG-*b*-PCL block copolymers.[42, 44, 45] Modification of the hydroxyl end groups of mPEG-*b*-OCLs with benzoyl or naphthoyl hardly affected the thermal behaviour of the block oligomers (data not shown). In chapter 3, it was shown that the two blocks of mPEG-*b*-oligo(L-lactate) did not phase separate, which resulted in the formation of hydrated nanoparticles with a size around 400 nm upon self-assembly in water.[35] It is anticipated that phase separation of the two blocks of mPEG-*b*-OCL will favour the formation of more compact core-shell structures in water.

The effect of end group modification on the critical aggregation concentration

The critical aggregation concentration (CAC) of the various block oligomers was determined with two different fluorescent probes. In general, the CAC values obtained with 1,8-ANS are higher than those obtained with pyrene (Table 2). A difference between fluorescent probes has been observed previously, and may be explained by differences in interactions between the amphiphile and the probe.[37, 40] As expected, the CAC decreased with increasing chain length of the hydrophobic block (>10 to 0.09 mg/mL determined with 1,8-ANS for mPEG750-*b*-$OCL_{2\ to\ 7}$, Table 2), and a linear relationship was observed between the DP of the OCL-block and the logarithm of the CAC of the block oligomers (Figure 3). Such a correlation was also observed in other homologous series of amphiphiles.[46] The CACs of the unmodified block oligomers are two orders of magnitude higher than those reported for high molecular weight PEG-*b*-PCL block copolymers,[18, 19] and are also higher than those of low molecular weight but polydisperse mPEG750-*b*-OCL.[34] The latter is ascribed to the presence of longer chains in the polydisperse oligomer mixture, compared to the fractionated oligomers studied in this paper. Interestingly, esterification of the hydroxyl end group of the block oligomer with an aromatic group dramatically decreased the CAC of the block oligomers. Table 2 and Figure 3 show that a 10- to 60-fold reduction of the CAC was obtained by benzoylation. The effect of naphthoylation is even larger, indicated for example by the 200-fold reduction of the CAC of mPEG750-*b*-OCL_4, measured with 1,8-ANS. It is noteworthy that these low CAC values are even comparable to those of high molecular weight PEG-*b*-PCL, which have already been used for the delivery of cyclosporin A *in vivo*.[47]

Table 2 Critical aggregation concentration of (modified) mPEG-*b*-OCL in PBS

x	mPEG750-*b*-OCL$_x$		Benzoylated mPEG750-*b*-OCL$_x$		Naphthoylated mPEG-*b*-OCL$_x$	
	CAC 1,8-ANS (mg/mL)[a]	CAC pyrene (mg/mL)[b]	CAC 1,8-ANS (mg/mL)[a]	CAC pyrene (mg/mL)[b]	CAC 1,8-ANS (mg/mL)[a]	CAC pyrene (mg/mL)[b]
1	NA[c]	NA[c]	5.1	0.50	0.38[d]	ND[e]
2	> 10	3.4	1.2	0.42	0.18	ND[e]
3	> 10	1.5	0.43	0.10	0.05	ND[e]
4	4.4	1.0	0.04	0.034	0.02	ND[e]
5	1.1	0.52	0.01	0.008	0.01	ND[e]
6	0.26	0.17	0.01	0.003	0.01	ND[e]
7	0.09	0.03	0.01	0.003	NA[c]	NA[c]

[a] *The standard error of the method was 10-15%.*
[b] *The standard error of the method was 5-10%.*
[c] *NA = Not available.*
[d] *This value may be slightly lower than the real CAC, as a result from the fluorescence of the naphthoyl end group: in the control samples (without 1,8-ANS), fluorescence is observed at block oligomer concentrations of 0.3 mg/mL and higher.*
[e] *Not detectable; the fluorescence of the naphthoyl end group interfered with the fluorescence of pyrene.*

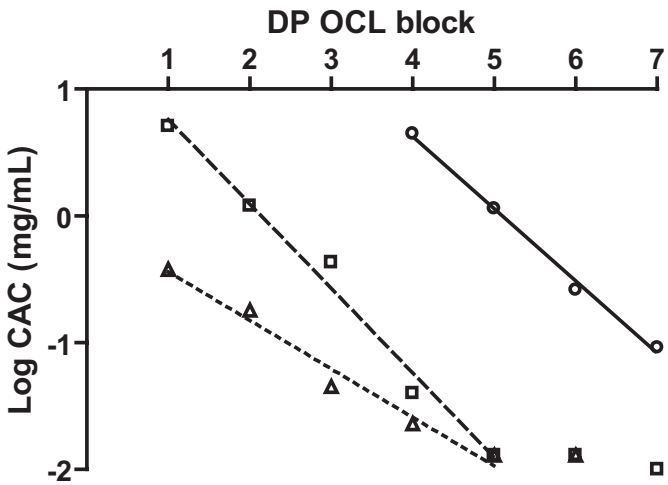

Figure 3 Critical aggregation concentration of mPEG750-*b*-OCL$_x$ (circles, straight line), benzoylated mPEG750-*b*-OCL$_x$ (squares, dashed line) and naphthoylated mPEG750-*b*-OCL$_x$ (triangles, dotted line) in phosphate buffered saline, determined with 1,8-ANS. Note: the data points of benzoylated and naphthoylated mPEG750-*b*-OCL$_{5 \text{ and } 6}$ overlap.

Remarkably, the CAC values found with the pyrene and the 1,8-ANS method levelled off at the lowest values of 0.003 mg/mL and 0.01 mg/mL, respectively, suggesting that we reached the detection limits of the methods. In literature, values lower than 0.001 mg/mL (pyrene method) were rarely reported either. Calculations based on partition equilibrium coefficients of pyrene and the volume fraction of the hydrophobic core of the micelles[34] indeed suggest that the total amount of pyrene in water and inside the hydrophobic core of the micelles is almost equal at the lowest amphiphile concentration. Since 1,8-ANS is more hydrophilic, it has a lower partition equilibrium coefficient, which explains the lower sensitivity of the method (0.01 mg/mL). This means that the effect of end group modification on the CAC may be even larger than suggested by the reported data.

Self-assembly of mPEG-*b*-oligo(ε-caprolactone)s with and without end group modification

After the particle formation by hydration of an oligomer film with PBS, followed by filtration, a block oligomer recovery of >90% was found with analytical GPC. This indicates that hardly any material was lost during the process. Dynamic light scattering (DLS) measurements demonstrated that the block oligomers with a relatively large PEG-fraction formed nanoparticles with a hydrodynamic diameter (Z_{ave}) of 30-200 nm (Figure 4), and a relatively high polydispersity index (PDI) of 0.2-0.6, which was observed in the previous chapter for mPEG-*b*-oligo(L-lactate)s as well.[35] Interestingly, mPEG750-*b*-OCL with a DP larger than 4 forms small, almost monodisperse nanoparticles (PDI < 0.1) with a diameter smaller than 15 nm (Figure 4). With the benzoylated and naphthoylated block oligomers, these small particles are even obtained at an OCL DP of 2 and higher. Our data suggest that a CAC lower than 1.5 mg/mL (determined with 1,8-ANS, see Table 2) favours the formation of sub-20 nm particles. Figure 4 demonstrates a growth in the particle diameter with increasing length of the hydrophobic block. The increase in diameter per caprolactone unit measures 1.4 nm, and benzoylation and naphthoylation result in an increase of 4 and 5 nm, respectively. Taking this into account, as well as the particle size in relation to the end-to-end distance of the block oligomers, the formed nanoparticles likely have a micellar morphology. For example, the end-to-end distance of a fully stretched mPEG750-*b*-OCL_6 chain is 11 nm, resulting in a theoretical micellar diameter of 22 nm. This is in reasonable agreement with the measured particle diameter of 9.3 nm, in which the oligomer chains will be at least partly coiled rather than fully stretched. Similarly, the length of a caprolactone unit (1 nm) corresponds well with the size increase. The effect of end group modification on the diameter is larger than the size of the benzoyl- or naphthoyl group (0.6 and 0.9 nm, respectively),

likely because of a different packing in the hydrophobic core, caused by the aromatic groups. The spherical shape of these small nanoparticles was confirmed by cryo-TEM. Figure 5 shows a picture of nanoparticles composed of benzoylated mPEG750-*b*-OCL_6 in PBS, which have a diameter of approximately 10 nm.

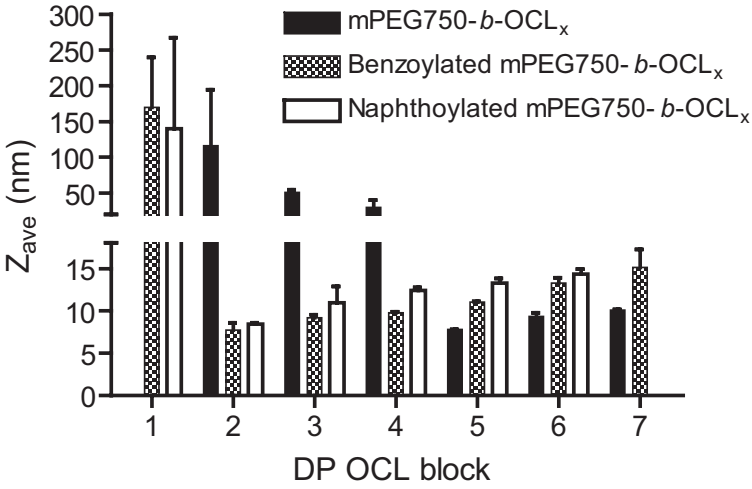

Figure 4 Hydrodynamic diameter (Z_{ave}) of (modified) mPEG750-*b*-OCL_x with different degree of polymerisation (DP) in phosphate buffered saline (10 mg/mL), determined by dynamic light scattering. Mean ± SD of 3 individual preparations.

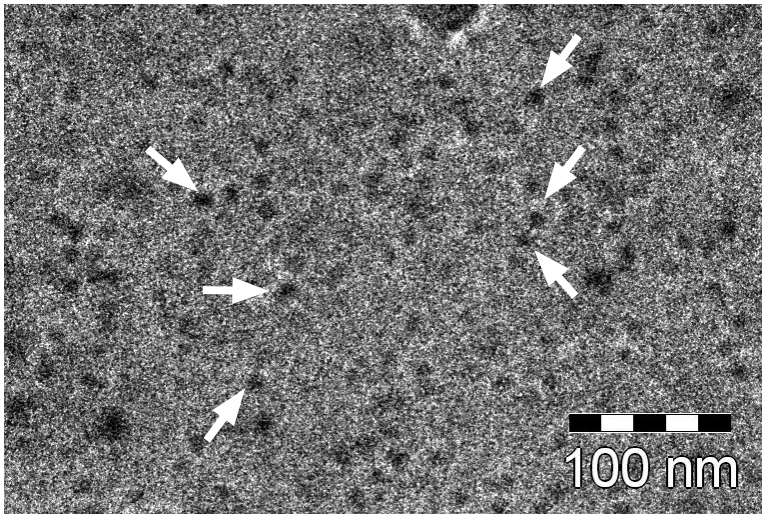

Figure 5 Cryo-TEM image of benzoylated mPEG750-*b*-OCL_6 particles at 10 mg/mL in PBS. Some of the nanoparticles are indicated by white arrows. The diameter of the nanoparticles is approximately 10 nm.

Temperature sensitivity and stability of the block oligomer dispersions

When heating a dispersion of mPEG750-*b*-OCL with a DP larger than 5, first a decrease in static light scattering was observed, reflecting the Krafft point (Kp) (Figure 6). The Kp represents the temperature at which the solubility of an amphiphilic polymer equals the CAC. Below the Kp the amphiphiles are precipitated, because the solubility is not sufficient to form micelles, whereas above the Kp the concentration of dissolved amphiphiles is high enough to favour the self-assembly into micelles. As expected, the Kp increased from <0 °C (for DP 2-4) to 32 °C when the DP of the OCL-block increased from 2 to 7 units (Figure 6). Similar behaviour was observed by Letchford *et al.*, who reported Kp's of 27, 30, and 31 °C for polydisperse mPEG750-*b*-OCLs, with an average OCL chain length of 2, 5 and 10 units, respectively.[34] Interestingly, the observed Kp's of the fractionated, unmodified mPEG750-*b*-OCLs are slightly above the onset of the melting endotherms of the OCL-block (see DSC of MEE-OCL, Figure 2a). This suggests that melting of the hydrophobic block increases the aqueous solubility of the block oligomer, and when the solubility reaches the CAC, the Kp is observed. Figure 7a shows a schematic representation of the block oligomer concentration in water (either molecularly dissolved or as micelles) vs temperature, illustrating the relation between DP, T_m, solubility, CAC, and Kp. With increasing DP, the onset of dissolution (represented by the inflection point of the curves) shifts to higher temperatures, because of an increased T_m of the hydrophobic block. Therefore, the Kp increases with increasing DP, as reflected by the horizontal arrow in Figure 7a, even though the CAC decreases with increasing DP. Surprisingly, the effect of the end group modification on the Kp is opposite to the effect of increasing DP: the modified mPEG-*b*-OCLs had a lower Kp (<0 to 25 °C) than their unmodified counterparts (Figure 6). This peculiar behaviour can be explained with the help of Figure 7b. As mentioned before, end group modification hardly affects the thermal behaviour of the block oligomers, and therefore the onset of dissolution is not changed. However, the CAC is greatly reduced (Table 2), which causes a reduction of the Kp, as illustrated by the arrows in Figure 7b.

Further heating of the dispersions resulted in the occurrence of a cloud point (Cp) in the dispersions of monodisperse mPEG750-*b*-OCL with a DP larger than 3 (Figure 6). The Cp is ascribed to the dehydration of the PEG-part of the block oligomers, causing aggregation of the self-assembled particles, which is reflected by an increase in turbidity. As expected, the Cp's decreased with increasing DP of the OCL-block, and the introduction of an aromatic group caused a decrease in the Cp's as well (Figure 6). Similar observations were described for polydisperse PEG-*b*-OCL,[34] PEG-*b*-poly(ε-caprolactone)-*co*-trimethylene carbonate (PCL-*co*-TMC)[48] and low molecular weight

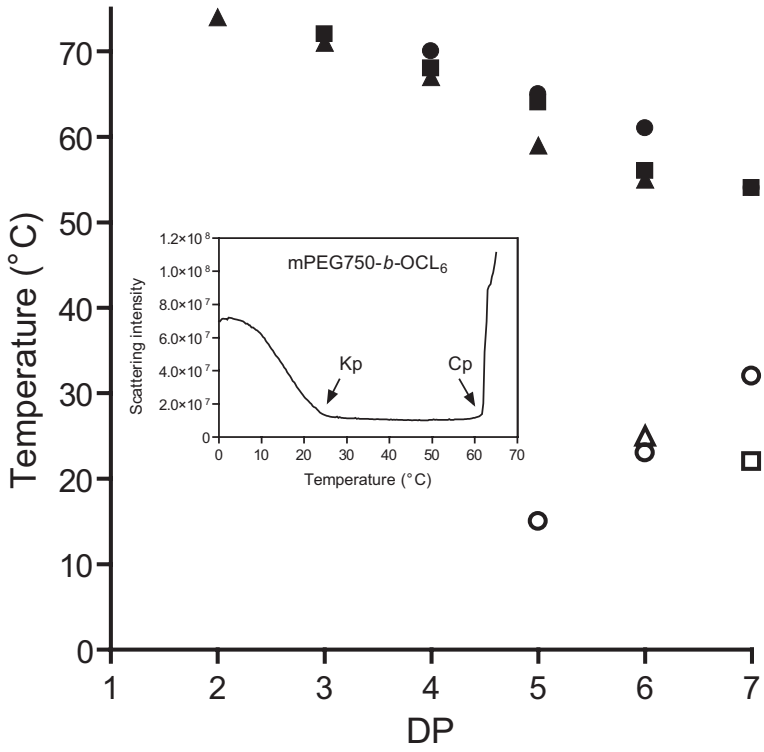

Figure 6 Krafft points (Kp, open symbols) and cloud points (Cp, closed symbols) of mPEG750-*b*-OCL_x (circles), benzoylated mPEG750-*b*-OCL_x (squares) and naphthoylated mPEG750-*b*-OCL_x (triangles). Note: The block oligomers with a low OCL DP < 5 (unmodified), <7 (benzoylated) and <6 (naphtoylated) do not display a Kp above 0 °C.

nonionic surfactants.[49] Preferably, the temperature sensitivity of amphiphiles used for drug delivery purposes should not interfere with their application at body temperature, nor with handling or storage at room temperature or 4 °C. This is illustrated by the low stability of the micelles composed of mPEG750-*b*-OCL_6, benzoylated mPEG750-*b*-OCL_7, and naphthoylated mPEG750-*b*-OCL_6, which precipitated within approximately two weeks, and of mPEG750-*b*-OCL_7, which precipitated within 1 h, when stored at room temperature (data not shown). This is likely due to the presence of their Krafft point close to or above the storage temperature (Figure 6). The oligomeric micelles formed by the other modified and unmodified mPEG-*b*-OCLs in PBS retained their small size for over a month when stored at room temperature, and for at least 2 weeks when incubated at 37 °C (data not shown).

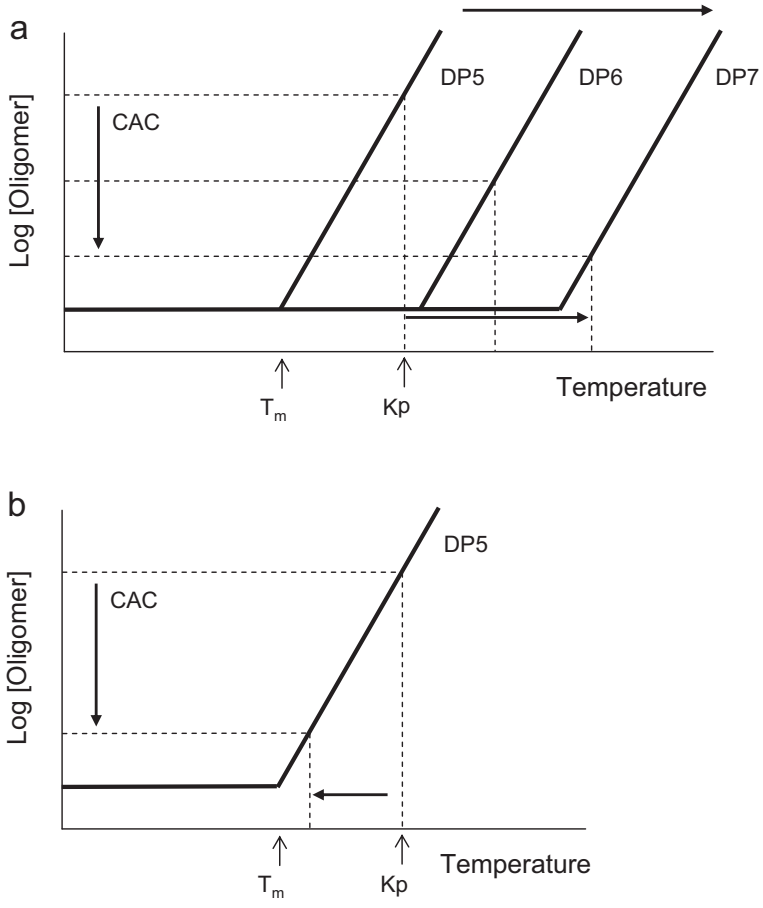

Figure 7 Schematic representation of the relation between the melting temperature (T_m), the solubility (Log [Oligomer], *i.e.* concentration of oligomer that is molecularly dissolved or present as micelles), the critical aggregation concentration (CAC) and the Krafft point (Kp), and the effect of the DP (a) and end group modification (b) thereon.

Conclusions

This study demonstrates that end group modified mPEG-*b*-oligo(ε-caprolactone)s with monodisperse hydrophobic blocks are very interesting amphiphiles for drug delivery purposes. They self-assemble into micelles with a diameter smaller than 15 nm, which may have attractive properties in terms of biodistribution and tissue penetration *in vivo*. Furthermore, end group modification with an aromatic group substantially decreased the CAC of the mPEG-*b*-OCLs, which even approached those of high molecular weight mPEG-*b*-PCL. This interesting observation will confer these micelles a higher stability towards dilution upon administration and longer retention of the loaded drug. These aspects will be the subject of future work to evaluate the pharmaceutical applicability of these oligomeric micelles.

References

1. Kabanov AV; Batrakova EV; Melik-Nubarov NS; Fedoseev NA; Dorodnich TY; Alakhov VY; Chekhonin VP; Nazarova IR; Kabanov VA, A new class of drug carriers: micelles of poly(oxyethylene)-poly(oxypropylene) block copolymers as microcontainers for drug targeting from blood in brain. *J Control Release* 22, 141-157 (1992).
2. Kwon GS; Yokoyama M; Okano T; Sakurai Y; Kataoka K, Biodistribution of micelle-forming polymer-drug conjugates. *Pharm Res* 10, 970-974 (1993).
3. Allen C; Maysinger D; Eisenberg A, Nano-engineering block copolymer aggregates for drug delivery. *Colloid Surface B* 16, 3-27 (1999).
4. Gaucher G; Dufresne MH; Sant VP; Kang N; Maysinger D; Leroux JC, Block copolymer micelles: preparation, characterization and application in drug delivery. *J Control Release* 109, 169-188 (2005).
5. Maeda H; Wu J; Sawa T; Matsumura Y; Hori K, Tumor vascular permeability and the EPR effect in macromolecular therapeutics: a review. *J Control Release* 65, 271-284 (2000).
6. Edlund U; Albertsson AC, Polyesters based on diacid monomers. *Adv Drug Deliver Rev* 55, 585-609 (2003).
7. Albertsson AC; K.Varma I, Recent developments in ring opening polymerization of lactones for biomedical applications. *Biomacromolecules* 4, 1446-1486 (2003).
8. Sinha VR; Bansal K; Kaushik R; Kumria R; Trehan A, Poly-ε-caprolactone microspheres and nanospheres: an overview. *Int J Pharm* 278, 1-23 (2004).
9. Woodle MC; Lasic DD, Sterically stabilized liposomes. *Biochim Biophys Acta* 1113, 171-199 (1992).
10. Storm G; Belliot SO; Daemen T; Lasic DD, Surface modification of nanoparticles to oppose uptake by the mononuclear phagocyte system. *Adv Drug Deliver Rev* 17, 31-48 (1995).
11. Torchilin VP; Trubetskoy VS, Which polymers can make nanoparticulate drug carriers long-circulating? *Adv Drug Deliver Rev* 16, 141-155 (1995).
12. Gref R; Domb A; Quellec P; Blunk T; Muller RH; Verbavatz JM; Langer R, The controlled intravenous delivery of drugs using PEG-coated sterically stabilized nanospheres. *Adv Drug Deliver Rev* 16, 215-233 (1995).
13. Burt HM; Zhang X; Toleikis P; Embree L; Hunter WL, Development of copolymers of poly(D,L-lactide) and methoxypolyethylene glycol as micellar carriers of paclitaxel. *Colloid Surface B* 16, 161-171 (1999).
14. Govender T; Riley T; Ehtezazi T; Garnett MC; Stolnik S; Illum L; Davis SS, Defining the drug incorporation properties of PLA-PEG nanoparticles. *Int J Pharm* 199, 95-110 (2000).
15. Peracchia MT; Gref R; Minamitake Y; Domb A; Lotan N; Langer R, PEG-coated nanospheres from amphiphilic diblock and multiblock copolymers: Investigation of their drug encapsulation and release characteristics. *J Control Release* 46, 223-231 (1997).
16. Shuai X; Ai H; Nasongkla N; Kim S; Gao J, Micellar carriers based on block copolymers of poly(ε-caprolactone) and poly(ethylene glycol) for doxorubicin delivery. *J Control Release* 98, 415-426 (2004).
17. Kim SY; Lee YM, Taxol-loaded block copolymer nanospheres composed of methoxy poly(ethylene glycol) and poly(epsilon-caprolactone) as novel anticancer drug carriers. *Biomaterials* 22, 1697-1704 (2001).
18. Forrest ML; Won CY; Malick AW; Kwon GS, In vitro release of the mTOR inhibitor rapamycin from poly(ethylene glycol)-*b*-poly(ε-caprolactone) micelles. *J Control Release* 110, 370-377 (2005).
19. Aliabadi HM; Mahmud A; Sharifabadi AD; Lavasanifar A, Micelles of methoxy poly(ethylene oxide)-b-poly(epsilon-caprolactone) as vehicles for the solubilization and controlled delivery of cyclosporine A. *J Control Release* 104, 301-311 (2005).
20. Lim Soo P; Lovric J; Davidson P; Maysinger D; Eisenberg A, Polycaprolactone-block-poly(ethylene oxide) micelles: A nanodelivery system for 17β-estradiol. *Mol Pharm* 2, 519-527 (2005).
21. Vonarbourg A; Passirani C; Saulnier P; Benoit JP, Parameters influencing the stealthiness of colloidal drug delivery systems. *Biomaterials* 27, 4356-4373 (2006).
22. Sun X; Rossin R; Turner JL; Becker ML; Joralemon MJ; Welch MJ; Wooley KL, An assessment of the effects of shell cross-linked nanoparticle size, core composition, and surface PEGylation on in vivo biodistribution. *Biomacromolecules* 6, 2541-2554 (2005).

23. Weissig V; Whiteman KR; Torchilin VP, Accumulation of protein-loaded long-circulating micelles and liposomes in subcutaneous Lewis lung carcinoma in mice. *Pharm Res* 15, 1552-1556 (1998).
24. Rosler A; Vandermeulen GW; Klok HA, Advanced drug delivery devices via self-assembly of amphiphilic block copolymers. *Adv Drug Deliver Rev* 53, 95-108 (2001).
25. Rodriguez-Hernandez J; Checot F; Gnanou Y; Lecommandoux S, Toward 'smart' nano-objects by self-assembly of block copolymers in solution. *Prog Polym Sci* 30, 691-724 (2005).
26. Shuai X; Merdan T; Schaper AK; Xi F; Kissel T, Core-cross-linked polymeric micelles as paclitaxel carriers. *Bioconjugate Chem* 15, 441-448 (2004).
27. Yokoyama M; Opanasopit P; Okano T; Kawano K; Maitani Y, Polymer design and incorporation methods for polymeric micelle carrier system containing water-insoluble anti-cancer agent camptothecin. *J Drug Target* 12, 373-384 (2004).
28. Opanasopit P; Yokoyama M; Watanabe M; Kawano K; Maitani Y; Okano T, Block copolymer design for camptothecin incorporation into polymeric micelles for passive tumor targeting. *Pharm Res* 21, 2001-2008 (2004).
29. Watanabe M; Kawano K; Yokoyama M; Opanasopit P; Okano T; Maitani Y, Preparation of camptothecin-loaded polymeric micelles and evaluation of their incorporation and circulation stability. *Int J Pharm* 308, 183-189 (2006).
30. Kabanov AV; Batrakova EV; Alakhov VY, Pluronic block copolymers as novel polymer therapeutics for drug and gene delivery. *J Control Release* 82, 189-212 (2002).
31. Harada A; Kataoka K, Chain length recognition: core-shell supramolecular assembly from oppositely charged block copolymers. *Science* 283, 65-67 (1999).
32. Yoshida E; Kunugi S, Micelle formation of poly(vinyl phenol)-block-polystyrene by alfa,omega-diamines. *J Polym Sci Pol Chem* 40, 3063-3067 (2002).
33. Kang N; Perron M-E; Prud'homme RE; Zhang Y; Gaucher G; Leroux J-C, Stereocomplex block copolymer micelles: Core-shell nanostructures with enhanced stability. *Nano Lett* 5, 315-319 (2005).
34. Letchford K; Zastre J; Liggins R; Burt H, Synthesis and micellar characterization of short block length methoxy poly(ethylene glycol)-block-poly(caprolactone) diblock copolymers. *Colloid Surface B* 35, 81-91 (2004).
35. Carstens MG; van Nostrum CF; Ramzi A; Meeldijk JD; Verrijk R; de Leede GJ; Crommelin DJA; Hennink WE, Poly(ethylene glycol)-oligolactates with monodisperse hydrophobic blocks: preparation, characterization, and behavior in water. *Langmuir* 21, 11446-11454 (2005).
36. Soga O; van Nostrum CF; Ramzi A; Visser T; Soulimani F; Frederik PM; Bomans PHH; Hennink WE, Physico-chemical characterization of degradable thermosensitive polymeric micelles. *Langmuir* 20, 9388-9395 (2004).
37. Nakahara Y; Kida T; Nakatsuji Y; Akashi M, New fluorescence method for the determination of the critical micelle concentration by photosensitive monoazacryptand derivatives. *Langmuir* 21, 6688-6695 (2005).
38. Walter A; Kuehl G; Barnes K; VanderWaerdt G, The vesicle-to-micelle transition of phosphatidylcholine vesicles induced by nonionic detergents: effects of sodium chloride, sucrose and urea. *BBA-Biomembranes* 1508, 20-33 (2000).
39. Abuin EB; Lissi EA; Aspee A; Gonzalez FD; Varas JM, Fluorescence of 8-anilinonaphthalene-1-sulfonate and properties of sodium dodecyl sulfate micelles in water-urea mixtures. *J Colloid Interf Sci* 186, 332-338 (1997).
40. Priev A; Zalipsky S; Cohen R; Barenholz Y, Determination of critical micelle concentration of lipopolymers and other amphiphiles: comparison of sound velocity and fluorescent measurements. *Langmuir* 18, 612-617 (2002).
41. Penco M; Sartore L; Bignotti F; D'Antone S; Di Landro L, Thermal properties of a new class of block copolymers based on segments of poly(D,L-lactic-glycolic acid) and poly(e-caprolactone). *Eur Polym J* 36, 901-908 (2000).
42. Cerrai P; Tricoli M; Andruzzi F; Paci M; Paci M, Polyether-polyester block copolymers by non-catalysed polymerization of ε-caprolactone with poly(ethylene glycol). *Polymer* 30, 338-343 (1989).
43. Sosnik A; Cohn D, Poly(ethylene glycol)-poly(epsilon-caprolactone) block oligomers as injectable materials. *Polymer* 44, 7033-7042 (2003).
44. He C; Sun J; Zhao T; Hong Z; Zhuang X; Chen X; Jing X, Formation of a unique crystal morphology for the poly(ethylene glycol)-poly(e-caprolactone) diblock copolymer. *Biomacromolecules* 7, 252-256 (2006).

45. Sun J; Chen X; He C; Jing X, Morphology and structure of single crystals of poly(ethylene glycol)-poly(ε-caprolactone) diblock copolymers. *Macromolecules* 39, 3717-3719 (2006).
46. Van Alstine JM; Sharp KA; Brooks DE, Critical micelle concentration dependence on head-group size in polyoxyethylene nonionic surfactants. *Colloid Surface* 17, 115-121 (1986).
47. Aliabadi HM; Brocks DR; Lavasanifar A, Polymeric micelles for the solubilization and delivery of cyclosporine A: pharmacokinetics and biodistribution. *Biomaterials* 26, 7251-7259 (2005).
48. Ould-Ouali L; Arien A; Rosenblatt J; Nathan A; Twaddle P; Matalenas T; Borgia M; Arnold S; Leroy D; Dinguizli M; Rouxhet L; Brewster M; Preat V, Biodegradable self-assembling PEG-copolymer as vehicle for poorly water-soluble drugs. *Pharm Res* 21, 1581-1590 (2004).
49. Schott H, Hydrophile-lipophile balance and cloud points of nonionic surfactants. *J Pharm Sci* 58, 1443-1449 (1969).

A mechanistic study on the chemical and enzymatic degradation of PEG-oligo(ε-caprolactone) micelles

5

Myrra G. Carstens,[a,b] Cornelus F. van Nostrum,[a] Ruud Verrijk,[b] Leo G.J. de Leede,[b] Daan J.A. Crommelin,[a] Wim E. Hennink[a]

[a] Department of Pharmaceutics, Utrecht Institute for Pharmaceutical Sciences (UIPS), Faculty of Pharmaceutical Sciences, Utrecht University, Utrecht, The Netherlands

[b] OctoPlus N.V., Leiden, the Netherlands

Journal of Pharmaceutical Sciences, **2007**. *In Press.*

Abstract

The chemical and enzymatic degradation of monodisperse oligo(ε-caprolactone) (OCL) and its amphiphilic block oligomer with methoxy poly(ethylene glycol) (mPEG) were investigated in order to obtain insight into the degradation of mPEG-*b*-OCL micelles. Chemical hydrolysis was studied as function of pH and dielectric constant of the medium, and enzymatic degradation was investigated at different enzyme and substrate concentrations. The degradation was monitored by HPLC and MS, and the micelle destabilisation with DLS. It was found that the hydrolytic cleavage followed pseudo first order kinetics, and that the rate depended on the pH and dielectric constant. Hydrolysis essentially occurred via a random scission process, and induced micelle destabilisation after approximately 1.5 degradation half-lives. At physiological pH and temperature, OCLs are very stable as reflected by an estimated half-life of mPEG-*b*-OCL micelles of several years. However, the presence of lipase resulted in an accelerated degradation with half-lives of a few days to hours. The enzymatic degradation of mPEG-*b*-OCL followed Michaelis-Menten kinetics. The results indicate that mPEG-*b*-OCL micelles are very stable *in vitro*, but their susceptibility to enzymes such as lipase makes these systems suitable for the hydrolysis-controlled release of drugs *in vivo*.

Introduction

Poly(ε-caprolactone) (PCL) is a hydrophobic polymer with good biocompatibility and biodegradability. It is therefore widely used in the biomedical field, for example in medical devices and tissue engineering,[1-3] and it has found applications in the pharmaceutical field, such as PCL microspheres and nanospheres that can be used for the controlled delivery of several types of drugs.[4] PCL is also frequently used as the hydrophobic block in amphiphilic block copolymers with poly(ethylene glycol) (PEG), which self-assemble in water into polymeric micelles.[5-12] These are core-shell structures, which can accommodate hydrophobic drugs in particular.[5, 6]

The degradability of PCL was recognised in the early seventies. Since then, its degradation has been extensively studied, for example in microspheres and nanospheres,[4, 13] as films,[13, 14] and implants *in vivo*.[15, 16] The degradation of PCL is described as a bulk process that can be divided into two phases. First, water is absorbed by the matrix, and subsequent chain scission results in reduction of the molecular weight.[4] The hydrolysis of the ester bonds is autocatalysed by the formed carboxylic acid during ester cleavage.[4, 17, 18] Second, weight loss occurs, caused by diffusion of the formed water soluble fragments out of the matrix.[4] During degradation the crystallinity of PCL increases, which is caused by preferential hydrolysis in the amorphous domains of the polyester.[4, 13, 17] Ester hydrolysis is catalysed by acid or by base,[19] and may be influenced by the presence of acidic or basic drugs as well.[17] Copolymerisation with the hydrophilic PEG has been reported to increase the degradation time.[20]

In addition to hydrolytic degradation, polyesters are susceptible to enzymatic degradation, for example by lipase.[13, 21-24] Lipases are present in many organisms, both intracellularly and extracellularly, and their natural function is to catalyse the hydrolysis of fatty acid esters of glycerol. Besides these triglycerides, lipase catalyses the degradation of polyesters such as PCL, poly(lactic acid) (PLA) and poly(trimethylene carbonate) (PTMC).[13, 21, 23, 25] Degradation of PCL *in vivo* will be a combination of both hydrolytic and enzymatic processes, which is illustrated by a slightly faster degradation of a PLA-*co*-PCL scaffold *in vivo* when compared to studies performed in buffer.[16]

In chapter 4, we reported on the self-assembly of low molecular weight mPEG-*b*-oligo(ε-caprolactone) with monodisperse hydrophobic blocks into small oligomeric micelles.[12] We also demonstrated that the introduction of an aromatic end group resulted in an extensive reduction of the critical aggregation concentration (CAC).[12] The overall stability of these micelles results from both physical and chemical stability. It is therefore important to know and understand their degradation behaviour. However, limited information is available on the degradation of these low molecular

weight compounds, since mainly high molecular weight polyesters were subject of investigation in the above mentioned studies. Moreover, the use of monodisperse oligomer chains, as in our studies, enables easy monitoring of the starting compound and degradation products in time by HPLC and MS, thereby providing more detailed insight into the kinetics and mechanisms.

A systematic study on the chemical degradation of monodisperse oligo(ε-caprolactone) is presented in this paper. Next, the degradation behaviour of its amphiphilic block oligomer with PEG was investigated, and the effect of the aggregation state thereon (*i.e.* as a molecularly dissolved block oligomer, and in a micellar dispersion). The effect of the ester bond hydrolysis on the micellar stability was studied, and based on the obtained data, the stability at physiological pH was estimated. Besides chemical hydrolysis, the enzymatic degradation and destabilisation of these block oligomer micelles by lipase were investigated. The results obtained provide more insight into the degradation-induced destabilisation of mPEG-*b*-oligo(ε-caprolactone) based drug carriers, and indicate that *in vivo* both chemical and enzymatic degradation may play a role.

Experimental section

Materials

Poly(ethylene glycol) mono(methyl ether) with a molecular weight of 750 Da (methoxy PEG750, mPEG750), ε-caprolactone (99%) and toluene were obtained from Acros Organics (Geel, Belgium). Stannous octoate (tin(II) bis(2-ethylhexanoate), $SnOct_2$, >95%), benzoyl chloride (99%), and pseudomonas lipase (30 U/mg, 1 unit produces 1 μmol glycerol from a triglyceride per min at pH 7.0 at 37 °C in the presence of bovine serum albumin) were purchased from Sigma Aldrich Chemie BV (Zwijndrecht, The Netherlands). Acetonitrile (ACN, HPLC gradient grade) was obtained from Biosolve LTD (Valkenswaard, The Netherlands), triethylamine (TEA, > 99%) from Merck (Darmstadt, Germany), and benzyl alcohol from Riedel de Haën (Seelze, Germany). All chemicals were used as received; buffers were filtered through a 20 nm filter (Anotop®, Whatmann, Breda, The Netherlands) prior to use.

Synthesis and purification of monodisperse oligo(ε-caprolactone) and its copolymers

Benzyl oligo(ε-caprolactone) (benzyl OCL) and mPEG-*b*-OCL (Figure 1a and b) with an average degree of polymerisation (DP) of 5 CL units were synthesised as described in chapter 4.[12] In brief, ring-opening polymerisation of ε-caprolactone (20 g), initiated by either benzyl alcohol or mPEG750 (0.2 equiv.) and catalysed by $SnOct_2$ (0.05 equiv.), was performed overnight at a temperature of 130 °C. Benzoylated mPEG750-*b*-OCL (Figure 1c) (mPEG750-*b*-OCL-Bz) was obtained by reacting the hydroxyl end group with a five fold excess of benzoyl chloride in the presence of an equimolar amount of triethyl amine as proton scavenger.[12]

To obtain monodisperse oligo(ε-caprolactone) oligomers, the polydisperse benzyl OCL and mPEG750-*b*-OCL-Bz were fractionated by preparative reversed phase HPLC (RP-HPLC), as reported in the previous chapter.[12] This procedure was slightly modified for the fractionation of benzyl OCL. In detail, a system composed of a Waters 600EF Quaternary gradient pump and a Waters 2700 sample manager was used. Five hundred μL of a 10% (w/w) solution of polydisperse benzyl OCL in 40/60 (w/w) ACN/H_2O was injected onto the column (Waters Xterra Prep MS C18, 10 μm, 19×250 mm, including a guard column). A gradient was run from 60% A (5/95 (w/w) ACN/H_2O) to 100% B (95/5 (w/w) ACN/H_2O) in 20 min, followed by isocratic elution with 100% B for 10 min. The flow rate was 10 mL/min, and the detection wavelength was 210 nm. Peak overlap necessitated a second fractionation to obtain material with

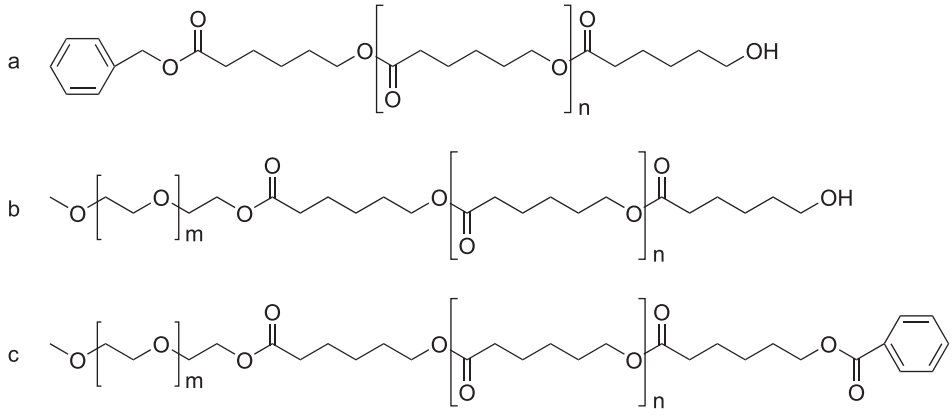

Figure 1 Chemical structures of benzyl oligo(ε-caprolactone) (benzyl OCL) (a), mPEG750-*b*-oligo(ε-caprolactone) (mPEG750-*b*-OCL) (b), and benzoylated mPEG750-*b*-oligo(ε-caprolactone) (mPEG750-*b*-OCL-Bz) (c).

a purity >95%. Two hundred and fifty µL of a 5% (w/w) solution of partly fractionated benzyl OCL in 80/20 (w/w) ACN/H_2O was injected and eluted with a gradient of 80% to 100% B in 20 min. Fractions were collected, and after evaporation of the solvents the products were characterised.

Analytical procedures

Electrospray Ionisation Mass Spectrometry

Electrospray ionisation mass spectrometry (ESI-MS) analysis of oligomer samples (0.1 mg/mL in 50/50 (v/v) ACN/H_2O) was performed using a Shimadzu LCMS QP8000.[12, 26] The cone voltage was +4.5 kV with a detector voltage of 1.5 kV. The CDL voltage was set at -10 V, the CDL temperature was 250 °C, and the deflector voltage was 80 V. The flow of the nebulising gas (N_2) was 4.5 L/min. Instrumental control was performed with a CLASS 8000 LCMS Software Package.

^{1}H NMR Spectroscopy

^{1}H NMR spectra were recorded using a Gemini spectrometer (Varian Associates Inc. NMR Instruments, Palo Alto, CA) operating at 300 MHz with $CDCl_3$ as a solvent. As reference line, the chloroform peak at 7.24 ppm was used.

HPLC analysis

HPLC analysis of the (degraded) (mPEG750-*b*-)OCL was performed using a model 2695 Alliance, consisting of a pump, autosampler and injector, and a model 2487 absorbance meter (Waters Chromatography BV).[12, 26] A LiChrospher 100 RP-18 (5 µm, 125×4 mm) including an RP-18 guard column (2×2 mm) (Merck) was used. A gradient was run from 100% A (5/95 (w/w) ACN/H_2O) to 100% B (95/5 (w/w) ACN/H_2O) in 30 min at a flow rate of 1 mL/min. The injection volume was 50 µL and the detection wavelength was 210 nm. Sample concentrations of benzyl OCL and mPEG750-*b*-OCL-Bz were 1 and 5 mg/mL, respectively. The chromatograms were analysed using Empower software (Empower Pro, Waters Chromatography BV).

Degradation studies of benzyl oligo(ε-caprolactone)

Standard degradation study

The hydrolytic degradation of benzyl OCL was studied according to the methods described by de Jong *et al.*[26] In a standard degradation experiment, 2.5 mL of a solution of monodisperse benzyl OCL_5 in acetonitrile (ACN, 2 mg/mL) was introduced in a 10 mL glass bottle. Directly after addition of 2.5 mL of the appropriate buffer, the solution was incubated in a thermostated water bath at 37 °C. Samples of 500 µL were withdrawn, diluted with 500 µL 50/50 (v/v) ACN/1M acetate buffer pH 4 to stop the degradation, and stored at 4 °C prior to analysis. At least 8 samples were taken in a time interval corresponding to 1-3 degradation half-lives. The pseudo first order degradation rate constant k_{obs} was determined from the slope of the plot of the logarithm of the residual oligomer concentration vs time.

Influence of pH

Buffers used were trifluoro acetic acid (TFA, pH 0.5 and 1), phosphate (pH 1.5; 2; 2.5 and 12), borate (pH 9 and 9.5) and carbonate (pH 10 and 11). Buffer concentrations were 100 mM and contained 0.02% (w/w) of sodium azide to prevent the growth of microorganisms. The buffer to ACN ratio was 50/50 (v/v). The pH of the ACN/buffer mixtures was measured using a HI 8314 membrane pH meter (Hanna Instruments) equipped with a HI1330 ceramic junction electrode.

Influence of the dielectric constant

The influence of the dielectric constant of the degradation medium on the hydrolysis kinetics was investigated by using different ratios of ACN/buffer pH 11, *i.e.* 40/60, 50/50, 60/40 and 70/30 (v/v). The dielectric constant was calculated according to the formula $\varepsilon = (\varepsilon_{ACN} \times ACN(\%) + \varepsilon_{H2O} \times buffer(\%))/100$, with ε_{H2O}=78.5 and ε_{ACN}=37.5. The concentration of benzyl OCL_5 in the final mixture was 1 mg/mL. Since the addition of ACN results in an elevated pH, the experimental k_{obs} values for the different ACN/buffer ratios were normalised to pH 11, assuming that the order in OH^- is 1.

Degradation mechanism

To study the degradation mechanism, the degradation product vs time curves at pH 1 and 12 were analysed according to the kinetic model described by van Nostrum *et al.*[27]

Degradation studies of oligo(ε-caprolactone) based diblock oligomers

Hydrolytic degradation

The degradation rate of mPEG750-*b*-OCL_5-Bz was investigated when molecularly dissolved in an ACN/buffer mixture, and as micelles in buffer only. MPEG750-*b*-OCL_5-Bz was either dissolved in ACN or dispersed in water by hydration of an oligomer film, at a concentration of 10 mg/mL. The samples were 1/1 diluted with buffer pH 11 and pH 12, resulting in a final pH of 11.8 and 12, respectively, and placed in the sample chamber of the HPLC system thermostated at 37 °C. At regular time points, a sample was taken and injected onto the RP-18 column. Elution was performed using an ACN/H_2O gradient as described in the section 'HPLC analysis'. To correct for the slightly lower pH in the ACN/buffer mixture, the experimental k_{obs} value was normalised to pH 12, assuming that the order in OH^- is 1. The destabilisation of the micelles in aqueous medium of pH 12 and at 37 °C was studied by measuring the particle size (Z_{ave}), polydispersity index (PDI) and scattering intensity (signal) by dynamic light scattering (DLS), using a Malvern CGS-3 multi-angle goniometer (Malvern Ltd., Malvern), thermostated at 37 °C, and a measurement angle of 90°.

Enzymatic degradation

The lipase-catalysed degradation of polydisperse mPEG750-*b*-OCL_{av5} was measured by titration of the generated acids using a pH-stat system, consisting of a Mettler DL21 titrator, equipped with a Mettler Toledo DG-111-sc KCl electrode.[28] In detail, mPEG750-*b*-OCL_{av5} was dispersed in water at concentrations ranging from 0.1-10 mg/mL, and the pH was set to 7.4. Forty mL of micellar dispersion were incubated at 37 °C and lipase was added, to yield enzyme concentrations of 3-38 mU/mL. The pH was kept constant by titration with 3 mM NaOH. The rate of base consumption during the first 10 min after lipase addition was used as a measure for the ester hydrolysis rate. Since the pH-stat method necessitates the use of relatively large amounts of block oligomer, this method could not be used to monitor the enzymatic degradation of fractionated mPEG750-*b*-OCL_5-Bz, of which only a limited amount was available.

The degradation and destabilisation of mPEG750-*b*-OCL_5-Bz micelles by lipase was investigated by HPLC and DLS, as described above for the hydrolytic degradation of these micelles. The studies were performed in 100 mM phosphate buffer pH 7.4 at an enzyme concentration of 3 mU/mL. HPLC analysis was also performed at lipase concentrations of 1.5 and 0.3 mU/mL.

Results and discussion

Preparation and characterisation of the oligo(ε-caprolactone) oligomers

Polydisperse benzyl OCL and mPEG750-*b*-OCL with an average degree of polymerisation (DP) of 5 (OCL_{av5}) were obtained by ring opening polymerisation of ε-caprolactone, and the hydroxyl end group was benzoylated as reported in chapter 4.[12] Monodisperse products were isolated by preparative HPLC, and the identity and purity were proven by ^{1}H NMR, ESI-MS and analytical HPLC.[12] Monodisperse benzyl OCL with a DP of 5 (benzyl OCL_5) and monodisperse benzoylated mPEG750-*b*-OCL_5 (mPEG750-*b*-OCL_5-Bz) were used in the degradation studies, and had a purity >95%. Polydisperse mPEG750-*b*-OCL_{av5} was used in one of the studies as well (Figure 1).

Hydrolytic degradation of benzyl oligo(ε-caprolactone)

Qualitative observations

The degradation of monodisperse benzyl OCL_5 (Figure 1a) was studied in a mixture of ACN and buffer of different pH. ACN was added to dissolve the hydrophobic benzyl OCL_5. Figure 2 shows the chromatograms of the degradation sample at different time points upon incubation at pH 11 and 37 °C. The degradation of benzyl OCL results in the formation of two types of oligomer fragments, one with a benzyl and a hydroxyl end group and one with a hydroxyl and a carboxyl end group, as illustrated in Figure 3. Ultimately, benzyl alcohol and 6-caproic acid are formed. With the HPLC method used, solely the degradation products with a benzyl end group are detected, since OCL has a very low UV-absorption at the detection wavelength used (210 nm). ESI-MS demonstrated that products without benzyl group are formed as well (data not shown). The chromatograms in Figure 2 demonstrate that upon degradation of benzyl OCL_5, small amounts of benzyl OCL_{1-4} are formed as the intermediate degradation products. When degradation proceeds, the intermediates are further degraded to finally obtain benzyl alcohol (and 6-caproic acid) as end stage degradation product. This is reflected by the curves in Figure 4, where the relative concentrations of the starting compound benzyl OCL_5 and of the degradation products with a lower DP are plotted against time. The chromatograms in Figure 2 demonstrate an equal rate of appearance of the intermediate degradation products in basic conditions, which indicates that a random chain scission process is involved in OCL hydrolysis. This is in contrast to oligolactate hydrolysis, where the hydroxyl end group is involved in preferred removal of the ultimate two lactic acid units, also called the back-biting mechanism.[26, 27]

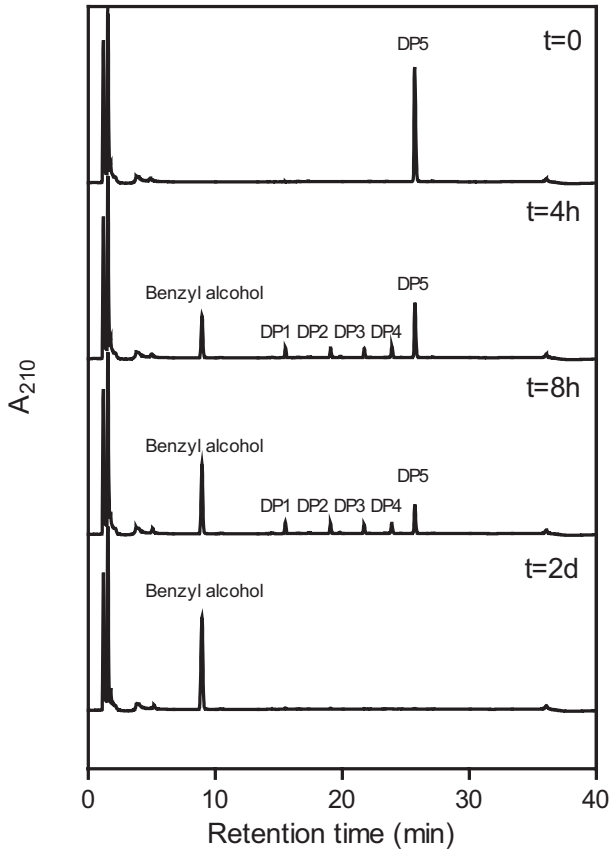

Figure 2 HPLC chromatograms of the degradation samples of monodisperse benzyl OCL_5 at pH 11 in 50/50 (v/v) ACN/buffer of 37 °C, at t=0, t=4 h, t=8 h and t=2 days. DP1-5 refers to the number of caprolactone (CL) units (degree of polymerisation) present in the benzylated oligomers.

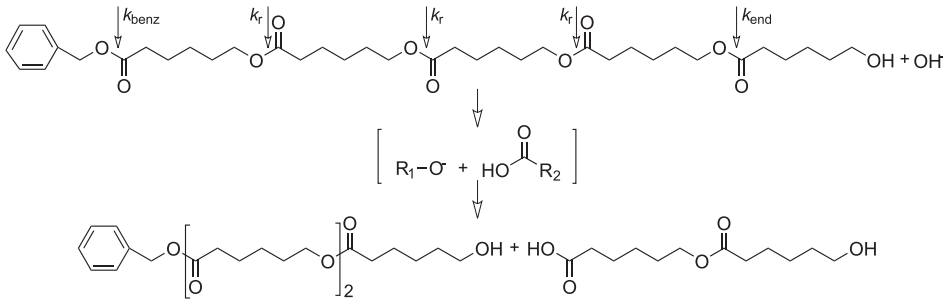

Figure 3 OH^- catalysed hydrolysis of benzyl OCL_5 into benzyl OCL_3 and OCL_2 as an example. k_{benz}, k_r and k_{end} refer to the degradation rate constants of the different types of ester bonds.

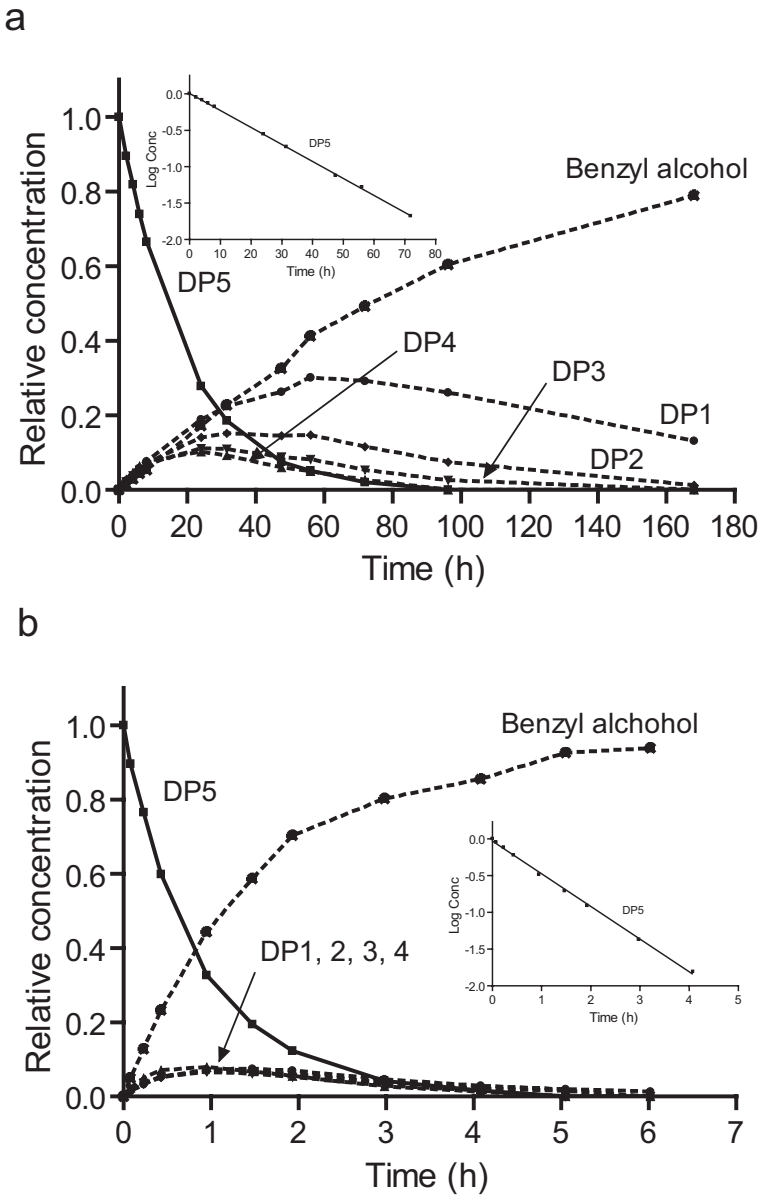

Figure 4 Degradation profile of benzyl OCL_5 at pH 1 (a) and pH 12 (b) in 50/50 (v/v) ACN/buffer at 37 °C. The insets show the logarithm of the concentration (Log Conc) of benzyl OCL_5 versus time. DP1-5 refers to the number of CL units.

Influence of the pH

At the pHs studied, benzyl OCL_5 degraded, as expected, according to pseudo-first order kinetics (linear relation between log k_{obs} and time; inserts Figure 4). Figure 5 shows the relation between log k_{obs} and pH. The slopes of the curves of pH vs log k_{obs} in acidic and basic conditions are -1.1 ± 0.1 and 1.0 ± 0.1, respectively, indicating specific proton- and hydroxyl-catalysed hydrolysis. This is in line with the results of oligolactate degradation.[26] Hydrolysis at physiological pH 7.4 has an estimated $t_{1/2}$ of 15 years in a 50/50 (v/v) ACN/buffer mixture (Table 1). Besides the effect on the degradation rate, the pH influences also the degradation mechanism (*vide infra*).

Influence of the dielectric constant

To be able to predict the degradation rate in buffer only, the influence of the dielectric constant (ε) of the dissolution medium (ACN/buffer) on k_{obs} was determined by studying the degradation of benzyl OCL_5 in different ACN/buffer mixtures. As shown in Figure 6, the log k_{obs} increased linearly with increasing ε, with a slope of 0.095 ± 0.003. A similar relationship was observed in the degradation of oligolactates, and it was ascribed to a lower reactivity of the ester towards hydrolysis resulting from stabilisation of the ground state by the organic solvent molecules.[26] Combining the effect of pH and ε on the degradation rate results in eq. 1,[27]

$$\log k' = \log k_{obs} + \Delta pH + \Delta \varepsilon_{ACN} \times 0.095 \qquad \text{(Eq. 1)}$$

where k' is the estimated degradation rate at a certain pH and volume percentage ACN in the mixture with aqueous buffer, k_{obs} is the measured degradation rate constant, ΔpH is the difference between the pH at which the degradation was measured and the pH at which the degradation rate is calculated, and $\Delta\varepsilon_{ACN}$ is the increase in ε when increasing the water content of the solvent mixture. The calculated degradation rate constant of benzyl OCL_5 in aqueous buffer at pH 7.4 and at 37 °C is 4.7×10^{-4} h^{-1}, corresponding to a $t_{1/2}$ of approximately 60 days (Table 1). Likely, this is an overestimation of the true degradation rate, since it is based on the degradation of molecularly dissolved benzyl OCL_5. However, due to its hydrophobicity, benzyl OCL_5 has a low solubility in buffer, which will result in a lower degradation rate.[26]

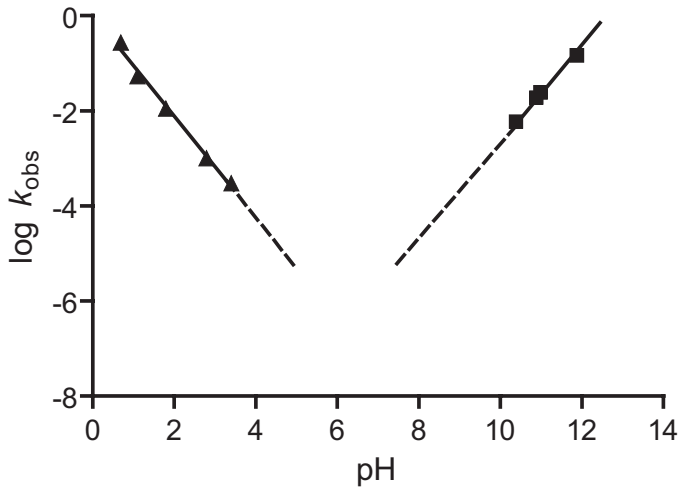

Figure 5 Log k_{obs} vs pH profile of benzyl OCL_5 (k_{obs} in h^{-1}). Degradation studies were performed at 37 °C in 50/50 (v/v) ACN/buffer, in a pH range of 0.5-3.5 and 10.5-12.5 at buffer concentrations of 100 mM. The variation in each k_{obs} value is 10% (n=3).

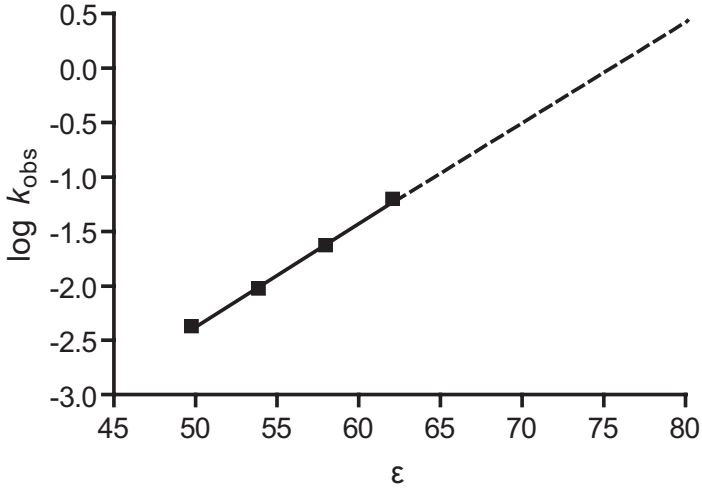

Figure 6 Relation between the dielectric constant (ε) of the degradation medium and log k_{obs} (k_{obs} in h^{-1}). Degradation studies were performed in mixtures with different ACN/buffer ratios at pH 11, 37 °C.

Table 1 Degradation rate constants and half-lives for the hydrolysis of benzyl OCL_5

	pH 1, 50% ACN	pH 12, 50% ACN	pH 7.4, 50% ACN	pH 7.4, buffer only
k_{obs} (h^{-1})[a]	5.5×10^{-2}	1.4×10^{-1}	5.2×10^{-6}	4.7×10^{-4}
$t_{1/2}$	13 h	4.9 h	15 years	62 days
k_r (h^{-1})	9.8×10^{-3}	2.1×10^{-2}		
k_{benz} (h^{-1})	8.5×10^{-3}	1.0×10^{-1}		
k_{end} (h^{-1})	9.8×10^{-3}	3.4×10^{-2}		

The variation in the values is 10% (n=3).
[a] Degradation rate constant k_{obs}; measured at pH 1 and pH 12, and calculated value at pH 7.4.

Degradation mechanism

The k_{obs} of benzyl OCL_5 can be considered the sum of the individual rate constants for hydrolysis of the different ester bonds in the OCL-chains. Since benzyl OCL_5 contains three different types of ester bonds, the scission process can be described by eq. 2:[27]

$$k_{obs} = k_{benz} + (n-2) \times k_r + k_{end} \qquad \text{(Eq. 2)}$$

where k_{benz} and k_{end} are the rate constants of the benzyl ester, and of the ultimate ester bond at the hydroxyl terminus, respectively, as indicated by the arrows in Figure 3. The different *k* values were determined by fitting of the degradation profiles (Figure 4).[27] The *k* values that gave the best predictions of the amounts of intermediate and final degradation products are listed in Table 1. It was demonstrated that indeed the reactivity of the hydroxyl terminus equals that of the esters in the OCL-chain. However, the benzyl ester degrades five times faster than the other esters at basic pH. This can be explained by the mechanism involved in basic ester hydrolysis. The nucleophilic attack by a hydroxide ion results in the formation of carboxylic acid and an alkoxide ion, which are then rapidly converted into a carboxylate anion and an alcohol, as illustrated by the example in Figure 3. Since the benzyl-O^- anion is a better leaving group than the R-CO-$(CH_2)_5$-O^- anion, the rate of basic hydrolysis of the benzyl ester is faster than that of the other esters in the OCL-chain.

Hydrolytic degradation of benzoylated mPEG-*b*-OCL

Upon incubation in ACN/buffer, the concentration of mPEG750-*b*-OCL_5-Bz decreased according to pseudo first order kinetics, similar to the homopolymer benzyl OCL_5 (data not shown). The degradation rate (k_{obs}) at pH 12 is almost the same as well (Table 2). Interestingly, when the degradation of mPEG750-*b*-OCL_5-Bz was studied as micellar dispersion in buffer only, an almost equal degradation rate was observed as in dissolved state in a 50/50 ACN/buffer mixture (Table 2). A micellar dispersion is an equilibrium between micelles and dissolved amphiphiles, but the concentration of mPEG750-*b*-OCL_5-Bz used in the degradation study (5 mg/mL) is much higher than its critical aggregation concentration (0.008 mg/mL),[12] which means that less than one percent of the molecules is dissolved. Although the dissolved oligomers are expected to degrade relatively fast because of the high ε of the buffer (calculated $t_{1/2}$ = 3.9 min at pH 12, Table 2), the majority of the oligomers is present in the micellar core. This has a low polarity, accounting for the low degradation rate ($t_{1/2}$ = 5.5 h). In fact, the small difference in degradation rates between the micelles and the dissolved molecules in 50/50 (v/v) ACN/buffer indicates that the micellar core may have a similar polarity as the cosolvent mixture.

HPLC analysis of the formation of degradation products did not indicate preferential cleavage of any of the ester bonds during micelle degradation or in the ACN/buffer mixture (data not shown). This is in contrast with literature data, where preferential cleavage of certain ester bonds has been suggested, rather than a random scission process. Both the involvement of the hydroxyl end group in chain end cleavage,[29, 30] and preferential cleavage of the PEG-PCL ester bond were reported.[31] Hu *et al.* proposed a two-stage degradation mechanism for PCL-*b*-PEG-*b*-PCL micelles. An initial stage of interfacial erosion was followed by bulk degradation in the micellar core, caused by preferential cleavage of the PEG-PCL ester bond.[31] The preferential cleavage of the ester bond adjacent to the PEG-block was observed in the degradation of PEG-PLGA nanoparticles as well.[32] The differences may be explained by the absence of a hydroxyl end group and by the low molecular weight of the block oligomers studied here. In contrast to high molecular weight PCL, OCL is liquid at 37 °C,[12] which may result in a higher water accessibility of the ester bonds inside the micellar core.

Figure 7 demonstrates the destabilisation of mPEG750-*b*-OCL_5-Bz micelles in buffer pH 12, measured by DLS. The increase in size, accompanied by the increasing and more fluctuating polydispersity index (PDI) and scattering intensity indicates that the micelles start to destabilise after approximately 5 h under these conditions, which corresponds well to the degradation half-life measured by HPLC. Such correlation was also found for other biodegradable micelles, for example PEG-*b*-poly(N-(2-hydroxyethyl) methacrylamide-oligolactate) ($HEMAm_{Lac}$) micelles.[33]

Table 2 Degradation rate constants and half-lives for the hydrolysis of mPEG750-*b*-OCL_5-Bz

	Measured		Calculated[b]	
	pH 12, dissolved in 50% ACN	pH 12, micelles in buffer	pH 12, dissolved in buffer[c]	pH 7.4, micelles in buffer[d]
k_{obs} (h^{-1})[a]	0.12	0.13	10.6	3.2×10^{-6}
$t_{1/2}$	5.8 h	5.5 h	3.9 min	25 years

[a] *Measured or calculated degradation rate constant k_{obs}. The variation in the values is 10%.*
[b] *Estimated with use of equation 2.*
[c] *Estimated based on the measured data in pH 12, dissolved in 50/50 (v/v) ACN/buffer.*
[d] *Estimated based on the measured data in pH 12, micelles in buffer.*

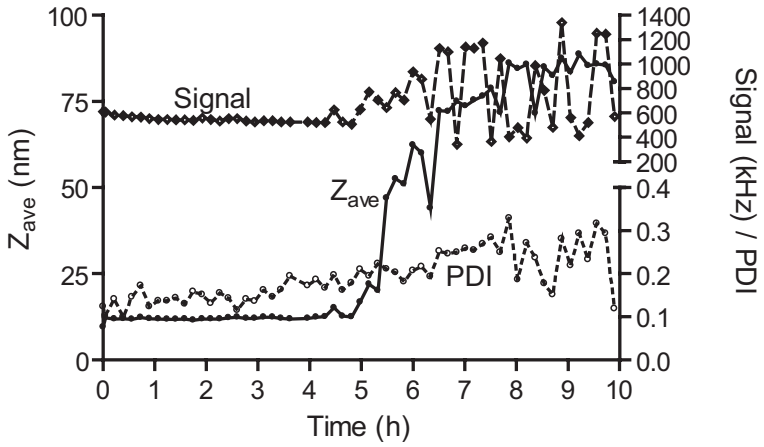

Figure 7 Destabilisation of micelles composed of mPEG750-*b*-OCL_5-Bz (5 mg/mL) upon incubation at pH 12 and 37 °C. Size (Z_{ave}) is plotted on the left Y-axis; polydispersity index (PDI) and scattering intensity (Signal) are plotted on the right Y-axis.

In chapter 4, it was found that mPEG750-*b*-OCL_5-Bz micelles in PBS retain their small size for at least two weeks at 37 °C.[12] This is confirmed by the results obtained here. In fact, by using equation 1, these micelles have an estimated degradation half-life of 25 years at pH 7.4 (Table 2). The results indicate that chemical degradation of these micelles is very slow, and will hardly play a role at physiological conditions. However, several enzymes are known to enhance the degradation rate of polyesters, as stated in the introduction. Therefore we studied the enzymatic degradation of micelles composed of OCL-based block oligomers in addition to chemical hydrolysis.

Enzymatic degradation of OCL-based block oligomers

Polydisperse mPEG750-b-OCL_{av5}

Figure 8 shows the enzymatic degradation rate of polydisperse mPEG750-*b*-OCL_{av5} by lipase, as function of the enzyme concentration (a) and the block oligomer concentration (b). The degradation rate is proportional to the enzyme concentration, which is in agreement with standard enzyme kinetics, and has also been reported by others.[21, 28, 34, 35] Interestingly, the relation between degradation rate and substrate concentration can be described by Michaelis-Menten kinetics (Figure 8b, eq. 3), which describes the enzymatically catalysed conversion of a dissolved substrate S into a product P,

$$V = V_{max} \frac{S}{K_m + S} \qquad \text{(Eq. 3)}$$

where V is the degradation rate, S the substrate concentration, K_m the Michaelis-Menten constant, and V_{max} the maximum degradation rate at high substrate concentrations, which is proportional to the enzyme concentration. Fitting of the data in Figure 8b by the Michaelis-Menten model revealed a V_{max} of 4.4 ± 0.2 μmol/min and a K_m of 2.2 ± 0.3 mg/mL at an enzyme concentration of 19 mU/mL.

The amphiphilic block oligomer mPEG750-*b*-OCL_{av5} forms micelles in water,[36] which is a dynamic equilibrium between free unimers and self-assembled oligomer chains, and there is a continuous exchange of unimers between the micelles and the bulk solution. The enzymatic degradation of mPEG750-*b*-OCL_{av5} was measured at oligomer concentrations above its CAC of 0.02 mg/mL,[36] which means that in theory both the self-assembled oligomers and the free unimers can be degraded by the enzyme, as illustrated by Figure 8c.

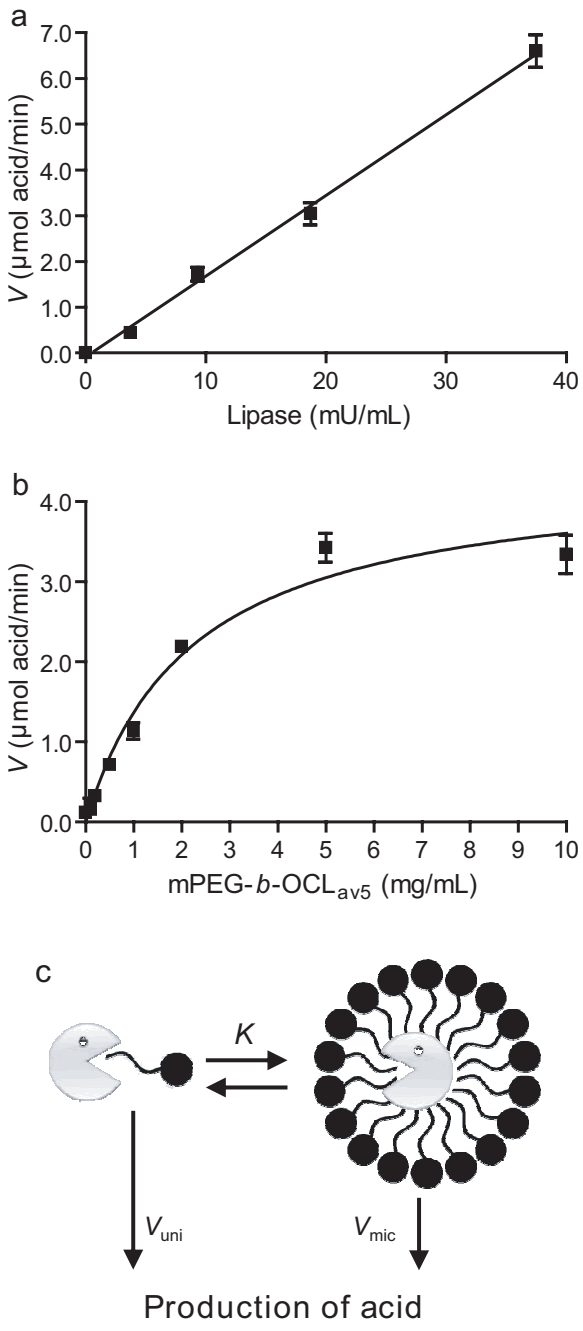

Figure 8 Enzymatic degradation rate V (± SD, n=3) of mPEG750-*b*-OCL_{av5} by lipase at pH 7.4 and 37 °C, at a fixed substrate concentration of 10 mg/mL (a), and at a fixed enzyme concentration of 19 mU/mL and oligomer concentrations above the critical aggregation concentration of 0.02 mg/mL[36] (b). Free unimers are in equilibrium with self-assembled oligomers, and both may be degraded by lipase into acid products (c).

First, we assume that the enzyme can only degrade the unimers in solution and the degradation rate, V_{uni}, is related to the concentration of unimers, S_{uni} (eq. 4).

$$V_{uni} = V_{\max,uni}\frac{S_{uni}}{K_{m,uni} + S_{uni}} \qquad \text{(Eq. 4)}$$

In an equilibrium situation, the concentration of unimers is independent of the total oligomer concentration in the dispersion, and equals the CAC (0.02 mg/mL for mPEG750-*b*-OCL_{av5}[36]). However, the enzymatic degradation of the unimers causes a shift of the equilibrium state, which means that unimer exchange rate has to be taken into account as well. The kinetics of this exchange process, or the so-called fast relaxation process of micelles, have been described by the Aniansson-Wall model, in which the association and dissociation of micelles is considered as a step-wise process, involving the entry and departure of one unimer at a time from the micelle (Figure 8c), and the exchange rate depends on the strength of the interactions in the micellar core.[37]

When the exchange of the block oligomers between the bulk solution and the micelles is faster than the enzymatic degradation, the concentration of unimers will remain constant during degradation, resulting from a continuous supply from the micelles. Since at a given enzyme concentration V_{max} and K_m are fixed values as well, V_{uni} will be constant and thus independent of the total oligomer concentration (*i.e.* zero order kinetics). On the other hand, when the unimer exchange rate is lower than the enzymatic degradation rate, the unimer exchange becomes the rate limiting step, and a steady state concentration of unimers will be present of which the concentration is below the CAC and proportional to the total oligomer concentration, *i.e.* $S_{uni} = K \times [\text{Oligo}]_{total}$, where the constant K represents the unimer exchange rate. This means that the overall degradation rate of the unimers can be described by equation 5, which is normal Michaelis-Menten kinetics, and can explain the relation observed in Figure 8b.

$$V_{uni} = V_{\max,uni}\frac{([\text{Oligo}]_{total} \times K)}{K_{m,uni} + ([\text{Oligo}]_{total} \times K)} = V_{\max,uni}\frac{[\text{Oligo}]_{total}}{(K_{m,uni}/K) + [\text{Oligo}]_{total}} \qquad \text{(Eq. 5)}$$

However, it can not be excluded that lipase is able to hydrolyse the ester bonds inside the micellar core as well (Figure 8c). This means that lipase-catalysed degradation of mPEG750-*b*-OCL_{av5} above its CAC can be described by the following equation:

$$V_{total} = V_{uni} + V_{mic} = \left(V_{\max,uni} \frac{[\text{Oligo}]_{total}}{(K_{m,\,uni}/K) + [\text{Oligo}]_{total}} \right) + \left(V_{\max,mic} \frac{S_{mic}}{K_{m,\,mic} + S_{mic}} \right) \quad \text{(Eq. 6)}$$

where the overall degradation rate (V_{total}) is a sum of the degradation rate of the unimers (V_{uni}) and that of the self-assembled block oligomers (V_{mic}). As pointed out above, V_{uni} is either constant (C in eq. 7) or depends on the total oligomer concentration $[\text{Oligo}]_{total}$ (eq. 6), when the enzymatic degradation rate of the unimers is lower or higher than the unimer exchange rate, respectively.

$$V_{total} = C + \left(V_{\max,mic} \frac{S_{mic}}{K_{m,\,mic} + S_{mic}} \right) \quad \text{(Eq. 7)}$$

Therefore, in the case that intramicellar degradation plays a role in the kinetics, the relation between the degradation rate and total oligomer concentration will follow the Michaelis-Menten model when the unimer exchange rate is low (eq. 6) or when the degradation of unimers hardly contributes to the overall degradation rate ($V_{uni} << V_{mic}$).

Summarising, Michaelis-Menten kinetics is expected when lipase degrades the unimers only and the unimer exchange is the rate limiting step, or when enzymatic degradation predominantly occurs in the micellar core. Based on the presented results it is not possible to discriminate unambiguously between the intramicellar or unimer degradation mechanism, and further investigation is ongoing . In literature, the enzymatic degradation of PEG-poly(3-hydroxybutyrate) (PHB)-*b*-PEG micelles was ascribed to penetration of the enzyme into the core,[38] and PEG-PCL nanoparticles were suggested to be 'eaten in a one-by-one fashion' by the enzyme.[34] However, in both studies the unimer exchange rate between the micelles and the bulk solution was not taken into account.

Benzoylated mPEG750-b-OCL$_5$

Since the limited amount of mPEG750-*b*-OCL$_5$-Bz available impeded the use of the pH-stat method to study its enzymatic degradation, the degradation of mPEG750-*b*-OCL$_5$-Bz (5 mg/mL) by lipase was monitored by HPLC (Figure 9). This figure shows that, in line with the results shown in Figure 8a, the degradation rate increases with increasing lipase concentration. At the lowest enzyme concentration, zero order kinetics is observed, reflected by the linear relation between concentration and time.

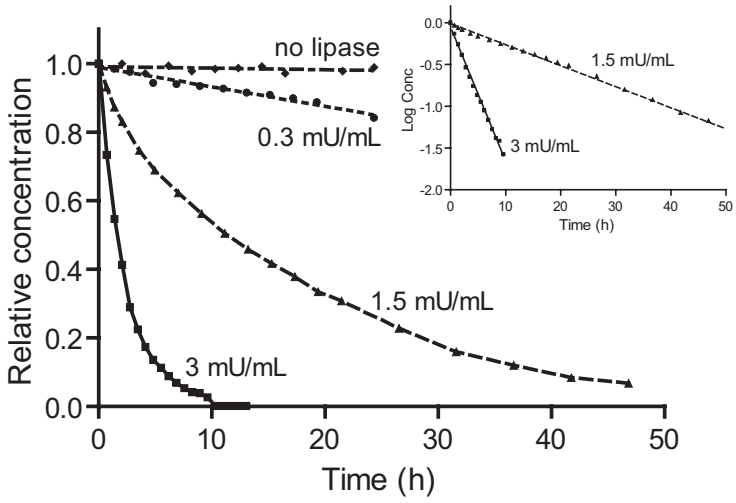

Figure 9 Enzymatic degradation of mPEG750-*b*-OCL_5-Bz (5 mg/mL) at different enzyme concentrations in pH 7.4 at 37 °C as monitored by HPLC. The relative concentration of mPEG750-*b*-OCL_5-Bz is plotted against time in hours. The inset shows the log concentration of mPEG750-*b*-OCL_5-Bz versus time at enzyme concentrations of 1.5 and 3.0 mU/mL.

Here, the degradation rate is relatively small, resulting in an almost constant substrate (block oligomer) concentration. At higher enzyme concentrations, the substrate concentration decreases in time, and apparent first order kinetics is observed (inset Figure 9).

Analysis of the chromatograms demonstrated that the decrease in the concentration of benzoylated mPEG750-*b*-OCL_5 was accompanied by an increase in the concentration of benzoic acid (data not shown). Remarkably, this was the only degradation product that could be detected, suggesting preferential cleavage of the benzoyl ester before further degradation of the OCL takes place. During the first hour of degradation at a lipase concentration of 3 mU/mL, 1.0 ± 0.1 mM benzoic acid was formed as measured by HPLC. Since products without a benzoyl group are not detected by the HPLC method, 6-caproic acid or non-benzoylated OCL-fragments may be formed as well, and therefore the total acid formation may be even higher. At the same oligomer and enzyme concentration, the initial hydrolysis rate of polydisperse mPEG750-*b*-OCL_{av5} lacking the benzoyl end group was only

0.6 ± 0.1 mM of total acid/h, measured by the pH-stat method, indicating indeed a higher susceptibility of the benzoyl ester bond towards enzymatic attack. This may be related to its higher hydrophobicity, resulting in a better binding to the enzyme. The influence of enzymatic degradation of mPEG750-*b*-OCL_5-Bz (5 mg/mL) at a lipase concentration of 3 mU/mL on the micelle stability is demonstrated in Figure 10. During degradation the scattering intensity decreases gradually from 300 kHz to background level (40 kHz). Remarkably, only a slight decrease in the micellar size and a constant polydispersity index was observed over more than 20 h, although after 12 h mPEG750-*b*-OCL_5-Bz was not detected anymore by HPLC (Figure 9). Based on the pH-stat results obtained with mPEG750-*b*-OCL_{av5} (lacking the benzoyl end group), only 40% of the total number of ester bonds is cleaved after 12 h, indicating that these observations may again be the result of the higher susceptibility of the benzoyl ester towards enzymatic degradation. Upon cleavage of the benzoyl ester, mPEG750-*b*-OCL_5 is formed, which is not detected by the HPLC-method. However, it is still an amphiphilic molecule that self-assembles into oligomeric micelles with a diameter of 8 nm, above its CAC of 0.5 mg/mL.[12] Due to the much higher CAC compared to that of the benzoylated oligomer (0.008 mg/mL[12]), the amount of micelles in the dispersion is lower, and consequently the scattering intensity decreases. Although much slower, as demonstrated in this chapter (Figure 8) the other ester bonds in the OCL-chain are subject to enzyme-catalysed hydrolysis as well, which eventually results in the dissolution of the micelles after approximately 30 h.

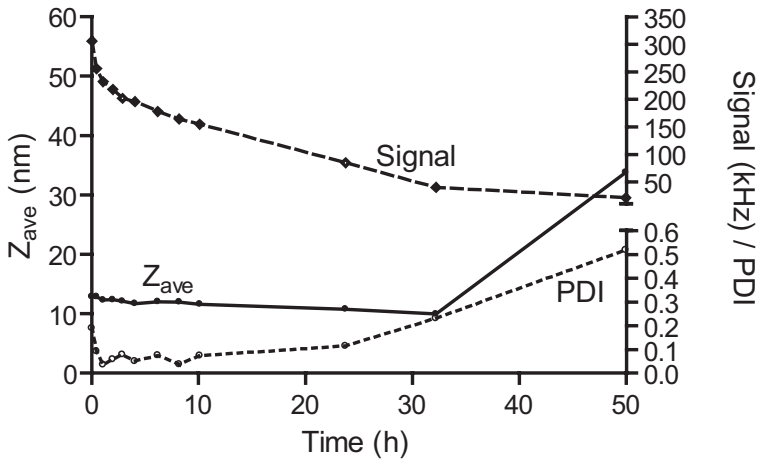

Figure 10 Destabilisation of micelles composed of mPEG750-*b*-OCL_5-Bz (5 mg/mL) in pH 7.4 at 37 °C and a lipase concentration of 3 mU/mL. Size (Z_{ave}) is plotted on the left Y-axis; polydispersity index (PDI) and scattering intensity (Signal) are plotted on the right Y-axis.

Conclusions

To gain insight into the destabilisation of mPEG750-*b*-OCL micelles, the degradation kinetics and mechanism of monodisperse OCL and its amphiphilic block oligomers with mPEG750 were investigated. It was demonstrated that monodisperse benzyl OCL was hydrolysed essentially via a random chain scission process. The presence of PEG hardly affected the degradation rate of the OCL esters in solution, but the formation of micelles in buffer resulted in a substantially increased half-life, which is ascribed to the low polarity of the micellar core. The hydrolytic degradation of OCL at physiological pH is a very slow process, which was markedly accelerated by the presence of lipase. The degradation half-life decreased from several years to a few days to hours, depending on the enzyme concentration. In conclusion, the results indicate that mPEG750-*b*-OCL micelles are stable systems in buffer. However, their susceptibility to hydrolytic enzymes such as lipase confers these systems good properties for the controlled delivery of drugs *in vivo*.

References

1. Ueda H; Tabata Y, Polyhydroxyalkanonate derivatives in current clinical applications and trials. *Adv Drug Deliver Rev* 55, 501-518 (2003).
2. Jagur-Grodzinski J, Polymers for tissue engineering, medical devices, and regenerative medicine. Concise general review of recent studies. *Polym Advan Technol* 17, 395-418 (2006).
3. Tessmar JK; Achim M. Göpferich, Customized PEG-derived copolymers for tissue-engineering applications. *Macromol Biosci* 7, 23-39 (2007).
4. Sinha VR; Bansal K; Kaushik R; Kumria R; Trehan A, Poly-ε-caprolactone microspheres and nanospheres: an overview. *Int J Pharm* 278, 1-23 (2004).
5. Gaucher G; Dufresne MH; Sant VP; Kang N; Maysinger D; Leroux JC, Block copolymer micelles: preparation, characterization and application in drug delivery. *J Control Release* 109, 169-188 (2005).
6. Allen C; Maysinger D; Eisenberg A, Nano-engineering block copolymer aggregates for drug delivery. *Colloid Surface B* 16, 3-27 (1999).
7. Shuai X; Ai H; Nasongkla N; Kim S; Gao J, Micellar carriers based on block copolymers of poly(ε-caprolactone) and poly(ethylene glycol) for doxorubicin delivery. *J Control Release* 98, 415-426 (2004).
8. Aliabadi HM; Brocks DR; Lavasanifar A, Polymeric micelles for the solubilization and delivery of cyclosporine A: pharmacokinetics and biodistribution. *Biomaterials* 26, 7251-7259 (2005).
9. Forrest ML; Won CY; Malick AW; Kwon GS, In vitro release of the mTOR inhibitor rapamycin from poly(ethylene glycol)-*b*-poly(e-caprolactone) micelles. *J Control Release* 110, 370-377 (2005).
10. Shi B; Fang C; You MX; Zhang Y; Fu S; Pei Y, Stealth MePEG-PCL micelles: effects of polymer composition on micelle physicochemical characteristics, *in vitro* drug release, *in vivo* pharmacokinetics in rats and biodistribution in S180 tumor bearing mice. *Colloid Polym Sci* 283, 954-967 (2005).
11. Zhang J; Wang L-Q; Wang H; Tu K, Micellization phenomena of amphiphilic block copolymers based on methoxy poly(ethylene glycol) and either crystalline or amorphous poly(caprolactone-*b*-lactide). *Biomacromolecules* 7, 2492-2500 (2006).
12. Carstens MG; Bevernage JJL; van Nostrum CF; van Steenbergen MJ; Flesch FM; Verrijk R; de Leede LGJ; Crommelin DJA; Hennink WE, Small oligomeric micelles based on end group modified mPEG-oligocaprolactone with monodisperse hydrophobic blocks. *Macromolecules* 40, 116-122 (2007).
13. Chen DR; Bei JZ; Wang SG, Polycaprolactone microparticles and their biodegradation. *Polym Degrad Stabil* 67, 455-459 (2000).
14. Pitt GG; Gratzl MM; Kimmel GL; Surles J; Sohindler A, Aliphatic polyesters II. The degradation of poly (DL-lactide), poly (ε-caprolactone), and their copolymers *in vivo*. *Biomaterials* 2, 215-220 (1981).
15. Sun H; Mei L; Song C; Cui X; Wang P, The *in vivo* degradation, absorption and excretion of PCL-based implant. *Biomaterials* 27, 1735-1740 (2006).
16. Jeong SI; Kim B-S; Lee YM; Ihn KJ; Kim SH; Kim YH, Morphology of elastic poly(ε-caprolactone) copolymers and *in vitro* and *in vivo* degradation behavior of their scaffolds. *Biomacromolecules* 5, 1303-1309 (2004).
17. Pitt CG; Gu Z-w, Modification of the rates of chain cleavage of poly(ε-caprolactone) and related polyesters in the solid state. *J Control Release* 4, 283-292 (1987).
18. Nishida H; Yamashita M; Nagashima M; Hattori N; Endo T; Tokiwa Y, Theoretical prediction of molecular weight on autocatalytic random hydrolysis of aliphatic polyesters. *Macromolecules* 33, 6595-6601 (2000).
19. Jung JH; Ree M; Kim H, Acid- and base-catalyzed hydrolyses of aliphatic polycarbonates and polyesters. *Catal Today* 115, 283-287 (2006).
20. Huang M-H; Li S; Hutmacher DW; Schantz J-T; Vacanti CA; Braud C; Vert M, Degradation and cell culture studies on block copolymers prepared by ring opening polymerisation of ε-caprolactone in the presence of poly(ethylene glycol). *J Biomed Mater Res A* 69A, 417-427 (2004).
21. Herzog K; Muller R-J; Deckwer W-D, Mechanism and kinetics of the enzymatic hydrolysis of polyester nanoparticles by lipases. *Polym Degrad Stabil* 91, 2486-2498 (2006).

22. He F; Li S; Garreau H; Vert M; Zhuo R, Enzyme-catalyzed polymerisation and degradation of copolyesters of ε-caprolactone and γ-butyrolactone. *Polymer* 46, 12682-12688 (2005).
23. Matsumura S; Tsukada K; Toshima K, Novel lipase-catalyzed ring-opening copolymerisation of lactide and trimethylene carbonate forming poly(ester carbonate)s. *Int J Biol Macromol* 25, 161-167 (1999).
24. Zeng J; Chen X; Liang Q; Xu X; Jing X, Enzymatic degradation of poly(L-lactide) and poly(ε-caprolactone) electrospun fibers. *Macromol Biosci* 4, 1118-1125 (2004).
25. Li S; Garreau H; Pauvert B; McGrath J; Toniolo A; Vert M, Enzymatic degradation of block copolymers prepared from ε-caprolactone and poly(ethylene glycol). *Biomacromolecules* 3, 525-530 (2002).
26. de Jong SJ; Arias ER; Rijkers DTS; van Nostrum CF; Kettenes-van den Bosch JJ; Hennink WE, New insights into the hydrolytic degradation of poly(lactic acid): participation of the alcohol terminus. *Polymer* 42, 2795-2802 (2001).
27. van Nostrum CF; Veldhuis TFJ; Bos GW; Hennink WE, Hydrolytic degradation of oligo(lactic acid): a kinetic and mechanistic study. *Polymer* 45, 6779-6787 (2004).
28. Marten E; Muller R-J; Deckwer W-D, Studies on the enzymatic hydrolysis of polyesters I. Low molecular mass model esters and aliphatic polyesters. *Polym Degrad Stabil* 80, 485-501 (2003).
29. Geng Y; Discher DE, Visualization of degradable worm micelle breakdown in relation to drug release. *Polymer* 47, 2519-2525 (2006).
30. Geng Y; Discher DE, Hydrolytic degradation of poly(ethylene oxide)-*block*-polycaprolactone worm micelles. *J Am Chem Soc* 127, 12780-12781 (2005).
31. Hu Y; Zhang L; Cao Y; Ge H; Jiang X; Yang C, Degradation behavior of poly(ε-caprolactone-*b*-poly(ethylene glycol)-*b*-poly(ε-caprolactone) micelles in aqueous solution. *Biomacromolecules* 5, 1756-1762 (2004).
32. Zweers MLT; Engbers GHM; Grijpma DW; Feijen J, In vitro degradation of nanoparticles prepared from polymers based on DL-lactide, glycolide and poly(ethylene oxide). *J Control Release* 100, 347-356 (2004).
33. Rijcken CJF; Veldhuis TFJ; Ramzi A; Meeldijk JD; van Nostrum CF; Hennink WE, Novel fast degradable thermosensitive polymeric micelles based on PEG-*block*-poly(*N*-(2-hydroxyethyl)methacrylamide-oligolactates). *Biomacromolecules* 6, 2343-2351 (2005).
34. Gan Z; Jim TF; Li M; Yuer Z; Wang S; Wu C, Enzymatic biodegradation of poly(ethylene oxide-ε-caprolactone) diblock copolymer and its potential biomedical applications. *Macromolecules* 32, 590-594 (1999).
35. Nie T; Zhao Y; Xie Z; Wu C, Micellar formation of poly(caprolactone-*block*-ethylene oxide-*block*-caprolactone) and its enzymatic biodegradation in aqueous dispersion. *Macromolecules* 36, 8825-8829 (2003).
36. Letchford K; Zastre J; Liggins R; Burt H, Synthesis and micellar characterization of short block length methoxy poly(ethylene glycol)-block-poly(caprolactone) diblock copolymers. *Colloid Surface B* 35, 81-91 (2004).
37. Attwood D; Florence AT, *Surfactant Systems: Their chemistry, pharmacy and biology*, Chapman and Hall Ltd., London, UK, p 108-111 (1983).
38. Chen C; Yu CH; Cheng YC; Yu PHF; Cheung MK, Biodegradable nanoparticles of amphiphilic triblock copolymers based on poly(3-hydroxybutyrate) and poly(ethylene glycol) as drug carriers. *Biomaterials* 27, 4804-4814 (2006).

Biodegradable oligomeric micelles for novel taxane formulations

6

Myrra G. Carstens,[a,b] Pascal H.J.L.F. de Jong,[a]

Cornelus F. van Nostrum,[a] Johan Kemmink,[c] Ruud Verrijk,[b]

Leo G.J. de Leede,[b] Daan J.A. Crommelin,[a] Wim E. Hennink[a]

[a] Department of Pharmaceutics, Utrecht Institute for Pharmaceutical Sciences (UIPS), Faculty of Pharmaceutical Sciences, Utrecht University, Utrecht, The Netherlands

[b] OctoPlus N.V., Leiden, the Netherlands

[c] Department of Medicinal Chemistry, UIPS, Faculty of Pharmaceutical Sciences, Utrecht University, Utrecht, The Netherlands

Submitted for publication

Abstract

Docetaxel (DCTX) and paclitaxel (PTX) are very potent anti-cancer drugs, but the currently available formulations, Taxotere® and Taxol®, respectively, are associated with vehicle-related toxicity. An attractive alternative to formulate these hydrophobic cytotoxic agents are polymeric micelles. In this study, the loading of taxanes into oligomeric micelles composed of mPEG750-*b*-oligo(ε-caprolactone)$_5$ (mPEG750-*b*-OCL$_5$) with a hydroxyl (OH), benzoyl (Bz) or naphthoyl (Np) end group was investigated. Next, the release characteristics and cytotoxicity of the loaded micelles were studied. MPEG750-*b*-OCL$_5$-OH micelles loaded with taxanes formed unstable particles with rapid leakage of the drug. In contrast, the presence of an aromatic end group (Bz or Np) resulted in the formation of small (10 nm), almost monodisperse micelles with stable encapsulation of 10% (w/w) of PTX or DCTX. This was ascribed to a better compatibility between the drug and the micellar core of oligomers with an aromatic end group as compared to oligomers with a hydroxyl end group. ^{1}H NMR studies showed that the micellar core was liquid and that PTX was molecularly dissolved in the core. The *in vitro* stability was studied in PBS at 37 °C, which showed that leakage of PTX from 10% and 5% (w/w) loaded mPEG750-*b*-OCL$_5$-Bz micelles started after 8 and 24 h, respectively. The presence of albumin did not affect the stability, suggesting that the micelles are not destabilised and the drug is not extracted from the micellar core by this protein. The cytotoxic effect of the taxane-loaded micelles on C26 tumour cells *in vitro* was comparable to that of the commercial formulations, but the empty micelles were far less toxic than the Cremophor EL® vehicle. The results show that mPEG-*b*-oligo(ε-caprolactone) micelles hold good promise for the formulation of taxanes.

Introduction

Paclitaxel (PTX) and docetaxel (DCTX) (Figure 1) belong to the taxane family of anti-neoplastic agents, and have been demonstrated to have good clinical efficacy in (amongst others) breast, ovarian, non-small cell lung and prostate cancer.[1, 2] Their cytotoxic effect is caused by interference with the microtubule function in the cell, which results in disrupted mitosis and cell death.[1, 3] Both PTX and DCTX are very potent anti-cancer agents, but they are highly hydrophobic and therefore poorly soluble in water. To overcome this solubility issue, for parenteral administration PTX is currently formulated in a mixture of Cremophor EL® (CrEL®), a polyoxyethylated castor oil vehicle, and ethanol (1/1 (v/v) CrEL®/EtOH). DCTX is slightly less hydrophobic than PTX, and is solubilised using Tween 80 (Tw80, polysorbate 80).[2, 4] These commercially available formulations of PTX and DCTX are called Taxol® and Taxotere®, respectively. Both CrEL® and Tw80 are not inert and have been associated with a number of adverse effects, such as hypersensitivity reactions and neurotoxicity.[2, 4] These vehicle-associated toxicities have led to the development of alternative methods to formulate these poorly soluble compounds,[2, 5] such as drug-polymer conjugates,[6] and nanoparticles composed of albumin-bound PTX (Abraxane®).[7] Because of the high hydrophobicity of taxanes, polymeric micelles are of particular interest for the formulation of these compounds. They are core-shell structures with a size of 10-100 nm, formed by the self-assembly of amphiphilic block copolymers.[8-14] Their hydrophobic core can accommodate hydrophobic drugs such as taxanes, and their hydrophilic shell, which usually consists of poly(ethylene glycol) (PEG), confers the micelles long circulating behaviour. These long circulation times, in combination with their small size, enable extravasation from the leaky vasculature at the tumour site, resulting in passive targeting and specific accumulation of the drug-loaded micelles in the tumour (*i.e.* the so-called enhanced permeability and retention (EPR) effect),[8-14] thus making polymeric micelles highly suitable for the (targeted) delivery of hydrophobic drugs to tumour tissue.

Both PTX and DCTX have been loaded into a variety of polymeric micelles, composed of *e.g.* PEG-*b*-poly(lactide) (PLA),[15-20] PEG-*b*-poly(benzylaspartate),[21] poly(N-vinylpyrrolidone) (PVP)-*b*-PLA,[22] PEG-*b*-poly(N-(2-hydroxypropyl methacryl amide dilactate) (PHPMAmDL),[23] poly(2-ethyl-2-oxazoline)-*b*-poly(ε-caprolactone) (PEtOx-*b*-PCL),[24] PEG-*b*-poly(styreneoxide) (PSO)[25] and core crosslinked PEG-*b*-PCL.[26] PTX- loaded PEG-*b*-PLA micelles have even reached clinical trials.[16] Although promising results were obtained with micellar PTX with regard to the anti-tumour effect *in vivo*,[19-22] these were mostly related to reduced toxicity and a higher maximum tolerated dose (MTD), rather than enhanced tumour accumulation of the (carrier loaded with) drug.[15, 19, 22] Likely, premature loss of the

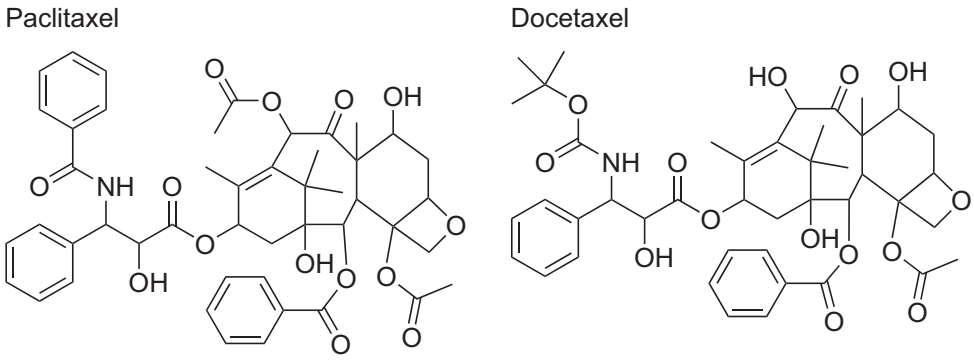

Figure 1 Chemical structures of the taxanes paclitaxel (PTX, left) and docetaxel (DCTX, right).

drug occurred, due to micelle destabilisation and/or extraction of the drug from the micelles by plasma proteins.[27-29] This was illustrated by biodistribution studies of a dual-labelled system of PTX in PEG-*b*-PLA micelles, in which rapid dissociation of the PTX from the micelle-forming block copolymers was observed after intravenous injection.[30] Several publications reported that the retention (and loading capacity) of a drug in the micelles can be improved by optimising the compatibility between the drug and the micellar core, *i.e.* 'matching' the drug and the core-forming polymer.[31-35]

We recently developed biodegradable oligomeric micelles, based on PEG-*b*-oligo(ε-caprolactone), as described in chapter 4.[36] Because of their small size (<20 nm), these micelles may have better properties than larger micelles used so far, in terms of biodistribution and tumour penetration. The PEG-*b*-oligo(ε-caprolactone) micelles can be easily prepared by the film-hydration method. Furthermore, the end group of the PEG-*b*-oligo(ε-caprolactone)s was modified with an aromatic group, which may serve as a tool to improve the compatibility between the core and the drug. Here, we investigated novel taxane formulations, composed of PEG-*b*-oligo(ε-caprolactone) based micelles. The aim of this study was to explore the effect of the composition of the hydrophobic block on the encapsulation and retention of PTX and DCTX, and to investigate their *in vitro* stability and cytotoxicity.

Experimental section

Materials

Chloroform-*d* ($CDCl_3$, 99.8% D), deuterium oxide (D_2O, 99.9%), docetaxel (DCTX, >97.0%), Cremophor EL® (CrEL®), polysorbate 80 (Tween80, Tw80), and albumin immobilised on crosslinked 4% beaded agarose (BSA-SepCL-4B, 14 mg BSA per mL packed gel) were purchased from Sigma Aldrich Chemie BV (Zwijndrecht, The Netherlands). Dichloromethane (DCM, peptide synthesis grade), and acetonitrile (ACN, HPLC gradient grade) were obtained from Biosolve Ltd. (Valkenswaard, The Netherlands). Paclitaxel (PTX) was from MP Biomedicals Inc. (Illkirch, France), and EtOH (absolute) from Mallinckrodt Baker BV (Deventer, The Netherlands). Poly(ethylene glycol)-*b*-oligo(ε-caprolactone) (mPEG-*b*-OCL) block oligomers with monodisperse hydrophobic blocks (4 or 5 CL-units) and different end groups (Figure 2) were prepared as described in chapter 4.[36] In brief, mPEG-*b*-OCL was synthesised by ring-opening polymerisation of ε-caprolactone (20 g, 175 mmol), initiated by mPEG750 (26 g, 35 mmol) and catalysed by $SnOct_2$ (0.71 g, 1.8 mmol) overnight at a temperature of 130 °C. Benzoylated and naphthoylated mPEG750-*b*-OCL (mPEG750-*b*-OCL-Bz, mPEG750-*b*-OCL-Np, respectively) (Figure 2b and c) were obtained by reacting the hydroxyl end group with a five fold excess of benzoyl or 2-naphthoyl chloride in the presence of an equimolar amount of triethyl amine as HCl scavenger. Subsequently, the polydisperse block oligomers were fractionated by preparative reversed phase HPLC (RP-HPLC), to obtain monodisperse hydrophobic blocks.[36]

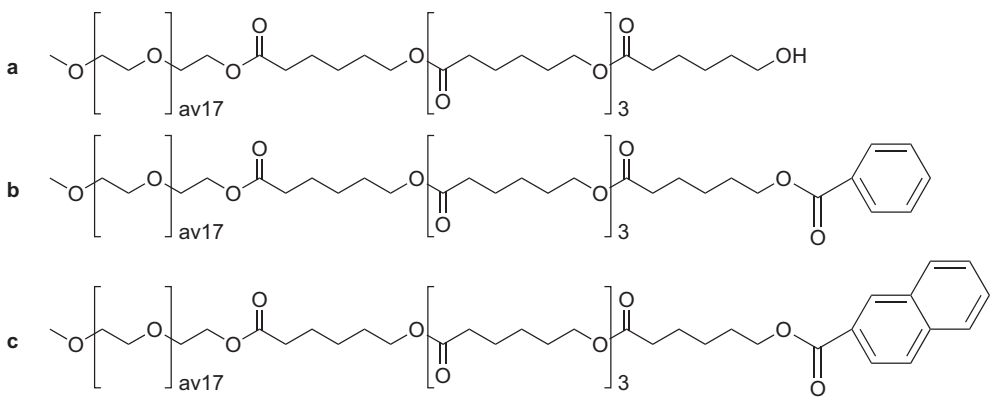

Figure 2 Chemical structures of mPEG750-*b*-oligo(ε-caprolactone)$_5$ (mPEG750-*b*-OCL_5-OH) (a), benzoylated mPEG750-*b*-OCL_5 (-Bz) (b) and naphthoylated mPEG750-*b*-OCL_5 (-Np) (c).

Phosphate buffered saline (PBS, pH 7.4) was obtained from Braun Melsungen AG (Melsungen, Germany), and was filtered through a 20 nm filter (Anotop®, Whatmann, Breda, The Netherlands) prior to use. Taxol® (6 mg/mL PTX, 16.7 mL) and Taxotere® (10 mg/mL DCTX in 2.0 mL premix solution) were purchased from Mayne Pharma BV (Brussels, Belgium), and Aventis Pharma SA (Antony Cedex, France), respectively.

Formation of taxane-loaded mPEG-*b*-OCL micelles

Micelles were formed by the film-hydration method, as described in chapter 4.[36] Typically, a film of block oligomer (10 mg) was formed by solvent evaporation from a 10 mg/mL solution of oligomer in dichloromethane in a 10 mL round bottomed flask. The film was dried for 30 min under an N_2 stream, followed by hydration with 1.0 mL PBS at room temperature. The resulting dispersion was filtered through a 200 nm filter (Anotop®, Whatmann, Breda, the Netherlands).[36] Drug was loaded into the micelles at different feed ratios by addition of 0.10, 0.20, 0.40 or 1.0 mL of a 5.0 mg/mL solution of the taxane (PTX or DCTX) in EtOH to the oligomer solution prior to evaporation of the solvent, representing feed ratios of 5, 10, 20 or 50 weight percentage relative to the oligomer (% w/w), respectively.

Analysis of the taxane-loaded mPEG-*b*-OCL micelles

Dynamic Light Scattering

The particle size and size distribution of loaded and unloaded mPEG-*b*-OCL-based micelles were measured by dynamic light scattering (DLS) using a Malvern CGS-3 multi-angle goniometer (Malvern Ltd,. Malvern), consisting of a HeNe laser source (λ = 632.8 nm, 22 mW output power), temperature controller (Julabo Waterbath) and a digital Correlator ALV-5000/EPP. Time correlation functions were analysed using the ALV-60X0 Software V.3.X provided by Malvern, to obtain the hydrodynamic diameter of the particles (Z_{ave}) and the particle size distribution (polydispersity index, PDI). The samples were measured at a scattering angle of 90°, at 25 °C or 37 °C, directly after preparation and after incubation for 30 min, 1 h, 2 h, 4 h, 8 h and 24 h.

Loading capacity

The amount of PTX or DCTX loaded into the micelles was determined according to an adapted literature method,[23, 37] using a Waters Acquity UPLC® system, consisting of a binary solvent manager, a sample manager and a TUV detector. An Acquity® BEH C8 1.7 µm column (2.1×50 mm) was used, and a gradient was run from 60% A (5/95 (w/w) ACN/H_2O) to 90% B (ACN) in 120 s, followed by isocratic elution at 100% B for 30 sec, at a flow rate of 0.5 mL/min, and a column temperature of 50 °C. The detection wavelength was 200 nm (40 datapoints per second), which enabled simultaneous detection of benzoylated block oligomer (mPEG-*b*-OCL-Bz). Samples taken directly after micelle preparation and after storage at room temperature for 24 h were diluted 30-60 times in 50/50 (w/w) ACN/H_2O, and 5 µL was injected. The chromatograms were analysed using Empower software (Empower Pro, Waters Chromatography BV). The amount of taxane (PTX or DCTX) present was calculated using a calibration curve, prepared in 50/50 (w/w) ACN/H_2O. The loading was calculated by equation 1.

$$\text{Loading Efficiency} = \frac{\text{mass of drug loaded}}{\text{mass of drug fed}} \times 100\% \qquad \text{(Eq. 1)}$$

^{1}H NMR spectroscopy

^{1}H NMR spectra were recorded using a Varian INOVA-500 spectrometer (Varian Associates Inc. NMR Instruments, Palo Alto, CA) operating at 500 MHz with $CDCl_3$ or D_2O as a solvent. As reference lines the chloroform peak at 7.24 ppm and the methyl peak of the mPEG-block at 3.40 ppm were used, respectively. Spatial information was derived from NOESY experiments (τ_m=300 ms). A spectral width of 5 kHz was used for all spectra. Samples of 10 mg/mL mPEG750-*b*-OLC_5-Bz with 10% (w/w) PTX dissolved in $CDCl_3$ or dispersed in D_2O were measured at 20 °C. Data were processed using Varian VNMR 6.1C (1D spectra) or NMRPipe (NOE spectra) software.[38]

In vitro stability

The *in vitro* stability of 5 and 10% (w/w) PTX- and DCTX-loaded mPEG750-*b*-OCL_5-Bz micelles was studied in PBS at 37 °C. Due to their low aqueous solubility, the released taxanes crystallised and subsequently precipitated. This resulted in continuous removal of the taxane from the release medium, and can be considered

the driving force for release. In detail, mPEG750-*b*-OCL_5-Bz micelles loaded with 5 or 10% taxane were prepared as described before, and incubated at 37 °C. The Z_{ave} and PDI were monitored by DLS. In addition, samples were taken from the dispersion at regular time points (10 min, 30 min, 1 h, 2 h, 4 h, 8 h, and 24 h), and centrifuged at 10000*g* for 1 min to remove the precipitate. After dilution of the supernatant in 50/50 (w/w) ACN/H_2O, the concentration of taxane and block oligomer was determined by UPLC®-UV, according to the method described above. The stability of the loaded micelles was also studied in the presence of bovine serum albumin (BSA). BSA immobilised on crosslinked 4% beaded agarose (BSA-SepCL-4B) was used, which has been applied to remove albumin-binding compounds from plasma, such as bilirubin and digitoxin.[39] In this study, 200 µL of a micelle dispersion in PBS (10 mg/mL mPEG750-*b*-OCL_5-Bz, containing 5% (w/w) PTX), was added to 1.8 mL of PBS, or a 50% (v/v) BSA-SepCL-4B-gel in PBS, corresponding to 12.6 mg BSA. The BSA concentration in the resulting dispersion was 6.3 mg/mL, and the molar ratio of PTX/BSA was 1/1.6, which means that a molar excess of BSA was present. Samples were taken at regular time points, and centrifuged for 1 min at 10000*g* to separate the micelles (supernatant) from the BSA-SepCL-4B and/or precipitated PTX. The supernatant was diluted in 50/50 (w/w) ACN/H_2O and both the PTX- and oligomer-concentration were determined by UPLC®-UV.

In vitro cytotoxicity studies

The *in vitro* cytotoxic effect of mPEG750-*b*-OCL_5-Bz micelles, with or without loading of 10% (w/w) PTX or DCTX, on C26 murine colon carcinoma cells was determined, and compared to Taxol®, Taxotere®, and the empty vehicles CrEL®/EtOH and Tw80/13% (w/w) EtOH. Loaded and empty micelles were prepared as described in the previous section of this chapter. Taxol® (6 mg/mL PTX) was diluted six fold with PBS, and the corresponding control formulation without PTX was prepared according to Lee *et al.*[24] In detail, 1.0 mL of CrEL® and 1.0 mL of EtOH were mixed, sonicated for 30 min, and subsequently diluted six fold with PBS. Taxotere® was prepared according to the instructions on the package leaflet,[40] *i.e.* the Tw80-solution containing DCTX was mixed gently with 13% (w/w) EtOH in water for injections, resulting in a 10 mg/mL DCTX premix solution, which was subsequently diluted 10-fold with PBS. The control without DCTX was prepared in the same manner, using Tw80. All stock solutions were diluted further with PBS to obtain taxane concentrations of 10^{-4} to 10 µg/mL, and the empty vehicles were treated equally.

C26 murine colon carcinoma cells were cultured at 37 °C in a 5% CO_2-containing humidified atmosphere in Dulbecco's modified Eagle's medium (DMEM), supplemented with 10% (v/v) heat-inactivated foetal calf serum, 100 IU/mL penicillin, 100 μg/mL streptomycin, and 0.25 μg/mL amphotericin B (Gibco, Breda, The Netherlands). Cells were seeded in a 96-well plate at a density of 5×10^3 cells per well. After 24 h, The culture medium was replaced by 100 μL of fresh medium, and 100 μL of the different taxane and control formulations were added. As a reference 100 μL of PBS were added. The cells were incubated for 72 h at 37 °C in a humidified atmosphere with 5% CO_2. After incubation, the cell viability was determined by an XTT colorimetric assay.[41] The experiments were repeated twice.

Results and discussion

Loading of the micelles

Empty and taxane-loaded micelles were prepared by hydration of an mPEG750-*b*-OCL_5-OH, -Bz, or -Np (see Figure 2) block oligomer film with or without different amounts of drug with PBS. Block oligomers with 5 CL units were used, because these oligomers (with an OH, Bz, or Np end group) had an acceptable temperature sensitivity profile, meaning a Krafft point below 4 °C and a cloud point above 37 °C, and were able to form sub 20-nm micelles, as described in chapter 4.[36] The *Z*-average hydrodynamic diameter (Z_{ave}) of the formed particles and the loading efficiency of taxanes at different feed ratios in the micelles are presented in Figure 3 and Table 1, respectively.

After hydration of a film composed of mPEG750-*b*-OCL_5 with a hydroxyl end group and 10% (w/w) PTX followed by filtration, around 90% of the initially added drug was recovered (Table 1), but DLS measurements demonstrated that very large aggregates (Z_{ave} >500 nm) rather than small micelles were formed (Figure 3). At a feed ratio of 20% (w/w) PTX in mPEG750-*b*-OCL_5-OH, less than 10% of the drug was present in the final preparation, indicating a low loading capacity. Again, relatively large and polydisperse particles were detected by DLS (Figure 3, Z_{ave} 17 ± 10 nm, PDI 0.4 ± 0.1). DCTX loading of mPEG750-*b*-OCL_5-OH micelles resulted in almost full recovery of the added drug (Table 1), but also with this taxane, the mPEG750-*b*-OCL_5-OH nanoparticles were rather polydisperse (PDI of 0.2 and 0.3 for a feed ratio of 10% and 20% (w/w) DCTX, respectively). Interestingly, when mPEG750-*b*-OCL_5 with an aromatic end group (Bz or Np) was used, almost quantitative encapsulation was obtained at a feed ratio of both 10 and 20% (w/w) of either PTX or DCTX (Table 1). The taxane concentrations were nearly 1 and 2 mg/mL, respectively, which is markedly higher than the aqueous solubility of PTX and DCTX (<1 μg/mL). Moreover, DLS measurements demonstrated that, in contrast to loaded mPEG750-*b*-OCL_5-OH particles, these particles were small (Z_{ave}=10-16 nm) and nearly monodisperse (PDI<0.1) (Figure 3), indicating that the aromatic end group is essential for the formation of well-defined taxane-loaded mPEG750-*b*-OCL_5 micelles. Even a feed ratio of 50% (w/w) PTX resulted in much higher PTX recovery in end group modified mPEG750-*b*-OCL_5-micelles than the unmodified ones, but at such high loading quite large and polydisperse particles were formed (Table 1). The highest loading capacity (approximately 20% (w/w) taxane) observed in the small, monodisperse micelles is considerably higher than those reported for both taxanes in micelles composed of PVP-*b*-PLA (max. 5% (w/w)),[22] PEOx-*b*-PCL (8%),[24] PEG-*b*-PSO (4%),[25] or core crosslinked PEG-*b*-PCL (5%),[26] and comparable to those reported for PTX in PEG-

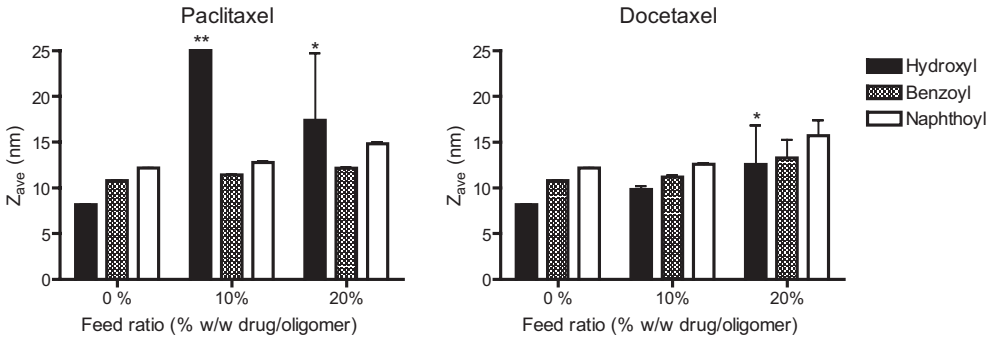

Figure 3 Particle size of (loaded) mPEG750-*b*-OCL_5 micelles with a hydroxyl, benzoyl or naphthoyl end group. Error bars represent the standard deviation (n=3). The polydispersity index (PDI) of the particles was < 0.1, except for the loaded mPEG750-*b*-OCL_5-OH micelles (*>0.2). **The particle size was larger than 500 nm.

Table 1 Loading efficiency (%) of paclitaxel and docetaxel in oligomeric micelles at different feed ratios[a] (n=3)

	Paclitaxel				Docetaxel	
End group	5% (w/w)	10% (w/w)	20% (w/w)	50% (w/w)	10% (w/w)	20% (w/w)
Hydroxyl	ND[b]	87 ± 12	8.5 ± 0.4	6.8 ± 0.2[d]	91 ± 7	99 ± 10
Benzoyl	80 ± 5[c]	89 ± 4	97 ± 1	94 ± 4[d]	89 ± 4	96 ± 1
Naphthoyl	ND[b]	89 ± 3	70 ± 18	65 ± 31[d]	96 ± 14	100 ± 5

[a] *Feed ratios were 5, 10, 20, or 50 weight percentage (% w/w) of taxane relative to the oligmer.*
[b] *ND = Not determined.*
[c] *The Z_{ave} was 12 nm, with a PDI of 0.06.*
[d] *The Z_{ave} was 23-200 nm with a PDI>0.2*

b-PHPMAmDL (22%),[23] or PEG-*b*-PLA micelles (25%).[18] The particle size slightly increased with increasing drug content, which was observed in other micellar systems as well.[23, 42]

At room temperature, the Z_{ave} and PDI of the micelles composed of mPEG750-*b*-OCL_5 with an aromatic end group (Bz or Np), loaded with 10% PTX or DCTX, remained stable for at least 24 h. Moreover, the taxanes were almost fully retained in these micelles during this time period, as determined by UPLC®-UV analysis (Table 2). At 20% (w/w) loading, the mPEG750-*b*-OCL_5-Bz or -Np micelles retained their small size and low polydispersity for 2-8 h, and after 24 h the taxane concentration in the formulation was 25-50% of the initially loaded drug (Table 2). The lower micellar stability upon higher drug loading was also observed in PTX-loaded PEG-polyester micelles.[30] It is related to exceeding the solubilisation capacity of the micelles, which results in release in the continuous phase, followed by crystallisation and precipitation of the drug.[13] In contrast to the end group modified mPEG750-*b*-OCL_5, it was not possible to form small and stable micelles composed of mPEG750-*b*-OCL_5-OH at a feed ratio of 10 or 20% (w/w) PTX or 20% (w/w) DCTX. At 10% (w/w) DCTX loading, the Z_{ave} and PDI remained stable for 8 h at room temperature, but at 24 h 60% of the loaded DCTX dose was released (Table 2). These data further confirm that an aromatic end group at the chain end of mPEG750-*b*-OCL_5 improves the solubilisation capacity of mPEG750-*b*-OCL_5 based micelles, and that it is necessary for the formation of stable taxane-loaded micelles.

Table 2 Stability of PTX- and DCTX- loaded oligomeric micelles at room temperature

	10% (w/w) Paclitaxel		20% (w/w) Paclitaxel	
End group	Stability (h)[a]	PTX at t=24h (%)[b]	Stability (h)[a]	PTX at t=24h (%)[b]
Hydroxyl	< 0.15	12 ± 3	< 0.15	8.0 ± 0.4
Benzoyl	> 24	88 ± 7	4	23.0 ± 0.2
Naphthoyl	> 24	77 ± 2	4	19 ± 2
	10% (w/w) Docetaxel		20% (w/w) Docetaxel	
End group	Stability (h)[a]	DCTX at t=24h (%)[b]	Stability (h)[a]	DCTX at t=24h (%)[b]
Hydroxyl	8	43 ± 9	< 0.15	11 ± 2
Benzoyl	> 24	74 ± 1	8	42 ± 24
Naphthoyl	> 24	84 ± 8	2	52 ± 33

[a] *Time (hours) until Z_{ave} > 20 nm or polydispersity index > 0.3.*
[b] *Amount of PTX or DCTX in the micellar dispersion at 24 h after preparation, presented as % of the amount of taxane fed ± standard deviation (n=3).*

The observed differences clearly demonstrate that the drug loading and stability of these micelles depends on both the micellar core and the taxane structure. This may be partly explained by the differences in hydrophobicity of both taxanes and the three micellar cores. The log P values of the OCL_5-OH, -Bz and -Np cores of the micelles, and of PTX and DCTX were calculated with the ClogP program (Table 3), which is based on the additive, constitutive character of partition coefficients, but also considers the interactions between neighbouring groups.[43] Likely, the higher hydrophobicity (reflected by the higher log P value) of the micellar core composed of OCL_5 with an aromatic end group (Bz or Np), when compared to OCL_5-OH, is responsible for the better encapsulation of both taxanes. Similarly, Lin *et al.* demonstrated differences in indomethacin loading in a series of PEG-*b*-polyester micelles, which was ascribed to differences in core hydrophobicity.[44] The slightly lower hydrophobicity of DCTX (as reflected by its lower log P value) when compared to PTX may be the reason for the better encapsulation and retention of DCTX in mPEG750-*b*-OCL_5-OH micelles. It may be anticipated that besides differences in hydrophobicity, specific interactions between the drugs and the micellar core play a role, such as enhanced hydrogen bonding between DCTX and the hydroxyl end group of mPEG750-*b*-OCL_5-OH. Moreover, both taxanes contain several aromatic rings, which may form π-π-interactions with the aromatic rings in the micellar core of the micelles composed of mPEG750-*b*-OCL_5-Bz or -Np. These type of interactions have been suggested to be involved in the encapsulation of another highly aromatic drug, camptothecin, into micelles composed of PEG-*b*-PBLA based block copolymers with different aromatic content. High contents of benzyl or methylnaphtyl in the core-forming polymers resulted in the encapsulation of camptothecin in high yields and high stability, which was ascribed to π-π-interactions between the drug and the core-forming polymer.[32]

Table 3 Log P values of the both taxanes and the three different micellar cores

Drug / Micellar core	Log P[a]
Paclitaxel (PTX)	4.7
Docetaxel (DCTX)	4.1
Oligo(ε-caprolactone)$_5$ (OCL_5-OH)	5.6
Benzoylated oligo(ε-caprolactone)$_5$ (OCL_5-Bz)	8.5
Naphthoylated oligo(ε-caprolactone)$_5$ (OCL_5-Np)	9.7

[a]*Calculated with the ClogP method, based on the additive-constitutive character of partition coefficients.*[43]

In addition to the nature of the micellar core, its size may affect the solubilisation capacity. Therefore the drug loading efficiency and stability of mPEG750-*b*-OCL_5-Bz micelles as reported above was compared to that of micelles composed of mPEG750-*b*-OCL_4-Bz, *i.e.* one unit of CL less. At a feed ratio of 10% (w/w) of PTX, it was found that mPEG750-*b*-OCL_4-Bz formed small and almost monodisperse micelles (Z_{ave} 10.0 ± 0.2 nm, PDI 0.02) with nearly complete encapsulation efficiency (83 ± 27%), similar to the block oligomer with 5 CL units (Figure 3, Table 1). However, whereas the 10% (w/w) PTX-loaded mPEG750-*b*-OCL_5-Bz micelles remained stable for at least 24 h, the loaded micelles with an OCL_4 chain increased in size at 8 h and after 24 h 40% was released. This indicates that indeed a larger core size has a positive influence on the solubilisation capacity of the micelles.

^{1}H NMR studies of the loaded micelles

One of the formulations, mPEG750-*b*-OCL_5-Bz loaded with 10% (w/w) PTX, was investigated by ^{1}H NMR, both as micelles in D_2O and dissolved in $CDCl_3$. The ^{1}H NMR spectrum of mPEG750-*b*-OCL_5-Bz with 10% (w/w) PTX in D_2O is presented in Figure 4. Interestingly, the D_2O-spectrum revealed signals from both the OCL_5-Bz block and the PTX, besides the signals of the PEG-block. This is in contrast to ^{1}H NMR studies with PEG-*b*-PLA, core crosslinked PEG-*b*-PCL, and PEG-*b*-PHPMAmDL micelles in D_2O, where only the PEG-signals were visible in the ^{1}H NMR spectrum.[26, 45-48] The absence of the signals of the hydrophobic blocks was related to the impaired mobility of these chains, as a result of the formation of a 'solid-like' core.[26, 45-48] Our data suggest that the core of PTX-loaded mPEG750-*b*-OCL_5-Bz micelles does not have a 'solid-like', but a liquid nature. This can be explained by the low melting temperature (5 °C) of this block oligomer, as reported in chapter 4,[36] causing a molten rather than a crystalline state at room temperature. Expansion of the aromatic region (7.0 to 8.4 ppm) of the spectra of mPEG750-*b*-OCL_5-Bz with 10% (w/w) PTX (inset Figure 4) clearly shows the aromatic signals of the block oligomer end group (7.40, 7.53 and 7.95 ppm) and of PTX. Comparison of the D_2O to the $CDCl_3$ spectrum shows a shift of the PTX-signals at 6.25 and 7.90 ppm (D_2O), which is related to a different chemical environment. Furthermore, peak broadening is observed, which indicates that the mobility of the oligomer chains is restricted in the viscous core of the micelles, when compared to chains dissolved in $CDCl_3$. Comparable results were obtained with Pluronics® (PEG-*b*-polypropylene-oxide (PPO)-*b*-PEG)[12] and PEG-PLA micelles above the glass transition temperature of PLA.[46] The presence of PTX-signals in the D_2O spectrum suggests that these molecules are present in dissolved, rather than crystallised or aggregated form. PTX also has a lower mobility than in $CDCl_3$, since it is dissolved in the viscous core,

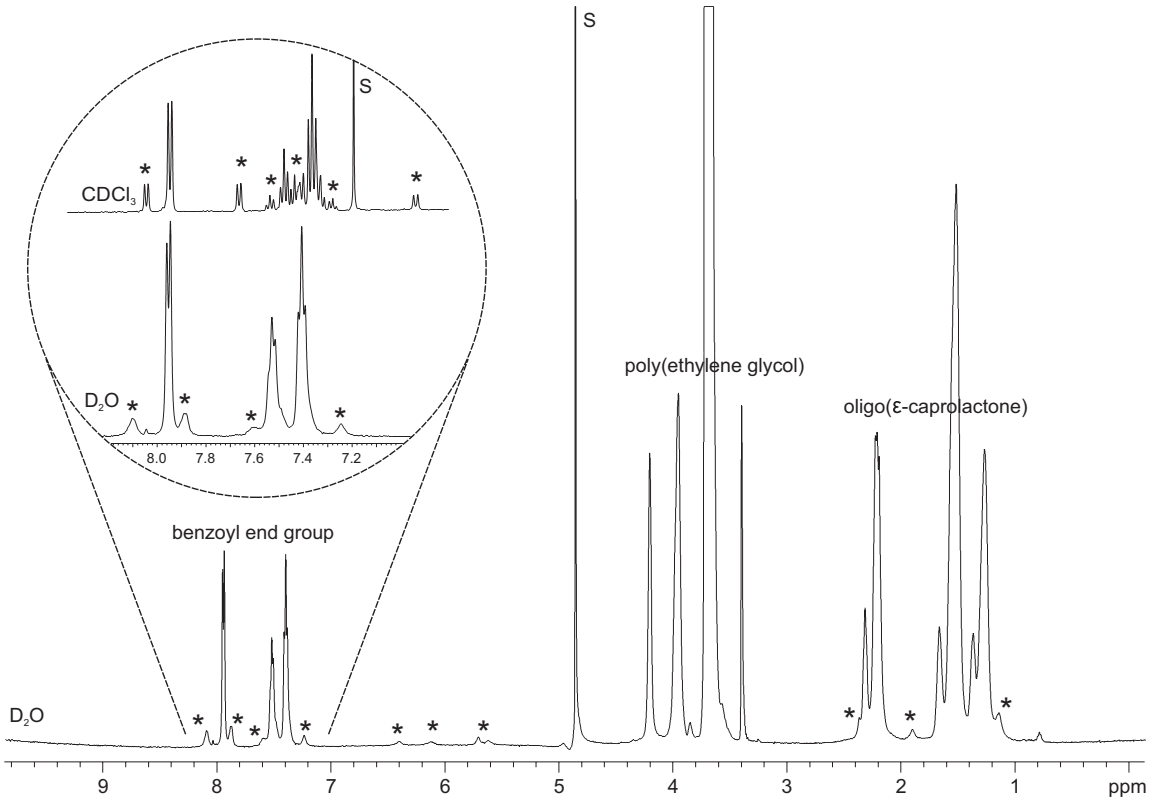

Figure 4 ^{1}H NMR spectrum of 10% PTX (w/w) loaded mPEG750-*b*-OCL_5-Bz micelles dispersed in D_2O. The aromatic region of the samples dissolved in $CDCl_3$ (top) and dispersed in D_2O (bottom) are expanded. The (small) signals of the PTX-protons are indicated by *; S represents the solvent peak of HDO and $CHCl_3$, respectively.

which has also been shown for camptothecin and Reichardt's dye upon encapsulation in poly(glycerolsuccinic acid) dendrimers.[49, 50]

To investigate the molecular interactions in the micellar core, an NOE spectrum in D_2O was recorded and compared to an NOE spectrum in $CDCl_3$. Figure 5 shows the expansion of the aromatic-aliphatic region in the spectrum in D_2O. The spectrum clearly demonstrates the presence of several cross-peaks between the aromatic protons (from the benzoyl end group of the oligomer and PTX) and the aliphatic protons (from the OCL-chain and the PTX-molecule). Specific cross-peaks between the core-forming block and the drug can be recognised between the methylene protons of the OCL-chain at 1.28 ppm and the aromatic protons of PTX at 8.11, 7.88 and 7.26 ppm. The recognition of other specific cross-peaks is hampered by the overlap of the OCL_5-Bz and PTX signals. All peaks observed in this region were absent in the $CDCl_3$ NOE spectrum (data not shown). This indicates that in D_2O these protons are in close proximity,[49, 51] as a result of the formation of a micellar OCL_5-Bz core encapsulating PTX, corroborating the results described above. NOE signals between the aromatic protons of PTX and the benzoyl end group of the block oligomer could not be detected due to peak overlap.

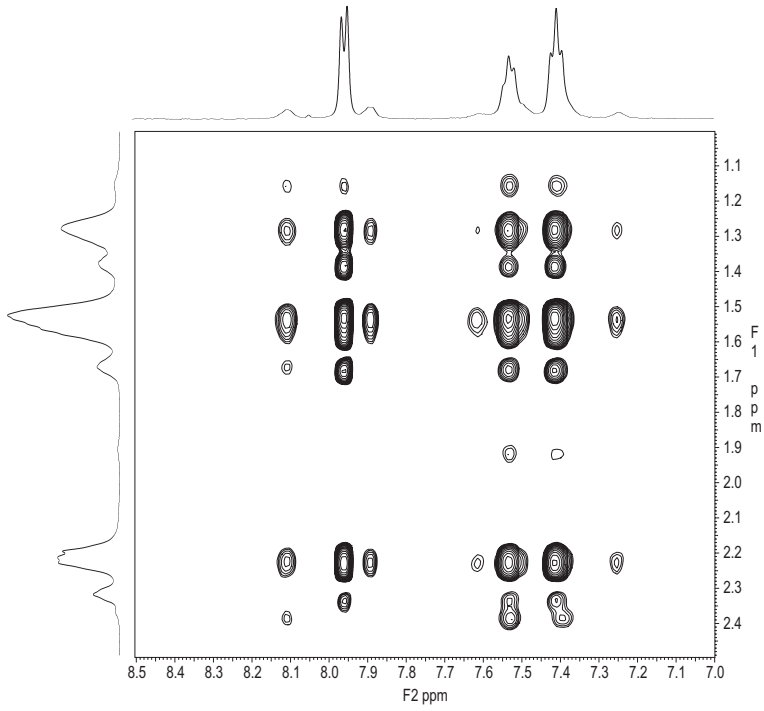

Figure 5 The aromatic-aliphatic region of the ^1H NMR NOESY of 10% (w/w) PTX loaded mPEG750-*b*-OCL_5-Bz micelles in D_2O (τ_m=300 ms).

In vitro stability

To study their *in vitro* stability, 5% and 10% (w/w) PTX- and DCTX-loaded mPEG750-*b*-OCL_5-Bz micelles were incubated at 37 °C. The samples taken were centrifuged to remove the precipitated taxane, and the concentration of block oligomer and taxane was determined by UPLC®-UV. Figure 6 demonstrates that during the first hours of incubation the concentration of both the block oligomer and PTX remained constant. After 8 h, the concentration of PTX in the 10% (w/w) sample started to decrease, which was not observed in the 5% (w/w) sample, whereas the oligomer concentration remained constant for both formulations. Correspondingly, the Z_{ave} and PDI of mPEG750-*b*-OCL_5-Bz micelles loaded with 10% (w/w) PTX started to increase after approximately 4 h incubation at 37 °C, and at 5% (w/w) PTX loading, Z_{ave} and PDI remained constant during at least 15 h (data not shown). Similar results were obtained with DCTX-loaded micelles (data not shown). In a subsequent experiment with 10-fold diluted 5% (w/w) loaded micelles, PTX release was also only observed after more than 24 h of incubation (*vide infra*, Figure 7).

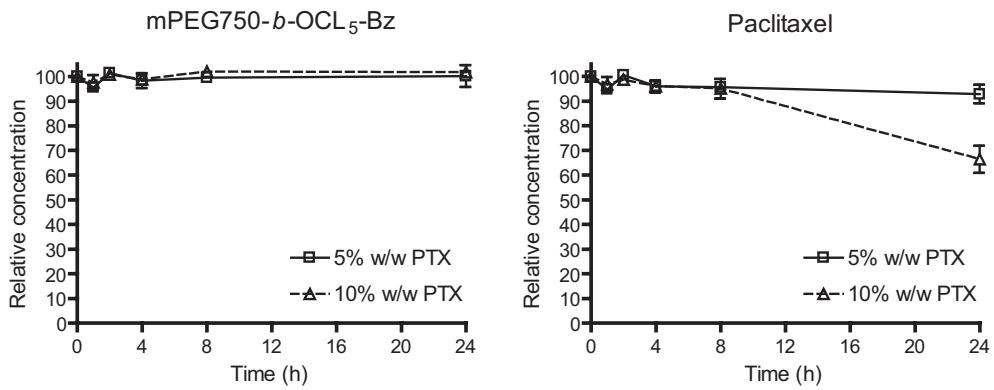

Figure 6 Concentration of mPEG750-*b*-OCL-Bz (left) and PTX (right) upon incubation of 5 and 10% (w/w) loaded micelles at 37 °C. The results are presented as percentage of the concentration at time 0.

In chapter 4 it was demonstrated that empty mPEG750-*b*-OCL_5-Bz micelles are stable for two weeks at 37 °C in PBS,[36] and in chapter 5 the degradation half-life of these micelles in buffer (pH 7.4) was estimated at several years.[52] The constant oligomer concentration observed here indicates that the micelle stability is not affected by the presence of PTX, but PTX slowly leaks from the micelles at relatively high loading. This PTX leakage likely accounts for the observed increase in size, since PTX has a low solubility in water, and may crystallise into particles larger than the micelles. Eventually PTX precipitated, resulting in the decreased PTX concentration measured at 24 h.

The interaction with serum proteins is important for the *in vivo* fate of drug delivery systems such as micelles. Serum proteins may adsorb on the micellar surface, thereby inducing opsonisation and subsequent clearance by the reticulo-endothelial system.[29, 53] Furthermore, they may accelerate the release of drugs from the micelles, especially in case of drugs with a high protein affinity,[27-29] such as PTX, which has a protein binding of 90% in serum.[54, 55] Therefore, the effect of BSA on the micellar integrity was investigated. Because it was not possible to separate the intact micelles from soluble BSA, albumin immobilised on agarose beads (BSA-SepCL-4B) was used, which can be easily separated by centrifugation. Such beads have been used to remove a variety of albumin-binding compounds from plasma, such as bilirubin and digitoxin.[39] MPEG750-*b*-OCL_5-Bz micelles loaded with 5% (w/w) PTX were incubated with BSA-SepCL-4B at a molar ratio of PTX/BSA of 1/1.6, which represents an excess of BSA as it is known that albumin can bind more than one PTX-molecule.[56, 57] As presented in Figure 7a, again, the oligomer concentration in the micellar dispersion remained constant in time, which suggests that at the experimental conditions, there is no adsorption of micelles or block oligomers to the BSA-coated beads. The absence of BSA adsorption at the micellar surface was also shown for ellipticine-loaded mPEG-*b*-P(5-benzyloxy-trimethylene carbonate) (PBTMC) micelles,[29] and Pluronics®,[58] which may be related to sufficient protection by the PEG-shell of the micelles. Figure 7b demonstrates that the presence of BSA-SepCL-4B did not affect the PTX release from 5% (w/w) loaded mPEG-*b*-OCL_5-Bz micelles, as both curves coincide. Although others did demonstrate binding of drugs loaded in polymeric micelles to BSA or serum proteins, their binding was always lower than that of the free drug.[27, 29] This indicates that the encapsulation in micelles has a protective effect with regard to protein binding, which is corroborated by the data described here.

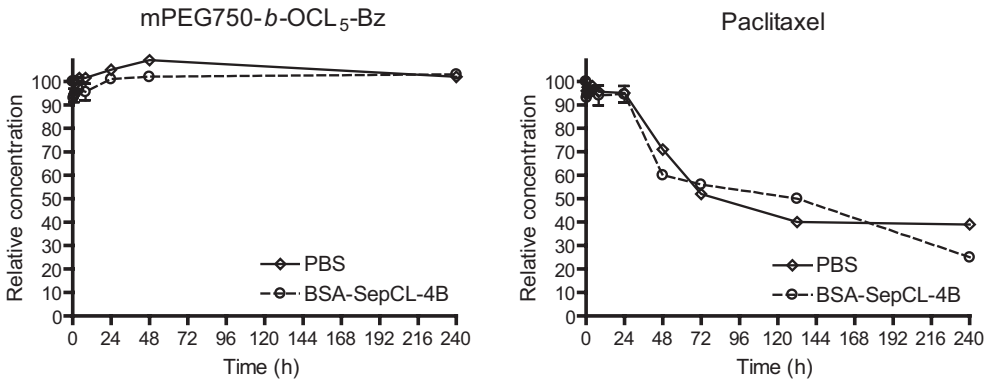

Figure 7 Concentration of mPEG750-*b*-OCL-Bz (left) and PTX (right) upon incubation of 5% (w/w) loaded micelles with BSA immobilised on agarose beads (BSA-SepCL-4B) and in PBS at 37 °C.

In vitro cytotoxicity

The cytotoxic effect of empty and 10% (w/w) taxane-loaded mPEG750-*b*-OCL_5-Bz micelles on C26 murine colon carcinoma cells was tested, and compared with the commercially available formulations Taxol® and Taxotere®. Table 4 shows that the cytotoxicity of the PTX- and DCTX-loaded micelles is comparable to Taxol® and Taxotere®, respectively. Importantly, the empty micelles are far less toxic than the 1/1 (v/v) CrEl®/EtOH used in the Taxol® formulation, as reflected by the higher cell viability upon incubation with the empty vehicles (Table 4). Moreover, neither the empty mPEG750-*b*-OCL_5-Bz micelles, nor Tw80 (used in the Taxotere® formulation) showed any cytotoxicity at the concentrations tested. Comparison of the cell viability after incubation with the loaded vehicles with the empty ones (Table 4), reveals that the cytotoxicity of Taxol® at 10 µg/mL PTX may be (partly) due to CrEL®/EtOH, whereas the effect of the loaded micelles and Taxotere® is solely caused by the drug. The results are in line with those obtained elsewhere with other PTX-loaded micelles, which were tested on C26 and other cancer cell lines.[22-24] The cytotoxicity of other DCTX-loaded micelles, which was similar to that of Taxotere®, has been demonstrated in literature as well.[25] The absence of vehicle-related cytotoxicity of Taxotere® may be explained by the better toxicity profile of Tw80, when compared to 'empty Taxol®', combined with the presence of a lower amount of excipient in the formulation (only 25/1 (w/w) Tw80/DCTX vs 88/1 (w/w) CrEl®/PTX in Taxol®). However, since some of the clinically observed adverse effects of Taxotere® have been ascribed to Tw80, rather than DCTX,[2, 4, 5] a Tw80-free formulation may still be preferred, which

Table 4 *In vitro* cytotoxicity of micellar taxanes vs Taxol®/Taxotere®

	IC_{50} (μg taxane /mL)[a]	Cell viability at 10 μg/mL taxane (% of PBS control)	Cell viability empty vehicle[b] (% of PBS control)
Taxol® (PTX)	0.02 ± 0.02	38 ± 5%	42 ± 4%
Taxotere® (DCTX)	0.01 ± 0.02	30 ± 2%	96 ± 10%
mPEG750-*b*-OCL_5-Bz micelles, PTX-loaded	0.03 ± 0.01	31 ± 2%	87 ± 17%
mPEG750-*b*-OCL_5-Bz micelles, DCTX-loaded	0.01± 0.01	29 ± 1%	87 ± 17%

[a] *IC_{50}: concentration (μg/mL) of taxane-loaded formulation that causes 50% cell death or growth inhibition.*
[b] *The concentration of the excipients (CrEL/EtOH, Tw80, block oligomer) is the same as in the loaded formulations at 10 μg/mL of taxane.*

can be achieved by using the biodegradable and biocompatible block oligomers described here. It may be anticipated that the low toxicity of the micelles allows higher dosing than Taxol® (and possibly Taxotere®), thereby improving the anti-tumour effect, as observed with other taxane-loaded micelles.[15, 19, 22]

It is important to note that at the reported IC_{50} values, the block oligomer concentrations (0.3 and 0.1 μg/mL for PTX- and DCTX-loaded micelles, respectively) are below the critical aggregation concentration (CAC) (10 μg/mL),[36] and therefore the taxanes are likely present in their free form. Calculations based on the administered dose of Taxol® and Taxotere® in patients and their plasma volume revealed a taxane concentration around 100 and 50 μg/mL in plasma, respectively. Here, at a taxane concentration of 10 μg/mL, where the mPEG750-*b*-OCL_5-Bz concentration (100 μg/mL) is above the CAC, the taxane-loaded micelles have a cytotoxicity of 70%, which is comparable to the toxicity of the commercial formulations at the same drug concentrations (Table 4). At this concentration, the taxanes may exert their intracellular effect after uptake of the loaded micelles or after extracellular release. The mechanism responsible for the cytotoxic effect will be subject of future studies.

Conclusions

In this study, both paclitaxel and docetaxel were successfully loaded in small (<20 nm) oligomeric micelles based on mPEG750-*b*-oligo(ε-caprolactone)$_5$. It was shown that the presence of an aromatic end group on the core-forming block is necessary to improve the loading and enhance the stability of the formulation of taxanes, indicating the importance of a good compatibility between the loaded drug and the micellar core. The micellar core has a liquid nature, in which paclitaxel is present in a dissolved state. *In vitro*, the release of paclitaxel occurs through leakage from the micelles, which is not affected by the presence of albumin. This, in combination with the observed low cytotoxic effect of the empty micelles on C26 cells demonstrates the feasibility of a novel taxane formulation based on mPEG-*b*-oligo(ε-caprolactone) micelles.

References

1. Gelmon K, The taxoids: paclitaxel and docetaxel. *Lancet* 344, 1267-1272 (1994).
2. Hennenfent KL; Govindan R, Novel formulations of taxanes: a review. Old wine in a new bottle? *Ann Oncol* 17, 735-749 (2006).
3. He L; Orr GA; Horwitz SB, Novel molecules that interact with microtubules and have functional activity similar to Taxol. *Drug Discov Today* 6, 1153-1164 (2001).
4. van Zuylen L; Verweij J; Sparreboom A, Role of formulation vehicles in taxane pharmacology. *Invest New Drug* 19, 125-141 (2001).
5. Engels FK; Mathot RA; Verweij J, Alternative drug formulations of docetaxel: a review. *Anti-cancer Drug* 18, 95-103 (2007).
6. Xie Z; Guan H; Chen X; Lu C; Chen L; Hu X; Shi Q; Jing X, A novel polymer-paclitaxel conjugate based on amphiphilic triblock copolymer. *J Control Release* 117, 210-216 (2007).
7. Ng SS; Sparreboom A; Shaked Y; Lee C; Man S; Desai N; Soon-Shiong P; Figg WD; Kerbel RS, Influence of formulation vehicle on metronomic taxane chemotherapy: albumin-bound versus cremophor EL-based paclitaxel. *Clin Cancer Res* 12, 4331-4338 (2006).
8. Torchilin VP, Structure and design of polymeric surfactant-based drug delivery systems. *J Control Release* 73, 137-172 (2001).
9. Gaucher G; Dufresne MH; Sant VP; Kang N; Maysinger D; Leroux JC, Block copolymer micelles: preparation, characterization and application in drug delivery. *J Control Release* 109, 169-188 (2005).
10. Kwon GS; Okano T, Polymeric micelles as new drug carriers. *Adv Drug Deliver Rev* 21, 107-116 (1996).
11. Jones M-C; Leroux J-C, Polymeric micelles - a new generation of colloidal drug carriers. *Eur J Pharm Biopharm* 48, 101-111 (1999).
12. Kwon GS, Polymeric micelles for delivery of poorly water-soluble compounds. *Crit Rev Ther Drug* 20, 357-403 (2003).
13. Torchilin VP, Micellar nanocarriers: pharmaceutical perspectives. *Pharm Res* 24, 1-16 (2007).
14. van Nostrum CF, Polymeric micelles to deliver photosensitizers for photodynamic therapy. *Adv Drug Deliver Rev* 56, 9-16 (2004).
15. Liggins RT; Burt HM, Polyether-polyester diblock copolymers for the preparation of paclitaxel loaded polymeric micelle formulations. *Adv Drug Deliver Rev* 54, 191-202 (2002).
16. Kim TY; Kim DW; Chung JY; Shin SG; Kim SC; Heo DS; Kim NK; Bang YJ, Phase I and pharmacokinetic study of Genexol-PM, a cremophor-free, polymeric micelle-formulated paclitaxel, in patients with advanced malignancies. *Clin Cancer Res* 10, 3708-3716 (2004).
17. Zhang X; Burt HM; Hoff DV; Dexter D; Mangold G; Degen D; Oktaba AM; Hunter WL, An investigation of the antitumour activity and biodistribution of polymeric micellar paclitaxel. *Cancer Chemoth Pharm* 40, 81-86 (1997).
18. Zhang X; Jackson JK; Burt HM, Development of amphiphilic diblock copolymers as micellar carriers of taxol. *Int J Pharm* 132, 195-206 (1996).
19. Kim SC; Kim DW; Shim YH; Bang JS; Oh HS; Wan Kim S; Seo MH, In vivo evaluation of polymeric micellar paclitaxel formulation: toxicity and efficacy. *J Control Release* 72, 191-202 (2001).
20. Zhang X; Burt HM; Mangold G; Dexter D; Hoff DV; Mayer L; Hunter WL, Anti-tumor efficacy and biodistribution of intravenous polymeric micellar paclitaxel. *Anti-Cancer Drug* 8, 696-701 (1997).
21. Hamaguchi T; Matsumura Y; Suzuki M; Shimizu K; Goda R; Nakamura I; Nakatomi I; Yokoyama M; Kataoka K; Kakizoe T, NK105, a paclitaxel-incorporating micellar nanoparticle formulation, can extend in vivo antitumour activity and reduce the neurotoxicity of paclitaxel. *Brit J Cancer* 92, 1240-1246 (2005).
22. Le Garrec D; Gori S; Luo L; Lessard D; Smith DC; Yessine MA; Ranger M; Leroux JC, Poly(N-vinylpyrrolidone)-block-poly(D,L-lactide) as a new polymeric solubilizer for hydrophobic anticancer drugs: in vitro and in vivo evaluation. *J Control Release* 99, 83-101 (2004).

23. Soga O; van Nostrum CF; Fens M; Rijcken CJF; Schiffelers RM; Storm G; Hennink WE, Thermosensitive and biodegradable polymeric micelles for paclitaxel delivery. *J Control Release* 103, 341-353 (2005).
24. Lee SC; Kim C; Kwon IC; Chung H; Jeong SY, Polymeric micelles of poly(2-ethyl-2-oxazoline)-block-poly(ε-caprolactone) copolymer as a carrier for paclitaxel. *J Control Release* 89, 437-446 (2003).
25. Elsabahy M; Perron ME; Bertrand N; Yu G; Leroux JC, Solubilization of docetaxel in poly(ethylene oxide)-block-poly(butylene/styrene oxide) micelles. *Biomacromolecules* 8, 2250-2257 (2007).
26. Shuai X; Merdan T; Schaper AK; Xi F; Kissel T, Core-cross-linked polymeric micelles as paclitaxel carriers. *Bioconjugate Chem* 15, 441-448 (2004).
27. Kwon GS; Naito M; Yokoyama M; Okano T; Sakurai Y; Kataoka K, Physical entrapment of adriamycin in AB block copolymer micelles. *Pharm Res* 12, 192-195 (1995).
28. Opanasopit P; Yokoyama M; Watanabe M; Kawano K; Maitani Y; Okano T, Influence of serum and albumins from different species on stability of camptothecin-loaded micelles. *J Control Release* 104, 313-321 (2005).
29. Liu J; Zeng F; Allen C, Influence of serum protein on polycarbonate-based copolymer micelles as a delivery system for a hydrophobic anti-cancer agent. *J Control Release* 103, 481-497 (2005).
30. Burt HM; Zhang X; Toleikis P; Embree L; Hunter WL, Development of copolymers of poly(D,L-lactide) and methoxypolyethylene glycol as micellar carriers of paclitaxel. *Colloid Surface B* 16, 161-171 (1999).
31. Liu J; Xiao Y; Allen C, Polymer-drug compatibility: a guide to the development of delivery systems for the anticancer agent, ellipticine. *J Pharm Sci* 93, 132-143 (2004).
32. Yokoyama M; Opanasopit P; Okano T; Kawano K; Maitani Y, Polymer design and incorporation methods for polymeric micelle carrier system containing water-insoluble anti-cancer agent camptothecin. *J Drug Target* 12, 373-384 (2004).
33. Watanabe M; Kawano K; Yokoyama M; Opanasopit P; Okano T; Maitani Y, Preparation of camptothecin-loaded polymeric micelles and evaluation of their incorporation and circulation stability. *Int J Pharm* 308, 183-189 (2006).
34. Forrest ML; Zhao A; Won CY; Malick AW; Kwon GS, Lipophilic prodrugs of Hsp90 inhibitor geldanamycin for nanoencapsulation in poly(ethylene glycol)-b-poly(epsilon-caprolactone) micelles. *J Control Release* 116, 139-149 (2006).
35. Lavasanifar A; Samuel J; Kwon GS, The effect of fatty acid substitution on the in vitro release of amphotericin B from micelles composed of poly(ethylene oxide)-block-poly(N-hexyl stearate-aspartamide). *J Control Release* 79, 165-172 (2002).
36. Carstens MG; Bevernage JJL; van Nostrum CF; van Steenbergen MJ; Flesch FM; Verrijk R; de Leede LGJ; Crommelin DJA; Hennink WE, Small oligomeric micelles based on end group modified mPEG-oligocaprolactone with monodisperse hydrophobic blocks. *Macromolecules* 40, 116-122 (2007).
37. Rao BM; Chakraborty A; Srinivasu MK; Devi ML; Kumar PR; Chandrasekhar KB; Srinivasan AK; Prasad AS; Ramanatham J, A stability-indicating HPLC assay method for docetaxel. *J Pharmaceut Biomed* 41, 676-681 (2006).
38. Delaglio F; Grzesiek S; Vuister GW; Zhu G; Pfeifer J; Bax A, NMRPipe: a multidimensional spectral processing system based on UNIX pipes. *J Biomol NMR* 6, 277-293 (1995).
39. Wilchek M; Miron T, Immobilization of enzymes and affinity ligands onto agarose via stable and uncharged carbamate linkage. *Biochem Int* 4, 629-635 (1982).
40. Sanofi-Aventis U.S. LLC Taxotere (docetaxel) Injection Concentrate. Preparation and Administration. http://www.taxotere.com/professional/about/preparation.do (May 4. 2007.)
41. Scudiero DA; Shoemaker RH; Paull KD; Monks A; Tierney S; Nofziger TH; Currens MJ; Seniff D; Boyd MR, Evaluation of a soluble tetrazolium/formazan assay for cell growth and drug sensitivity in culture using human and other tumor cell lines. *Cancer Res* 48, 4827-4833 (1988).
42. Nagarajan R, Solubilization of guest molecules into polymeric aggregates. *Polym Advan Technol* 12, 23-43 (2001).
43. Daylight Chemical Information Systems Inc. CLogP. http://www.daylight.com/daycgi/clogp (June 4. 2007)
44. Lin WJ; Juang LW; Lin CC, Stability and release performance of a series of pegylated copolymeric micelles. *Pharm Res* 20, 668-673 (2003).

45. Hrkach JS; Peracchia MT; Bomb A; Lotan N; Langer R, Nanotechnology for biomaterials engineering: structural characterization of amphiphilic polymeric nanoparticles by 1H NMR spectroscopy. *Biomaterials* 18, 27-30 (1997).
46. Heald CR; Stolnik S; Kujawinski KS; De Matteis C; Garnett MC; Illum L; Davis SS; Purkiss SC; Barlow RJ; Gellert PR, Poly(lactic acid)-poly(ethylene oxide) (PLA-PEG) nanoparticles: NMR studies of the central solidlike PLA core and the liquid PEG corona. *Langmuir* 18, 3669-3675 (2002).
47. Yamamoto Y; Yasugi K; Harada A; Nagasaki Y; Kataoka K, Temperature-related change in the properties relevant to drug delivery of poly(ethylene glycol)-poly(D,L-lactide) block copolymer micelles in aqueous milieu. *J Control Release* 82, 359-371 (2002).
48. Soga O; van Nostrum CF; Ramzi A; Visser T; Soulimani F; Frederik PM; Bomans PHH; Hennink WE, Physicochemical characterization of degradable thermosensitive polymeric micelles. *Langmuir* 20, 9388-9395 (2004).
49. Morgan MT; Carnahan MA; Immoos CE; Ribeiro AA; Finkelstein S; Lee SJ; Grinstaff MW, Dendritic molecular capsules for hydrophobic compounds. *J Am Chem Soc* 125, 15485-15489 (2003).
50. Morgan MT; Nakanishi Y; Kroll DJ; Griset AP; Carnahan MA; Wathier M; Oberlies NH; Manikumar G; Wani MC; Grinstaff MW, Dendrimer-encapsulated camptothecins: Increased solubility, cellular uptake, and cellular retention affords enhanced anticancer activity in vitro. *Cancer Res* 66, 11913-11921 (2006).
51. Vakil R; Kwon GS, Poly(ethylene glycol)-*b*-poly(ε-caprolactone) and PEG-phospholipid form stable mixed micelles in aqueous media. *Langmuir* 22, 9723-9729 (2006).
52. Carstens MG; van Nostrum CF; Verrijk R; de Leede LGJ; Crommelin DJA; Hennink WE, A mechanistic study of the chemical and enzymatic degradation of PEG-oligo(ε-caprolactone) micelles. *J Pharm Sci* In Press (2007).
53. Patel HM; Moghimi SM, Serum-mediated recognition of liposomes by phagocytic cells of the reticuloendothelial system - The concept of tissue specificity. *Adv Drug Deliver Rev* 32, 45-60 (1998).
54. Sonnichsen DS; Relling MV, Clinical pharmacokinetics of paclitaxel. *Clin Pharmacokinet* 27, 256-269 (1994).
55. Kumar GN; Walle UK; Bhalla KN; Walle T, Binding of taxol to human plasma, albumin and alpha 1-acid glycoprotein. *Res Commun Chem Path* 80, 337-344 (1993).
56. Purcell M; Neault JF; Tajmir-Riahi HA, Interaction of taxol with human serum albumin. *BBA-Protein Struct M* 1478, 61-68 (2000).
57. Paal K; Muller J; Hegedus L, High affinity binding of paclitaxel to human serum albumin. *Eur J Biochem* 268, 2187-2191 (2001).
58. Kabanov AV; Nazarova IR; Astafieva IV; Batrakova EV; Alakhov VY; Yaroslavov AA; Kabanov VA, Micelle formation and solubilization of fluorescent probes in poly(oxyethylene-b-oxypropylene-b-oxyethylene) solutions. *Macromolecules* 28, 2303-2314 (1995).

Summary and Perspectives

7

Summary

In order to develop a promising drug candidate into a clinical product many hurdles need to be taken, which can be related to the proper formulation of the compound, and its efficacy and safety *in vivo*.[1] A variety of nanosized drug carriers have been developed to overcome formulation problems related to, for example, low solubility or stability, and to improve the therapeutic index of the encapsulated drug by ameliorating the pharmacokinetics and/or the biodistribution after intraveneous injection.[2-5] Self-assembled nanoparticles have received increasing interest in the last decades.[6-8] These are supramolecular structures composed of amphiphilic macromolecular compounds, often block copolymers. In particular nanosized polymeric vesicles and micelles are interesting systems for the (targeted) delivery of hydrophilic and hydrophobic drugs, respectively (Figure 1). Their small size and hydrophilic surface are attractive features to achieve long circulatory behaviour after intravenous admininstration, enabling extravasation and accumulation at tumour sites or inflamed areas by the so-called enhanced permeability and retention (EPR) effect. Other favourable characteristics of these systems are their ease of preparation and their tailorability, as the use of (semi-)synthetic polymers offers the possibility to modulate the carriers' properties and to control the release of the loaded drug.[9, 10]

Poly(ethylene glycol) (PEG)-polyesters, especially PEG-*b*-polylactate (PLA) and PEG-*b*-poly(ε-caprolactone) (PCL), have been extensively studied for the development of self-assembled drug delivery systems. These polymers are biocompatible, and the degradability of the polyester block may enable controlled release and facilitate excretion of the carrier after administration.

The amphiphiles studied in this thesis are well-defined low molecular weight (MW) PEG-*b*-oligoesters. The effects of block oligomer structure on their self-assembling properties were investigated in detail, and their suitability to design novel nanoscopic drug carriers was evaluated.

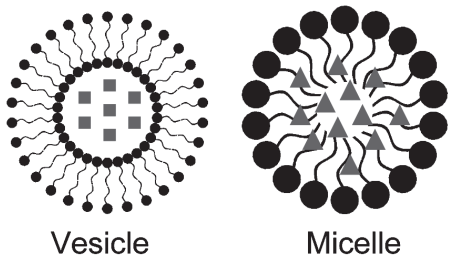

Figure 1 Polymeric vesicle (left) and micelle (right), loaded with hydrophilic (squares) and hydrophobic (triangles) drugs.

Chapter one provides an introduction to nanosized polymeric drug delivery systems, including self-assembled systems, and their preparation methods and morphogenic factors. Subsequently, the aim and outline of this thesis are presented.

Polymeric micelles are discussed in more detail in **Chapter two**, which presents an extensive literature overview on the longevity, stability and stimuli sensitivity of these carriers. Importantly, polymeric micelles can accommodate hydrophobic drugs in their core, which are usually difficult to formulate. Ideally, these carriers have long circulating properties after intravenous administration (longevity), without premature loss of the encapsulated drug (stability), to allow efficient accumulation of the drug at the target site. Here, the drug should be released, preferably in a controlled manner, either by time or site specific degradation, or by destabilisation induced by an external trigger (stimuli sensitivity). Longevity can be accomplished by the use of an adequate surface coating to provide steric protection, and a small (submicron) size of the nanocarrier. To design polymeric micelles, PEG has been most often used as hydrophilic block. The shell thickness, surface density and flexibility have been identified as important parameters for effective shielding of the nanoparticles. Other flexible polymers have been used as hydrophilic block as well, such as poly(N-vinylpyrrolidone) (PVP) and poly(2-ethyl-2-oxazoline) (PEtOz). Furthermore, several strategies have been applied to stabilise polymeric micelles, by physical or chemical crosslinking, and to improve drug retention by optimisation of the compatibility between the drug and the micellar core. Finally, a variety of stimuli sensitive micelles have been designed, using temperature, pH, light and (enzymatic) degradation to destabilise polymeric micelles and simultaneously induce the drug release. The large versatility of polymeric micelles characteristics explains their potential for the site specific delivery of drugs.

In **Chapter three** the self-assembly of methoxyPEG-*b*-oligo(L-lactate) (mPEG-*b*-OLA) with monodisperse hydrophobic blocks (mPEG350, mPEG550, and mPEG750; OLA degree of polymerisation (DP) 4-10) was studied. Interestingly, above their critical aggregation concentration (CAC) of 0.4-1 mg/mL, these mPEG-*b*-OLAs formed nanoparticles by the film-hydration (also called 'film-casting') method, with a hydrodynamic radius of 130-300 nm, whereas polydisperse mPEG-*b*-OLAs formed large aggregates. Further characterisation of the nanoparticles by static light scattering (SLS) revealed an aggregated morphology, and a density of only 0.6-25 mg/mL. This indicates that the particles are highly hydrated, and explains why they could not be visualised by cryogenic transmission electron microscopy (cryo-TEM). Furthermore, differential scanning calorimetry (DSC) demonstrated that the PEG- and OLA-block are miscible, contributing to the high water absorbing capacity of the nanoaggregates. Presumably, PEG that is present in the outer layer contributes to the stability of the

particles composed of oligomers with mPEG550 and mPEG750. Because of their self-emulsifying properties, combined with their expected biodegradability and biocompatibility, mPEG-*b*-oligo(L-lactate)s may be used for the solubilisation of therapeutic proteins and drugs.

However, upon intravenous injection, the oligomer concentration after dilution in the blood should be above the CAC, to prevent rapid destabilisation. This means that relatively high amounts of mPEG-*b*-OLA are needed for intravenous administration, because of their high CAC. Consequently, systems with a lower CAC would be more attractive, and therefore block oligomers with a more hydrophobic oligoester were synthesised and investigated for the preparation of polymeric micelles (**Chapter four**). The block oligomers were composed of an mPEG-block with a molecular weight of 750 Da and a monodisperse oligo(ε-caprolactone) (OCL)-block of 1-7 units, and their hydroxyl end groups were unmodified, or derivatised with either a benzoyl or naphthoyl group. As anticipated, much lower CACs were obtained with the unmodified mPEG-*b*-OCLs, as compared to mPEG-*b*-OLAs. The CAC decreased with increasing length of the OCL-chain. Importantly, the introduction of an aromatic end group resulted in a substantial decrease in the CAC. Even a CAC of 0.003 mg/mL was measured for benzoylated mPEG750-*b*-OCL_6, which approached that of high MW mPEG-*b*-PCL as reported in literature.[11] Furthermore, DSC showed that, in contrast to mPEG-*b*-OLA, the two blocks of mPEG-*b*-OCLs were phase separated. In aqueous solution, these block oligomers formed small and almost monodisperse oligomeric micelles with a hydrodynamic diameter of 8-15 nm, which may have attractive properties for drug delivery applications in terms of biodistribution and tissue penetration.[12-16] The micelles had a spherical shape, as demonstrated by cryo-TEM, and their size could be tailored by the molecular weight of the hydrophobic block. These small oligomeric micelles in PBS were stable for over a month at room temperature, and for at least 2 weeks at 37 °C, with the exception of the micelles composed of mPEG750-*b*-$OCL_{6\text{ and }7}$, benzoylated mPEG750-*b*-OCL_7, and naphthoylated mPEG750-*b*-OCL_6. The low stability of the latter three types of micelles was related to an unfavourable temperature sensitivity profile, as they displayed Krafft points (*i.e.* the temperature at with the solubility equals the CAC) at temperatures between 0 and 25 °C. At temperatures above 60 °C, cloud points were observed in all samples. With regard to their application at 37 °C and handling or storage at room temperature or at lower temperature, amphiphilic oligomers with a cloud point above 37 °C and a Krafft point below 4 °C are desired. Altogether, the physical stability of mPEG-*b*-OCL based micelles was ameliorated by the introduction of an aromatic end group, enabling an optimal combination of a low CAC and a good temperature sensitivity profile.

The chemical stability of these block oligomers was addressed in **Chapter five**. To gain insight into the degradation kinetics and mechanism, first, the hydrolysis of monodisperse benzyl OCL was studied. It was demonstrated that hydrolytic cleavage of the ester bonds in the oligomers occurred essentially via a random scission process. In line with the degradation of OLA,[17] pseudo first order kinetics were observed and the degradation rate depended on the pH and dielectric constant of the degradation medium. The presence of PEG hardly affected the degradation rate of the OCL-esters when molecularly dissolved in a mixture of acetonitrile and buffer. Dispersion of mPEG-*b*-OCL as micelles in buffer resulted in slower degradation, which was ascribed to the low polarity of the micellar core. As expected, the ester hydrolysis induced micelle destabilisation after approximately 1.5 degradation half-lives. The estimated half-life of mPEG-*b*-OCL micelles at physiological pH and temperature was several years, indicating that chemical hydrolysis of OCL will hardly play a role in the destabilisation of mPEG-*b*-OCL micelles *in vivo*. It is however known that polyesters can be degraded by enzymes such as lipase, which are present in many organisms, both intracellularly and extracellularly.[18, 19] Indeed, the presence of lipase accelerated the degradation and destabilisation of the mPEG-*b*-OCL micelles to half-lives of a few days to hours, depending on the lipase concentration. This indicates that, despite the slow chemical hydrolysis, degradation-induced destabilisation and subsequent drug release from these mPEG-*b*-OCL micelles is feasible by the action of enzymes *in vivo*.

In **Chapter six** PEG-*b*-OCL based micelles were loaded with paclitaxel (PTX) and docetaxel (DCTX). These hydrophobic anti-cancer agents are highly potent, but their current clinically used formulations (Taxol® and Taxotere®, respectively) are associated with vehicle-related toxicity.[20, 21] Importantly, it was shown that the use of benzoyl (Bz) or naphthoyl (Np) end group-modified mPEG750-*b*-OCL_5 resulted in small-sized micelles with stable encapsulation of 10% (w/w) of taxane, in contrast to non-modified mPEG750-*b*-OCL_5. Characterisation of the loaded micelles in D_2O by ^1H NMR demonstrated the liquid nature of the micellar core, in which PTX was dissolved. *In vitro* stability studies (PBS, 37 °C) showed that PTX was retained in the mPEG750-*b*-OCL_5-Bz micelles for 8 h, and was then released by leakage, rather than by micelle destabilisation. The integrity of the PTX-loaded mPEG750-*b*-OCL_5-Bz micelles was not affected by the presence of albumin, suggesting that albumin neither destabilised the micelle, nor extracted the drug from the micellar core. The taxane-loaded micelles had a comparable cytotoxic effect on C26-cells to that of the commercial formulations Taxol® and Taxotere®, whereas the empty micelles, in contrast to Cremophor EL®, were not toxic up to 0.1 mg/mL. Taken together, the results indicate that these micelles have superior properties for the formulation of taxanes.

Discussion and future perspectives

Self-assembly of block oligomers

The self-assembled polymeric drug delivery systems most frequently described in literature are composed of high MW block copolymers, and only a limited number of oligomer-based systems have been reported. These low MW block oligomers often have a relatively high CAC, resulting in a limited stability of the formed systems upon intravenous administration.[6] In **Chapter four** of this thesis it was demonstrated that it is possible synthesise block oligomers with a low CAC. End group modification of mPEG-*b*-OCL with an aromatic group resulted in CAC-values that approached those of high MW copolymers. A further reduction of the CAC may be achieved by introducing multiple aromatic groups in the oligoester backbone, by using for example benzyl substituted monomers in the polymerisation reaction, such as benzyl carboxylate-caprolactone,[22] 4-phenyl-ε-caprolactone,[23] or benzyloxymethyl glycolide.[24] It should be noted that it may not always be possible to measure extremely low CAC-values by using fluorescent probes like pyrene, whose fluorescence is influenced by the polarity of the environment.[25, 26] These compounds have a partition equilibrium coefficient, and at low CAC the total volume fraction of the hydrophobic cores of the micelles is insufficient to incorporate the fluorescent probe, representing the detection limit of the method.[27] This phenomenon was observed when determining the CAC-values of the mPEG-*b*-OCL based oligomers, which levelled off at low values (**Chapter four**). This means that the CAC of these oligomers might be even lower than the reported values. The CAC detection limit can be lowered by using a more hydrophobic probe.[27] Alternative techniques to determine the CAC include potentiometry, measurement of surface tension, light scattering, or intrinsic fluorescence of tryptophan residues in peptide amphiphiles.[28-30] Comparative studies should be considered to explore whether alternative methods can be used to obtain a better approximation of the CAC of mPEG-*b*-oligoesters.

One of the advantages of the use of block oligomers for the design of self-assembled nanocarriers is the possibility to prepare well-defined materials with a low polydispersity, which is often more difficult in case of high MW polymers. Good control of the molecular structure of the polymer/oligomer may translate in control of its physicochemical properties and fate *in vivo*. The PEG-oligoesters studied in this thesis were polydisperse after synthesis (M_w/M_n = 1.4) but they could be fractionated by preparative reversed phase HPLC to obtain amphiphiles with monodisperse hydrophobic blocks. In **Chapter four** it was shown that almost monodisperse micelles were formed by fractionated mPEG-*b*-OCLs, and that their size could be tailored by the chain length of the OCL. Fractionation of the mPEG-*b*-oligoesters by preparative HPLC

has a limited capacity and it is rather laborious, which will hamper easy up-scaling. It should be noted that the use of monodisperse materials is interesting from a scientific point of view, but it may not always be necessary for drug delivery purposes. Future studies should reveal whether some degree of heterodispersity is acceptable for practical applications, and confirm that heterodisperse block oligomers can be reproducibly prepared as well. An alternative method to reduce the polydispersity of the mPEG-*b*-oligoesters may be precipitation after the polymerisation reaction, by using selective solvents or solvent mixtures to remove high and/or low MW material. Next to ring opening polymerisation catalysed by organometallic compounds like $SnOct_2$, as applied in this thesis, polyesters can also be synthesised by enzymatic polymerisation. This method uses relatively mild reaction conditions and has a high enantio- and regioselectivity, and may be interesting to explore for the preparation of well-defined oligoesters with a low polydispersity.[31-33]

The small size of low MW block oligomers allows the formation of small micelles, as demonstrated by the formation of sub-20 nm micelles by mPEG-*b*-OCL based block oligomers in **Chapter four** of this thesis. Considering their size, these particles are expected to be especially suitable for the delivery of drugs to tumours with a low cut-off size of the vessel wall.[15, 16, 34, 35] However, the particle size is not only a key factor determining their fate *in vivo*, but it also affects the space available for drug solubilisation/encapsulation. In **Chapter six** it was demonstrated that when the OCL chain length in mPEG750-*b*-OCL-Bz micelles was decreased from 5 to 4 caprolactone units, the PTX loading capacity was reduced. The limited space in small micelles can be (partly) compensated by adjusting the molecular structure of the micellar core, to better 'match' with the drug, as shown in **Chapter six,** where the introduction of an aromatic end group onto mPEG750-*b*-OCL_5 resulted in loading capacities of 20% (w/w) of PTX and DCTX. It is relevant to explore to what extent a high and stable drug loading can be achieved with these oligomeric micelles, and whether the compatibility between the drug and the micellar core can be further improved, also with regard to stable encapsulation for future *in vivo* applications. A possible strategy is the introduction of benzyl groups in the oligoester backbone, which was also suggested for CAC-reduction. A perfect 'match' may be obtained by attaching the drug to the core-forming block, either to the hydroxyl end group of the oligoester, or to the backbone after the introduction of functional groups.[24] The latter approach has been applied by the group of Kataoka, who covalently bound doxorubicin (DOX) to mPEG-*b*-poly(aspartate) (P(Asp)) polymer.[36] This resulted in an increased loading capacity and stability of additional free DOX, and it was demonstrated that the presence of free drug was essential for a good anti-tumour effect *in vivo*.[36, 37] Phase I studies with this formulation, NK911, revealed that NK911 exhibited longer half-lives, a lower clearance, and a larger area under the curve (AUC) as compared to free DOX,

suggesting prolonged circulation times. A phase II clinical trial is currently ongoing.[38] Evidently, when changing the oligomer structure to improve the compatibility with the drug, the possible changes in the properties of the micelle (*e.g.* size, CAC, temperature sensitivity) should also be taken into consideration.

In this thesis the self-assembled systems were formed by the film-hydration method (also called 'film-casting' method). This method is relatively easy, and it has been reported that a higher loading of hydrophobic drugs into polymeric micelles can be obtained when compared to the solvent-evaporation method (o/w emulsion method) or the dialysis method.[39] The film-hydration method has been widely applied in the formation of liposomes.[4] In fact, this method is highly suitable for the encapsulation of hydrophilic proteins or peptides in vesicular structures, since contact of the protein or peptide with the organic solvent is avoided. A disadvantage of the film-hydration method is that up-scaling is rather difficult. Considering the ease of self-assembly by mPEG-*b*-oligoesters upon the film-hydration method, bulk hydration may be a suitable alternative, which should be evaluated in future studies. Important aspects are the effect on the drug loading capacity, and particle size (distribution) of the drug-loaded micelles, and how this procedure can be optimised by for example sonication or extrusion steps. The solvent-evaporation method can also be easily scaled up, and it is a method in which many parameters can be varied, such as the type and amount of solvent used, and the polymer and drug concentration.[6, 7, 40] Thereby the particles' characteristics and even the morphology can be tailored, and it may be interesting to investigate these aspects with mPEG-*b*-oligoesters as well.

Degradation of PEG-*b*-oligoesters

The biodegradability of a drug carrier system is a favourable property to prevent its accumulation in the body, and to allow (controlled) release of the loaded drug, preferably at its target site. The data on the hydrolytic degradation of oligo(ε-caprolactone), presented in **Chapter five** of this thesis, demonstrated that the chemical hydrolysis rate at physiological pH and temperature is very slow, and will hardly play a role *in vivo.* However, **Chapter five** also showed that mPEG-*b*-OCL micelles are susceptible to enzymatic degradation by lipase, suggesting that degradation-induced release is possible *in vivo*. The utilisation of enzymatic degradability is an interesting approach in the design of drug delivery systems, not only because it discloses a new class of biodegradable materials, but also because the presence of specific enzymes in cellular compartments,[41-43] or their up-regulation in pathological tissues[44, 45] can be used as an environmental trigger to allow target specific drug release. This approach was for instance applied to design polymer-drug conjugates such as poly(N-

(2-hydroxypropyl) methacrylamide) (PHPMA)-DOX, which are coupled via a peptidyl linkage that can be cleaved by specific lysosomal enzymes.[46, 47] In this thesis the enzymatic degradability of mPEG-*b*-OCL micelles was shown *in vitro*, using a model enzyme in PBS. Additional studies are necessary for a better approximation of the much more complicated *in vivo* situation, where a cocktail of enzymes is present, the substrate specificity and enzymatic activity are different, and competing substrates are involved. These studies should include investigation of the degradation by other (model) enzymes like proteinase K,[48, 49] and degradation studies in cell lysates and serum. Furthermore, the feasibility of site specific degradation of PEG-*b*-oligoesters in pathological tissues, either intracellularly or extracellularly, should be evaluated.

Micelle-cell interactions

The interaction of the mPEG-*b*-oligoester nanoparticles with cells was hardly addressed in this thesis, but it is an interesting aspect for future studies. In **Chapter six** data on the cytotoxic effect of taxane-loaded and empty benzoylated mPEG-*b*-OCL micelles on C26-cells are presented. These demonstrated high cytotoxicity of the loaded micelles, whereas the empty micelles were non-toxic in the concentration range tested. As the fate of the micelles is not known, it is unclear whether the taxanes are released outside or inside the cells, and consequently, whether they reach their intracellular target associated with the micelles or as a free drug.[50] Remarkably, several studies have suggested the cellular uptake of polymeric micelles via endocytic pathways, despite the presence of a protective PEG-shell.[51-57] The results of such studies are influenced by many factors, such as the cell line used, incubation time, micelle concentration, the type of block copolymer and the labelling procedure. In addition, the uptake mechanism and subsequent intracellular routing strongly depend on the particle size,[58-61] implicating that uptake and cellular localisation studies with the well-defined sub-20 nm micelles described in this thesis are highly interesting. Labelling is necessary to allow the visualisation and detection of the micelles in cells. This can be achieved by coupling of a fluorescent moiety to the hydroxyl end group of mPEG-*b*-oligoesters, which enables (confocal) fluorescence microscopy.[51, 53, 54, 57] Inhibitor studies with specific blockers of the various uptake mechanisms, and co-localisation studies with fluorescent compounds encapsulated in the micelles, as well as organelle specific dyes will provide insight into the uptake mechanism of these micelles and their intracellular fate.[51, 58] Alternatively, the micelles (and loaded drug) can be radioactively labelled, and the intracellular localisation can be established after subcellular fractionation.[62, 63]

In addition to cellular uptake and localisation, it is important to understand the pharmacodynamic effects of the micellar building blocks. For example, there is evidence that PEG-*b*-PCL inhibits the P-glycoprotein efflux pump in Caco-2 cells.[64, 65] This protein is present in the intestine, where it limits the bioavailability of several orally administered drugs.[66, 67] Importantly, P-glycoprotein is also overexpressed in various multi-drug resistant (MDR) tumours, mediating the efflux of a variety of substrates, such as DOX, etoposide, vinblastine, and PTX.[68-70] In fact, it was demonstrated that inhibition of the P-glycoprotein efflux pump is an effective strategy to overcome multi-drug resistance.[68, 71, 72] Amphiphilic Pluronics® (PEG-poly(propylene oxide)-PEG triblock copolymers) have also been identified as P-glycoprotein inhibitors, accounting for the 'chemo-sensitisation' of MDR tumours to anti-cancer drugs, in particular DOX.[73-75] DOX-loaded Pluronic® micelles are currently in clinical development.[76] Regarding the reported effect of high MW PEG-*b*-PCL, the mPEG-*b*-OCL oligomers studied in this thesis may be able to improve anti-tumour therapy of MDR tumours via this mechanism as well.

In vivo applications

Several studies have demonstrated good anti-tumour efficacy of polymeric micelles loaded with anti-cancer drugs in animal models. Examples are cisplatin-incorporated PEG-poly(glutamic acid),[77] DOX-loaded and covalently bound to PEG-P(Asp),[78] micellar camptothecin,[79, 80] and several types of PTX-loaded micelles.[81-85] Moreover, some micellar anti-cancer formulations have entered clinical trials, and showed promising results in patients.[76, 86-89] Besides cancer, polymeric micelles may also be applied for the formulation of hydrophobic drugs to treat infections, or chronic inflammatory diseases like rheumatoid arthritis and psoriasis.[90-95]

Next to their ability to carry hydrophobic compounds, which are usually difficult to formulate, a number of reasons can be given for the demonstrated value of polymeric micelles for the formulation of anti-cancer agents.

Firstly, the loading of a drug into polymeric micelles alters its pharmacokinetics and biodistribution. For example, intravenous administration of polymeric micelles containing camptothecin,[79] cisplatin,[77] DOX (NK911),[78] and PTX (NK105)[84] to mice resulted in prolonged circulation times and improved tumour accumulation of the drug, compared to the free drug. The latter formulations, NK911 and NK105, even showed superior pharmacokinetics and biodistribution in patients.[87, 88] Although these results strongly suggest that the polymeric micelles act as a carrier system, they only give indirect information on the fate of the micelles *in vivo*. As solely the biodistribution of the drug is studied, it is unclear whether the drug is associated with the

micelle, and whether the micelles are still intact. In an *in vivo* biodistribution study of [^{14}C]-labelled PEG-P(Asp), to which DOX was conjugated, the PEG-P(Asp)-DOX conjugates displayed longer circulation times and higher tumour accumulation than free [^{14}C]-DOX, indicating that this particular micellar system is indeed a drug carrier.[96]

Secondly, an improved anti-tumour effect of micellar anti-cancer drugs can be obtained because of a lower toxicity of the polymeric micelles when compared to commercial formulations, which allows higher dosing. It has been demonstrated in mice that PTX-loaded PEG-*b*-PLA or PVP-*b*-PLA micelles displayed poor biodistribution and tumour accumulation, but the maximum tolerated dose was higher than that of Taxol®, resulting in more effective treatment of the tumour.[81-83, 85] The improved toxicity profile of PTX in PEG-*b*-PLA micelles (Genexol-PM) was also found in patients.[86, 89] Although a reduction of the toxicity results in an increased therapeutic index, in these cases the polymeric micelles act as solubilising agents, rather than real drug carriers aiming at specific drug delivery to the target site. This was illustrated by biodistribution studies of a dual-labelled system of PTX in PEG-*b*-PLA micelles, which showed that PTX was rapidly dissociated from the micellar components after intravenous injection.[97]

Thirdly, the added value of polymeric micelles may be related to a pharmacodynamic effect of the micellar building blocks themselves. The prime example of this mechanism are DOX-loaded Pluronic® micelles (SP1049C). As discussed previously, cellular drug efflux can be inhibited by Pluronic®, accounting for the improved anti-tumour efficacy of the loaded DOX in MDR-tumours,[73-75] which was even observed in some patients with advanced resistant solid tumours.[76]

To evaluate the *in vivo* performance of the mPEG-*b*-OCL based micelles developed in this thesis, an introductory biodistribution study in tumour bearing mice was performed. The blood clearance and tissue distribution of PTX loaded in mPEG750-*b*-OCL_5-Bz micelles were determined after a single intravenous injection, and compared with the commercially available formulation Taxol® (Table 1, Figure 2). Regarding the circulation time and biodistribution of PTX, no improvement was observed when in comparing the micelle formulation with Taxol®. Based on these data it is difficult to identify a mechanism explaining the rapid blood clearance of the PTX loaded in the micelles. Regarding the size of the micelles, rapid renal excretion is unlikely, as they are larger than the renal filtration cut-off size. As described above, rapid blood clearance and low tumour accumulation has been observed with other micellar formulations as well,[81-83, 85] and strongly indicate that, despite the anticipated stabilisation by the benzoyl end group, these block oligomers are solubilisers, rather than a real carrier system. Still, it can be envisaged that they have advanta-

Table 1 PTX blood levels and tumour concentrations after administration of PTX-loaded micelles and Taxol® in C26-tumour bearing Balb/C mice[a]

Time (h)	[^{14}C]-PTX in mPEG-*b*-OCL-Bz micelles		[^{14}C]-PTX in Taxol®	
	Blood (%ID±SD)	Tumour (%ID/g±SD)	Blood (%ID±SD)	Tumour (%ID/g±SD)
0.2	1.4±0.4	1.0±0.2	2.5±0.8	0.7±0.2
1	1.0±0.3	1.2±0.4	1.0±0.3	1.0±0.1
2	0.2±0.1	ND[b]	0.5±0.2	ND[b]
5	0.0±0.0	0.8±0.2	0.1±0.1	0.8±0.3
8	0.0±0.0	0.7±0.2	0.0±0.0	0.5±0.2
24	0.0±0.0	0.3±0.1	0.0±0.0	0.3±0.1

[a] *BALB/c mice with a subcutaneously established C26-tumour received a single intravenous injection of either [^{14}C]-paclitaxel (PTX, 10% (w/w)) loaded mPEG750-b-OCL$_5$-Bz micelles or Taxol®, supplemented with [^{14}C]-PTX. Hundred μL of each formulation were injected into the tail vein, at a PTX-concentration of 1 mg/mL. Results are expressed as percentage of the initially injected dose of radioactivity (% ID, the estimated blood volume is 2 mL per mouse) or % ID per gram tumour tissue (% ID/g) ± standard deviation (SD, n=4-5), at various time points after administration, in hours.*

[b] *Not determined.*

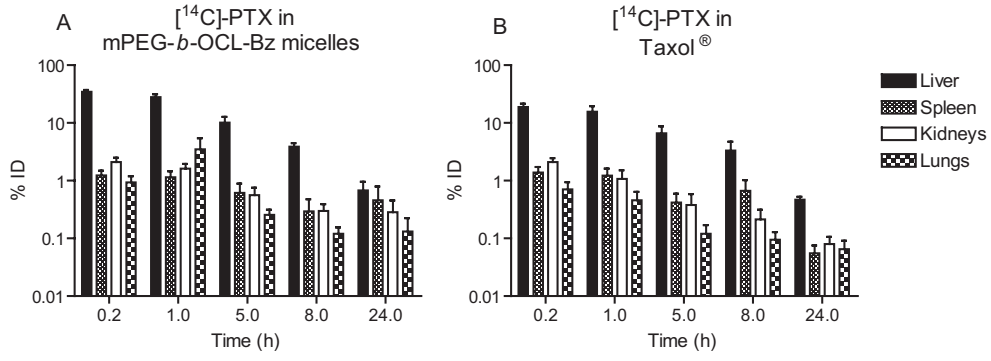

Figure 2 Biodistribution of PTX after administration of PTX-loaded mPEG750-*b*-OCL$_5$-Bz micelles (A) and Taxol® (B) in C26-tumour bearing BALB/c mice. The bars represent % ID ± SD (n=4-5) in the different tissues at various time points after administration, in hours.

geous properties for the formulation of hydrophobic anti-cancer drugs, because of their degradability (**Chapter five**), high solubilisation capacity, low *in vitro* toxicity (**Chapter six**), and possible effect on P-glycoprotein *in vivo*.

To benefit from the small size of mPEG-*b*-OCL based micelles, which may be favourable in terms of biodistribution and tumour penetration of the loaded drug *in vivo*,[12-16] additional stabilisation is necessary. Increasing the drug retention and/or the micellar integrity will result in improved drug carrier properties of these micelles, and a variety of strategies to achieve this have been presented in **Chapter two**. As discussed earlier in this chapter, the drug loading and retention may be further improved by a better 'matching' of the micellar core with the loaded compound. In addition, the CAC may be further reduced, to increase the micellar stability. However, perhaps the most promising approach for additional stabilisation of these micelles is covalent crosslinking, preferably in combination with the two strategies described above. The oligoester core can be easily crosslinked after the introduction of a polymerisable group. High MW PEG-*b*-polyester micelles have been crosslinked in this way by functionalisation of the hydroxyl end group of the hydrophobic block with (meth)acrylate groups, which were crosslinked after micelle formation by thermal or photo-induced polymerisation.[98-100] As this crosslinking procedure is not possible when using benzoylated or naphthoylated mPEG-*b*-OCL due to the lack of a functional group, crosslinkable groups should be introduced in the oligoester backbone, for example by copolymerisation with allyl glycidyl ether[101] or α-allyl(valerolactone).[102] Alternatively, a crosslinkable spacer could be introduced between the PEG- and oligoester-block, to allow interfacial crosslinking.

It may be anticipated that these stabilised small-sized nanocarriers will accumulate in tumour tissue by passive targeting, as a result of the EPR-effect. The tumour accumulation of these systems may be further improved by the coupling of homing devices, like antibodies, sugar moieties, transferrin, RGD-peptides (arginine-glycine-aspartic acid) or folate to allow active targeting.[103-109] In order to couple cell specific ligands to the surface of the mPEG-*b*-oligoester nanoparticles described in this thesis, it is necessary to introduce a functional group at the distal end of the PEG-chain, such as an aldehyde,[107] or an amino group.[110]

Whereas the stability of polymeric micelles after intravenous administration remains a major challenge, the conditions encountered upon other administration routes may cause fewer problems. Examples are subcutaneous administration, transdermal delivery or inhalation therapy, where the limited volume of fluid at the site of disposition will result in less extensive dilution upon administration. Since sterically stabilised nanoparticles can be taken up from an interstitial site into the lymphatic system, the sub-20 nm micelles developed in this thesis may be used to achieve lymphatic

targeting after subcutaneous administration, for therapeutic but also for diagnostic purposes.[111-115] Their small size could also be a benefit for transdermal delivery, as the permeation via the hair follicles increases with decreasing particle size.[116-119] Besides, PEG-oligoester micelles may be applied for pulmonary delivery of hydrophobic drugs, to increase the residence time of the drug in the lung, or to target specific sites in the respiratory tract.[120-122] In particular hydrophobic drugs often rapidly pass the epithelial barrier to end up in the systemic circulation, which is undesirable in case of local treatment of diseases such as lung cancer or pulmonary infections, and may be retarded by their encapsulation in polymeric micelles.

Conclusion

The PEG-*b*-oligoesters studied in this thesis represent an interesting class of amphiphilic molecules, which possess attractive properties for pharmaceutical applications. These include good control of the molecular composition and high tailorability, as well as biodegradability and low toxicity. As they offer numerous opportunities for further improvement, they are promising candidates for the development of drug carrier systems, which may be suitable for several applications.

References

1. Pritchard JF; Jurima-Romet M; Reimer ML; Mortimer E; Rolfe B; Cayen MN, Making better drugs: Decision gates in non-clinical drug development. *Nat Rev Drug Discov* 2, 542-553 (2003).
2. Allen TM; Cullis PR, Drug delivery systems: entering the mainstream. *Science* 303, 1818-1822 (2004).
3. Barratt GM, Therapeutic applications of colloidal drug carriers. *Pharm Sci Technol To* 3, 163-171 (2000).
4. Storm G; Crommelin DJA, Liposomes: quo vadis? *Pharm Sci Technol To* 1, 19-31 (1998).
5. Khandare J; Minko T, Polymer-drug conjugates: Progress in polymeric prodrugs. *Prog Polym Sci* 31, 359-397 (2006).
6. Allen C; Maysinger D; Eisenberg A, Nano-engineering block copolymer aggregates for drug delivery. *Colloid Surface B* 16, 3-27 (1999).
7. Letchford K; Burt H, A review of the formation and classification of amphiphilic block copolymer nanoparticulate structures: micelles, manospheres, nanocapsules and polymersomes. *Eur J Pharm Biopharm* 65, 259-269 (2007).
8. Gaucher G; Dufresne MH; Sant VP; Kang N; Maysinger D; Leroux JC, Block copolymer micelles: preparation, characterization and application in drug delivery. *J Control Release* 109, 169-188 (2005).
9. Qiu LY; Bae YH, Polymer architecture and drug delivery. *Pharm Res* 23, 1-30 (2006).
10. Hawker CJ; Wooley KL, The convergence of synthetic organic and polymer chemistries. *Science* 309, 1200-1205 (2005).
11. Aliabadi HM; Mahmud A; Sharifabadi AD; Lavasanifar A, Micelles of methoxy poly(ethylene oxide)-b-poly(epsilon-caprolactone) as vehicles for the solubilization and controlled delivery of cyclosporine A. *J Control Release* 104, 301-311 (2005).
12. Vonarbourg A; Passirani C; Saulnier P; Benoit JP, Parameters influencing the stealthiness of colloidal drug delivery systems. *Biomaterials* 27, 4356-4373 (2006).
13. Sun X; Rossin R; Turner JL; Becker ML; Joralemon MJ; Welch MJ; Wooley KL, An assessment of the effects of shell cross-linked nanoparticle size, core composition, and surface PEGylation on in vivo biodistribution. *Biomacromolecules* 6, 2541-2554 (2005).
14. Weissig V; Whiteman KR; Torchilin VP, Accumulation of protein-loaded long-circulating micelles and liposomes in subcutaneous Lewis lung carcinoma in mice. *Pharm Res* 15, 1552-1556 (1998).
15. Hobbs SK; Monsky WL; Yuan F; Roberts WG; Griffith L; Torchilin VP; Jain RK, Regulation of transport pathways in tumor vessels: role of tumor type and microenvironment. *P Natl Acad Sci USA* 95, 4607-4612 (1998).
16. Yuan F; Dellian M; Fukumura D; Leunig M; Berk DA; Torchilin VP; Jain RK, Vascular permeability in a human tumor xenograft: molecular size dependence and cutoff size. *Cancer Res* 55, 3752-3756 (1995).
17. De Jong SJ; Arias ER; Rijkers DTS; van Nostrum CF; Kettenes-van den Bosch JJ; Hennink WE, New insights into the hydrolytic degradation of poly(lactic acid): participation of the alcohol terminus. *Polymer* 42, 2795-2802 (2001).
18. Herzog K; Muller R-J; Deckwer W-D, Mechanism and kinetics of the enzymatic hydrolysis of polyester nanoparticles by lipases. *Polym Degrad Stabil* 91, 2486-2498 (2006).
19. Chen DR; Bei JZ; Wang SG, Polycaprolactone microparticles and their biodegradation. *Polym Degrad Stabil* 67, 455-459 (2000).
20. Hennenfent KL; Govindan R, Novel formulations of taxanes: a review. Old wine in a new bottle? *Ann Oncol* 17, 735-749 (2006).
21. van Zuylen L; Verweij J; Sparreboom A, Role of formulation vehicles in taxane pharmacology. *Invest New Drugs* 19, 125-141 (2001).
22. Mahmud A; Xiong XB; Lavasanifar A, Novel self-associating poly(ethylene oxide)-block-poly(ε-caprolactone) block copolymers with functional side groups on the polyester block for drug delivery. *Macromolecules* 39, 9419-9428 (2006).
23. Lee R-S; Hung C-B, Synthesis and characterization of amphiphilic block copolymers from poly(ethylene glycol)methyl ether and 4-methyl-epsilon-caprolactone or 4-phenyl-epsilon-caprolactone. *Polymer* 48, 2605-2612 (2007).

24. Leemhuis M; van Nostrum CF; Kruijtzer JAW; Zhong ZY; ten Breteler MR; Dijkstra PJ; Feijen J; Hennink WE, Functionalized poly(alpha-hydroxy acid)s via ring-opening polymerization: Toward hydrophilic polyesters with pendant hydroxyl groups. *Macromolecules* 39, 3500-3508 (2006).
25. Wilhelm M; Zhao CL; Wang Y; Xu R; Winnik MA; Mura JL; Riess G; Croucher MD, Poly(styrene-ethylene oxide) block copolymer micelle formation in water: a fluorescence probe study. *Macromolecules* 24, 1033-1040 (1991).
26. Soga O; van Nostrum CF; Ramzi A; Visser T; Soulimani F; Frederik PM; Bomans PHH; Hennink WE, Physicochemical characterization of degradable thermosensitive polymeric micelles. *Langmuir* 20, 9388-9395 (2004).
27. Nakahara Y; Kida T; Nakatsuji Y; Akashi M, New fluorescence method for the determination of the critical micelle concentration by photosensitive monoazacryptand derivatives. *Langmuir* 21, 6688-6695 (2005).
28. Kastantin M; Ananthanarayanan B; Lin B; Ressl J; Black M; Tirrell M, Increase of fluorescence anisotropy upon self-assembly in headgroup-labeled surfactants. *Macromol Biosci* 7, 189-194 (2007).
29. Van Hell AJ; Costa C; Flesch FM; Sutter M; Jiskoot W; Crommelin DJA; Hennink WE; Mastrobattista E, Self-assembly of recombinant amphiphilic oligopeptides into vesicles. *Biomacromolecules,* In Press (2007) .
30. Attwood D; Florence AT, *Surfactant Systems: Their chemistry, pharmacy and biology*, Chapman and Hall Ltd., London, UK, p 72 (1983).
31. Panova AA; Kaplan DL, Mechanistic limitations in the synthesis of polyesters by lipase-catalyzed ring-opening polymerization. *Biotechnol Bioeng* 84, 103-113 (2003).
32. Albertsson AC; K.Varma I, Recent developments in ring opening polymerization of lactones for biomedical applications. *Biomacromolecules* 4, 1446-1486 (2003).
33. Kobayashi S; Uyama H; Kimura S, Enzymatic Polymerization. *Chem Rev* 101, 3793-3818 (2001).
34. Weissig V; Whiteman KR; Torchilin VP, Accumulation of protein-loaded long-circulating micelles and liposomes in subcutaneous lewis lung carcinoma in mice. *Pharm Res* V15, 1552-1556 (1998).
35. Nishiyama N; Kataoka K, Current state, achievements, and future prospects of polymeric micelles as nanocarriers for drug and gene delivery. *Pharmacol Therapeut* 112, 630-648 (2006).
36. Yokoyama M; Fukushima S; Uehara R; Okamoto K; Kataoka K; Sakurai Y; Okano T, Characterization of physical entrapment and chemical conjugation of adriamycin in polymeric micelles and their design for in vivo delivery to a solid tumor. *J Control Release* 50, 79-92 (1998).
37. Nakanishi T; Fukushima S; Okamoto K; Suzuki M; Matsumura Y; Yokoyama M; Okano T; Sakurai Y; Kataoka K, Development of the polymer micelle carrier system for doxorubicin. *J Control Release* 74, 295-302 (2001).
38. Matsumura Y; Hamaguchi T; Ura T; Muro K; Yamada Y; Shimada Y; Shirao K; Okusaka T; Ueno H; Ikeda M; Watanabe N, Phase I clinical trial and pharmacokinetic evaluation of NK911, a micelle-encapsulated doxorubicin. *Brit J Cancer* 91, 1775-1781 (2004).
39. Yokoyama M; Opanasopit P; Okano T; Kawano K; Maitani Y, Polymer design and incorporation methods for polymeric micelle carrier system containing water-insoluble anti-cancer agent camptothecin. *J Drug Target* 12, 373-384 (2004).
40. Jain S; Bates FS, On the origins of morphological complexity in block copolymer surfactants. *Science* 300, 460-464 (2003).
41. Du H; Grabowski GA, Lysosomal acid lipase and atherosclerosis. *Curr Opin Lipidol* 15, 539-544 (2004).
42. Chayen J; Bitensky L, Lysosomal enzymes and inflammation with particular reference to rheumatoid diseases. *Ann Rheum Dis* 30, 522-536 (1971).
43. Roberts R, Lysosomal cysteine proteases: structure, function and inhibition of cathepsins. *Drug News Perspect* 18, 605-614 (2005).
44. Koblinski JE; Ahram M; Sloane BF, Unraveling the role of proteases in cancer. *Clin Chim Acta* 291, 113-135 (2000).
45. Muller-Ladner U, Molecular and cellular interactions in rheumatoid synovium. *Curr Opin Rheumatol* 8, 210-220 (1996).
46. Duncan R; Gac-Breton S; Keane R; Musila R; Sat YN; Satchi R; Searle F, Polymer-drug conjugates, PDEPT and PELT: basic principles for design and transfer from the laboratory to clinic. *J Control Release* 74, 135-146 (2001).

47. Vicent MJ; Duncan R, Polymer conjugates: nanosized medicines for treating cancer. *Trends Biotechnol* 24, 39-47 (2006).
48. Lim H-A; Raku T; Tokiwa Y, Hydrolysis of polyesters by serine proteases. *Biotechnol Lett* 27, 459-464 (2005).
49. Zeng J; Chen X; Liang Q; Xu X; Jing X, Enzymatic degradation of poly(L-lactide) and poly(ε-caprolactone) electrospun fibers. *Macromol Biosci* 4, 1118-1125 (2004).
50. Marcucci F; Lefoulon F, Active targeting with particulate drug carriers in tumor therapy: fundamentals and recent progress. *Drug Discov Today* 9, 219-228 (2004).
51. Savic R; Luo L; Eisenberg A; Maysinger D, Micellar nanocontainers distribute to defined cytoplasmic organelles. *Science* 300, 615-618 (2003).
52. Savic R; Eisenberg A; Maysinger D, Block copolymer micelles as delivery vehicles of hydrophobic drugs: Micelle-cell interactions. *J Drug Target* 14, 343-355 (2006).
53. Luo L; Tam J; Maysinger D; Eisenberg A, Cellular internalization of poly(ethylene oxide)-b-poly(epsilon-caprolactone) diblock copolymer micelles. *Bioconjugate Chem* 13, 1259-1265 (2002).
54. Rapoport N; Marin A; Luo Y; Prestwich GD; Muniruzzaman MD, Intracellular uptake and trafficking of Pluronic micelles in drug-sensitive and MDR cells: effect on the intracellular drug localization. *J Pharm Sci* 91, 157-170 (2002).
55. Shuai X; Ai H; Nasongkla N; Kim S; Gao J, Micellar carriers based on block copolymers of poly(ε-caprolactone) and poly(ethylene glycol) for doxorubicin delivery. *J Control Release* 98, 415-426 (2004).
56. Mahmud A; Lavasanifar A, The effect of block copolymer structure on the internalization of polymeric micelles by human breast cancer cells. *Colloid Surface B* 45, 82-89 (2005).
57. Soga O; van Nostrum CF; Fens M; Rijcken CJF; Schiffelers RM; Storm G; Hennink WE, Thermosensitive and biodegradable polymeric micelles for paclitaxel delivery. *J Control Release* 103, 341-353 (2005).
58. Rejman J; Oberle V; Zuhorn IS; Hoekstra D, Size-dependent internalization of particles via the pathways of clathrin- and caveolae-mediated endocytosis. *Biochem J* 377, 159-169 (2004).
59. Lai SK; Hida K; Man ST; Chen C; Machamer C; Schroer TA; Hanes J, Privileged delivery of polymer nanoparticles to the perinuclear region of live cells via a non-clathrin, non-degradative pathway. *Biomaterials* 28, 2876-2884 (2007).
60. Pante N; Kann M, Nuclear pore complex is able to transport macromolecules with diameters of about 39 nm. *Mol Biol Cell* 13, 425-434 (2002).
61. Zauner W; Farrow NA; Haines AM, In vitro uptake of polystyrene microspheres: effect of particle size, cell line and cell density. *J Control Release* 71, 39-51 (2001).
62. Lecocq M; Andrianaivo F; Warnier M-T; Coninck SW-D; Wattiaux R; Jadot M, Uptake by mouse liver and intracellular fate of plasmid DNA after a rapid tail vein injection of a small or a large volume. *J Gene Med* 5, 142-156 (2003).
63. Manunta M; Izzo L; Duncan R; Jones AT, Establishment of subcellular fractionation techniques to monitor the intracellular fate of polymer therapeutics II. Identification of endosomal and lysosomal compartments in HepG2 cells combining single-step subcellular fractionation with fluorescent imaging. *J Drug Target* 15, 37-50 (2007).
64. Zastre J; Jackson JK; Wong W; Burt HM, Methoxypolyethylene glycol-block-polycaprolactone diblock copolymers reduce P-glycoprotein efflux in the absence of a membrane fluidization effect while stimulating P-glycoprotein ATPase activity. *J Pharm Sci* 96, 864-875 (2007).
65. Zastre J; Jackson J; Burt H, Evidence for modulation of P-glycoprotein-mediated efflux by methoxypolyethylene glycol-block-polycaprolactone amphiphilic diblock copolymers. *Pharm Res* 21, 1489-1497 (2004).
66. Van Asperen J; van Tellingen OH; Beijnen JH, The pharmacological role of P-glycoprotein in the intestinal epothelium. *Pharmacol Res* 37, 429-435 (1998).
67. Wacher VJ; Salphati L; Benet LZ, Active secretion and enterocytic drug metabolism barriers to drug absorption. *Adv Drug Deliver Rev* 46, 89-102 (2001).
68. Lum BL; Gosland MP; Kaubisch S; Sikic BI, Molecular targets in oncology: implications of the multidrug resistance gene. *Pharmacotherapy* 13, 88-109 (1993).
69. Fardel O; Lecureur V; Guillouzo A, The P-glycoprotein multidrug transporter. *Gen Pharmacol* 27, 1283-1291 (1996).

70. Goldstein LJ; Pastan I; Gottesman MM, Multidrug resistance in human cancer. *Crit Rev Oncol Hematol* 12, 243-253 (1992).

71. Nobili S; Landini I; Giglioni B; Mini E, Pharmacological strategies for overcoming multidrug resistance. *Curr Drug Targets* 7, 861-879 (2006).

72. Thomas H; Coley HM, Overcoming multidrug resistance in cancer: an update on the clinical strategy of inhibiting P-glycoprotein. *Cancer Control* 10, 159-165 (2003).

73. Kabanov AV; Batrakova EV; Alakhov VY, Pluronic block copolymers for overcoming drug resistance in cancer. *Adv Drug Deliver Rev* 54, 759-779 (2002).

74. Batrakova EV; Li S; Li Y; Alakhov VY; Kabanov AV, Effect of Pluronic P85 on ATPase Activity of Drug Efflux Transporters. *Pharm Res* 21, 2226-2233 (2004).

75. Venne A; Li S; Mandeville R; Kabanov A; Alakhov V, Hypersensitizing effect of pluronic L61 on cytotoxic activity, transport, and subcellular distribution of doxorubicin in multiple drug-resistant cells. *Cancer Res* 56, 3626-3629 (1996).

76. Danson S; Ferry D; Alakhov V; Margison J; Kerr D; Jowle D; Brampton M; Halbert G; Ranson M, Phase I dose escalation and pharmacokinetic study of pluronic polymer-bound doxorubicin (SP1049C) in patients with advanced cancer. *Brit J Cancer* 90, 2085-2091 (2004).

77. Nishiyama N; Okazaki S; Cabral H; Miyamoto M; Kato Y; Sugiyama Y; Nishio K; Matsumura Y; Kataoka K, Novel cisplatin-incorporated polymeric micelles can eradicate solid tumors in mice. *Cancer Res* 63, 8977-8983 (2003).

78. Nakanishi T; Fukushima S; Okamoto K; Suzuki M; Matsumura Y; Yokoyama M; Okano T; Sakurai Y; Kataoka K, Development of the polymer micelle carrier system for doxorubicin. *J Control Release* 74, 295-302 (2001).

79. Kawano K; Watanabe M; Yamamoto T; Yokoyama M; Opanasopit P; Okano T; Maitani Y, Enhanced antitumor effect of camptothecin loaded in long-circulating polymeric micelles. *J Control Release* 112, 329-332 (2006).

80. Koizumi F; Kitagawa M; Negishi T; Onda T; Matsumoto S-i; Hamaguchi T; Matsumura Y, Novel SN-38-incorporating polymeric micelles, NK012, eradicate vascular endothelial growth factor-secreting bulky tumors. *Cancer Res* 66, 10048-10056 (2006).

81. Zhang X; Burt HM; Mangold G; Dexter D; Hoff DV; Mayer L; Hunter WL, Anti-tumor efficacy and biodistribution of intravenous polymeric micellar paclitaxel. *Anti-Cancer Drug* 8, 696-701 (1997).

82. Kim SC; Kim DW; Shim YH; Bang JS; Oh HS; Wan Kim S; Seo MH, In vivo evaluation of polymeric micellar paclitaxel formulation: toxicity and efficacy. *J Control Release* 72, 191-202 (2001).

83. Le Garrec D; Gori S; Luo L; Lessard D; Smith DC; Yessine MA; Ranger M; Leroux JC, Poly(N-vinylpyrrolidone)-block-poly(D,L-lactide) as a new polymeric solubilizer for hydrophobic anticancer drugs: in vitro and in vivo evaluation. *J Control Release* 99, 83-101 (2004).

84. Hamaguchi T; Matsumura Y; Suzuki M; Shimizu K; Goda R; Nakamura I; Nakatomi I; Yokoyama M; Kataoka K; Kakizoe T, NK105, a paclitaxel-incorporating micellar nanoparticle formulation, can extend in vivo antitumour activity and reduce the neurotoxicity of paclitaxel. *Brit J Cancer* 92, 1240-1246 (2005).

85. Liggins RT; Burt HM, Polyether-polyester diblock copolymers for the preparation of paclitaxel loaded polymeric micelle formulations. *Adv Drug Deliver Rev* 54, 191-202 (2002).

86. Kim TY; Kim DW; Chung JY; Shin SG; Kim SC; Heo DS; Kim NK; Bang YJ, Phase I and pharmacokinetic study of Genexol-PM, a cremophor-free, polymeric micelle-formulated paclitaxel, in patients with advanced malignancies. *Clin Cancer Res* 10, 3708-3716 (2004).

87. Matsumura Y; Hamaguchi T; Ura T; Muro K; Yamada Y; Shimada Y; Shirao K; Okusaka T; Ueno H; Ikeda M; Watanabe N, Phase I clinical trial and pharmacokinetic evaluation of NK911, a micelle-encapsulated doxorubicin. *Brit J Cancer* 91, 1775-1781 (2004).

88. Kato K; Hamaguchi T; Yasui H; Okusaka T; Ueno H; Ikeda M; Shirao K; Shimada Y; Nakahama H; Muro K; Matsumura Y, Phase I study of NK105, a paclitaxel-incorporating micellar nanoparticle, in patients with advanced cancer. *J Clin Oncol* 24, 2018 (2006).

89. Lee KS; Chung HC; Im SA; Park YH; Kim CS; Kim SB; Rha SY; Lee MY; Ro J, Multicenter phase II trial of Genexol-PM, a Cremophor-free, polymeric micelle formulation of paclitaxel, in patients with metastatic breast cancer. *Breast Cancer Res Tr*, (2007).

90. Zhang JX; Yan MQ; Li XH; Qiu LY; Li XD; Li XJ; Jin Y; Zhu KJ, Local delivery of indomethacin to arthritis-bearing rats through polymeric micelles based on amphiphilic polyphosphazenes. *Pharm Res*, In Press (2007).
91. Beauchesne PR; Chung NS; Wasan KM, Cyclosporine A: a review of current oral and intravenous delivery systems. *Drug Dev Ind Pharm* 33, 211-220 (2007).
92. Ehrlich A; Booher S; Becerra Y; Borris DL; Figg WD; Turner ML; Blauvelt A, Micellar paclitaxel improves severe psoriasis in a prospective phase II pilot study. *J Am Acad Dermatol* 50, 533-540 (2004).
93. Kwon GS, Polymeric micelles for delivery of poorly water-soluble compounds. *Crit Rev Ther Drug* 20, 357-403 (2003).
94. Lavasanifar A; Samuel J; Kwon GS, The effect of fatty acid substitution on the in vitro release of amphotericin B from micelles composed of poly(ethylene oxide)-block-poly(N-hexyl stearate-aspartamide). *J Control Release* 79, 165-172 (2002).
95. Yi Y; Yoon HJ; Kim BO; Shim M; Kim SO; Hwang SJ; Seo MH, A mixed polymeric micellar formulation of itraconazole: Characteristics, toxicity and pharmacokinetics. *J Control Release* 117, 59-67 (2007).
96. Kwon G; Suwa S; Yokoyama M; Okano T; Sakurai Y; Kataoka K, Enhanced tumor accumulation and prolonged circulation times of micelle-forming poly (ethylene oxide-aspartate) block copolymer-adriamycin conjugates. *J Control Release* 29, 17-23 (1994).
97. Burt HM; Zhang X; Toleikis P; Embree L; Hunter WL, Development of copolymers of poly(D,L-lactide) and methoxypolyethylene glycol as micellar carriers of paclitaxel. *Colloid Surface B* 16, 161-171 (1999).
98. Shuai X; Merdan T; Schaper AK; Xi F; Kissel T, Core-cross-linked polymeric micelles as paclitaxel carriers. *Bioconjugate Chem* 15, 441-448 (2004).
99. Iijima M; Nagasaki Y; Okada T; Kato M; Kataoka K, Core-polymerized reactive micelles from heterotechelic amphiphilic block copolymers. *Macromolecules* 32, 1140-1146 (1999).
100. Kim J; Emoto K; Iijima M; Nagasaki Y; Aoyagi T; Okano T; Sakurai Y; Kataoka K, Core-stabilized polymeric micelle as potential drug carrier: increased solubilization of taxol. *Polym Advan Technol* 10, 647-654 (1999).
101. Nadeau V; Leclair G; Sant S; Rabanel J-M; Quesnel R; Hildgen P, Synthesis of new versatile functionalized polyesters for biomedical applications. *Polymer* 46, 11263-11272 (2005).
102. Parrish B; Quansah JK; Emrick T, Functional polyesters prepared by polymerization of α-allyl(valerolactone) and its copolymerization with ε–caprolactone and δ-valerolactone. *J Polym Sci Pol Chem* 40, 1983-1990 (2002).
103. Torchilin VP, Targeted polymeric micelles for delivery of poorly soluble drugs. *Cell Mol Life Sci* 61, 2549-2559 (2004).
104. Torchilin VP; Lukyanov AN; Gao Z; Papahadjopoulos-Sternberg B, Immunomicelles: targeted pharmaceutical carriers for poorly soluble drugs. *P Natl Acad Sci USA* 100, 6039-6044 (2003).
105. Jeong YI; Seo SJ; Park IK; Lee HC; Kang IC; Akaike T; Cho CS, Cellular recognition of paclitaxel-loaded polymeric nanoparticles composed of poly(gamma-benzyl L-glutamate) and poly(ethylene glycol) diblock copolymer endcapped with galactose moiety. *Int J Pharm* 296, 151-161 (2005).
106. Vinogradov S; Batrakova E; Li S; Kabanov A, Polyion complex micelles with protein-modified corona for receptor-mediated delivery of oligonucleotides into cells. *Bioconjugate Chem* 10, 851-860 (1999).
107. Xiong XB; Mahmud A; Uludag H; Lavasanifar A, Conjugation of arginine-glycine-aspartic acid peptides to poly(ethylene oxide)-b-poly(epsilon-caprolactone) micelles for enhanced intracellular drug delivery to metastatic tumor cells. *Biomacromolecules* 8, 874-884 (2007).
108. Park EK; Kim SY; Lee SB; Lee YM, Folate-conjugated methoxy poly(ethylene glycol)/poly(epsilon-caprolactone) amphiphilic block copolymeric micelles for tumor-targeted drug delivery. *J Control Release* 109, 158-168 (2005).
109. Wang Y; Yu L; Han L; Sha X; Fang X, Difunctional Pluronic copolymer micelles for paclitaxel delivery: Synergistic effect of folate-mediated targeting and Pluronic-mediated overcoming multidrug resistance in tumor cell lines. *Int J Pharm* 337, 63-73 (2007).
110. Xu Z; Gu W; Huang J; Sui H; Zhou Z; Yang Y; Yan Z; Li Y, In vitro and in vivo evaluation of actively targetable nanoparticles for paclitaxel delivery. *Int J Pharm* 288, 361-368 (2005).
111. Nishioka Y; Yoshino H, Lymphatic targeting with nanoparticulate system. *Adv Drug Deliver Rev* 47, 55-64 (2001).

112. Hawley AE; Illum L; Davis SS, Lymph node localisation of biodegradable nanospheres surface modified with poloxamer and poloxamine block co-polymers. *FEBS Lett* 400, 319-323 (1997).

113. Illum L; Church AE; Butterworth MD; Arien A; Whetstone J; Davis SS, Development of systems for targeting the regional lymph nodes for diagnostic imaging: in vivo behaviour of colloidal PEG-coated magnetite nanospheres in the rat following interstitial administration. *Pharm Res* 18, 640-645 (2001).

114. Trubetskoy VS, Polymeric micelles as carriers of diagnostic agents. *Adv Drug Deliver Rev* 37, 81-88 (1999).

115. Torchilin VP, PEG-based micelles as carriers of contrast agents for different imaging modalities. *Adv Drug Deliver Rev* 54, 235-252 (2002).

116. Shim J; Seok Kang H; Park WS; Han SH; Kim J; Chang IS, Transdermal delivery of mixnoxidil with block copolymer nanoparticles. *J Control Release* 97, 477-484 (2004).

117. Vogt A; Combadiere B; Hadam S; Stieler KM; Lademann J; Schaefer H; Autran B; Sterry W; Blume-Peytavi U, 40 nm, but not 750 or 1,500 nm, nanoparticles enter epidermal CD1a+ cells after transcutaneous application on human skin. *J Invest Dermatol* 126, 1316-1322 (2006).

118. Alvarez-Roman R; Naik A; Kalia YN; Guy RH; Fessi H, Skin penetration and distribution of polymeric nanoparticles. *J Control Release* 99, 53-62 (2004).

119. Cevc G, Lipid vesicles and other colloids as drug carriers on the skin. *Adv Drug Deliver Rev* 56, 675-711 (2004).

120. Zeng XM; Martin GP; Marriott C, The controlled delivery of drugs to the lung. *Int J Pharm* 124, 149-164 (1995).

121. Pandey R; G.K.Khuller, Antitubercular inhaled therapy: opportunities, progress and challenges. *J Antimicrob Chemoth* 55, 430-435 (2005).

122. Cryan S-A, Carrier-based strategies for targeting protein and peptide drugs to the lungs. *AAPS J* 7, E20-E41 (2005).

Appendices

Samenvatting in het Nederlands

Inleiding

De recente ontwikkelingen in op het gebied van de chemie, biotechnologie en moderne screenings-methodes ('high-throughput screening') hebben geleid tot de ontdekking en selectie van een groot aantal potentieel werkzame stoffen (farmaca). Echter, een goede activiteit is niet de enige voorwaarde voor een succesvol geneesmiddel, en tijdens de ontwikkeling van een veelbelovend kandidaat-farmacon tot een klinisch[a] werkzaam en bruikbaar product moeten vaak vele hindernissen worden overwonnen. Enerzijds kunnen deze gerelateerd zijn aan de formulering[b] van het geneesmiddel. De formulering tot een product dat geschikt is voor parenterale toediening[c] kan bijvoorbeeld worden bemoeilijkt door een slechte oplosbaarheid van het farmacon in water, of een geringe stabiliteit. Anderzijds kan het geneesmiddel een lage therapeutische index[d] hebben. Snelle eliminatie uit het lichaam en/of het of onvoldoende bereiken van de plek van werking kunnen leiden tot een lage effectiviteit, terwijl distributie naar gezonde organen en weefsels ernstige bijwerkingen tot gevolg kan hebben.

Deze ongunstige eigenschappen kunnen worden verhuld door het farmacon in te sluiten in nanodeeltjes, en de laatste jaren is er vooral veel onderzoek gedaan naar zelf-assemblerende systemen. Deze systemen bestaan uit zogenoemde amfifiele moleculen, zoals blok-copolymeren,[e] die bestaan uit een hydrofoob ('watervrezend') en een hydrofiel ('waterlievend') gedeelte. Amfifiele blok-copolymeren kunnen in water vele structuren vormen, zoals vesicles en micellen. Vesicles zijn blaasjes met een waterige kern omgeven door een polymeren bilaag, waarin hydrofiele farmaca kunnen worden ingesloten. Micellen bestaan uit een hydrofobe kern en een hydrofiele schil, en kunnen worden beladen met hydrofobe, slecht water-oplosbare farmaca. Polymeren vesicles en micellen met een grootte tot enkele tientallen nanometers (nanoscopisch) zijn interessante systemen voor de doelgerichte aflevering van respectievelijk hydrofiele en hydrofobe geneesmiddelen. Hun kleine afmeting en hydrofiele oppervlak zijn aantrekkelijke eigenschappen om lange circulatietijden te verkrijgen na intraveneuze toediening.[f] Bovendien kunnen ze gebruik maken van het feit dat in

[a] *in de kliniek*
[b] *samenstelling; het maken van een samenstelling*
[c] *door middel van een injectie*
[d] *verhouding tussen de toxische en de effectieve dosis*
[e] Gr. *poly = veel, meros = deel; een polymeer is een molecuul bestaande uit een keten van identieke delen (monomere eenheden); een blok-copolymeer bestaan uit verschillende type eenheden, die gerangschikt zijn in blokken.*
[f] *in de ader*

bepaalde pathologische[g] gebieden, zoals tumoren of ontstoken weefsel, de bloedvaten 'lek' zijn. De nanodeeltjes kunnen hier de bloedbaan verlaten en specifiek ophopen op de plek van werking. Een andere gunstige eigenschap van deze systemen is hun bereidingsgemak, omdat ze spontaan gevormd worden in water. Daarnaast biedt de variatie in de samenstelling van (semi-)synthetische polymeren de mogelijkheid om de eigenschappen van de nanodeeltjes te optimaliseren en de afgifte van het farmacon te sturen.

Poly(ethylene glycol) (PEG)-*b*-polyesters, zoals PEG-*b*-polylactaat (PLA) en PEG-*b*-polycaprolacton (PCL) zijn amfifiele blok-copolymeren, die uitgebreid bestudeerd zijn voor de ontwikkeling van zelf-assemblerende systemen voor de aflevering van farmaca. Deze polymeren zijn biocompatibel[h] en bovendien is het polyester-blok bioafbreekbaar. Hierdoor kan het farmacon gecontroleerd worden afgegeven en kan ophoping van het polymeer na herhaalde toediening worden voorkomen.

In dit proefschrift zijn goed-gedefinieerde amfifiele laag-moleculaire PEG-oligoësters gebruikt. De effecten van de samenstelling van het blok-oligomeer[i] op de zelf-assemblerende eigenschappen zijn in detail bestudeerd, en hun toepasbaarheid voor de ontwikkeling van nieuwe nanoscopische geneesmiddeldragers is geëvalueerd.

Polymeren geneesmiddeldragers

In **hoofdstuk één** wordt een aantal nanoscopische polymeren systemen besproken, die gebruikt worden voor de formulering van geneesmiddelen, waaronder zelf-assemblerende systemen. Verder worden de bereidingsmethodes van dit soort systemen beschreven, evenals de factoren die bepalend zijn voor het type structuur dat wordt gevormd (zoals micellen of vesicles). Vervolgens is het doel en opzet van dit proefschrift uiteengezet.

Hoofdstuk twee bespreekt polymeren micellen in meer detail en presenteert een uitgebreid literatuuroverzicht van de vele mogelijkheden van deze systemen voor de doelgerichte aflevering van farmaca. Terwijl hydrofobe geneesmiddelen vaak lastig te formuleren zijn door hun lage water-oplosbaarheid, zijn polymeren micellen hier bij uitstek geschikt voor. De ideale polymeren micel heeft na intraveneuze toediening een lange circulatietijd in de bloedbaan, zonder voortijdig verlies van het ingesloten farmacon. Hierdoor kan efficiënte accumulatie in het doel orgaan (bijv. de

[g] *ziekelijk, afwijkend*
[h] *verenigbaar met biologische systemen (i.e. zonder toxische of schadelijke effecten)*
[i] Gr. *oligo = weinig, meros = deel; vergelijkbaar met een polymeer, maar met een kleiner aantal eenheden*

tumor) worden bereikt. Vaak worden dit soort 'lichaamsvreemde' deeltjes door het immuunsysteem herkend, wat leidt tot snelle eliminatie uit het lichaam en een korte verblijfsduur in de bloedbaan. Een efficiënte hydrofiele oppervlakte-coating, en een klein (submicron) formaat van de geneesmiddeldrager kunnen wel resulteren in lange circulatietijden. In polymeren micellen wordt meestal poly(ethylene glycol) (PEG) gebruikt als hydrofiel, schil-vormend blok, waarbij de dikte, de dichtheid en de flexibiliteit van de schil van belang zijn voor de gewenste lange circulatietijd. Daarnaast zijn er verschillende strategieën beschreven om de polymeren micellen te stabiliseren, door verhoogde fysische[j] interacties en/of covalente bindingen[k] tussen de polymeren waaruit de micel bestaat, en door de structuur van de micellaire kern en het farmacon beter op elkaar af te stemmen. Op deze manieren kan het vroegtijdig uiteenvallen en/of verlies van het farmacon worden voorkomen. Zodra de beladen micellen hun plek van werking hebben bereikt, moet het farmacon worden afgegeven, bij voorkeur op een gecontroleerde manier. In de literatuur zijn verschillende zogenoemde 'stimulusgevoelige' micellen beschreven, die uiteenvallen onder invloed van licht, een verandering in temperatuur of pH,[l] of door tijd- of plaats-specifieke afbraak.

Zelf-assemblerende PEG-oligoësters

In **hoofdstuk drie** zijn de zelf-assemblerende eigenschappen van mPEG-*b*-oligo(L-lactaten) (OLA) onderzocht. Na synthese zijn deze blok-oligomeren gezuiverd door middel van een scheidingstechniek (zogenoemde 'preparatieve HPLC'), om producten met een monodispers[m] hydrofoob blok te verkrijgen (PEG-molecuulgewicht van 350, 550 of 750 Da, OLA-keten van 4, 6, 8 of 10 eenheden). Boven een oligomeerconcentratie van 0.4-1 mg/mL (de zogenoemde kritische aggregatie concentratie, KAC), werden door hydratatie van een oligomeerfilm nanodeeltjes met een straal van 130-300 nm gevormd. Deze deeltjes bleken nano-aggregaten te zijn, met een hoog watergehalte, wat vermoedelijk kan worden toegeschreven aan de mengbaarheid van de beide blokken van het oligomeer, PEG en OLA. De in deze studie aangetoonde zelf-emulgerende eigenschappen van PEG-*b*-OLA, in combinatie met hun biocompatibiliteit en afbreekbaarheid, zijn aantrekkelijke eigenschappen voor farmaceutische toepassing. Het is echter wel van belang dat na intraveneuze toediening de oligomeerconcentratie in bloed boven de KAC blijft, om te voorkomen dat de nanodeeltjes snel uiteenvallen. Dat betekent dat, gezien hun hoge KAC, relatief grote hoeveelheden van PEG-*b*-OLA geïnjecteerd moeten worden, en het

[j] fysica = natuurkunde
[k] chemische binding, binding tussen atomen
[l] zuurgraad
[m] in een monodispers polymeer zijn alle ketens even lang (tegenstelling: polydispers)

is duidelijk dat systemen met een lagere KAC de voorkeur hebben. Daarom zijn in **hoofdstuk vier** de zelf-assemblerende eigenschappen bestudeerd van blok-oligomeren met een meer hydrofoob oligoësterblok, oligo(ε-caprolacton) (OCL). De bestudeerde oligomeren bestonden uit een PEG-blok van 750 Da en 1-7 caprolacton-eenheden. Het einde van de OCL-keten bestond uit een hydroxyl (OH) of een sterk hydrofobe, aromatische groep[n] (benzoyl of naphthoyl). De KAC van deze oligomeren was inderdaad een stuk lager dan die van PEG-*b*-OLA. De laagste waarden werden gemeten voor de langste OCL-ketens, en de aanwezigheid van een aromatische eindgroep resulteerde zelfs in waarden van 3 µg/mL. Vergelijkbare waarden zijn gevonden voor PEG-PCL (met langere hydrofobe caprolacton-ketens). Formuleringen gebaseerd op PEG-PCL, die succesvol zijn toegepast *in vivo*,[o] zijn al bekend zijn uit de literatuur. Daarnaast waren de beide blokken van PEG-*b*-OCL oligomeren, in tegenstelling tot PEG-*b*-OLA, niet mengbaar. In water vormden de PEG-*b*-OCL oligomeren zeer kleine micellen, met een diameter van 8-15 nm, afhankelijk van de grootte van het hydrofobe blok. Deze kleine afmeting is mogelijk gunstig voor de penetratie van tumoren *in vivo*. Naast de KAC is ook het temperatuurgevoelige gedrag in water een belangrijke stabiliteitsbepalende factor. Bij lage temperaturen kan een zogenoemd Krafft-punt optreden, waar de oplosbaarheid van het oligomeer in water gelijk is aan de KAC. Beneden deze temperatuur slaat het oligomeer neer. Aan de andere kant kunnen hoge temperaturen leiden tot de (gedeeltelijke) verwijdering van de beschermende watermantel die aanwezig is om de micellen, waardoor de micellen gaan aggregeren ('samenklonteren'). Dit wordt waargenomen als een zogenoemd troebelingspunt. Gezien hun toepassing bij 37 °C en hun bereiding en opslag bij kamertemperatuur of in de koelkast, hebben oligomeren met een Krafft-punt onder de 4 °C en een troebelingspunt boven de 37 °C de voorkeur. De meeste PEG-*b*-OCL oligomeren voldoen hieraan. Deze zijn meer dan een maand stabiel bij kamertemperatuur en ten minste twee weken bij 37 °C. Door de introductie van een aromatische eindgroep kon een optimale combinatie van een lage KAC en een gunstige temperatuurgevoeligheid worden bereikt, en dus een hoge fysische stabiliteit van de micellen.

De chemische stabiliteit van deze PEG-*b*-OCL micellen is het onderwerp van **hoofdstuk vijf**. Afbraakstudies toonden aan dat het verbreken van de esterbindingen in de OCL-keten leidde tot het uiteenvallen van de micellen, na ongeveer 1,5 afbraak-halfwaardetijd.[p] De geschatte halfwaardetijd van PEG-*b*-OCL micellen bij fysiologische[q] pH en temperatuur (pH 7.4, 37 °C) was in de orde van jaren, en chemische afbraak van de micellen speelt waarschijnlijk dus nauwelijks een rol *in vivo*. Het is

[n] Scheik. *een molecuul met een specifieke structuur die zorgt voor sterk hydrofobe eigenschappen*
[o] Lat. *in het levende organisme*
[p] *tijd waarin de beginhoeveelheid (oligomeer) tot de helft is verminderd (als gevolg van afbraak)*
[q] *fysiologie = de leer van de normale levensverschijnselen van de mens (of dier / plant)*

echter bekend dat polyesters ook kunnen worden afgebroken door enzymen[r] zoals lipase. In dit hoofdstuk is aangetoond dat ook de PEG-*b*-OCL micellen enzymatisch afbreekbaar zijn, en afhankelijk van de enzymconcentratie zijn halfwaardetijden van enkele dagen tot uren gemeten. Dit geeft aan dat ook *in vivo* het uiteenvallen van de micellen kan worden geïnduceerd door afbraak, waardoor vervolgens het ingesloten farmacon wordt afgegeven.

In **hoofdstuk zes** is de belading van PEG-*b*-OCL micellen met paclitaxel (PTX) en docetaxel (DCTX) bestudeerd. Dit zijn hydrofobe stoffen met een hoge antitumor activiteit, en de formuleringen die momenteel klinisch worden toegepast zijn respectievelijk Taxol® en Taxotere®. Deze hebben echter vele bijwerkingen, die gedeeltelijk worden toegeschreven aan de hulpstoffen in deze formuleringen, Cremophor EL®, respectievelijk polysorbaat 80. Net als in hoofdstuk vier, blijkt ook hier het positieve effect van de aanwezigheid van een aromatische eindgroep, aangezien deze essentieel was voor de stabiele belading van PEG-*b*-OCL micellen met substantiële hoeveelheden PTX of DCTX. *In vitro*[s] stabiliteitsstudies bij fysiologische pH en temperatuur (PBS, pH 7.4, 37 °C) toonden aan dat PTX gedurende 8 uur werd vastgehouden in micellen bestaande uit PEG-*b*-OCL met een benzoyl eindgroep, waarna afgifte plaatsvond door 'lekken' van het farmacon uit de nog intacte micellen. De aanwezigheid van albumine, een belangrijk eiwit in bloed, had hier geen invloed op. De *in vitro* toxiciteit van de PTX- of DCTX- beladen micellen op tumorcellen was vergelijkbaar met het effect van Taxol® en Taxotere®. De onbeladen micellen zijn echter veel minder toxisch dan Cremophor EL®, wat een belangrijk voordeel is met het oog op de mogelijke bijwerkingen *in vivo*.

Toekomstperspectieven

Het onderzoek in dit proefschrift laat zien dat ook laag-moleculaire blok-oligomeren kunnen worden gebruikt voor de ontwikkeling van geneesmiddel-afleversystemen. De introductie van een aromatische eindgroep zorgde niet alleen voor een betere fysische stabiliteit, maar ook voor betere belading met farmaca. Het concept van de introductie van aromatische groepen kan nog verder worden uitgewerkt door meerdere groepen in de oligomeer-keten te introduceren, waardoor mogelijk een nog lagere KAC en hogere en/of meer stabiele belading kan worden bereikt.

[r] *katalysator die bepaalde processen (in het organisme) veroorzaakt of bevordert*
[s] Lat. *in glas, d.w.z. in een reageerbuis, op de labtafel*

In een inleidende *in vivo* studie in tumor-dragende muizen (**hoofdstuk zeven**) zijn geen verlengde circulatietijden en/of verhoogde tumoropname gevonden na intraveneuze injectie van PTX geformuleerd in PEG-*b*-OCL micellen, in vergelijking met Taxol®. Dit wijst erop dat deze micellen het farmacon solubiliseren,[t] maar dat van een echt transportsysteem nog geen sprake is, ondanks de toegepaste stabilisatie door de benzoyl eindgroep. Toch hebben deze micellen verschillende eigenschappen die gunstig kunnen zijn voor de formulering van hydrofobe antitumor geneesmiddelen, zoals een hoge belading, hun bioafbreekbaarheid, en lage toxiciteit *in vitro*. Bovendien zijn deze micellen misschien zeer geschikt voor andere toedieningsroutes, waar minder problemen met de stabiliteit zijn te verwachten, zoals subcutane injectie[u] of inhalatie. Voor de toepassing van deze micellen als transportsysteem na intraveneuze injectie is echter verdere stabilisatie nodig. Naast verlaging van de KAC en verbetering van de belading, kan de stabiliteit van deze micellen mogelijk geoptimaliseerd worden door ze te crosslinken door middel van covalente bindingen.

Conclusie

De PEG-oligoësters die in dit proefschrift zijn bestudeerd, vormen een interessante klasse van amfifiele moleculen met aantrekkelijke eigenschappen voor farmaceutische toepassingen, gezien hun bioafbreekbaarheid en lage toxiciteit. Bovendien kan hun moleculaire samenstelling goed worden gedefiniëerd, en zijn er talrijke mogelijkheden om de structuren te variëren en verder te optimaliseren. Kortom, PEG-oligoësters zijn veelbelovende structuren voor de ontwikkeling van geneesmiddel-afleversystemen, met diverse therapeutische toepassingen.

[t] *in (waterige) oplossing brengen*
[u] *onder de huid*

Abbreviations

ACN	acetonitrile
1,8-ANS	8-anilino-1-naphthalene sulfonic acid magnesium salt
AUC	area under the curve
BSA-SepCL-4B	albumin immobilised on crosslinked 4% beaded agarose
Bz	benzoyl (end group)
CAC	critical aggregation concentration
CCL	core crosslinked micelles
$CDCl_3$	deuterated chloroform
CL	(ε-)caprolactone
CMC	critical micelle concentration
CMT	critical micelle temperature
CP	Cp = cloud point
CrEL®	Cremophor EL® = polyoxyethylated castor oil
Cryo-TEM	cryogenic transmission electron microscopy
CT	computed tomography
d	doublet (NMR)
D_2O	deuterated water
DCM	dichloromethane
DCTX	docetaxel
Dex	dextran
DLS	dynamic light scattering
DMEM	Dulbecco's modified Eagle's medium
DMF	dimethylformamide
DOX	doxorubicin
DP	degree of polymerisation
DSC	differential scanning calorimetry
DSPE	distearoyl phosphatidyl ethanolamine
equiv	equivalent
ESI-MS	electrospray ionisation mass spectrometry
EtOH	ethanol
FDA	food and drug administration
F_H	hydrophilic molecular weight fraction
F_L	lipophilic molecular weight fraction
ΔG	Gibbs free energy
GPC	gel permeation chromatography
ΔH	(melting) enthalpy
HES	hydroxyethyl starch
(RP) HPLC	(reversed phase) high performance liquid chromatography

IC_{50}	half maximal inhibitory concentration
% ID	percentage of the injected dose
(N)IR	(near) infrared (light)
iv	intravenous
k_{benz}	reaction rate constant of benzyl ester degradation
k_{end}	reaction rate constant of ester degradation at the hydroxyl terminus
K_m	Michaelis-Menten constant
k_{obs}	$k_{observed}$ = reaction rate constant
Kp	Krafft point
k_r	reaction rate constant of ester degradation in the OCL chain
KAC	kritische aggregatie concentratie (NL)
m	multiplet (NMR)
M/I ratio	monomer/initiator ratio
m/z	mass/charge ratio (ESI-MS)
MDR	multi drug resistant
MEE	2-(2-methoxyethoxy) ethanol
min	minute(s)
M_n	number average molecular weight
MRI	magnetic resonance imaging
MTD	maximum tolerated dose
MW	molecular weight
$M_{w(NP)}$	weight average molecular weight (of the nanoparticles)
N_{agg}	aggregation number
NCE	new chemical entity
NMR	nuclear magnetic resonance
NOESY	nuclear overhauser enhancement spectroscopy
Np	naphthoyl (end group)
OCL	oligo(ε-caprolactone)
OLA	oligo(L-lactate)
$[Oligo]_{total}$	$[Oligomer]_{total}$ = total oligomer concentration
P(AAm)	poly(acryl amide)
P(Asp)	poly(aspartate) = poly(aspartic acid)
P4VP	poly(4-vinyl pyridine)
PAA	poly(acrylic acid)
PBA	poly(*tert*-butyl acrylate)
PBD	poly(butadiene)
PBLA	poly(β-benzyl L-aspartate)
$PBLA_{mod}$	$PBLA_{modified}$ = modified poly(β-benzyl L-aspartate)
PBLG	poly(γ-benzyl L-glutamate)
PBS	phosphate buffered saline

PBTMC	poly(5-benzyloxy-trimethylene carbonate)
PCL	poly(ε-caprolactone)
PDEA	poly(2-(diethylamino) ethyl methacrylate)
PDI	polydispersity index (particle size distribution)
PDLLA	poly(DL-lactate)
PDMAAm	poly(N,N-dimethyl acrylamide)
PDMAEMA	poly(N,N-dimethylamino-2-ethyl methacrylate)
PDPA	poly(diisopropylamino ethyl methacrylate)
PE	phosphatidyl ethanolamine
PEA	phenylalanine
(m)PEG	(methoxy) poly(ethylene glycol)
PEI	poly(ethylene imine)
PEO	poly(ethylene oxide)
PEtOx	poly(2-ethyl-2-oxazoline)
PEVP	poly(N-ethyl-4-vinylpyridinium)
PGA	poly(γ-glutamic acid)
PGMA	poly(glycerol monomethacrylate)
PHB	poly(3-hydroxybutyrate)
$PHEMA_{Lac}$	poly(N-(2-hydroxyethyl) methacrylamide-oligolactate)
$PHEMAm_{Lac}$	poly(N-(2-hydroxyethyl) methacrylamide-oligolactate)
PHIS	poly(L-histidine)
PHPMA	poly(N-(2-hydroxypropyl) methacryl amide)
$PHPMA_{Lac}$	poly(N-(2-hydroxylpropyl) methacrylamide-oligolactate)
PHPMAmDL	poly(N-(2-hydroxylpropyl) methacrylamide dilactate)
$PHPMAm_{Lac}$	poly(N-(2-hydroxylpropyl) methacrylamide-oligolactate)
PIC	polyion complex (micelle)
P*i*PrOx	poly(2-isopropyl-2-oxazoline)
PL	phospholipid
PLA	polylactate = poly(lactic acid)
PLGA	poly(lactic-*co*-glycolic acid)
PMA	poly(methyl acrylate) = poly(methacrylic acid)
PMEMA	poly(2-(N-mopholino)ethyl methacrylate)
PMMA	poly(methyl methacrylate)
PMPC	poly(2-(methacryloyloxy) ethyl phosphorylcholine)
PNIPAAm	poly(N-isopropyl acrylamide)
POE	poly(ortho ester)
P(Lys)	poly(L-lysine)
PPO	poly(propylene oxide)
PS	poly(styrene)
PSD	poly(methacryloyl sulfadimethoxine)

PSO	poly(styrene oxide)
PSS	poly(styrene sulfonate)
PTMC	poly(trimethylene carbonate)
PTX	paclitaxel
PVA	poly(vinyl alcohol)
PVP	poly(N-vinyl pyrrolidone)
q	quartet (NMR)
QD	quantum dot
RES	reticuloendothelial system
R_g	radius of gyration
R_h	hydrodynamic radius
s	second(s)
s	singlet (NMR)
S	substrate concentration
SD	standard deviation
SDS	sodium dodecyl sulphate
SLS	static light scattering
$SnOct_2$	tin(II) bis(2-etylhexanoate) = stannous octoate
t	triplet (NMR)
$t_{1/2}$	half-life (of degradation)
TEA	triethylamine
TFA	trifluoro acetic acid
T_g	glass transition temperature
T_m	melting temperature
TUV	tunable UV/VIS (detector)
Tw80	Tween 80 = polysorbate 80
UPLC®	ultra performance liquid chromatography
UV	ultraviolet (light)
% (v/v)	volume percentage
V	(enzymatic) degradation rate
VIS	visible (light)
V_{max}	maximum enzymatic degradation rate at high substrate concentration
V_{mic}	$V_{micelle}$ = enzymatic degradation rate of the self-assembled oligomers
V_{total}	overall enzymatic degradation rate
V_{uni}	V_{unimer} = enzymatic degradation rate of unimers in solution
vs	versus
% (w/w)	weight percentage
Z_{ave}	*Z*-average hydrodynamic diameter
ρ_{NP}	density of the nanoparticles
τ_m	mixing time (NOESY)

Curriculum Vitae

Date of birth	January 30th, 1978
Place of birth	Waalwijk, The Netherlands

Education

1990-1996	Grammar school, Dr. Mollercollege, Waalwijk (NL)
1996-2000	Pharmacy, Utrecht University (NL), cum laude. Participation in the Honours Programme of the Faculty of Pharmaceutical Sciences, Utrecht University (NL). Awarded by the Royal Dutch Pharmacy Association (KNMP) as best undergraduate student of 2001 in Utrecht.
2000-2003	Post-graduate Pharmacy, Utrecht University (NL), licensed pharmacist.

Work Experience

02/1999 - 08/1999	Research project at the Dpt. of Nuclear Medicine, UMC St. Radboud, Nijmegen (NL). Subject: Pharmacokinetics of PEG-liposomes.
09/1999 - 12/1999	Essay at the Dpt. of Pharmaceutics, Utrecht University (NL). Subject: Therapeutic potency of angiogenic markers in rheumatoid arthritis.
10/1999 - 12/1999	Internship: Dpt. of Regulatory Affairs, N.V. Organon, Oss (NL). Training in different pharmacies: • Apotheek Buys (community), Utrecht (NL). • VU University Medical Center (hospital), Amsterdam (NL). • Oxford Radcliffe Hospitals (hospital), Oxford (UK).
03/2003-09/2007	Ph.D. student at OctoPlus N.V., Leiden / Dpt. of Pharmaceutics, Utrecht University, Utrecht (NL). Promotors: Prof. Dr. Ir. W.E. Hennink and Prof. Dr. D.J.A. Crommelin. Title: Preparation and *in vivo* performance of novel biodegradable oligomeric nanoparticles for drug delivery.

Curriculum Vitae

Geboortedatum	30 januari, 1978
Geboorteplaats	Waalwijk

Onderwijs

1990-1996	Gymnasium, Dr. Mollercollege, Waalwijk (NL)
1996-2000	Farmacie, Universiteit Utrecht (NL), cum laude. Deelname aan het Excellent Tracé van de Faculteit Farmaceutische Wetenschappen, Universiteit Utrecht (NL). Winnaar KNMP-prijs 2001, voor beste doctoraal student van het jaar in Utrecht.
2000-2003	Post-doctoraal Farmacie, Universiteit Utrecht (NL), afgesloten met het behalen van het apothekers-diploma.

Werkervaring

02/1999 - 08/1999	Onderzoeksproject bij de afdeling Nucleare Geneeskunde, UMC St. Radboud, Nijmegen (NL). Onderwerp: Farmacokinetiek van PEG-liposomen.
09/1999 - 12/1999	Scriptie bij de vakgroep Biofarmacie en Farmaceutische Technologie, Universiteit Utrecht (NL). Onderwerp: Therapeutische potentie van anti-antiogene markers in rheumatoïde artitis.
10/1999 - 12/1999	Stage bij de Registratie-afdeling van N.V. Organon, Oss (NL) Stage in verschillende apotheken: • Apotheek Buys, Utrecht (NL). • VU medisch centrum, Amsterdam (NL). • Oxford Radcliffe Hospitals, Oxford (UK).
03/2003-09/2007	AIO bij OctoPlus N.V., Leiden / vakgroep Biofarmacie en Farmaceutische Technologie, Universiteit Utrecht (NL). Promotoren: Prof. Dr. Ir. W.E. Hennink en Prof. Dr. D.J.A. Crommelin. Titel: Bereiding en *in vivo* evaluatie van nieuwe biodegradeerbare oligomeren nanodeeltjes voor de aflevering van geneesmiddelen.

List of publications

Publications

Carstens MG; de Jong PHJLF; van Nostrum CF; Kemmink J; Verrijk R; De Leede LGJ; Crommelin DJA; Hennink WE, Biodegradable oligomeric micelles for novel taxane formulations. *Submitted for publication.*

Carstens MG; Rijcken CJF; van Nostrum CF; Hennink WE, Pharmaceutical micelles: combining longevity, stability and stimuli-sensitivity. *Submitted for publication.*

Carstens MG; van Nostrum CF; Verrijk R; de Leede LGJ; Crommelin DJA; Hennink WE, A mechanistic study on the chemical and enzymatic degradation of PEG-oligo(ε-caprolactone) micelles. *J Pharm Sci,* In Press (2007).

Carstens MG; Bevernage JJL; van Nostrum CF; van Steenbergen MJ; Flesch FM; Verrijk R; de Leede LGJ; Crommelin DJA; Hennink WE, Small oligomeric micelles based on end group modified mPEG-oligocaprolactone with monodisperse hydrophobic blocks. *Macromolecules* 40, 116-122 (2007).

Carstens MG; van Nostrum CF; Ramzi A; Meeldijk JD; Verrijk R; de Leede LGJ; Crommelin DJA; Hennink WE, Poly(ethylene glycol)-oligolactates with monodisperse hydrophobic blocks: preparation, characterization, and behavior in water. *Langmuir* 21, 11446-11454 (2005).

Romberg B; Oussoren C; Snel CJ; **Carstens MG**; Hennink WE; Storm G, Pharmacokinetics of poly(hydroxyethyl-L-asparagine)-coated liposomes is superior over that of PEG-coated liposomes at low lipid dose and upon repeated administration. *BBA - Biomembranes* 1768, 737-743 (2007).

Carstens MG; Romberg B; Laverman P; Boerman OC; Oussoren C; Storm G, Observations on the disappearance of the stealth property of PEGylated liposomes. Effects of lipid dose and dosing frequency. In: *Liposome Technology*, 3rd ed. (G. Gregoriadis, Ed.), CRC press: London, Vol. III, p 79-93 (2006).

Laverman P; **Carstens MG**; Boerman OC; Dams ET; Oyen WJ; van Rooijen N; Corstens FH; Storm G, Factors affecting the accelerated blood clearance of polyethylene glycol-liposomes upon repeated injection. *J Pharmacol Exp Ther* 298, 607-612 (2001).

Laverman P; **Carstens MG**; Storm G; Moghimi SM, Recognition and clearance of methoxypoly(ethyleneglycol)2000-grafted liposomes by macrophages with enhanced phagocytic capacity. Implications in experimental and clinical oncology. *BBA - Gen Subjects* 1526, 227-229 (2001).

Selected Abstracts

Carstens MG; van Nostrum CF.; Verrijk R; de Leede LGJ; Crommelin DJA; Hennink WE, PEG-oligocaprolactone based oligomeric micelles: the effect of hydrophobic chain length and end group on self assembly and drug encapsulation. *Third Pharmaceutical Sciences World Congress*, Amsterdam, The Netherlands, April 2007. Oral presentation at the pre-satellite meeting, poster presentation at the main congress.

Carstens MG; van Nostrum CF.; Verrijk R; de Leede LGJ; Crommelin DJA; Hennink WE, PEG-oligocaprolactone based oligomeric micelles: the effect of hydrophobic chain length and end group on self assembly and drug encapsulation. Poster presentation at the *13th International Symposium on Recent Advances in Drug Delivery Systems*, Salt Lake City, USA, February 2007.

Carstens MG; van Nostrum CF; Verrijk R; de Leede LGJ; Crommelin DJA; Hennink WE, Self-assembled PEG-oligo-ε-caprolactone nanoparticles for drug delivery: the effect of hydrophobic chain length and end group. Oral presentation at the *Dutch Polymer Days*, Lunteren, The Netherlands, February 2007.

Carstens MG; van Nostrum CF; Verrijk R; de Leede LGJ; Crommelin DJA; Hennink WE, Micellization of PEG-oligocaprolactones: the effect of end group and chain length. Oral presentation at the *Autumn meeting of the Belgian-Dutch Biopharmaceutical Society*, Leiden, The Netherlands, November 2007.

Carstens MG; van Nostrum CF; Ramzi A; Meeldijk JD; Verrijk R; de Leede LGJ; Crommelin DJA; Hennink WE, Self assembly of PEG-oligolactates with monodisperse hydrophobic blocks. Poster presentation at the *33rd Annual Meeting & Exposition of the Controlled Release Society*, Vienna, Austria, July 2006.

Carstens MG; van Nostrum CF; Ramzi A; Meeldijk JD; Verrijk R; de Leede, LGJ; Crommelin DJA; Hennink WE, Self assembly of PEG-oligolactates with monodisperse hydrophobic blocks. Poster presentation at the *9th European Symposium on Controlled Drug Delivery*, Noordwijk aan Zee, The Netherlands, April 2006.

Carstens MG; van Nostrum CF; Ramzi A; Meeldijk JD; Verrijk R; de Leede LGJ; Crommelin DJA; Hennink WE, Self assembly of PEG-Oligolactates with monodisperse hydrophobic blocks. Oral presentation at the *European Workshop on Particulate Systems*, Geneva, Switzerland, March 2006.

Dankwoord / Acknowledgements

Tijd voor de laatste pagina's van dit proefschrift. En zeker niet de minste, want hoewel mijn naam de enige is op de voorkant van dit proefschrift, is dit werk ook de verdienste van de vele mensen die me geholpen, gesteund en gestimuleerd hebben tijdens mijn AIO-periode. Voor jullie dit dankwoord.

Om te beginnen wil ik graag mijn promotoren bedanken, Wim Hennink en Daan Crommelin. Jullie kennis, enthousiasme en kritische kijk waren essentieel voor de inhoud van dit proefschrift. Daarnaast hebben jullie me begeleid in mijn ontwikkeling als wetenschapper, een betere basis kan ik me niet wensen! Wim, je aanpak maakte soms onzeker, maar haalde ook een vastberadenheid in me naar boven, en heeft me erg gestimuleerd. Door je directe manier van communiceren wist ik altijd wat ik aan je had, en ik vond erg fijn dat je kamerdeur altijd openstond voor vragen, problemen en ideeën. De snelheid waarmee jij manuscripten nakijkt is ongeëvenaard, en je wist natuurlijk altijd precies de vinger op de zere plek te leggen. Daan, je bent voor mij vanaf mijn studietijd altijd een soort mentor geweest, en ik ben blij dat je als tweede promotor bij mijn eerste stap in de wetenschappelijke wereld betrokken bent. Naast je waardevolle input tijdens de projectbijeenkomsten en je altijd kritische vragen over mijn werk, wil ik je bedanken voor je vertrouwen, en voor de gesprekken over de farmaceutische wetenschap en hoe die wereld in elkaar zit.

Behalve Wim was René van Nostrum, mijn eerste co-promotor, verantwoordelijk voor de dagelijkse begeleiding tijdens mijn AIO-tijd. Rene, ook jij was altijd bereid om me te helpen om keuzes te maken tussen de vele ideeën die we weer hadden bedacht om verder te komen. Van je schrijfstijl, en vooral hoe de verhalen van de nodige 'jus' te voorzien, heb ik veel geleerd.

Graag wil ik ook OctoPlus NV, en met name Joost Holthuis, bedanken voor het mogelijk maken van dit onderzoek. Ik ben 4 jaar als AIO bij jullie in dienst geweest. Hoewel ik waarschijnlijk de enige werknemer was die moest aanbellen en als gast werd behandeld, heb ik me altijd erg welkom gevoeld en was ik er trots op dat ik één van jullie was. Ruud Verrijk en Leo de Leede waren nauw betrokken bij mijn project. Ondanks jullie drukke agenda wisten jullie tijd vrij te maken voor de projectbesprekingen, die vaak in Utrecht plaatsvonden. Ruud, je aanstekelijke enthousiasme en je eindeloze stroom van ideeën waren erg inspirerend en hebben mooie discussies opgeleverd. Ik vind het fijn dat je straks als mijn tweede co-promotor achter de tafel zit. Leo, ook jou wil ik bedanken voor het vertrouwen dat je in me stelde, en voor je input bij de projectbesprekingen en brainstormsessies. Remco en Delphine, bedankt voor jullie nuttige adviezen in de beginperiode van mijn onderzoek.

I would like to thank the members of the review committee, dr. Glenn Kwon, dr. Martien Cohen Stuart, dr. Jan van Hest, dr. Alexander Kros en dr. Gert Storm for reviewing my thesis. Gert, hoewel dit proefschrift gevuld is met polymeren deeltjes, heb ik gemerkt dat dat prima samengaat met mijn 'liefde' voor liposomen, die je in leven hebt gehouden door me te vragen met Birgit een boek-hoofdstuk over de kinetiek van PEG-liposomen te schrijven.

Hans Meeldijk van Electron Microscopy Utrecht wil ik graag bedanken voor de vele cryoTEM-foto's die hij gemaakt heeft van mijn samples, waarvan er een is opgenomen in hoofdstuk 3. De EM-foto's die in de beginfase van mijn onderzoek zijn gemaakt bij de afdeling Electronenmicroscopie aan de Universiteit van Maastricht, door dr. Peter Frederik en Paul Bomans hebben helaas dit proefschrift niet gehaald. Dat geldt ook voor de MALDI-spectra die Mirjam Damen van Biomedische Analyse heeft opgenomen, en de resultaten van de Langmuir-Blodgett monolayer studies bij de Soft Matter Chemistry Group in Leiden, waar ik geholpen ben door dr. Alexander Kros en Hana Marsden. Toch bedankt voor jullie hulp!

Ook mijn collega's en ex-collega's van de vakgroep Biofarmacie en Farmaceutische technologie wil ik natuurlijk niet overslaan in dit dankwoord. Jullie hulp bij de experimenten, kritische vragen, luisterende oren, en niet te vergeten de gezelligheid tijdens de pauzes, lab-uitjes, borrels en barbecues waren onmisbaar. Kortom, iedereen bedankt voor een geweldige tijd waar ik altijd met veel plezier aan zal terug denken!

Een aantal collega's wil ik graag nog even met name noemen, en ik hoop dat ik daarbij niemand over het hoofd zie. Mies, je hebt me veel geleerd over de wondere wereld van de chromatografie, en als eeuwige optimist ging je altijd met een lach aan de slag met de zoveelste 'uitdaging' die de apparatuur ons weer bracht. Martin, je hebt me ingewerkt in de celkweek en me geholpen met een aantal proeven. Ik hoop in de toekomst nog veel aan je tips te hebben. In het dierenlab was Cor mijn steun- en toeverlaat. Je hebt me een hoop werk uit handen genomen. Helaas leverden de muizen-proeven niet op wat we gehoopt hadden, maar dat lag meer aan mijn bollen dan aan aan jouw inzet! Mijn dank ook aan de heren chemici, Mark, Jordy en Jan Willem voor jullie adviezen bij mijn syntheses (al waren die soms niet zo verstandig..). Aissa, zonder jouw ingewikkelde berekeningen en kennis van SLS was hoofdstuk 3 er niet geweest en waren de PEG-oligolactaat-deeltjes nog steeds een raadsel. Frits, jij hebt na vele pogingen die piepkleine PEG-oligocaprolacton-deeltjes weten te vast te leggen, en er staat dan ook een mooie foto van in hoofdstuk 4. Je enthousiasme en bereidheid anderen te helpen gaven me veel energie. Zonder Barbara was ik redderloos verloren geweest met alle formulieren, bedankt voor het invullen daarvan, en voor het mooie naambordje op deur van onze 'type-kamer'.

I would also like to thank the students whom I guided during my PhD. Emilie, Jan, Macieij and Pascal, you performed a lot of work for this thesis and were welcome assistants during my research.

Mijn labmaatjes op Z513, en later op Z521, Karin, Theo, Cristianne, Jordy, Tina en Najim hebben de nodige buien van mij voorbij zien komen, maar mede dankzij jullie werd er elke dag gelachen en kwam ik met veel plezier naar mijn werk. Ook tijdens de congressen buiten de deur hebben we vanalles ondernomen om behalve nieuwe kennis ook nieuwe indrukken op te doen. Birgit, jij hebt me op dat snowboard weten te krijgen, en Holger, jij bent de enige die dat nog een tweede keer heeft meegemaakt. Ik zal onze avonturen in de States niet snel vergeten. Marjan, bedankt voor je hulp bij mijn toekomstplannen en de gezellige tijd in Cardiff.

De laatste maanden was het ploeteren geblazen op de AIO-kamer, maar gelukkig was ik niet de enige. Sophie en Cris, de output van onze 'type-kamer' heeft onze begeleiders aardig bezig gehouden, en er zijn heel wat kopjes thee, koffie en koekjes door gegaan. We hebben er wat moois van gemaakt met zijn drietjes, bedankt voor jullie steun en gezelligheid.

Cris, jij was meer dan een labmaatje, eigenlijk was je meer mijn 'sparring partner'. We hebben de kans om samen een review te schrijven dan ook met beide handen aangepakt. In mijn eentje had ik hoofdstuk 2 nooit op dit niveau gekregen! We hebben vele inspirerende discussies gevoerd over self-assembling particles, over slechte artikelen en over het leven, en ik bewonder je toewijding en doorzettingsvermogen.

Na alle gezelligheid bij de zwemvereniging en tijdens onze studie kwam ik jou, Suzanne, weer tegen als collega bij Biofarmacie, en al jouw enthousiaste verhalen hebben daar misschien wel een rol in gehad. Ik vond het erg bijzonder om paranimf te zijn bij je promotie, en ik heb je gemist toen je naar Leiden bent vertrokken voor je nieuwe baan.

De 'andere OctoPlus-AIO', Karin, bij jou werd ik ondergebracht toen ik begon met mijn onderzoek, en het klikte meteen. Helaas zijn we maar kort labgenootjes geweest, maar gelukkig lang genoeg om contact te houden na je overstap naar OctoPlus. Jij weet hoe belangrijk het is om in jezelf te geloven, en dat heb je me regelmatig op het hart gedrukt. Misschien moet je dat straks als paranimf nog maar eens tegen me zeggen.

Mijn andere paranimf, Naomi, al bij het begin van mijn onderzoek wist ik dat ik jou hiervoor wilde vragen en ik ben blij dat je me wilt bijstaan. We zijn al weer meer dan 10 jaar vriendinnen, en tijdens onze etentjes hebben altijd we zoveel te bespreken dat de tijd voorbij vliegt.

Ook de Mollerbende stond altijd garant voor de nodige afleiding buiten het werk, verjaardagen, house-warmings, jazzfestivals, er was altijd wel een smoes te verzinnen om af te spreken. Marleen, Boukje, Marike en Marjorie, het kostte soms veel moeite een meidenweekendje te plannen, maar dat was wel altijd dikke pret, net als onze vakantie naar Gran Canaria. Ik hoop dat er nog vele zullen volgen!

Ondanks dat jullie misschien niet altijd begrepen wat ik op het lab uitspookte, leefde ook mijn familie en schoon-familie (wat klinkt dat leuk) mee tijdens de ups en downs van mijn onderzoek. Bedankt voor jullie interesse en opbeurende woorden, en zie hier het resultaat. Martine, terwijl ik hier mijn best doe om niemand te vergeten in dit dankwoord, ben jij bezig er een prachtboekje van te maken. En zoals dat hoort met een proefschrift, met de nodige tegenslagen, maar het wordt een schitterend boekje. Ontzettend bedankt, je maakt er echt iets bijzonders van!

Papa, mama, Vilja, jullie hebben het er niet gemakkelijker op gemaakt, maar ik had het zonder jullie zeker niet gekund. Dit is ook een beetje jullie boekje. Papa, jij wilde altijd alles weten over mijn onderzoek, mijn artikelen en ik geloof dat je ook nog aardig begreep wat ik allemaal het doen was. Mama, ik hoop dat jouw oneindige moed en positivisme in onze genen zit, en dat ik er een beetje van heb meegekregen. Vilja, mijn allerliefste zusje, wat kun jij mensen altijd weer heerlijk met beide benen op de grond zetten. Ik hou van jullie en ik ben er trots op hoe we ons door alles heen slaan.

De laatste woorden heb ik bewaard voor de belangrijkste persoon in mijn leven, mijn kersverse echtgenoot. Lieve Karst, ik heb je wel eens verteld dat ik eindelijk begrijp waarom de partner altijd zo uitgebreid bedankt wordt in het dankwoord. Ik sluit me daar volledig bij aan. Hoe veel boterhammen heb je wel niet voor me gesmeerd en hoe vaak heb je me niet een spiegel voorgehouden? Je was er altijd om me op te vangen als de grond onder mijn voeten weg leek te zakken, of gewoon als ik weer eens 'last had' van mijn ambities. Dankjewel voor je onvoorwaardelijke steun en je brede schouders. Je hebt me de wereld laten zien, en me een onvergetelijke dag bezorgd begin juli (It's you, it's you..). Wat de toekomst ook mag brengen, samen met jou kan ik het aan!